Westinghouse Non-Proprietary Class 3

T69 980804 384

WCAP-15046

♦ ♦ ♦ ♦ ♦ ♦ ♦ ♦

ANALYSIS OF CAPSULE U FROM THE TENNESSEE VALLEY AUTHORITY WATTS BAR UNIT 1 REACTOR VESSEL RADIATION SURVEILLANCE PROGRAM

Westinghouse Energy Systems

WESTINGHOUSE NON-PROPRIETARY CLASS 3

WCAP-15046

Analysis of Capsule U from the Tennessee Valley Authority Watts Bar Unit 1 Reactor Vessel Radiation Surveillance Program

T. J. Laubham
G.K. Roberts
J.F. Williams

June 1998

Work Performed Under Shop Order WGYP-106

Prepared by the Westinghouse Electric Company
for the Tennessee Valley Authority

Approved: C. H. Boyd
C. H . Boyd, Manager
Equipment & Materials Technology

Approved: [signature]
D. M . Trombola, Manager
Mechanical Systems Integration

WESTINGHOUSE ELECTRIC COMPANY
Nuclear Services Division
P.O. Box 355
Pittsburgh, Pennsylvania 15230-0355

PREFACE

This report has been technically reviewed and verified by:

Reviewer:

Sections 1 through 5, 7, 8, Appendices A and B	Ed Terek	Ed Terek
Section 6	John Perock	J. Perock

EXECUTIVE SUMMARY

The purpose of this report is to document the results of the testing of surveillance capsule U from Watts Bar Unit 1. Capsule U was removed at 1.20 EFPY and post irradiation mechanical tests of the Charpy V-notch and tensile specimens was performed, along with a fluence evaluation. The peak clad base/metal vessel fluence after 1.20 EFPY of plant operation was 5.05×10^{18} n/cm^2. A brief summary of the Charpy V-notch testing can be found in Section 1 and the updated capsule removal schedule can be found in Section 7.

TABLE OF CONTENTS

SECTION	TITLE	PAGE
1.0	SUMMARY OF RESULTS	1
2.0	INTRODUCTION	4
3.0	BACKGROUND	5
4.0	DESCRIPTION OF PROGRAM	7
5.0	TESTING OF SPECIMENS FROM CAPSULE U	13
	5.1 Overview	13
	5.2 Charpy V-Notch Impact Test Results	15
	5.3 Tensile Test Results	18
	5.4 1/2T Compact Tension Specimen Tests	18
6.0	RADIATION ANALYSIS AND NEUTRON DOSIMETRY	58
	6.1 Introduction	58
	6.2 Discrete Ordinates Analysis	59
	6.3 Neutron Dosimetry	63
	6.4 Projections of Reactor Vessel Exposure	68
7.0	SURVEILLANCE CAPSULE REMOVAL SCHEDULE	89
8.0	REFERENCES	90

TABLE OF CONTENTS

APPENDIX A - LOAD-TIME RECORDS FOR CHARPY SPECIMEN TESTS

APPENDIX B - CHARPY V-NOTCH PLOTS FOR EACH CAPSULE USING HYPERBOLIC TAGENT CURVE-FITTING METHOD

LIST OF TABLES

Table	Title	Page
4-1	Chemical Composition (wt%) of the Watts Bar Unit 1 Reactor Vessel Beltline Region Surveillance Material	9
4-2	Heat Treatment of the Watts Bar Unit 1 Reactor Vessel Surveillance Material	10
5-1	Charpy V-Notch Data for the Watts Bar Unit 1 Intermediate Shell Forging 05 Irradiated to a Fluence of 5.05×10^{18} n/cm^2 (E > 1.0 MeV) (Tangential Orientation)	19
5-2	Charpy V-notch Data for the Watts Bar Unit 1 Intermediate Shell Forging 05 Irradiated to a Fluence of 5.05×10^{18} n/cm^2 (E > 1.0 MeV) (Axial Orientation)	20
5-3	Charpy V-notch Data for the Watts Bar Unit 1 Surveillance Weld Metal Irradiated to a Fluence of 5.05×10^{18} n/cm^2 (E > 1.0 MeV)	21
5-4	Charpy V-notch Data for the Watts Bar Unit 1 Heat-Affected-Zone Material Irradiated to a Fluence of 5.05×10^{18} n/cm^2 (E > 1.0 MeV)	22
5-5	Instrumented Charpy Impact Test Results for the Watts Bar Unit 1 Intermediate Shell Forging 05 Irradiated to a Fluence of 5.05×10^{18} n/cm^2 (E > 1.0 MeV) (Tangential Orientation)	23
5-6	Instrumented Charpy Impact Test Results for the Watts Bar Unit 1 Intermediate Shell Forging 05 Irradiated to a Fluence of 5.05×10^{18} n/cm^2 (E > 1.0 MeV) (Axial Orientation)	24
5-7	Instrumented Charpy Impact Test Results for the Watts Bar Unit 1 Surveillance Weld Metal Irradiated to a Fluence of 5.05×10^{18} n/cm^2 (E > 1.0 MeV)	25

LIST OF TABLES (CONTINUED)

Table	Title	Page
5-8	Instrumented Charpy Impact Test Results for the Watts Bar Unit 1 Heat-Affected-Zone (HAZ) Metal Irradiated to a Fluence of 5.05×10^{18} n/cm^2 (E > 1.0 MeV)	26
5-9	Effect Irradiation to 5.05×10^{18} n/cm^2 (E > 1.0 MeV) on the Notch Toughness Properties of the Watts Bar Unit 1 Reactor Vessel Surveillance Materials	27
5-10	Comparison of the Watts Bar Unit 1 Surveillance Material 30 ft-lb Transition Temperature Shifts and Upper Shelf Energy Decreases with Regulatory Guide 1.99, Revision 2, Predictions	28
5-11	Tensile Properties of the Watts Bar Unit 1 Reactor Vessel Surveillance Materials Irradiated to 5.05×10^{18} n/cm^2 (E > 1.0 MeV)	29
6-1	Calculated Fast Neutron Exposure Rates and Iron Atom Displacement Rates at the Surveillance Capsule Center	72
6-2	Calculated Azimuthal Variation of Fast Neutron Exposure Rates and Iron Atom Displacement Rates at the Reactor Vessel Clad/Base Metal Interface	73
6-3	Relative Radial Distribution of ϕ(E > 1.0 MeV) Within the Reactor Vessel Wall	74
6-4	Relative Radial Distribution of ϕ(E > 0.1 MeV) Within the Reactor Vessel Wall	75
6-5	Relative Radial Distribution of dpa/sec Within the Reactor Vessel Wall	76
6-6	Nuclear Parameters Used in the Evaluation of Neutron Sensors	77

LIST OF TABLES (CONTINUED)

Table	Title	Page
6-7	Monthly Thermal Generation During The First Fuel Cycle of the Watts Bar 1 Reactor	78
6-8	Measured Sensor Activities and Reaction Rates - Surveillance Capsule U	79
6-9	Summary of Neutron Dosimetry Results Surveillance Capsule U	80
6-10	Comparison of Measured, Calculated and Best Estimate Reaction Rates at the Surveillance Capsule Center	81
6-11	Best Estimate Neutron Energy Spectrum at the Center of Surveillance Capsule - Capsule U	82
6-12	Comparison of Calculated and Best Estimate Integrated Neutron Exposure of Watts Bar 1 Surveillance Capsule U	83
6-13	Azimuthal Variations of the Neutron Exposure Projections on the Reactor Vessel Clad/Base Metal Interface at Core Midplane	84
6-14	Neutron Exposure Exposure Values Within The Watts Bar Unit 1 Reactor Vessel	86
6-15	Updated Lead Factors for Watts Bar 1 Surveillance Capsules	88
7-1	Watts Bar Unit 1 Reactor Vessel Surveillance Capsule Withdrawal Schedule	89

LIST OF ILLUSTRATIONS

Figure	Title	Page
4-1	Arrangement of Surveillance Capsules in the Watts Bar Unit 1 Reactor Vessel	11
4-2	Capsule U Diagram Showing the Location of Specimens, Thermal Monitors, and Dosimeters	12
5-1	Charpy V-Notch Impact Energy vs. Temperature for Watts Bar Unit 1 Reactor Vessel Intermediate Shell Forging 05 (Tangential Orientation)	30
5-2	Charpy V-Notch Lateral Expansion vs. Temperature for Watts Bar Unit 1 Reactor Vessel Intermediate Shell Forging 05 (Tangential Orientation)	31
5-3	Charpy V-Notch Percent Shear vs. Temperature for Watts Bar Unit 1 Reactor Vessel Intermediate Shell Forging 05 (Tangential Orientation)	32
5-4	Charpy V-Notch Impact Energy vs. Temperature for Watts Bar Unit 1 Reactor Vessel Intermediate Shell Forging 05 (Axial Orientation)	33
5-5	Charpy V-Notch Lateral Expansion vs. Temperature for Watts Bar Unit 1 Reactor Vessel Intermediate Shell Forging 05 (Axial Orientation)	34
5-6	Charpy V-Notch Percent Shear vs. Temperature for Watts Bar Unit 1 Reactor Vessel Intermediate Shell Forging 05 (Axial Orientation)	35
5-7	Charpy V-Notch Impact Energy vs. Temperature for Watts Bar Unit 1 Reactor Vessel Weld Metal	36
5-8	Charpy V-Notch Lateral Expansion vs. Temperature for Watts Bar Unit 1 Reactor Vessel Weld Metal	37

LIST OF ILLUSTRATIONS (CONTINUED)

Figure	Title	Page
5-9	Charpy V-Notch Percent Shear vs. Temperature for Watts Bar Unit 1 Reactor Vessel Weld Metal	38
5-10	Charpy V-Notch Impact Energy vs. Temperature for Watts Bar Unit 1 Reactor Vessel Heat-Affected-Zone Material	39
5-11	Charpy V-Notch Lateral Expansion vs. Temperature for Watts Bar Unit 1 Reactor Vessel Heat-Affected-Zone Material	40
5-12	Charpy V-Notch Percent Shear vs. Temperature for Watts Bar Unit 1 Reactor Vessel Heat-Affected-Zone Material	41
5-13	Charpy Impact Specimen Fracture Surfaces for Watts Bar Unit 1 Reactor Vessel Intermediate Shell Forging 05 (Tangential Orientation)	42
5-14	Charpy Impact Specimen Fracture Surfaces for Watts Bar Unit 1 Reactor Vessel Intermediate Shell Forging 05 (Axial Orientation)	43
5-15	Charpy Impact Specimen Fracture Surfaces for Watts Bar Unit 1 Reactor Vessel Weld Metal	44
5-16	Charpy Impact Specimen Fracture Surfaces for Watts Bar Unit 1 Reactor Vessel Heat-Affected-Zone Metal	45
5-17	Tensile Properties for Watts Bar Unit 1 Reactor Vessel Intermediate Shell Forging 05 (Tangential Orientation)	46
5-18	Tensile Properties for Watts Bar Unit 1 Reactor Vessel Intermediate Shell Forging 05 (Axial Orientation)	47

LIST OF ILLUSTRATIONS (CONTINUED)

Figure	Title	Page
5-19	Tensile Properties for Watts Bar Unit 1 Reactor Vessel Weld Metal	48
5-20	Fractured Tensile Specimens from Watts Bar Unit 1 Reactor Vessel Intermediate Shell Forging 05 (Tangential Orientation)	49
5-21	Fractured Tensile Specimens from Watts Bar Unit 1 Reactor Vessel Intermediate Shell Forging 05 (Axial Orientation)	50
5-22	Fractured Tensile Specimens from Watts Bar Unit 1 Reactor Vessel Weld Metal	51
5-23	Engineering Stress-Strain Curves for Intermediate Shell Forging 05 Tensile Specimens WL1 and WL2 (Tangential Orientation)	52
5-24	Engineering Stress-Strain Curve for Intermediate Shell Forging 05 Tensile Specimen WL3 (Tangential Orientation)	53
5-25	Engineering Stress-Strain Curves for Intermediate Shell Forging 05 Tensile Specimens WT1 and WT2 (Axial Orientation)	54
5-26	Engineering Stress-Strain Curve for Intermediate Shell Forging 05 Tensile Specimen WT3 (Axial Orientation)	55
5-27	Engineering Stress-Strain Curves for Weld Metal Tensile Specimens WW1 and WW2	56
5-28	Engineering Stress-Strain Curve for Weld Metal Tensile Specimen WW3	57
6-1	Plan View of a Dual Reactor Vessel Surveillance Capsule	71

SECTION 1.0
SUMMARY OF RESULTS

The analysis of the reactor vessel materials contained in surveillance capsule U, the second capsule to be removed from the Watts Bar Unit 1 reactor pressure vessel, led to the following conclusions:

- The capsule received an average fast neutron fluence (E > 1.0 MeV) of 5.05 x 10^{18} n/cm^2 after 1.20 effective full power years (EFPY) of plant operation.

- Irradiation of the reactor vessel intermediate shell forging 05 Charpy specimens, oriented with the longitudinal axis of the specimen parallel to the major working direction (tangential orientation), to 5.05 x 10^{18} n/cm^2 (E > 1.0 MeV) resulted in a 30 ft-lb transition temperature increase of 98°F and a 50 ft-lb transition temperature increase of 102°F. This results in an irradiated 30 ft-lb transition temperature of 41°F and an irradiated 50 ft-lb transition temperature of 86°F for the tangential oriented specimens.

- Irradiation of the reactor vessel intermediate shell forging 05 Charpy specimens, oriented with the longitudinal axis of the specimen perpendicular to the major working direction of the plate (axial orientation), to 5.05 x 10^{18} n/cm^2 (E > 1.0 MeV) resulted in a 30 ft-lb transition temperature increase of 29°F and a 50 ft-lb transition temperature increase of 35°F. This results in an irradiated 30 ft-lb transition temperature of 74°F and an irradiated 50 ft-lb transition temperature of 149°F for axial oriented specimens.

- Irradiation of the weld metal Charpy specimens to 5.05 x 10^{18} n/cm^2 (E > 1.0 MeV) resulted in a 30 ft-lb transition temperature decrease of 6°F and a 50 ft-lb transition temperature increase of 12°F. This results in an irradiated 30 ft-lb transition temperature of -38°F and an irradiated 50 ft-lb transition temperature of 6°F.

- Irradiation of the weld Heat-Affected-Zone (HAZ) metal Charpy specimens to 5.05 x 10^{18} n/cm^2 (E > 1.0 MeV) resulted in a 30 ft-lb transition temperature increase of 52°F and a 50 ft-lb transition temperature increase of 53°F. This results in an irradiated 30 ft-lb transition temperature of -5°F and an irradiated 50 ft-lb transition temperature of 44°F.

- The average upper shelf energy of the intermediate shell forging 05 (tangential orientation) resulted in an average energy decrease of 25 ft-lb after irradiation to 5.05×10^{18} n/cm^2 (E > 1.0 MeV). This results in an irradiated average upper shelf energy of 107 ft-lb for the tangential oriented specimens.

- The average upper shelf energy of the intermediate shell forging 05 (axial orientation) resulted in an average energy increase of 10 ft-lb after irradiation to 5.05×10^{18} n/cm^2 (E > 1.0 MeV). This results in an irradiated average upper shelf energy of 72 ft-lb for the axially oriented specimens.

- The average upper shelf energy of the weld metal Charpy specimens resulted in an average energy increase of 12 ft-lb after irradiation to 5.05×10^{18} n/cm^2 (E > 1.0 MeV). This results in an irradiated average upper shelf energy of 143 ft-lb for the weld metal specimens.

- The average upper shelf energy of the weld HAZ metal Charpy specimens resulted in an average energy decrease of 10 ft-lb after irradiation to 5.05×10^{18} n/cm^2 (E > 1.0 MeV). This results in an irradiated average upper shelf energy of 79 ft-lb for the weld HAZ metal.

- A comparison of the Watts Bar Unit 1 reactor vessel beltline material test results with the Regulatory Guide 1.99, Revision 2[1], predictions led to the following conclusions:

  - The measured 30 ft-lb shift in transition temperature of all surveillance materials contained in capsule U is less than the Regulatory Guide 1.99, Revision 2, predictions.

  - The measured decrease in USE of all surveillance materials contained capsule U is less than the Regulatory Guide 1.99, Revision 2, predictions.

- The best estimate end-of-license (32 EFPY) neutron fluence (E > 1.0 MeV) at the core midplane for the Watts Bar Unit 1 reactor vessel using the Regulatory Guide 1.99, Revision 2 attenuation formula (ie. # 3) is as follows:

Vessel inner radius*	= 3.38×10^{19} n/cm^2
Vessel 1/4 thickness	= 2.03×10^{19} n/cm^2
Vessel 3/4 thickness	= 7.37×10^{18} n/cm^2

* Clad/base metal interface

- All beltline materials, with exception to the intermediate shell forging 05, are expected to have an upper shelf energy (USE) greater than 50 ft-lb through end of license (EOL, 32 EFPY) as required by 10CFR50, Appendix G[2].

In September of 1993, Westinghouse completed an evaluation to demonstrate that all Westinghouse Owners Group (WOG) Plant reactor vessels have a margin of safety, relative to USE, equivalent to that required by Appendix G of the ASME Code. This was accomplished by performing generic bounding evaluations per the proposed ASME Section XI, Appendix X. This evaluation is documented in WCAP-13587, Revision 1[36], "Reactor Vessel Upper Shelf Energy Bounding Evaluation for Westinghouse Pressurized Water Reactors" and provides the minimum USE for a four loop Westinghouse NSSS plant. The minimum acceptable USE for a 4 loop plant is 43 ft-lb. The projected minimum EOL USE for the Watts Bar Unit 1 intermediate shell forging 05 is greater than 43 ft-lb. Hence, the bounding WOG evaluation shows that the Watts Bar Unit 1 intermediate shell forging 05 will maintain an equivalent margin, with respect to USE per the requirements of 10 CFR Part 50, Appendix G, through EOL (ie. Maintain this margin through EOL). In addition, the results of capsule U testing indicate that the measured EOL USE for the axially oriented Charpy specimens actually increased by approximately 11 ft-lb. However, for the Watts Bar Unit 1 reactor vessel only one capsule has been tested to date. Once another set of surveillance data becomes available, the surveillance data can be used to project the EOL USE of the Watts Bar Unit 1 intermediate shell forging 05.

SECTION 2.0
INTRODUCTION

This report presents the results of the examination of Capsule U, the first capsule to be removed from the reactor in the continuing surveillance program which monitors the effects of neutron irradiation on the Tennessee Valley Authority Watts Bar Unit 1 reactor pressure vessel materials under actual operating conditions.

The surveillance program for the Tennessee Valley Authority Watts Bar Unit 1 reactor pressure vessel materials was designed and recommended by the Westinghouse Electric Corporation. A description of the surveillance program and the preirradiation mechanical properties of the reactor vessel materials is presented in WCAP-9298, "Tennessee Valley Authority Watts Bar Unit No. 1 Reactor Vessel Radiation Surveillance Program"[3]. The surveillance program was planned to cover the 40-year design life of the reactor pressure vessel and was based on ASTM E185-73, "Standard Recommended Practice Surveillance Tests for Nuclear Reactor Vessels". Capsule U was removed from the reactor after 1.20 EFPY of exposure and shipped to the Westinghouse Science and Technology Center Hot Cell Facility, where the postirradiation mechanical testing of the Charpy V-notch impact and tensile surveillance specimens was performed.

This report summarizes the testing of and the post-irradiation data obtained from surveillance capsule U removed from the Tennessee Valley Authority Watts Bar Unit 1 reactor vessel and discusses the analysis of the data.

SECTION 3.0
BACKGROUND

The ability of the large steel pressure vessel containing the reactor core and its primary coolant to resist fracture constitutes an important factor in ensuring safety in the nuclear industry. The beltline region of the reactor pressure vessel is the most critical region of the vessel because it is subjected to significant fast neutron bombardment. The overall effects of fast neutron irradiation on the mechanical properties of low alloy, ferritic pressure vessel steels such as A508 Class 2 Forging (base material of the Watts Bar Unit 1 reactor pressure vessel beltline) are well documented in the literature. Generally, low alloy ferritic materials show an increase in hardness and tensile properties and a decrease in ductility and toughness during high-energy irradiation.

A method for ensuring the integrity of reactor pressure vessels has been presented in "Fracture Toughness Criteria for Protection Against Failure," Appendix G to Section XI of the ASME Boiler and Pressure Vessel Code[4]. The method uses fracture mechanics concepts and is based on the reference nil-ductility transition temperature (RT_{NDT}).

RT_{NDT} is defined as the greater of either the drop weight nil-ductility transition temperature (NDTT per ASTM E-208[5]) or the temperature 60°F less than the 50 ft-lb (and 35-mil lateral expansion) temperature as determined from Charpy specimens oriented perpendicular (Axial) to the major working direction of the forging. The RT_{NDT} of a given material is used to index that material to a reference stress intensity factor curve (K_{Ia} curve) which appears in Appendix G to the ASME Code[4]. The K_{Ia} curve is a lower bound of dynamic, crack arrest, and static fracture toughness results obtained from several heats of pressure vessel steel. When a given material is indexed to the K_{Ia} curve, allowable stress intensity factors can be obtained for this material as a function of temperature. Allowable operating limits can then be determined using these allowable stress intensity factors.

RT_{NDT} and, in turn, the operating limits of nuclear power plants can be adjusted to account for the effects of radiation on the reactor vessel material properties. The changes in mechanical properties of a given reactor pressure vessel steel, due to irradiation, can be monitored by a reactor surveillance program, such as the Watts Bar Unit 1 reactor vessel radiation surveillance program[3], in which a surveillance capsule is periodically removed from the operating nuclear reactor and the encapsulated specimens tested. The increase in the average Charpy V-notch 30 ft-lb temperature (ΔRT_{NDT}) due to irradiation is added to the initial RT_{NDT}, along with a margin (M) to cover uncertainties, to adjust the RT_{NDT} (ART) for radiation embrittlement. This ART (RT_{NDT} initial + M + ΔRT_{NDT}) is used to index the material to the K_{Ia} curve and, in turn, to set operating limits for the nuclear power plant that take into account the effects of irradiation on the reactor vessel materials.

SECTION 4.0
DESCRIPTION OF PROGRAM

Six surveillance capsules for monitoring the effects of neutron exposure on the Watts Bar Unit 1 reactor pressure vessel core region (beltline) materials were inserted in the reactor vessel prior to initial plant start-up. The six capsules were positioned in the reactor vessel between the neutron pads and the vessel wall as shown in Figure 4-1. The vertical center of the capsules is opposite the vertical center of the core. The capsules contain specimens made from intermediate shell forging 05, weld metal fabricated with weld wire heat number 895075 with Grau L.O. (LW320) flux, lot P46, which is identical to that used in the actual fabrication of the closing girth seam weld between forgings 04 and 05.

Capsule U was removed after 1.20 effective full power years (EFPY) of plant operation. This capsule contained Charpy V-notch, tensile, and 1/2T-CT fracture mechanics specimens made from intermediate shell forging 05 and submerged arc weld metal identical to the reactor vessel beltline region welds. In addition, this capsule contained Charpy V-notch specimens from the weld Heat-Affected-Zone (HAZ) of intermediate shell forging 05.

Test material obtained from intermediate shell forging 05 (after the thermal heat treatment and forming of the forging) was taken at least one plate thickness from the quenched ends of the forging. All test specimens were machined from the 1/4 thickness location of the forging after performing a simulated post-weld stress-relieving treatment on the test material. Specimens from weld metal and heat-affected-zone metal were machined from a stress-relieved weldment joining intermediate and lower shell forgings 05 and 04. All heat-affected-zone specimens were obtained from the weld heat-affected-zone of intermediate shell forging 05.

Charpy V-notch impact specimens from intermediate shell forging 05 were machined with some in the tangential orientation (longitudinal axis of the specimen parallel to the major working direction) and some in the axial orientation (longitudinal axis of the specimen perpendicular to the major working direction). The core region weld Charpy impact specimens were machined from the weldment such that the long dimension of each Charpy specimen was perpendicular to the weld direction. The notch of the weld metal Charpy specimens was machined such that the direction of crack propagation in the specimen was in the welding direction.

Tensile specimens from intermediate shell forging 05 were machined in both the tangential and axial orientation. Tensile specimens from the weld metal were oriented with the long dimension of the specimen perpendicular to the weld direction.

Bend bar specimens were machined from forging 05 with the longitudinal axis of the specimen oriented in the rolling direction of the forging such that the simulated crack would propagate in a direction normal ro the rolling direction of the forging. All bend bar specimens were fatigue precracked according to ASTM E399.

Compact tension test specimens from forging 05 were machined in both the axial and tangential orientations. Compact tension test specimens from the weld metal were machined normal to the weld direction with the notch oriented in the direction of the weld. All specimens were fatigue precracked according to ASTM E399.

The chemical composition and heat treatment of the surveillance material is presented in Tables 4-1 and 4-2. The chemical analysis reported in Table 4-1 was obtained from unirradiated material used in the surveillance program[3].

Capsule U contained dosimeter wires of pure copper, iron, nickel, and aluminum-0.15 weight percent cobalt (cadmium-shielded and unshielded). In addition, cadmium shielded dosimeters of neptunium (Np^{237}) and uranium (U^{238}) were placed in the capsule to measure the integrated flux at specific neutron energy levels.

The capsule contained thermal monitors made from two low-melting-point eutectic alloys and sealed in Pyrex tubes. These thermal monitors were used to define the maximum temperature attained by the test specimens during irradiation. The composition of the two eutectic alloys and their melting points are as follows:

2.5% Ag, 97.5% Pb	Melting Point: 579°F (304°C)
1.75% Ag, 0.75% Sn, 97.5% Pb	Melting Point: 590°F (310°C)

The arrangement of the various mechanical specimens, dosimeters and thermal monitors contained in capsule U is shown in Figure 4-2.

TABLE 4-1

Chemical Composition (wt%) of the Watts Bar Unit 1 Reactor Vessel Beltline Region Materials[3]

Element	Intermediate Shell Forging 05[(a)]		Weld Metal[(b & c)]	
C	0.20	0.21	0.080	0.069
S	0.016	0.014	0.007	0.010
N	0.009	---	0.019	---
Co	<0.01	0.012	0.007	---
Cu	0.17	0.14	0.031	0.05
Si	0.25	0.25	0.27	0.22
Mo	0.57	0.61	0.54	0.56
Ni	0.80	0.79	0.75	0.70
Mn	0.73	0.68	1.94	1.97
Cr	0.32	0.34	0.023	0.05
V	<0.01	<0.02	0.001	---
P	0.012	0.013	0.015	0.010
Al	<0.019	0.049	0.019	---
Sn	0.010	---	0.003	---

Notes:

a) All analysis except for N and Sn were conducted by Rotterdam Dockyard Company/Krupp ladle analysis; N and Sn analysis were performed by Westinghouse.

b) The surveillance weldment is identical to the closing girth seam weldment between forging 04 and 05. The closing seam used weld wire heat number 895075 with Grau L.O. (LW320) flux, lot P46, except for the 1-inch root pass at the ID of the vessel. This root pass used weld wire heat number 899680 with type Grau L.O. (LW320) flux, lot P23, with as as-deposited copper and phosphorus content of 0.03 and 0.009, respectively. The surveillance weldment specimens were not removed from this root area.

c) The left column results were obtained from Westinghouse analyses, while the results in the right column results were obtained from analyses conducted by Rotterdam Dockyard Company.

TABLE 4-2			
Heat Treatment of the Watts Bar Unit 1 Reactor Vessel Surveillance Material[3]			
Material	Temperature (°F)	Time (hrs.)	Coolant
Intermediate Shell Forging 05	1675 - 1700	3 ½	Water-quenched
	1230 - 1240	6	Air Cooled
	1140 ± 25	21	Furnace Cooled
Weldment	1140 ± 25	14 hr., 56 min	Furnace Cooled

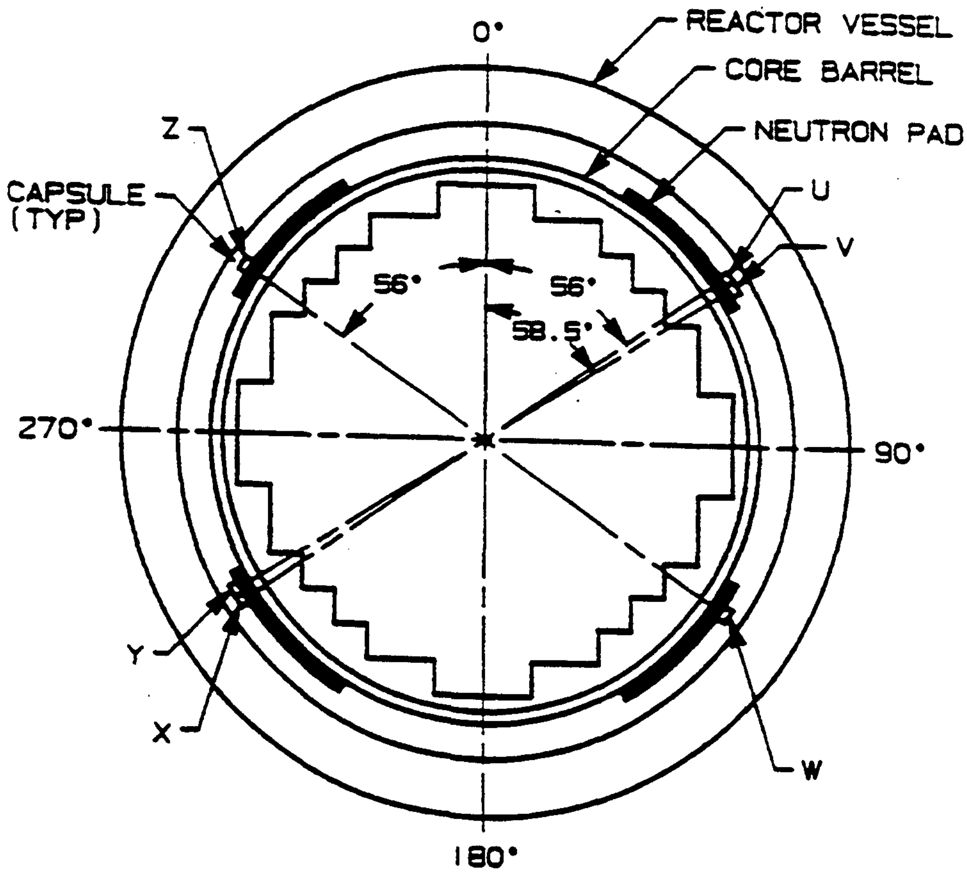

Figure 4-1. Arrangement of Surveillance Capsules in the Watts Bar Unit 1 Reactor Vessel

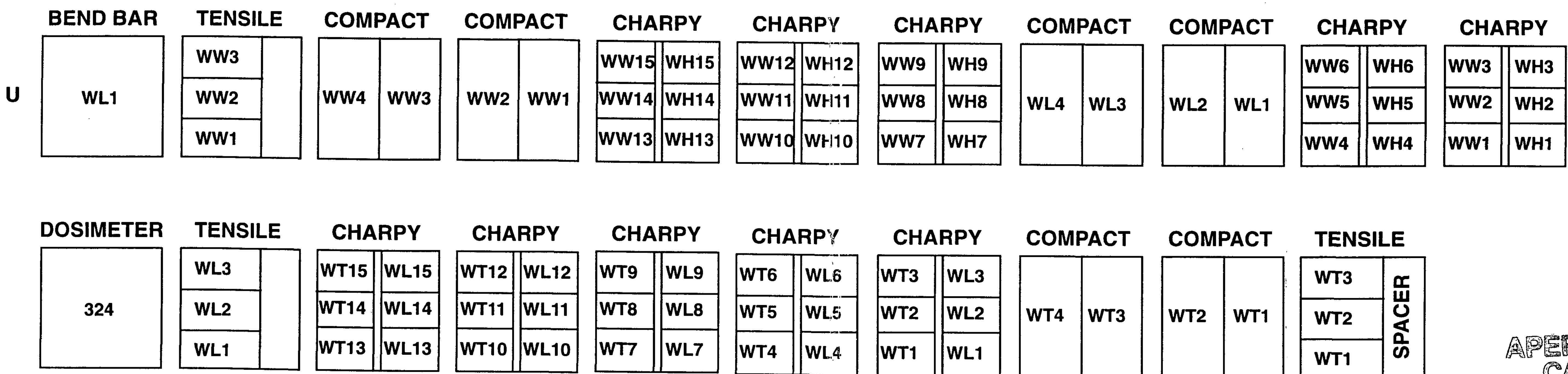

LEGEND:

WL - INTERMEDIATE FORGING 05, HEAT NO. 527536 (TANGENTIAL)

WT - INTERMEDIATE FORGING 05, HEAT NO. 527536 (AXIAL)

WW - WELD METAL

WH - HEAT AFFECTED ZONE MATERIAL

9810200226-01

Figure 4-2. Capsule U Diagram Showing the Location of Specimens, Thermal Monitors, and Dosimeters

SECTION 5.0

TESTING OF SPECIMENS FROM CAPSULE U

5.1 Overview

The post-irradiation mechanical testing of the Charpy V-notch impact specimens and tensile specimens was performed in the Remote Metallographic Facility (RMF) at the Westinghouse Science and Technology Center. Testing was performed in accordance with 10CFR50, Appendices G and H[2], ASTM Specification E185-82[6], and Westinghouse Procedure RMF 8402, Revision 2 as modified by Westinghouse RMF Procedures 8102, Revision 1, and 8103, Revision 1.

Upon receipt of the capsule at the hot cell laboratory, the specimens and spacer blocks were carefully removed, inspected for identification number, and checked against the master list in WCAP-9298[3]. No discrepancies were found.

Examination of the two low-melting point 579°F (304°C) and 590°F (310°C) eutectic alloys indicated no melting of either type of thermal monitor. Based on this examination, the maximum temperature to which the test specimens were exposed was less than 579°F (304°C).

The Charpy impact tests were performed per ASTM Specification E23-93a[7] and RMF Procedure 8103, Revision 1, on a Tinius-Olsen Model 74, 358J machine. The tup (striker) of the Charpy impact test machine is instrumented with a GRC 830-I instrumentation system, feeding information into an IBM compatible 486 computer. With this system, load-time and energy-time signals can be recorded in addition to the standard measurement of Charpy energy (E_D). From the load-time curve (Appendix A), the load of general yielding (P_{GY}), the time to general yielding (t_{GY}), the maximum load (P_M), and the time to maximum load (t_M) can be determined. Under some test conditions, a sharp drop in load indicative of fast fracture was observed. The load at which fast fracture was initiated is identified as the fast fracture load (P_F), and the load at which fast fracture terminated is identified as the arrest load (P_A). The energy at maximum load (E_M) was determined by comparing the energy-time record and the load-time record. The energy at maximum load is approximately equivalent to the energy required to initiate a crack in the specimen. Therefore, the propagation energy for the crack (E_p) is the difference between the total energy to fracture (E_D) and the energy at maximum load (E_M).

The yield stress (s_Y) was calculated from the three-point bend formula having the following expression:

$$\sigma_Y = (P_{GY} * L) / [B * (W - a)^2 * C] \quad (1)$$

where:	L	=	distance between the specimen supports in the impact machine
	B	=	the width of the specimen measured parallel to the notch
	W	=	height of the specimen, measured perpendicularly to the notch
	a	=	notch depth

The constant C is dependent on the notch flank angle (f), notch root radius (r) and the type of loading (ie. pure bending or three-point bending). In three-point bending, for a Charpy specimen in which f = 45° and r = 0.010 inch, Equation 1 is valid with C = 1.21. Therefore, (for L = 4W),

$$\sigma_Y = (P_{GY} * L) / [B * (W - a)^2 * 1.21] = (3.3 * P_{GY} * W) / [B * (W - a)^2] \quad (2)$$

For the Charpy specimen, B = 0.394 inch, W = 0.394 inch and a = 0.079 inch. Equation 2 then reduces to:

$$\sigma_Y = 33.3 * P_{GY} \quad (3)$$

where σ_Y is in units of psi and P_{GY} is in units of lbs. The flow stress was calculated from the average of the yield and maximum loads, also using the three-point bend formula.

The symbol A in columns 4, 5, and 6 of Tables 5-5 through 5-8 is the cross-section area under the notch of the Charpy specimens:

$$A = B * (W - a) = 0.1241 \text{ sq. in.} \quad (4)$$

Percent shear was determined from post-fracture photographs using the ratio-of-areas methods in compliance with ASTM Specification A370-92[8]. The lateral expansion was measured using a dial gage rig similar to that shown in the same specification.

Tensile tests were performed on a 20,000-pound Instron, split-console test machine (Model 1115) per ASTM Specification E8-93[9] and E21-92[10], and RMF Procedure 8102, Revision 1. All pull rods, grips, and pins were made of Inconel 718. The upper pull rod was connected through a universal joint to improve axiality of loading. The tests were conducted at a constant crosshead speed of 0.05 inches per minute throughout the test.

Extension measurements were made with a linear variable displacement transducer extensometer. The extensometer knife edges were spring-loaded to the specimen and operated through specimen failure. The extensometer gage length was 1.00 inch. The extensometer is rated as Class B-2 per ASTM E83-93[11].

Elevated test temperatures were obtained with a three-zone electric resistance split-tube furnace with a 9-inch hot zone. All tests were conducted in air. Because of the difficulty in remotely attaching a thermocouple directly to the specimen, the following procedure was used to monitor specimen temperatures. Chromel-Alumel thermocouples were positioned at the center and at each end of the gage section of a dummy specimen and in each tensile machine griper. In the test configuration, with a slight load on the specimen, a plot of specimen temperature versus upper and lower tensile machine griper and controller temperatures was developed over the range from room temperature to 550°F. During the actual testing, the grip temperatures were used to obtain desired specimen temperatures. Experiments have indicated that this method is accurate to ±2°F.

The yield load, ultimate load, fracture load, total elongation, and uniform elongation were determined directly from the load-extension curve. The yield strength, ultimate strength, and fracture strength were calculated using the original cross-sectional area. The final diameter and final gage length were determined from post-fracture photographs. The fracture area used to calculate the fracture stress (true stress at fracture) and percent reduction in area was computed using the final diameter measurement.

5.2 Charpy V-Notch Impact Test Results

The results of the Charpy V-notch impact tests performed on the various materials contained in capsule U, which received a fluence of 5.05 x 10^{18} n/cm^2(E > 1.0 MeV) in 1.20 EFPY of operation, are presented in Tables 5-1 through 5-8 and are compared with unirradiated results[3] as shown in Figures 5-1 through 5-12.

The transition temperature increases and upper shelf energy decreases for the capsule U materials are summarized in Table 5-9. These results led to the following conclusions:

Irradiation of the reactor vessel intermediate shell forging 05 Charpy specimens, oriented with the longitudinal axis of the specimen parallel to the major working direction (tangential orientation), to 5.05 x 10^{18} n/cm^2 (E > 1.0 MeV) resulted in a 30 ft-lb transition temperature increase of 98°F and a 50 ft-lb transition temperature increase of 102°F. This results in an irradiated 30 ft-lb transition temperature of 41°F and an irradiated 50 ft-lb transition temperature of 86°F for the tangential oriented specimens.

Irradiation of the reactor vessel intermediate shell forging 05 Charpy specimens, oriented with the longitudinal axis of the specimen perpendicular to the major working direction of the plate (axial orientation), to 5.05 x 10^{18} n/cm^2 (E > 1.0 MeV) resulted in a 30 ft-lb transition temperature increase of 29°F and a 50 ft-lb transition temperature increase of 35°F. This results in an irradiated 30 ft-lb transition temperature of 74°F and an irradiated 50 ft-lb transition temperature of 149°F for axial oriented specimens.

Irradiation of the weld metal Charpy specimens to 5.05 x 10^{18} n/cm^2 (E > 1.0 MeV) resulted in a 30 ft-lb transition temperature decrease of 6°F and a 50 ft-lb transition temperature increase of 12°F. This results in an irradiated 30 ft-lb transition temperature of -38°F and an irradiated 50 ft-lb transition temperature of 6°F.

Irradiation of the weld Heat-Affected-Zone (HAZ) metal Charpy specimens to 5.05 x 10^{18} n/cm^2 (E > 1.0 MeV) resulted in a 30 ft-lb transition temperature increase of 52°F and a 50 ft-lb transition temperature increase of 53°F. This results in an irradiated 30 ft-lb transition temperature of -5°F and an irradiated 50 ft-lb transition temperature of 44°F.

The average upper shelf energy of the intermediate shell forging 05 (tangential orientation) resulted in an average energy decrease of 25 ft-lb after irradiation to 5.05 x 10^{18} n/cm^2 (E > 1.0 MeV). This results in an irradiated average upper shelf energy of 107 ft-lb for the tangentially oriented specimens.

The average upper shelf energy of the intermediate shell forging 05 (axial orientation) resulted in an average energy increase of 10 ft-lb after irradiation to 5.05 x 10^{18} n/cm^2 (E > 1.0 MeV). This results in an irradiated average upper shelf energy of 72 ft-lb for the axially oriented specimens.

The average upper shelf energy of the weld metal Charpy specimens resulted in an average energy increase of 12 ft-lb after irradiation to 5.05 x 10^{18} n/cm^2 (E > 1.0 MeV). This results in an irradiated average upper shelf energy of 143 ft-lb for the weld metal specimens.

The average upper shelf energy of the weld HAZ metal Charpy specimens resulted in an average energy decrease of 10 ft-lb after irradiation to 5.05 x 10^{18} n/cm^2 (E > 1.0 MeV). This results in an irradiated average upper shelf energy of 79 ft-lb for the weld HAZ metal.

A comparison of the Watts Bar Unit 1 reactor vessel beltline material test results with the Regulatory Guide 1.99, Revision 2[1], predictions is given in Table 5-10 and led to the following conclusions:

- The measured 30 ft-lb shift in transition temperature and measured decrease in USE of all surveillance materials contained in capsule U are less than the Regulatory Guide 1.99, Revision 2, predictions.

The fracture appearance of each irradiated Charpy specimen from the various surveillance capsule U materials is shown in Figures 5-13 through 5-16 and shows an increasingly ductile or tougher appearance with increasing test temperature.

All beltline materials, with exception to the intermediate shell forging 05, are expected to have an upper shelf energy (USE) greater than 50 ft-lb through end of license (EOL, 32 EFPY) as required by 10CFR50, Appendix G[2]. In September of 1993, Westinghouse completed an evaluation to demonstrate that all Westinghouse Owners Group (WOG) Plant reactor vessels have a margin of safety, relative to USE, equivalent to that required by Appendix G of the ASME Code. This was accomplished by performing generic bounding evaluations per the proposed ASME Section XI, Appendix X. This evaluation is documented in WCAP-13587, Rev.1[36] provides the minimum USE, 43 ft-lb, for a four loop Westinghouse NSSS plant. The projected minimum EOL USE for the Watts Bar Unit 1 intermediate shell forging 05 is greater than 43 ft-lb. Hence, the bounding WOG evaluation shows that the Watts Bar Unit 1 intermediate shell forging 05 will maintain an equivalent margin through EOL, with respect to USE per the requirements of 10 CFR Part 50, Appendix G. In addition, the results of capsule U testing indicate that the measured EOL USE actually increased by approximately 11 ft-lb. However, for the Watts Bar Unit 1 reactor vessel only one capsule has been tested to date. Once another set of surveillance data becomes available, the surveillance data can be used to project the EOL USE of the Watts Bar Unit 1 intermediate shell forging 05.

The load-time records for individual instrumented Charpy specimen tests are shown in Appendix A.

The Charpy V-notch data presented in WCAP-9298[3] were based on hand-fit Charpy curves using engineering judgement. However, the results presented in this report are based on a re-plot of all capsule data using CVGRAPH, Version 4.1. which is a hyperbolic tangent curve-fitting program. Appendix B presents the CVGRAPH, Version 4.1, Charpy V-notch plots and the program input data.

5.3 Tensile Test Results

The results of the tensile tests performed on the various materials contained in capsule U irradiated to 5.05×10^{18} n/cm^2 (E > 1.0 MeV) are presented in Table 5-11 and are compared with unirradiated results[3] as shown in Figures 5-17 through 5-19.

The results of the tensile tests performed on the intermediate shell forging 05 (Tangential orientation) indicated that irradiation to 5.05×10^{18} n/cm^2 (E > 1.0 MeV) caused approximately a 4 to 7 ksi increase in the 0.2 percent offset yield strength and approximately a 5 to 8 ksi increase in the ultimate tensile strength when compared to unirradiated data[3] (Figure 5-17).

The results of the tensile tests performed on the intermediate shell forging 05 (axial orientation) indicated that irradiation to 5.05×10^{18} n/cm^2 (E > 1.0 MeV) caused a 5 ksi increase in the 0.2 percent offset yield strength and approximately a 3 to 6 ksi increase in the ultimate tensile strength when compared to unirradiated data[3] (Figure 5-18).

The results of the tensile tests performed on the surveillance weld metal indicated that irradiation to 5.05 x 10^{18} n/cm^2 (E > 1.0 MeV) caused a 6 to 9 ksi increase in the 0.2 percent offset yield strength and a 4 to 9 ksi increase in the ultimate tensile strength when compared to unirradiated data[3] (Figure 5-19).

The fractured tensile specimens for the intermediate shell forging 05 material are shown in Figures 5-20 and 5-21, while the fractured tensile specimens for the surveillance weld metal are shown in Figure 5-22. The engineering stress-strain curves for the tensile tests are shown in Figures 5-23 through 5-28.

5.4 1/2T Compact Tension and Bend Bar Specimen Tests

Per the surveillance capsule testing contract, the 1/2T Compact Tension Specimens and Bend Bars were not tested and are being stored at the Westinghouse Science and Technology Center Hot Cell facility.

TABLE 5-1

Charpy V-notch Data for the Watts Bar Unit 1 Intermediate Shell Forging 05
Irradiated to a Fluence of 5.05×10^{18} n/cm^2 (E > 1.0 MeV)
(Tangential Orientation)

Sample Number	Temperature		Impact Energy		Lateral Expansion		Shear
	F	C	ft-lbs	Joules	mils	mm	%
WL7	-105	-76	8	11	2	0.05	2
WL1	-25	-32	9	12	4	0.10	5
WL9	0	-18	25	34	15	0.38	10
WL12	10	-12	32	43	17	0.43	15
WL2	25	-4	28	38	19	0.48	15
WL4	50	10	47	64	29	0.74	20
WL3	70	21	38	52	25	0.64	20
WL11	75	24	13	18	6	0.15	5
WL5	100	38	60	81	44	1.12	25
WL13	125	52	66	89	49	1.24	40
WL10	150	66	85	115	57	1.45	75
WL6	200	93	101	137	72	1.83	100
WL14	250	121	111	150	76	1.93	100
WL8	300	149	102	138	73	1.85	100
WL15	350	177	112	152	72	1.83	100

TABLE 5-2

Charpy V-notch Data for the Watts Bar Unit 1 Intermediate Shell Forging 05
Irradiated to a Fluence of 5.05 x 10^{18} n/cm^2 (E > 1.0 MeV)
(Axial Orientation)

Sample Number	Temperature		Impact Energy		Lateral Expansion		Shear
	F	C	ft-lbs	Joules	mils	mm	%
WT5	-100	-73	4	5	2	0.05	2
WT12	-20	-29	8	11	2	0.05	5
WT2	10	-12	9	12	4	0.10	10
WT14	50	10	23	31	18	0.46	20
WT6	75	24	33	45	25	0.64	20
WT7	75	24	56	76	49	1.24	60
WT11	100	38	30	41	26	0.66	20
WT3	125	52	38	52	33	0.84	30
WT9	150	66	38	52	34	0.86	30
WT4	175	79	47	64	46	1.17	60
WT1	225	107	80	108	60	1.52	100
WT13	250	121	71	96	56	1.42	100
WT10	300	149	73	99	56	1.42	100
WT8	350	177	76	103	60	1.52	100
WT15	400	204	61	83	52	1.32	100

TABLE 5-3

Charpy V-notch Data for the Watts Bar Unit 1 Surveillance Weld Metal Irradiated to a Fluence of 5.05 x 10^{18} n/cm^2 (E > 1.0 MeV)

Sample	Temperature		Impact Energy		Lateral Expansion		Shear
Number	F	C	ft-lbs	Joules	mils	mm	%
WW6	-100	-73	7	9	3	0.08	5
WW4	-50	-46	17	23	11	0.28	10
WW1	-25	-32	25	34	19	0.48	25
WW7	0	-18	36	49	25	0.64	25
WW11	20	-7	65	88	50	1.27	70
WW10	35	2	75	102	49	1.24	80
WW12	50	10	76	103	51	1.30	80
WW13	75	24	127	172	87	2.21	95
WW8	75	24	91	123	58	1.47	90
WW9	100	38	95	129	67	1.70	90
WW2	125	52	93	126	71	1.80	80
WW5	150	66	99	134	73	1.85	85
WW15	250	121	145	197	84	2.13	100
WW3	300	149	138	187	84	2.13	100
WW14	350	177	147	199	67	1.70	100

TABLE 5-4

Charpy V-notch Data for the Watts Bar Unit 1 Heat Affected Zone Material Irradiated to a Fluence of 5.05 x 10^{18} n/cm^2 (E > 1.0 MeV)

Sample Number	Temperature		Impact Energy		Lateral Expansion		Shear
	F	C	ft-lbs	Joules	mils	mm	%
WH11	-175	-115	3	4	2	0.05	0
WH9	-100	-73	8	11	1	0.03	5
WH2	-25	-32	26	35	10	0.25	10
WH14	0	-18	37	50	21	0.53	15
WH5	25	-4	55	75	40	1.02	15
WH15	40	4	36	49	25	0.64	20
WH7	50	10	39	53	27	0.69	20
WH13	60	16	36	49	27	0.69	20
WH8	70	21	79	107	58	1.47	5
WH12	75	24	95	129	56	1.42	25
WH3	75	24	15	20	5	0.13	40
WH10	100	38	99	134	68	1.73	75
WH1	150	66	68	92	52	1.32	100
WH4	250	121	86	117	50	1.27	100
WH6	300	149	83	113	53	1.35	100

TABLE 5-5

Instrumented Charpy Impact Test Results for the Watts Bar Unit 1 Intermediate Shell Forging 05
Irradiated to a Fluence of 5.05 x 10^{18} n/cm² (E > 1.0 MeV) (Tangential Orientation)

Sample No.	Test Temp. (°F)	Charpy Energy E_D (ft-lb)	Normalized Energies (ft-lb/in²) Charpy E_D/A	Max. E_M/A	Prop. E_P/A	Yield Load P_{GY} (lb)	Time to Yield t_{GY} (msec)	Max. Load P_M (lb)	Time to Max. t_M (msec)	Fast Fract. Load P_F (lb)	Arrest Load P_A (lb)	Yield Stress s_Y (ksi)	Flow Stress (ksi)
WL7	-105	8	64	34	30	3672	0.16	3683	0.16	3672	0	122	122
WL1	-25	9	72	47	26	4208	0.18	4214	0.18	4208	0	140	140
WL9	0	25	201	168	33	4255	0.17	4663	0.38	4661	0	141	148
WL12	10	32	258	215	43	3862	0.16	4694	0.47	4694	0	128	142
WL2	25	28	225	186	39	4086	0.17	4641	0.42	4528	0	136	145
WL4	50	47	378	328	50	3799	0.16	4714	0.67	4705	0	126	141
WL3	70	38	306	236	69	3832	0.16	4698	0.51	4580	0	127	142
WL11	75	13	105	62	43	4271	0.16	4843	0.2	4836	0	142	151
WL5	100	60	483	304	179	3552	0.16	4609	0.65	4323	448	118	136
WL13	125	66	531	310	221	3670	0.17	4471	0.67	4153	833	122	135
WL10	150	85	684	314	370	3455	0.16	4473	0.68	3448	1507	115	132
WL6	200	101	813	294	519	3351	0.16	4331	0.66	N/A	N/A	111	128
WL14	250	111	894	314	580	3300	0.16	4462	0.69	N/A	N/A	110	129
WL8	300	102	821	288	534	3254	0.16	4224	0.66	N/A	N/A	108	124
WL15	350	112	902	303	599	3259	0.16	4342	0.68	N/A	N/A	108	126

N/A - Not Applicable - Fully ductile fracture.

TABLE 5-6

Instrumented Charpy Impact Test Results for the Watts Bar Unit 1 Intermediate Shell Forging 05 Irradiated to a Fluence of 5.05×10^{18} n/cm^2 (E > 1.0 MeV) (Axial Orientation)

Sample No.	Test Temp. (°F)	Charpy Energy E_D (ft-lb)	Normalized Energies (ft-lb/in^2) Charpy E_D/A	Max. E_M/A	Prop. E_P/A	Yield Load P_{GY} (lb)	Time to Yield t_{GY} (msec)	Max. Load P_M (lb)	Time to Max. t_M (msec)	Fast Fract. Load P_F (lb)	Arrest Load P_A (lb)	Yield Stress s_Y (ksi)	Flow Stress (ksi)
WT5	-100	4	32	15	17	1943	0.11	1999	0.12	1943	0	65	65
WT12	-20	8	64	40	25	3834	0.17	3838	0.17	3834	0	127	127
WT2	10	9	72	45	27	3907	0.17	3926	0.18	3754	0	130	130
WT14	50	23	185	63	122	3645	0.16	4083	0.22	4038	0	121	128
WT6	75	33	266	194	72	3597	0.16	4312	0.46	3983	814	119	131
WT7	75	56	451	196	255	3265	0.16	3987	0.49	3410	2569	108	120
WT11	100	30	242	152	89	3515	0.16	4054	0.39	4026	1043	117	126
WT3	125	38	306	179	127	3379	0.16	4105	0.45	4053	1297	112	124
WT9	150	38	306	166	140	3352	0.16	3960	0.43	3939	1598	111	121
WT4	175	47	378	172	207	3319	0.16	3923	0.45	3873	2436	110	120
WT1	225	80	644	219	425	3349	0.16	4280	0.52	N/A	N/A	111	127
WT13	250	71	572	207	365	3288	0.16	4185	0.51	N/A	N/A	109	124
WT10	300	73	588	193	395	3070	0.16	3895	0.51	N/A	N/A	102	116
WT8	350	76	612	206	406	3158	0.16	4054	0.52	N/A	N/A	105	120
WT15	400	61	491	161	330	2880	0.16	3531	0.46	N/A	N/A	96	106

N/A - Not Applicable - Fully ductile fracture.

TABLE 5-7													
Instrumented Charpy Impact Test Results for the Watts Bar Unit 1 Surveillance Weld Metal Irradiated to a Fluence of 5.05 x 10^{18} n/cm^2 (E > 1.0 MeV)													
			Normalized Energies (ft-lb/in^2)										
Sample No.	Test Temp. (°F)	Charpy Energy E_D (ft-lb)	Charpy E_D/A	Max. E_M/A	Prop. E_P/A	Yield Load P_{GY} (lb)	Time to Yield t_{GY} (msec)	Max. Load P_M (lb)	Time to Max. t_M (msec)	Fast Fract. Load P_F (lb)	Arrest Load P_A (lb)	Yield Stress s_Y (ksi)	Flow Stress (ksi)
WW6	-100	7	56	31	25	3385	0.15	3394	0.15	3385	243	112	113
WW4	-50	17	137	64	73	4144	0.17	4388	0.21	4206	0	138	142
WW1	-25	25	201	64	137	3886	0.16	4311	0.21	4169	1298	129	136
WW7	0	36	290	209	81	3668	0.16	4367	0.48	4335	1420	122	133
WW11	20	65	523	224	299	3617	0.16	4312	0.52	4290	2769	120	132
WW10	35	75	604	316	288	3599	0.16	4409	0.69	4116	1735	120	133
WW12	50	76	612	311	301	3594	0.16	4389	0.68	4137	2486	119	133
WW13	75	127	1023	283	740	2964	0.15	4068	0.68	1969	1616	98	117
WW8	75	91	733	310	423	3676	0.17	4334	0.69	2882	1330	122	133
WW9	100	95	765	305	460	3308	0.16	4194	0.7	3271	2142	110	125
WW2	125	93	749	298	451	3265	0.16	4188	0.7	3634	2510	108	124
WW5	150	99	797	294	503	3261	0.16	4141	0.69	1646	848	108	123
WW15	250	145	1168	361	806	3151	0.16	4114	0.83	N/A	N/A	105	121
WW3	300	138	1111	346	765	2928	0.16	3983	0.83	N/A	N/A	97	115
WW14	350	147	1184	353	831	3128	0.16	4007	0.83	N/A	N/A	104	118

N/A - Not Applicable - Fully ductile fracture.

TABLE 5-8

Instrumented Charpy Impact Test Results for the Watts Bar Unit 1 Heat-Affected-Zone (HAZ) Metal Irradiated to a Fluence of 5.05×10^{18} n/cm^2 (E > 1.0 MeV)

Sample No.	Test Temp. (°F)	Charpy Energy E_D (ft-lb)	Normalized Energies (ft-lb/in^2) Charpy E_D/A	Normalized Energies (ft-lb/in^2) Max. E_M/A	Normalized Energies (ft-lb/in^2) Prop. E_P/A	Yield Load P_{GY} (lb)	Time to Yield t_{GY} (msec)	Max. Load P_M (lb)	Time to Max. t_M (msec)	Fast Fract. Load P_F (lb)	Arrest Load P_A (lb)	Yield Stress S_Y (ksi)	Flow Stress (ksi)
WH11	-175	3	24	9	15	1219	0.11	1223	0.11	1219	0	40	41
WH9	-100	8	64	40	24	4089	0.16	4106	0.16	4089	192	136	136
WH2	-25	26	209	74	135	4180	0.16	4674	0.22	4501	428	139	147
WH14	0	37	298	211	87	3970	0.16	4615	0.46	4543	1508	132	143
WH5	25	55	443	213	229	3969	0.16	4510	0.47	4096	2722	132	141
WH15	40	36	290	67	223	4069	0.17	4340	0.22	4121	2663	135	140
WH7	50	39	314	159	155	3982	0.17	4295	0.39	4135	2128	132	137
WH13	60	36	290	63	227	3809	0.16	4224	0.21	4105	2206	127	133
WH8	70	79	636	336	300	3856	0.16	4713	0.68	4537	2979	128	142
WH12	75	95	765	302	463	3456	0.16	4356	0.67	N/A	N/A	115	130
WH3	75	15	121	67	54	4216	0.17	4601	0.22	4597	0	140	146
WH10	100	99	797	240	557	3565	0.16	4427	0.55	2063	1525	118	133
WH1	150	68	548	199	349	3564	0.16	4216	0.47	N/A	N/A	118	129
WH4	250	86	692	304	389	3507	0.16	4412	0.67	N/A	N/A	116	132
WH6	300	83	668	277	391	3116	0.16	4067	0.66	N/A	N/A	103	119

N/A - Not Applicable - Fully ductile fracture.

TABLE 5-9												
Effect of Irradiation to 5.05 x 10^{18} n/cm^2 (E > 1.0 MeV) on the Notch Toughness Properties of the Watts Bar Unit 1 Reactor Vessel Surveillance Materials												
Material	Average 30 (ft-lb) [(a)] Transition Temperature (°F)			Average 35 mil Lateral [(b)] Expansion Temperature (°F)			Average 50 ft-lb [(a)] Transition Temperature (°F)			Average Energy Absorption [(a)] at Full Shear (ft-lb)		
	Unirradiated	Irradiated	ΔT	Unirradiated	Irradiated	ΔT	Unirradiated	Irradiated	ΔT	Unirradiated	Irradiated	ΔE
Inter. Shell Forging05 (Tangential)	-57	41	98	-9	91	100	-16	86	102	132	107	-25
Inter. Shell Forging 05 (Axial)	45	74	29	84	114	30	114	149	35	62	72	10
Weld Metal	-32	-38	-6	-9	8	17	-6	6	12	131	143	12
HAZ Metal	-57	-5	52	0	52	52	-9	44	53	89	79	-10

(a) "Average" is defined as the value read from the curve fit through the data points of the Charpy tests (see Figures 5-1, 5-4, 5-7 and 5-10).

(b) "Average" is defined as the value read from the curve fit through the data points of the Charpy tests (see Figures 5-2, 5-5, 5-8 and 5-11).

TABLE 5-10

Comparison of the Watts Bar Unit 1 Surveillance Material 30 ft-lb Transition Temperature Shifts and Upper Shelf Energy Decreases with Regulatory Guide 1.99, Revision 2, Predictions

Material	Capsule	Fluence (n/cm^2, E > 1.0 MeV)	30 ft-lb Transition Temperature Shift		Upper Shelf Energy Decrease	
			Predicted (°F) [a]	Measured (°F) [b]	Predicted (%) [a]	Measured (%) [c]
Intermediate Shell Forging 05 (Tangential)	U	5.05×10^{18}	100	98	22	19
Intermediate Shell Forging 05 (Axial)	U	5.05×10^{18}	100	29	22	0
Weld Metal	U	5.05×10^{18}	33	0	16	0
HAZ Metal	U	5.05×10^{18}	--	51	---	11

(a) Based on Regulatory Guide 1.99, Revision 2, methodology using the mean weight percent values of copper and nickel of the surveillance material.

(b) Calculated using measured Charpy data plotted using CVGRAPH, Version 4.1(See Appendix C) with exception to the weld, which recorded a value of -6. This physically should not occur, thus a value of zero was entered.

(c) Values are based on the definition of upper shelf energy given in ASTM E185-82.

TABLE 5-11										
Tensile Properties of the Watts Bar Unit 1 Reactor Vessel Surveillance Materials Irradiated to 5.05 x 10^{18} n/cm² (E > 1.0 MeV)										
Material	Sample Number	Test Temp. (°F)	0.2% Yield Strength (ksi)	Ultimate Strength (ksi)	Fracture Load (kip)	Fracture Stress (ksi)	Fracture Strength (ksi)	Uniform Elongation (%)	Total Elongation (%)	Reduction in Area (%)
Intermediate Shell Forging 05 (Tangential)	WL1	100	81.5	101.8	3.38	219.2	68.8	11.4	24.1	69
	WL2	200	76.9	96.4	3.20	167.3	65.1	9.9	21.3	61
	WL3	550	73.3	99	3.75	212.2	76.4	10.8	22.4	64
Intermediate Shell Forging 05 (Axial)	WT1	125	79.5	99.8	3.70	166.9	75.4	10.6	18.8	55
	WT2	200	76.4	95.5	3.60	156.8	73.3	10.2	19.4	53
	WT3	550	72.3	95.1	3.88	165.1	79.0	9.6	17.0	52
Weld Metal	WW1	50	81.5	95.7	2.80	21.6	57.0	13.7	29.4	74
	WW2	200	72.8	84.5	2.55	201.3	51.9	12.0	26.6	74
	WW3	550	68.8	83.6	2.60	198.9	53.0	10.5	22.7	73

SHELL FORGING 05 TANGENTIAL

CVGRAPH 4.1 Hyperbolic Tangent Curve Printed at 08:29:26 on 03-10-1998

Results

Curve	Fluence	LSE	d-LSE	USE	d-USE	T @ 30	d-T @ 30	T @ 50	d-T @ 50
1	0	2.19	0	131.5	0	-57.21	0	-15.58	0
2	0	2.19	0	106.5	-25	40.72	97.93	86.14	101.72

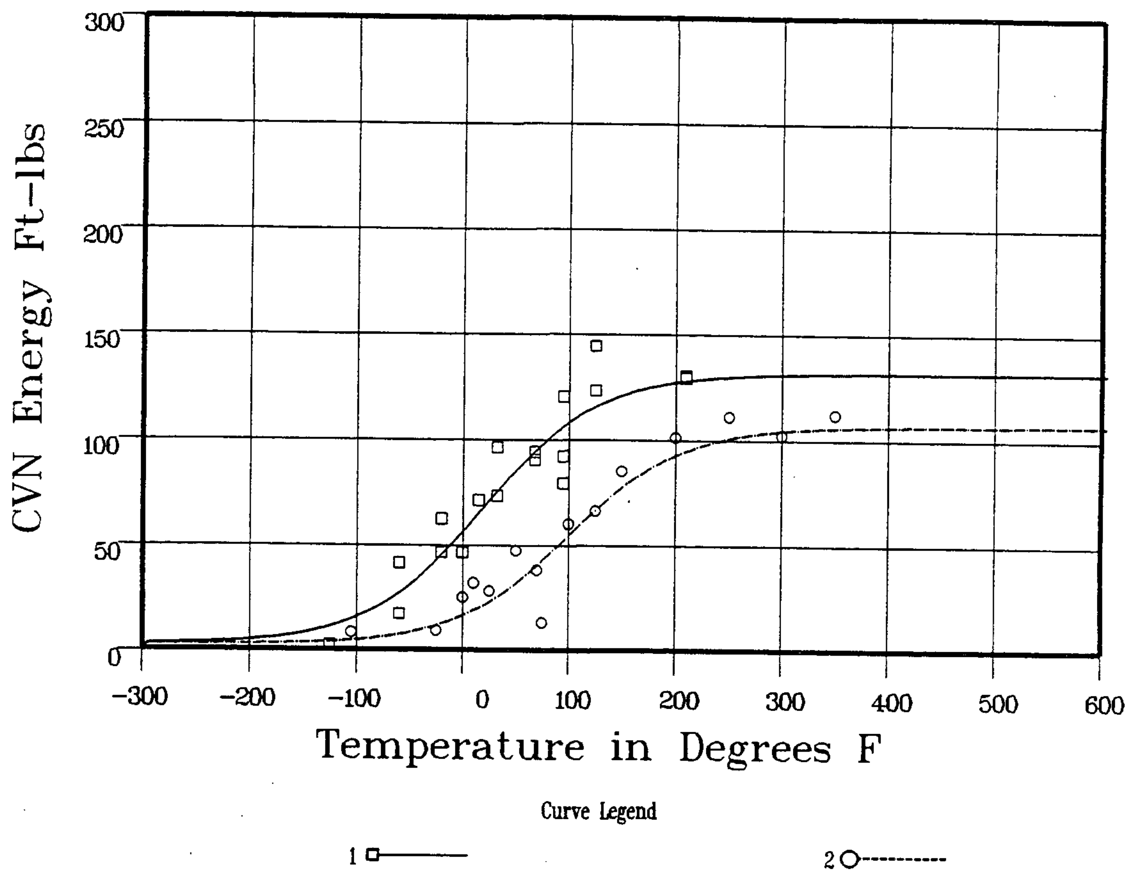

Data Set(s) Plotted

Curve	Plant	Capsule	Material	Ori.	Heat#
1	WB1	UNIRR	FORGING SA508CL2		LT527536 (RING 05)
2	WB1	U	FORGING SA508CL2		LT527536 (RING 05)

Figure 5-1 Charpy V-Notch Impact Energy vs. Temperature for Watts Bar Unit 1 Reactor Vessel Intermediate Shell Forging 05 (Tangential Orientation)

SHELL FORGING 05 TANGENTIAL

CVGRAPH 4.1 Hyperbolic Tangent Curve Printed at 08:39:29 on 03-10-1998

Results

Curve	Fluence	USE	d-USE	T @ LE35	d-T @ LE35
1	0	80.28	0	-8.91	0
2	0	76.47	-3.8	91.47	100.39

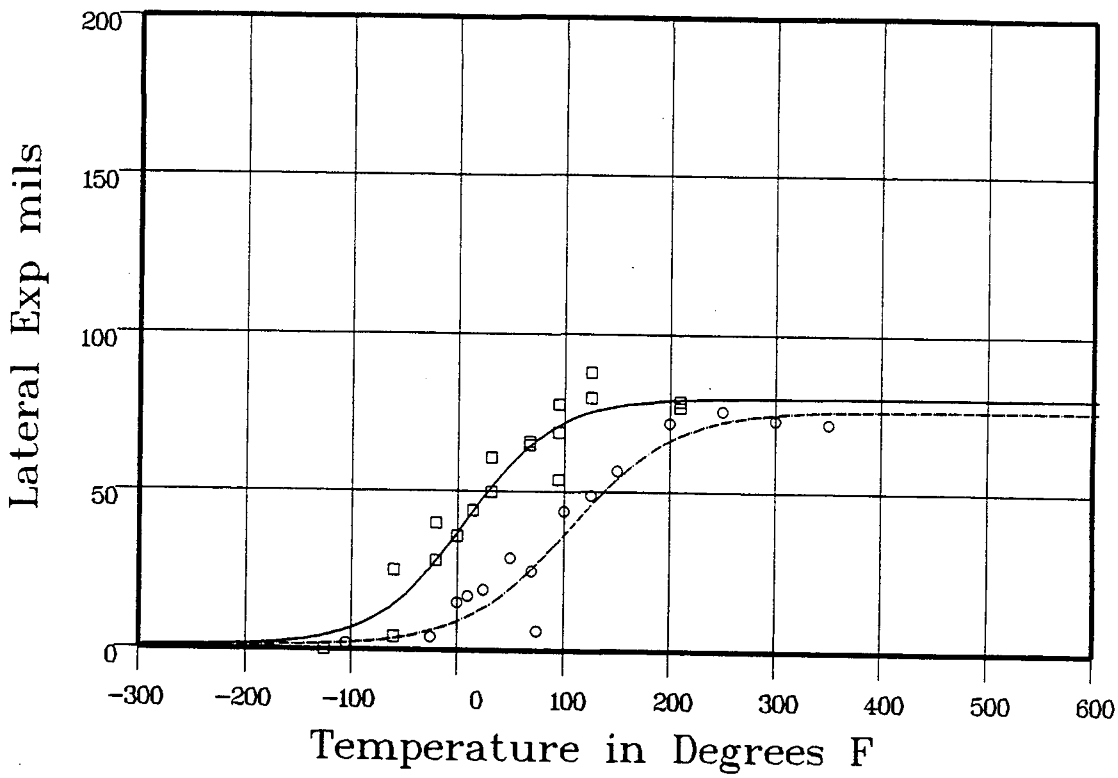

Curve Legend

1 □———— 2 O----------

Data Set(s) Plotted

Curve	Plant	Capsule	Material	Ori.	Heat#
1	WB1	UNIRR	FORGING SA508CL2	LT	527536 (RING 05)
2	WB1	U	FORGING SA508CL2	LT	527536 (RING 05)

Figure 5-2 Charpy V-Notch Lateral Expansion vs. Temperature for Watts Bar Unit 1 Reactor Vessel Intermediate Shell Forging 05 (Tangential Orientation)

SHELL FORGING 05 TANGENTIAL

CVGRAPH 4.1 Hyperbolic Tangent Curve Printed at 08:43:26 on 03-10-1998

Results

Curve	Fluence	T @ 50% Shear	d-T @ 50% Shear
1	0	34.88	0
2	0	126.56	91.68

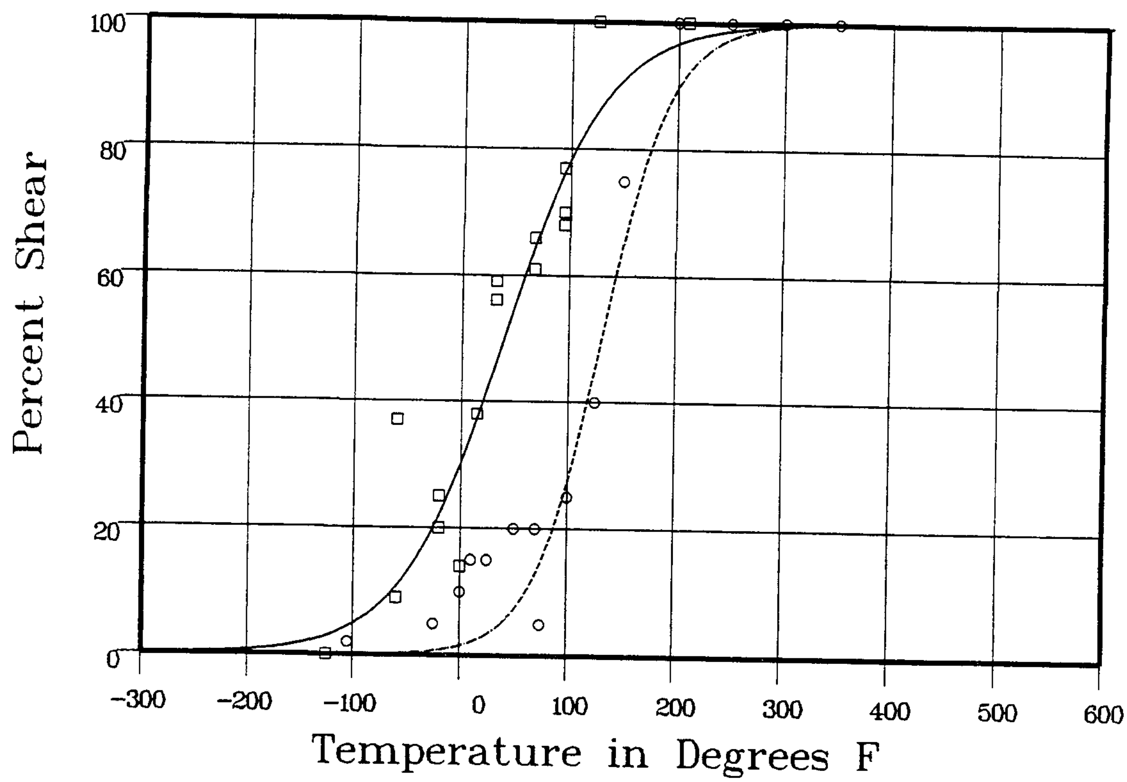

Curve Legend

1 □——— 2 ○----------

Data Set(s) Plotted

Curve	Plant	Capsule	Material	Ori.	Heat#
1	WB1	UNIRR	FORGING SA508CL2	LT	527536 (RING 05)
2	WB1	U	FORGING SA508CL2	LT	527536 (RING 05)

Figure 5-3 Charpy V-Notch Percent Shear vs. Temperature for Watts Bar Unit 1 Reactor Vessel Intermediate Shell Forging 05 (Tangential Orientation)

SHELL FORGING 05 AXIAL

CVGRAPH 4.1 Hyperbolic Tangent Curve Printed at 09:28:28 on 03-10-1998

Results

Curve	Fluence	LSE	d-LSE	USE	d-USE	T @ 30	d-T @ 30	T @ 50	d-T @ 50
1	0	2.2	0	61.59	0	44.85	0	114.37	0
2	0	2.19	0	72.19	10.59	73.82	28.97	148.64	34.26

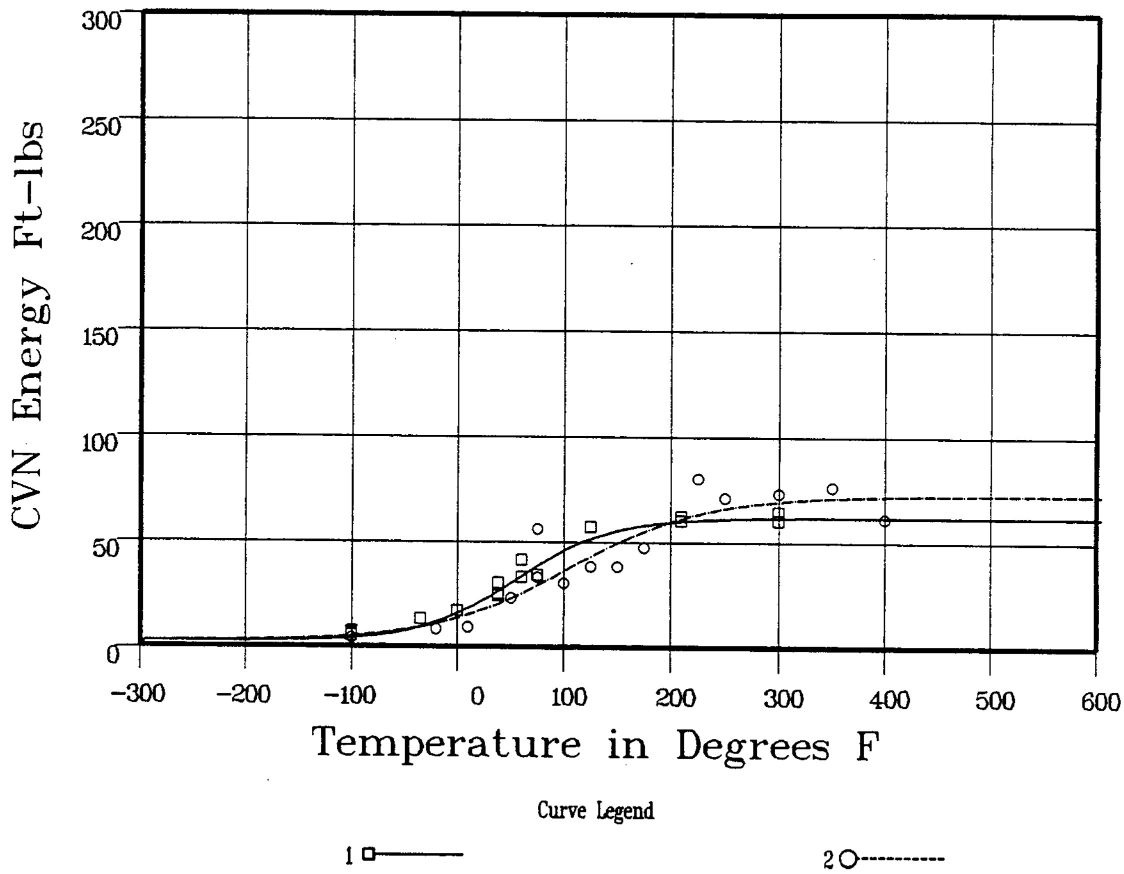

Data Set(s) Plotted

Curve	Plant	Capsule	Material	Ori.	Heat#
1	WB1	UNIRR	FORGING SA508CL2		TI527536 (RING 05)
2	WB1	U	FORGING SA508CL2		TI527536 (RING 05)

Figure 5-4 Charpy V-Notch Impact Energy vs. Temperature for Watts Bar Unit 1 Reactor Vessel Intermediate Shell Forging 05 (Axial Orientation)

SHELL FORGING 05 AXIAL

CVGRAPH 4.1 Hyperbolic Tangent Curve Printed at 10:01:16 on 03-10-1998

Results

Curve	Fluence	USE	d-USE	T @ LE35	d-T @ LE35
1	0	58.17	0	84.08	0
2	0	57.39	-.78	113.58	29.5

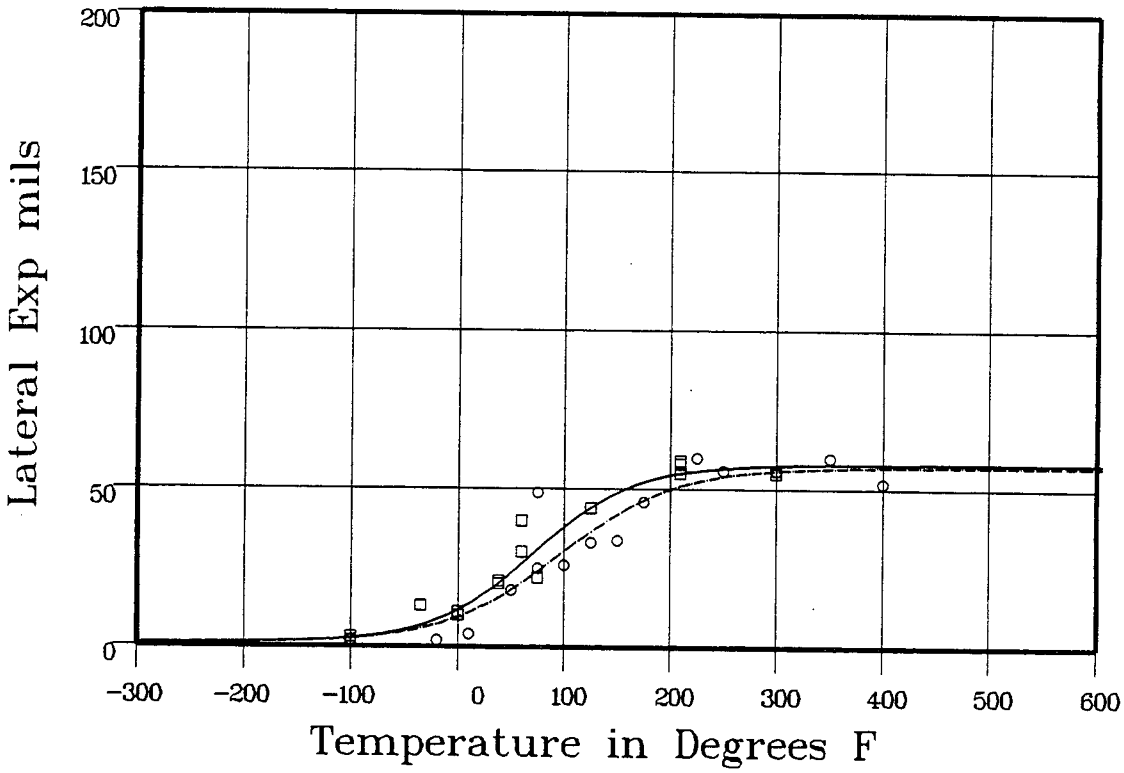

Curve Legend

1 □———— 2 ○----------

Data Set(s) Plotted

Curve	Plant	Capsule	Material	Ori.	Heat#
1	WB1	UNIRR	FORGING SA508CL2		TI527536 (RING 05)
2	WB1	U	FORGING SA508CL2		TI527536 (RING 05)

Figure 5-5 Charpy V-Notch Lateral Expansion vs. Temperature for Watts Bar Unit 1 Reactor Vessel Intermediate Shell Forging 05 (Axial Orientation)

SHELL FORGING 05 AXIAL

CVGRAPH 4.1 Hyperbolic Tangent Curve Printed at 10:06:36 on 03-10-1998

Results

Curve	Fluence	T @ 50% Shear	d-T @ 50% Shear
1	0	54.84	0
2	0	144.42	89.57

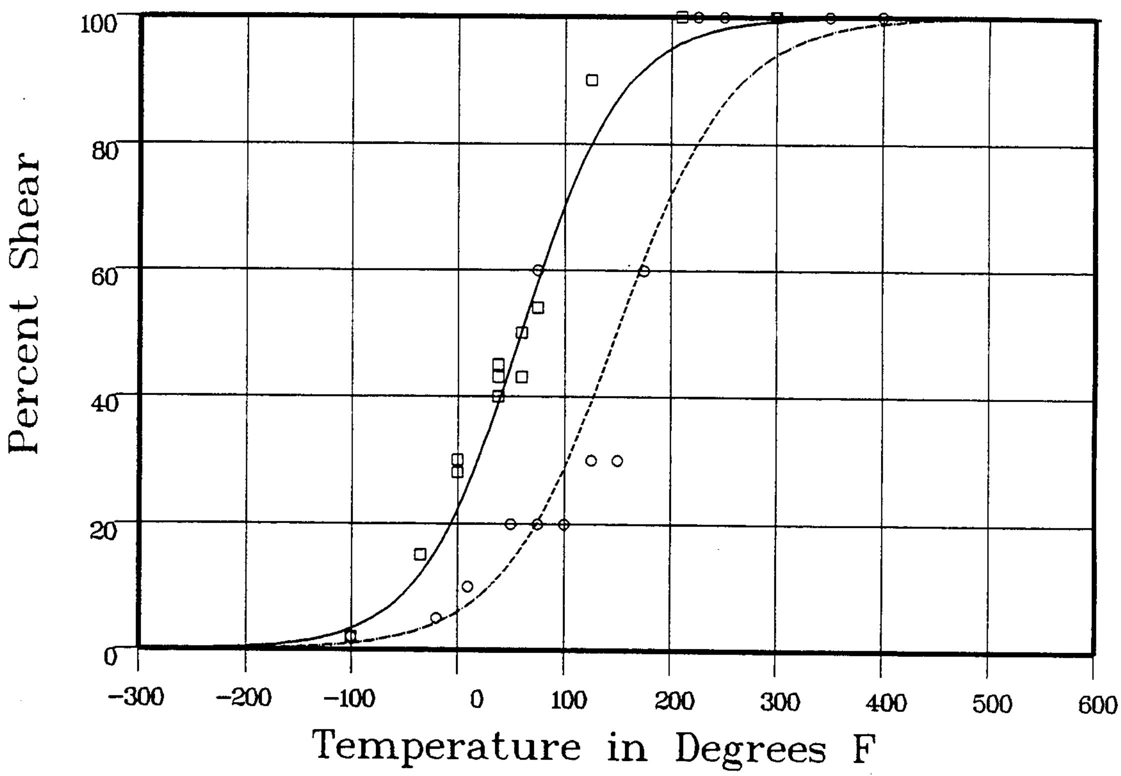

Curve Legend

1 □——— 2 ○---------

Data Set(s) Plotted

Curve	Plant	Capsule	Material	Ori.	Heat#
1	WB1	UNIRR	FORGING SA508CL2		TI527536 (RING 05)
2	WB1	U	FORGING SA508CL2		TI527536 (RING 05)

Figure 5-6 Charpy V-Notch Percent Shear vs. Temperature for Watts Bar Unit 1 Reactor Vessel Intermediate Shell Forging 05 (Axial Orientation)

WELD

CVGRAPH 4.1 Hyperbolic Tangent Curve Printed at 13:02:20 on 03-10-1998

Results

Curve	Fluence	LSE	d-LSE	USE	d-USE	T @ 30	d-T @ 30	T @ 50	d-T @ 50
1	0	2.19	0	130.8	0	-31.63	0	-6.22	0
2	0	2.19	0	143.3	12.5	-38.17	-6.53	6.14	12.37

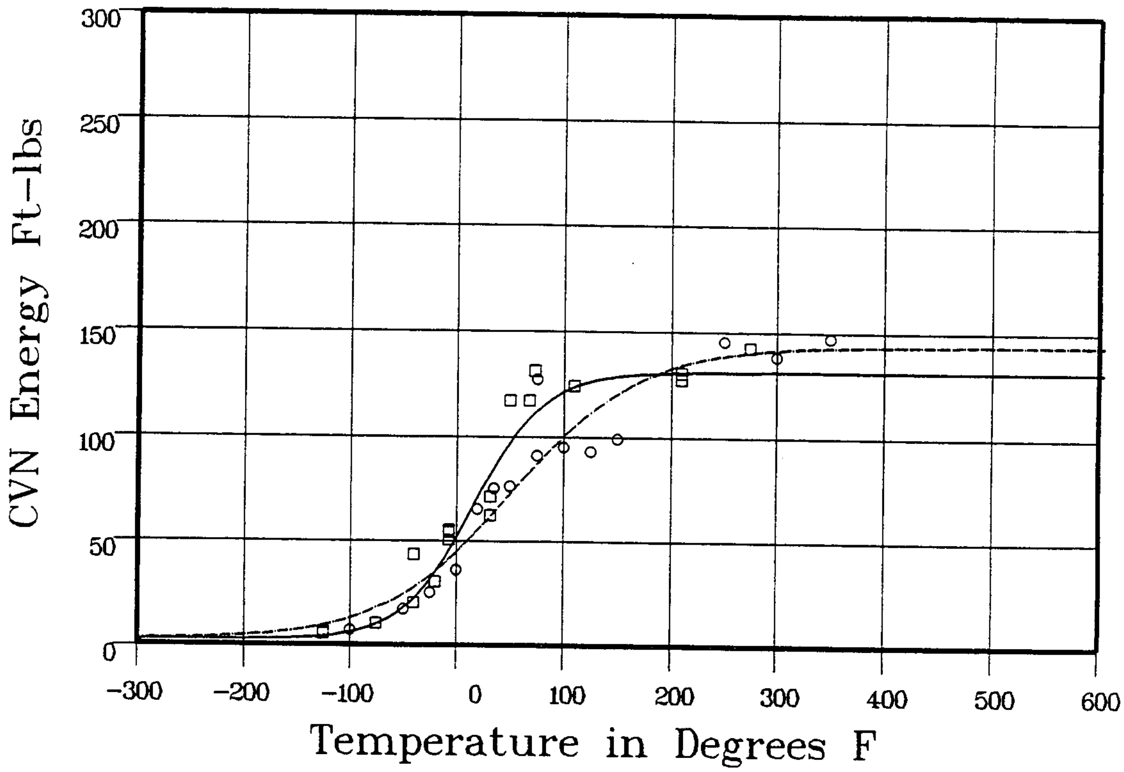

Curve Legend

1 □——— 2 ○----------

Data Set(s) Plotted

Curve	Plant	Capsule	Material	Ori.	Heat#
1	WB1	UNIRR	WELD		WIRE HEAT:895075
2	WB1	U	WELD		WIRE HEAT:895075

Figure 5-7 Charpy V-Notch Impact Energy vs. Temperature for Watts Bar Unit 1 Reactor Vessel Weld Metal

WELD

CVGRAPH 4.1 Hyperbolic Tangent Curve Printed at 13:09:03 on 03-10-1998

Results

Curve	Fluence	USE	d-USE	T @ LE35	d-T @ LE35
1	0	87.85	0	-9.44	0
2	0	76.94	-10.9	7.8	17.24

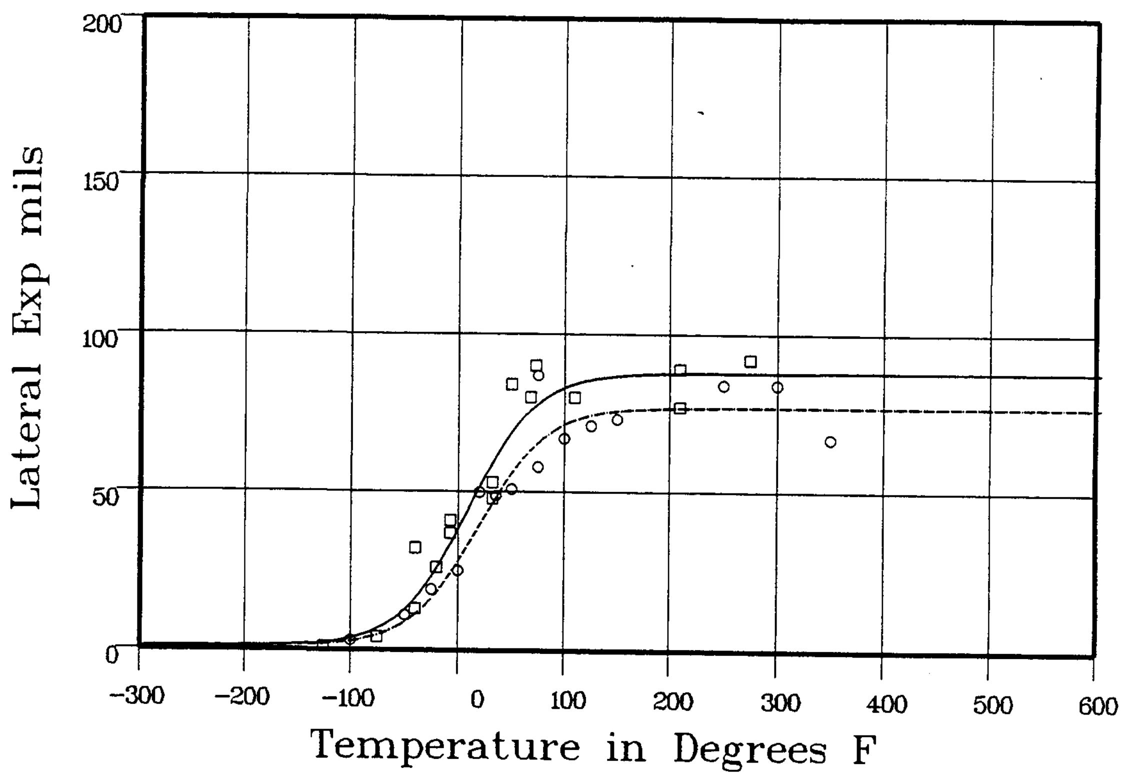

Curve Legend

1 □———— 2 ○----------

Data Set(s) Plotted

Curve	Plant	Capsule	Material	Ori.	Heat#
1	WB1	UNIRR	WELD	WIRE	HEAT:895075
2	WB1	U	WELD	WIRE	HEAT:895075

Figure 5-8 Charpy V-Notch Lateral Expansion vs. Temperature for Watts Bar Unit 1 Reactor Vessel Weld Metal

WELD

CVGRAPH 4.1 Hyperbolic Tangent Curve Printed at 13:12:39 on 03-10-1998

Results

Curve	Fluence	T @ 50% Shear	d-T @ 50% Shear
1	0	-1.4	0
2	0	9.66	11.07

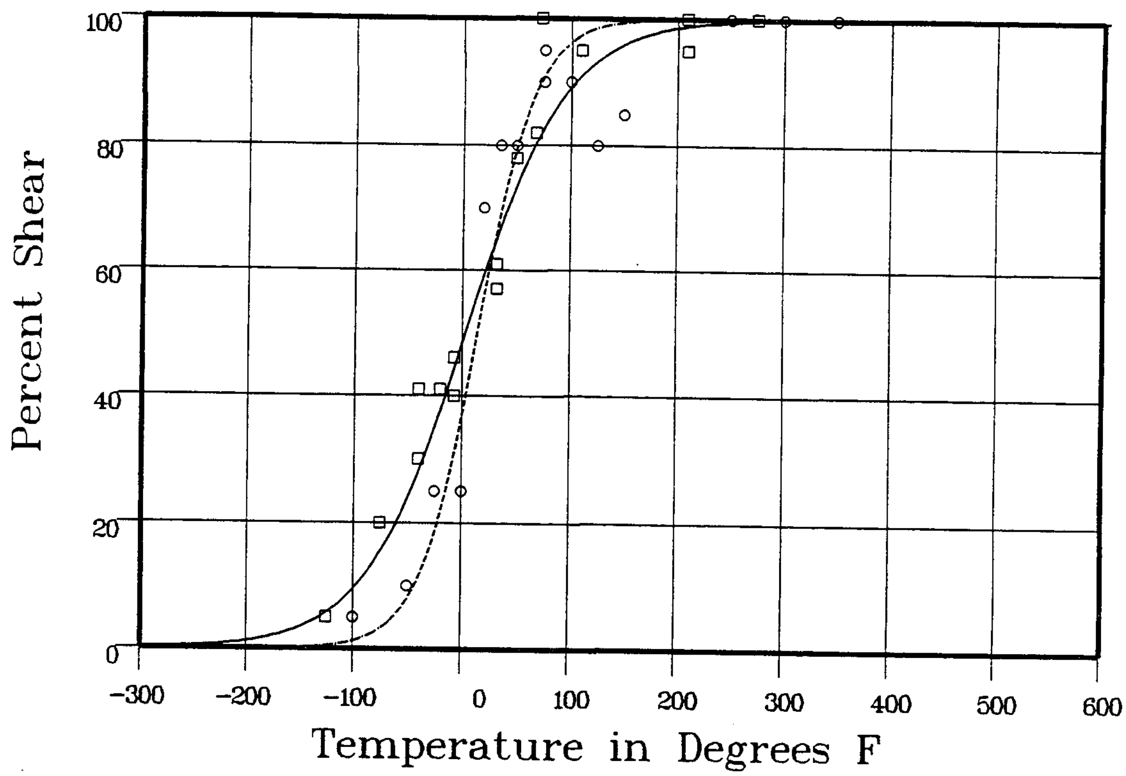

Curve Legend

1 □——— 2 ○----------

Data Set(s) Plotted

Curve	Plant	Capsule	Material	Ori.	Heat#
1	WB1	UNIRR	WELD	WIRE	HEAT:895075
2	WB1	U	WELD	WIRE	HEAT:895075

Figure 5-9 Charpy V-Notch Percent Shear vs. Temperature for Watts Bar Unit 1 Reactor Vessel Weld Metal

HEAT-AFFECTED-ZONE

CVGRAPH 4.1 Hyperbolic Tangent Curve Printed at 13:17:42 on 03-10-1998

Results

Curve	Fluence	LSE	d-LSE	USE	d-USE	T @ 30	d-T @ 30	T @ 50	d-T @ 50
1	0	2.19	0	89	0	-56.64	0	-9.09	0
2	0	2.19	0	79	-10	-5.48	51.16	43.64	52.73

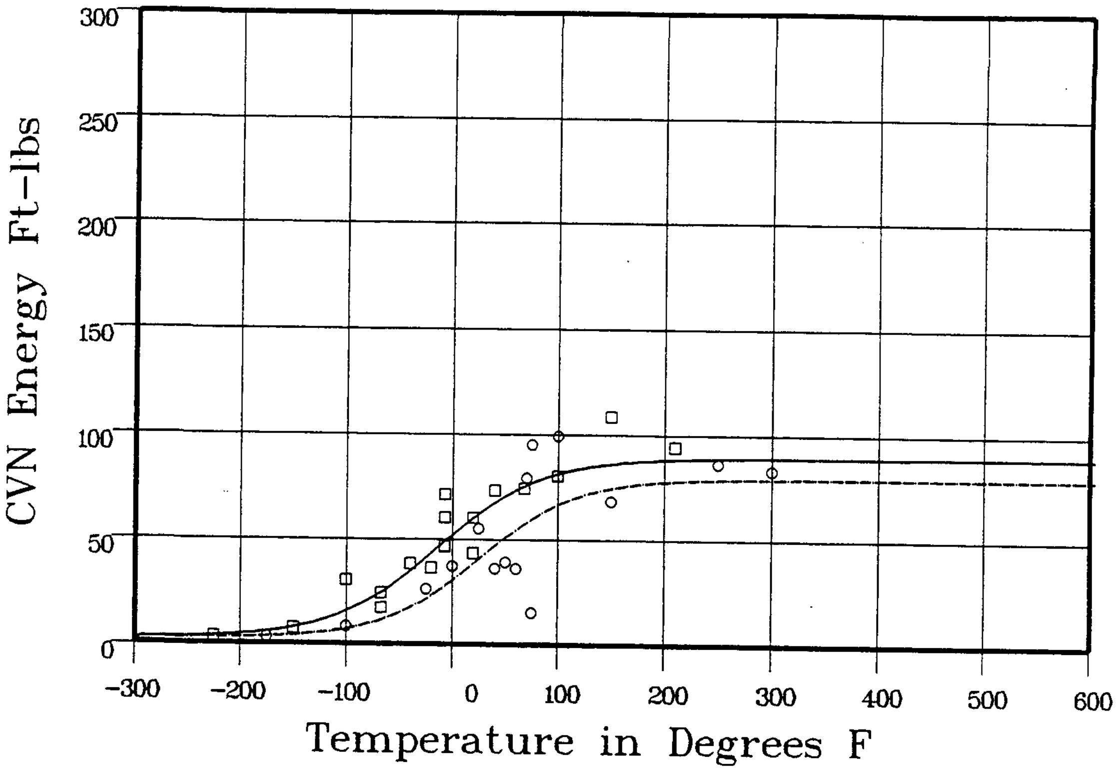

Curve Legend

1 □——— 2 ○---------

Data Set(s) Plotted

Curve	Plant	Capsule	Material	Ori.	Heat#
1	WB1	UNIRR	HEAT AFFD ZONE	WIRE	HEAT:895075
2	WB1	U	HEAT AFFD ZONE	WIRE	HEAT:895075

Figure 5-10 Charpy V-Notch Impact Energy vs. Temperature for Watts Bar Unit 1 Reactor Vessel Heat-Affected-Zone Material

HEAT–AFFECTED–ZONE

CVGRAPH 4.1 Hyperbolic Tangent Curve Printed at 08:16:52 on 03-11-1998

Results

Curve	Fluence	USE	d-USE	T @ LE35	d-T @ LE35
1	0	66.13	0	-29	0
2	0	54.47	-11.65	51.68	51.97

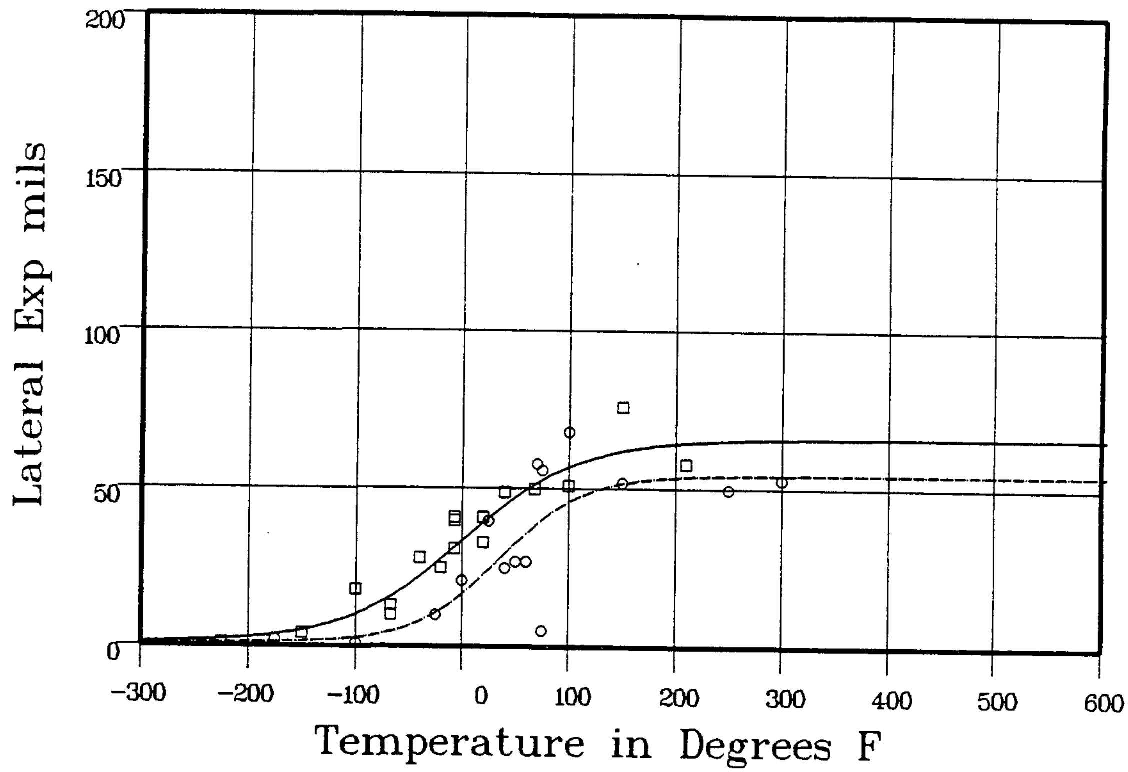

Curve Legend

1 □———— 2 ○----------

Data Set(s) Plotted

Curve	Plant	Capsule	Material	Ori.	Heat#
1	WB1	UNIRR	HEAT AFFD ZONE	WIRE	HEAT:895075
2	WB1	U	HEAT AFFD ZONE	WIRE	HEAT:895075

Figure 5-11 Charpy V-Notch Lateral Expansion vs. Temperature for Watts Bar Unit 1 Reactor Vessel Heat-Affected-Zone Material

HEAT–AFFECTED–ZONE

CVGRAPH 4.1 Hyperbolic Tangent Curve Printed at 08:23:55 on 03-11-1998

Results

Curve	Fluence	T @ 50% Shear	d-T @ 50% Shear
1	0	-22.37	0
2	0	88.18	110.55

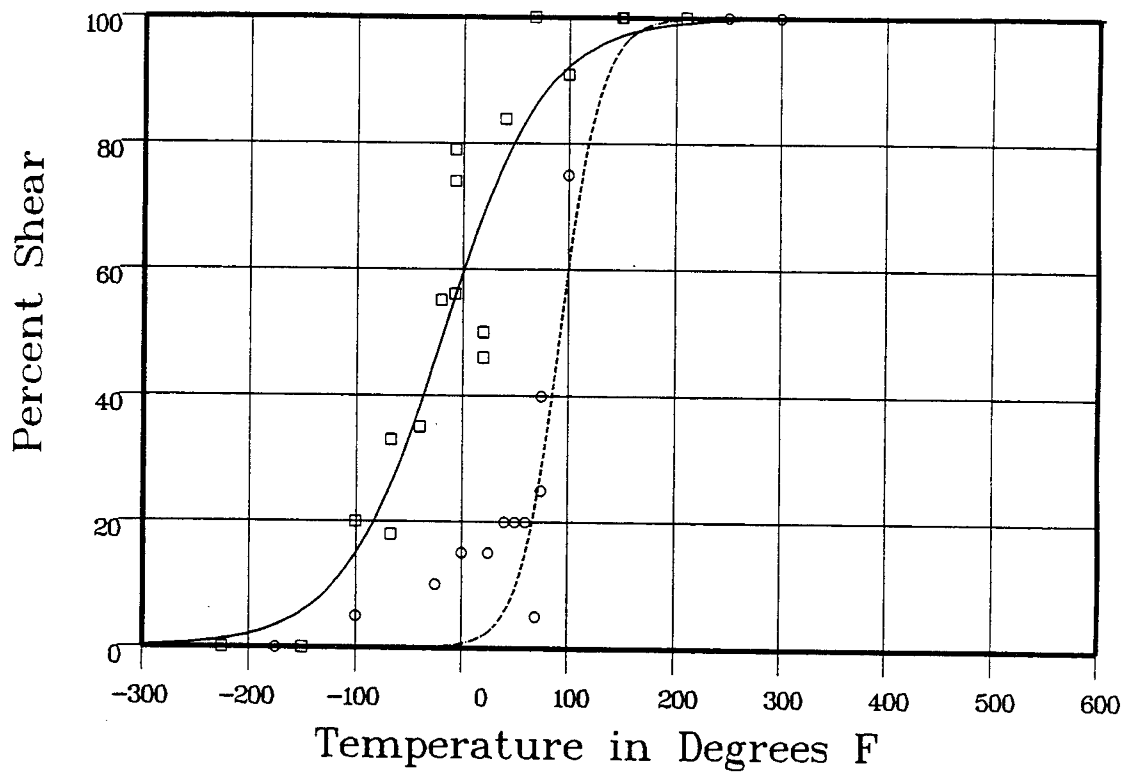

Curve Legend

1 □——— 2 ○----------

Data Set(s) Plotted

Curve	Plant	Capsule	Material	Ori.	Heat#
1	WB1	UNIRR	HEAT AFFD ZONE		WIRE HEAT:895075
2	WB1	U	HEAT AFFD ZONE		WIRE HEAT:895075

Figure 5-12 Charpy V-Notch Percent Shear vs. Temperature for Watts Bar Unit 1 Reactor Vessel Heat-Affected-Zone Material

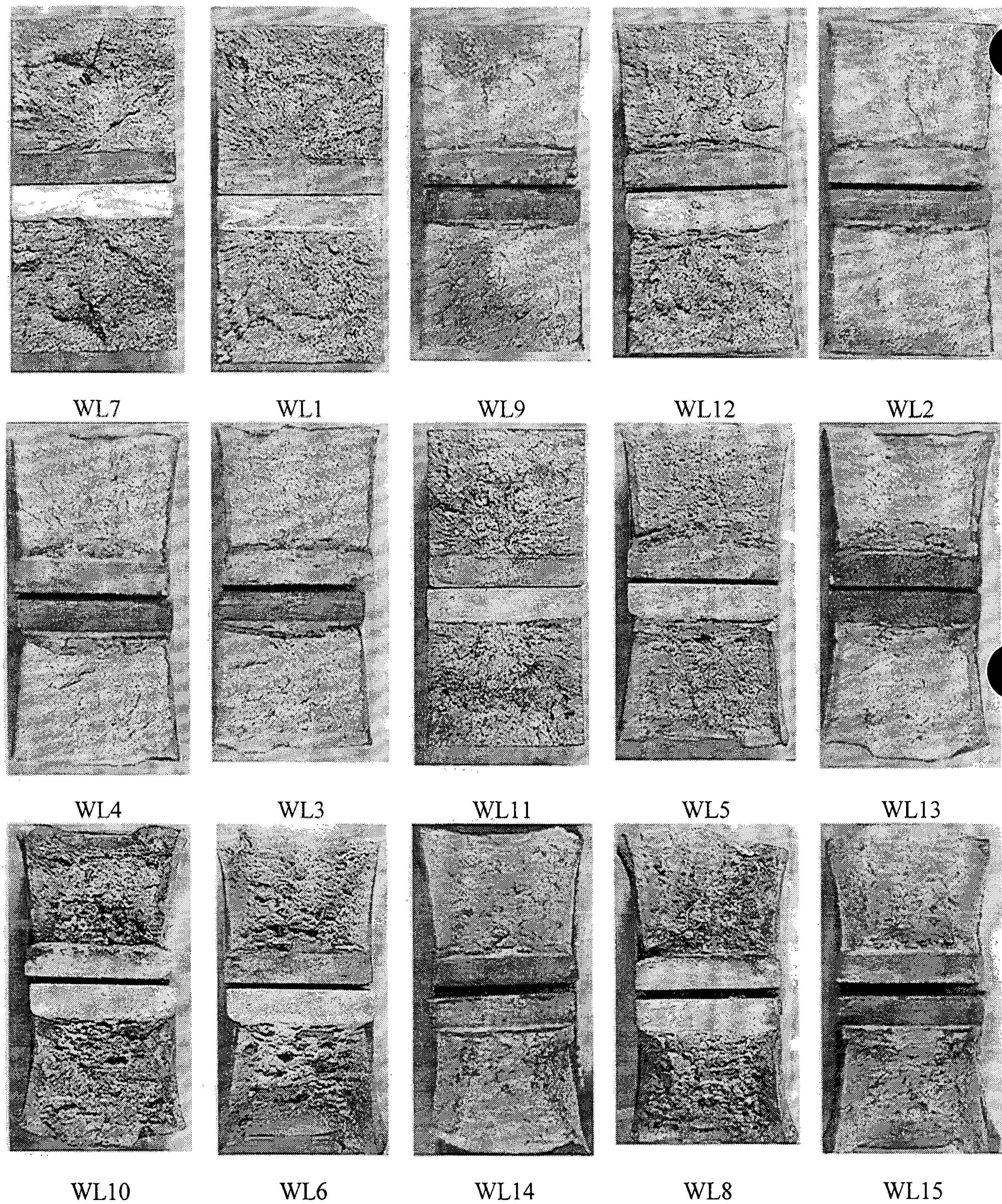

Figure 5-13 Charpy Impact Specimen Fracture Surfaces for Watts Bar Unit 1 Reactor Vessel Intermediate Shell Forging 05 (Tangential Orientation)

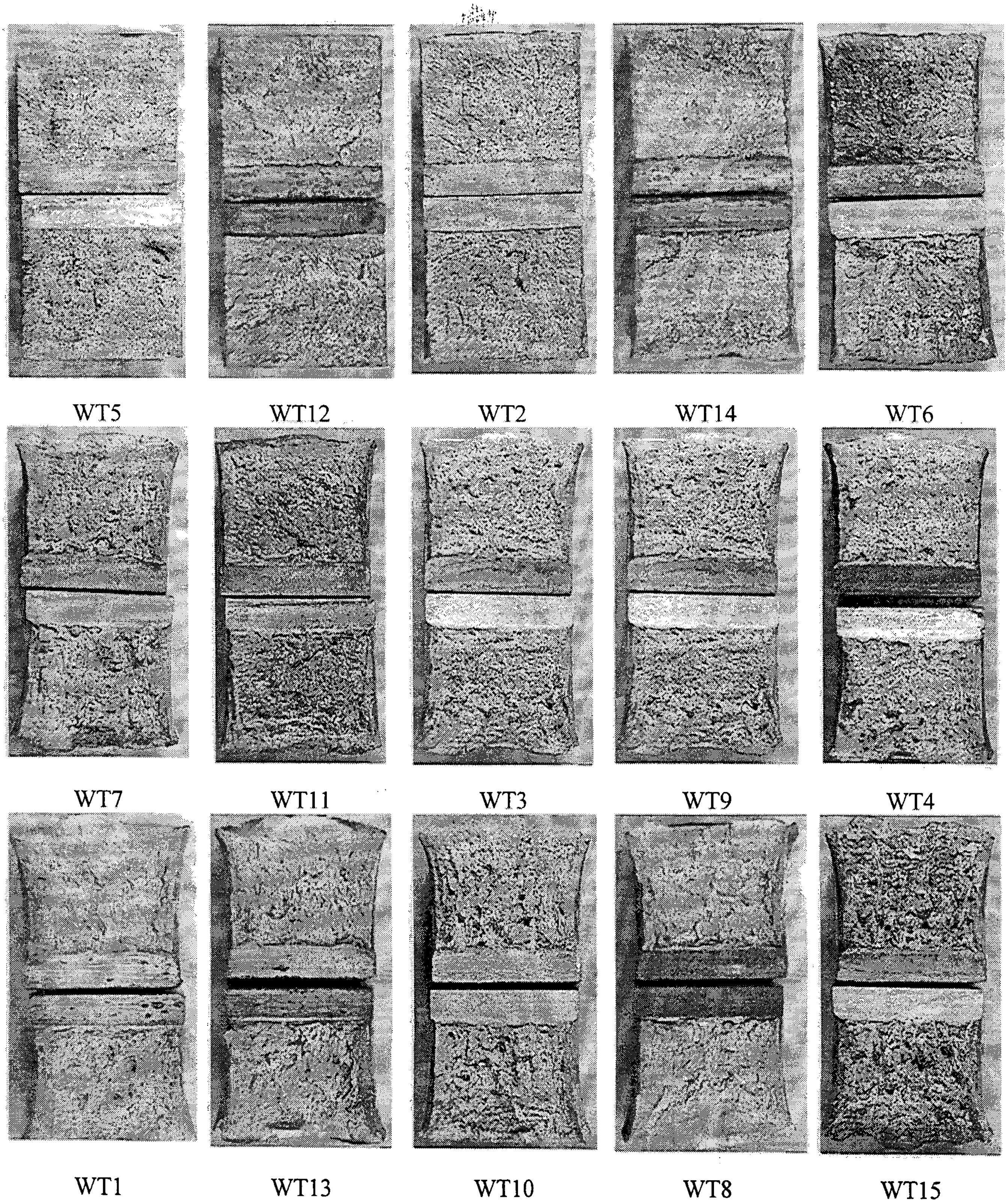

Figure 5-14 Charpy Impact Specimen Fracture Surfaces for Watts Bar Unit 1 Reactor Vessel Intermediate Shell Forging 05 (Axial Orientation)

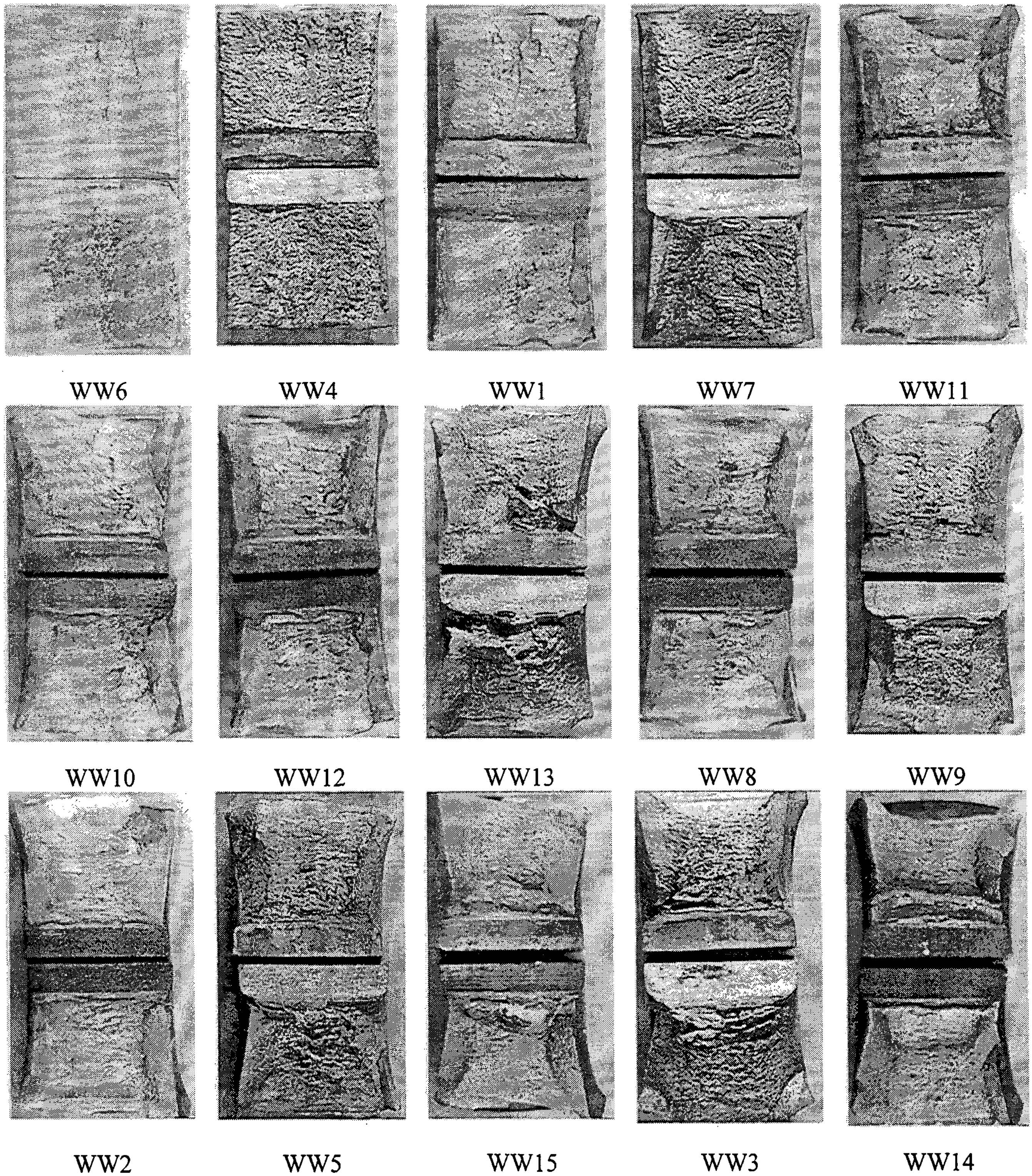

Figure 5-15 Charpy Impact Specimen Fracture Surfaces for Watts Bar Unit 1 Reactor Vessel Weld Metal

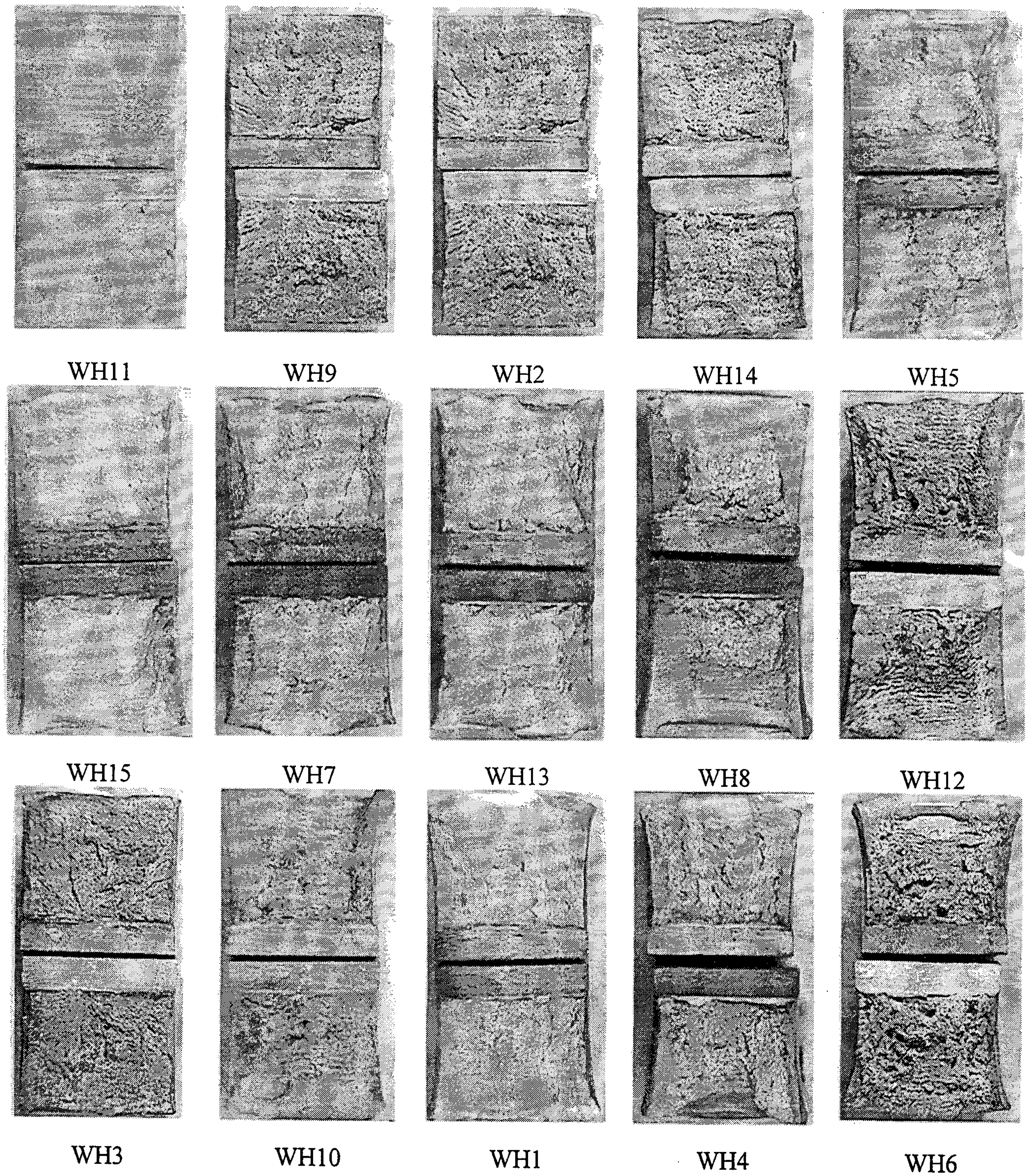

Figure 5-16 Charpy Impact Specimen Fracture Surfaces for Watts Bar Unit 1 Reactor Vessel Heat-Affected-Zone Metal

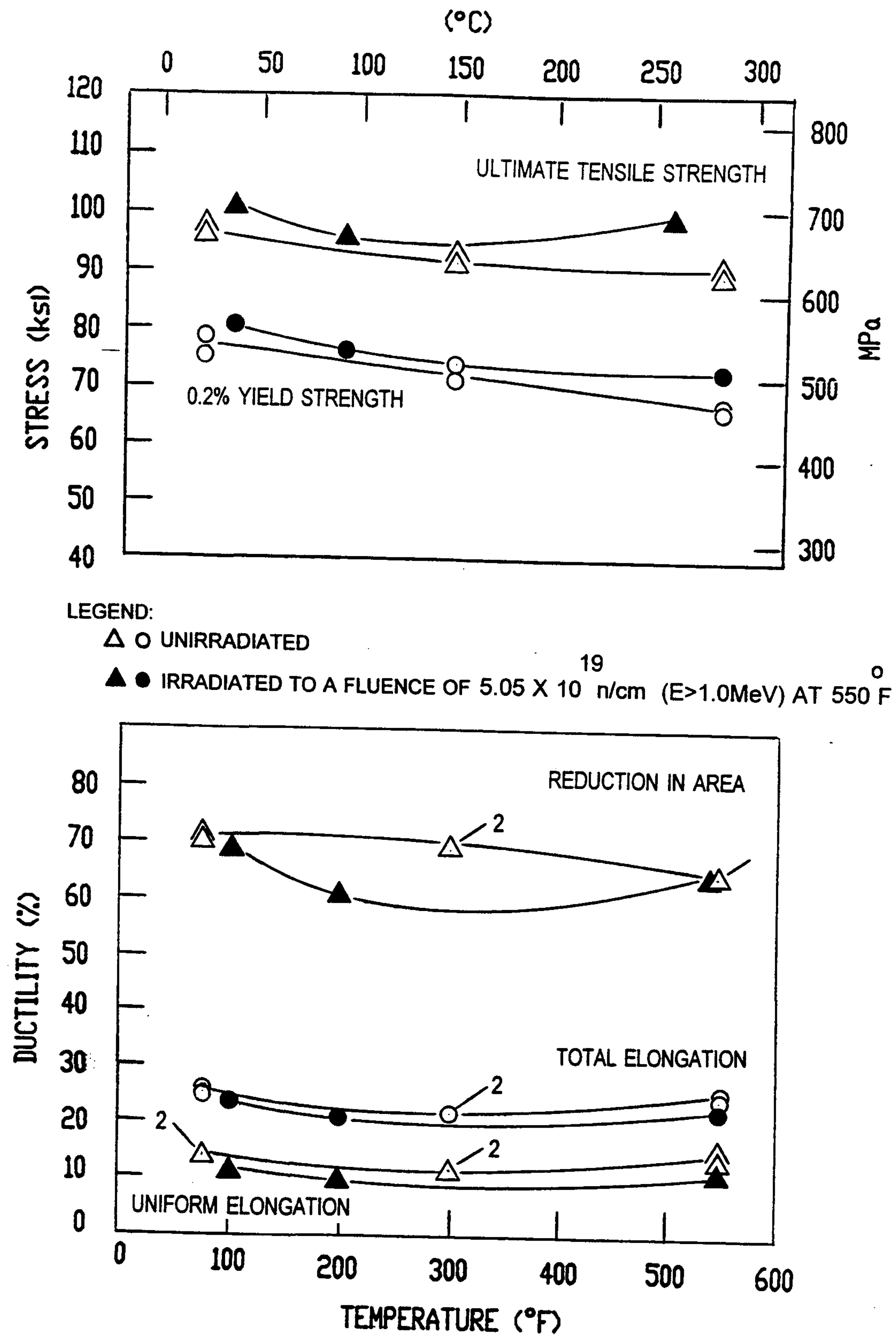

Figure 5-17 Tensile Properties for Watts Bar Unit 1 Reactor Vessel Intermediate Shell Forging 05 (Tangential Orientation)

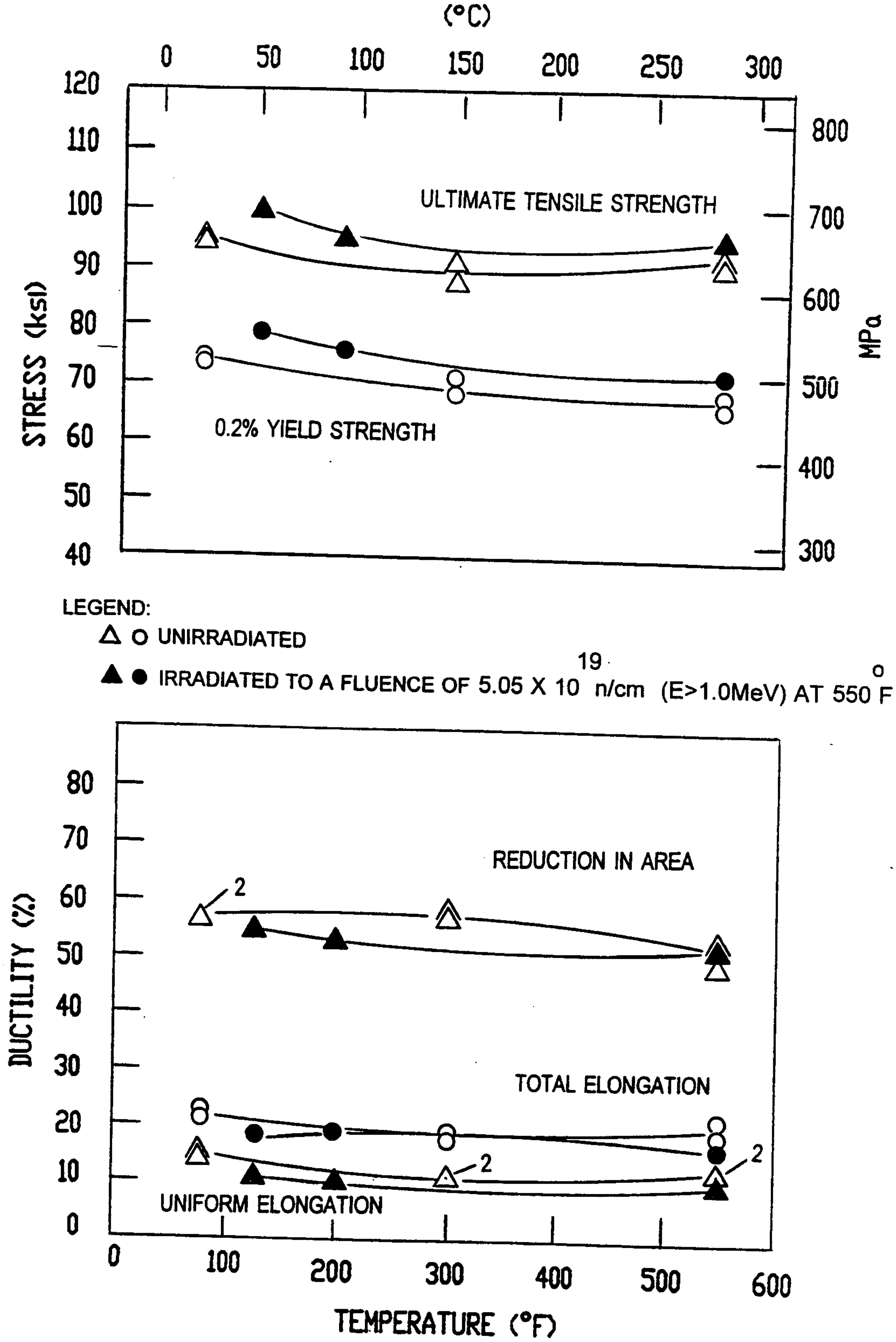

Figure 5-18 Tensile Properties for Watts Bar Unit 1 Reactor Vessel Intermediate Shell Forging 05 (Axial Orientation)

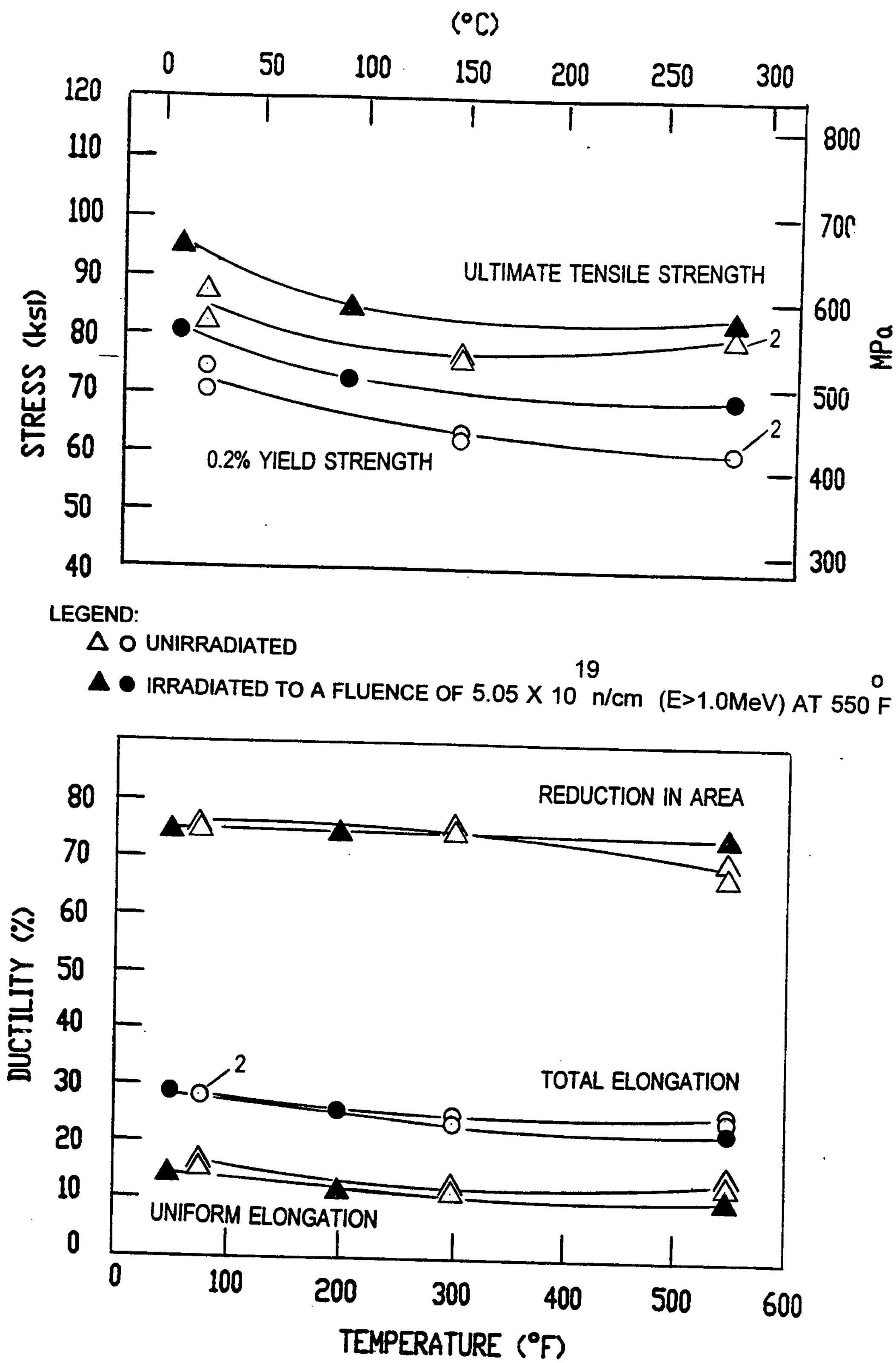

Figure 5-19 Tensile Properties for Watts Bar Unit 1 Reactor Vessel Weld Metal

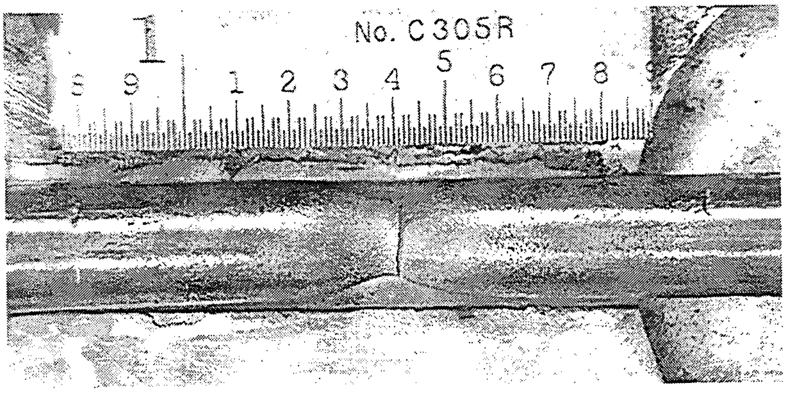

Specimen WL1 Tested at 100°F

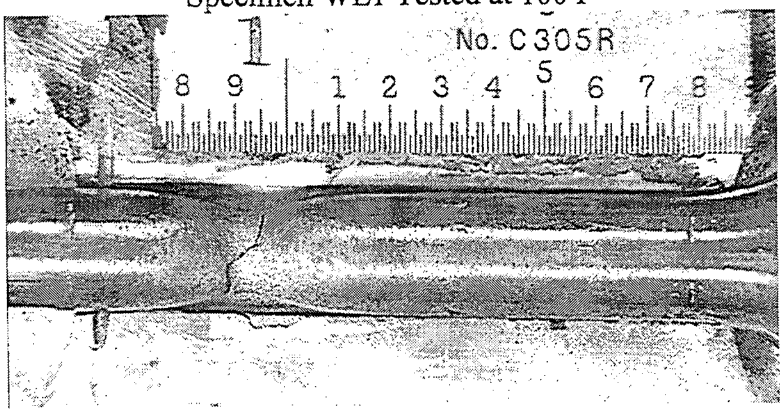

Specimen WL2 Tested at 200°F

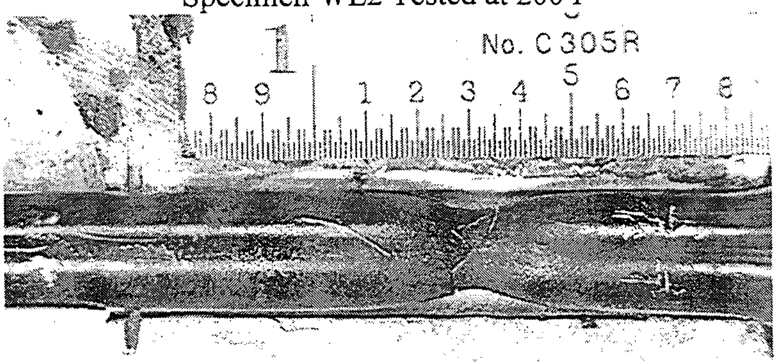

Specimen WL3 Tested at 550°F

Figure 5-20 Fractured Tensile Specimens from Watts Bar Unit 1 Reactor Vessel Intermediate Shell Forging 05 (Tangential Orientation)

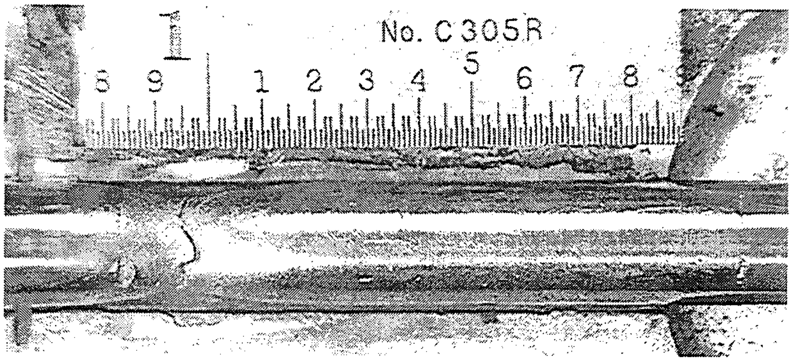

Specimen WT1 Tested at 125°F

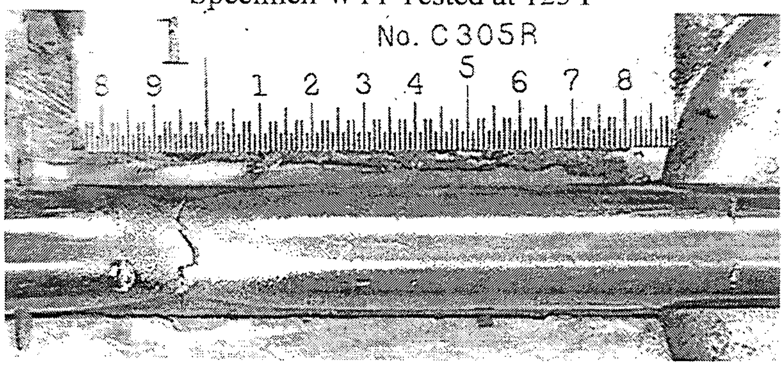

Specimen WT2 Tested at 200°F

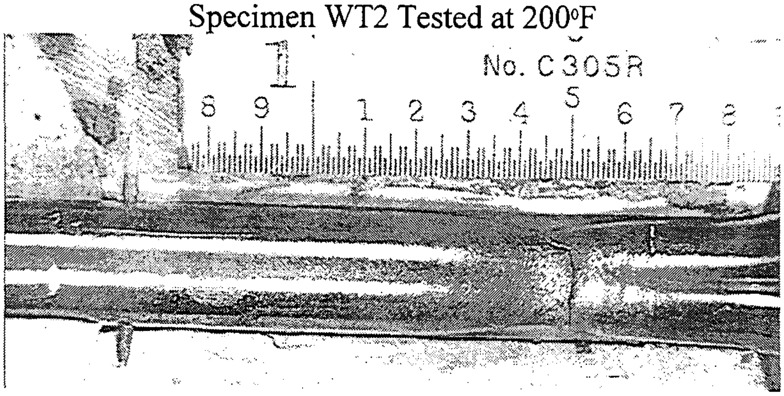

Specimen WT3 Tested at 550°F

Figure 5-21 Fractured Tensile Specimens from Watts Bar Unit 1 Reactor Vessel Intermediate Shell Forging 05 (Axial Orientation)

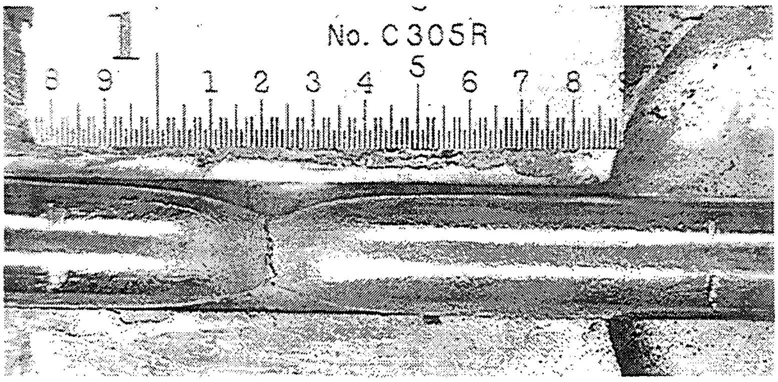

Specimen WW1 Tested at 50°F

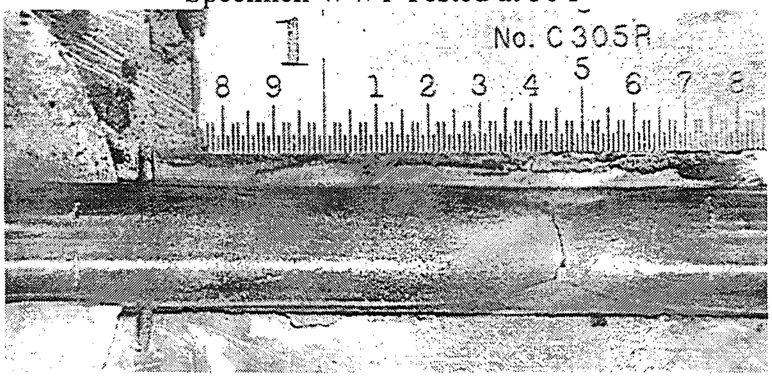

Specimen WW2 Tested at 200°F

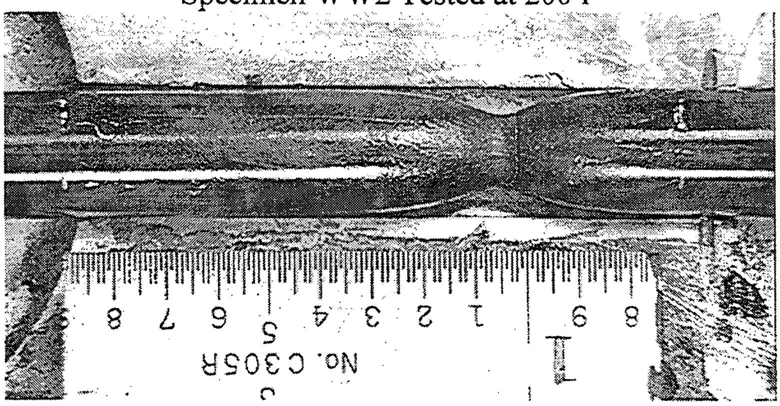

Specimen WW3 Tested at 550°F

Figure 5-22 Fractured Tensile Specimens from Watts Bar Unit 1 Reactor Vessel Weld Metal

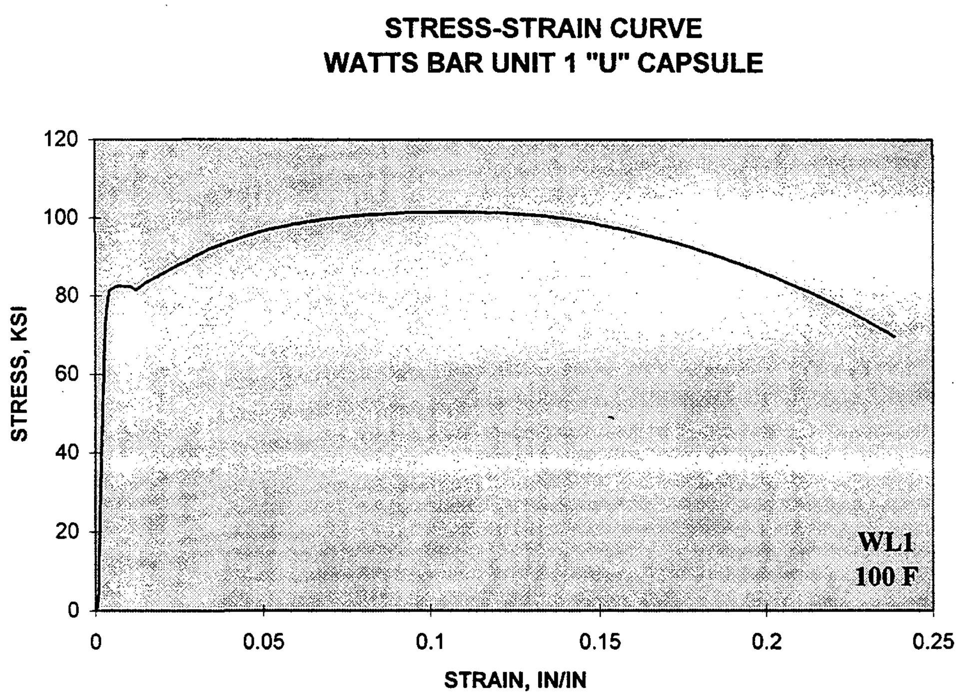

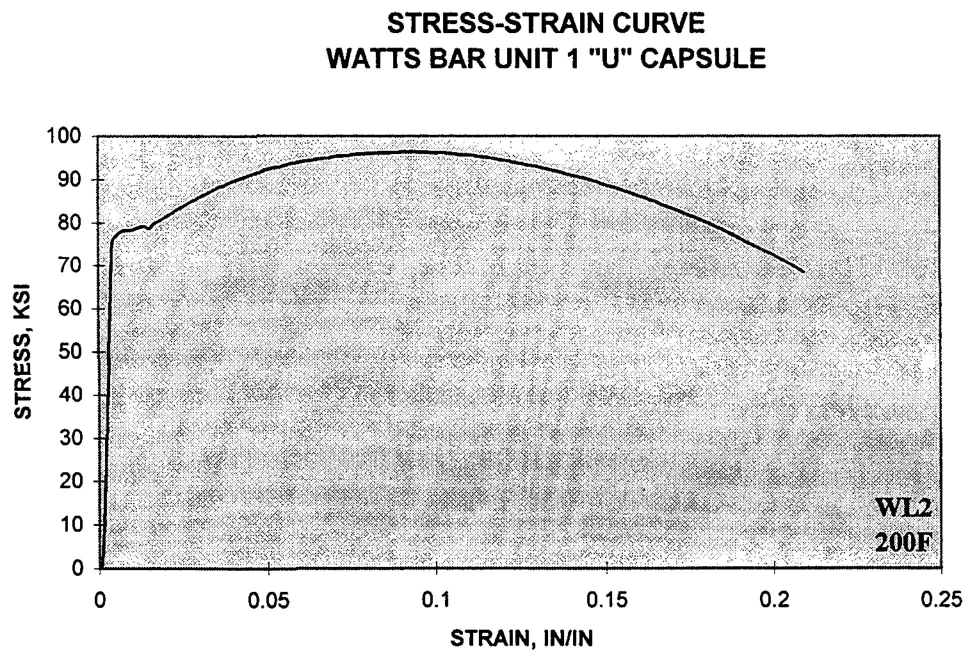

Figure 5-23 Engineering Stress-Strain Curves for Intermediate Shell Forging 05 Tensile Specimens WL1 and WL2 (Tangential Orientation)

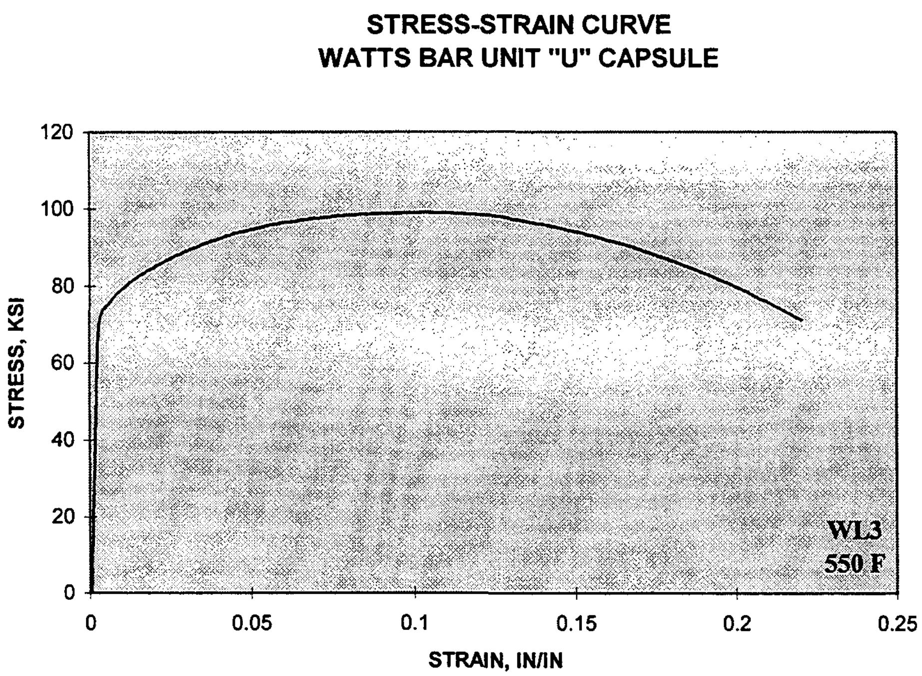

Figure 5-24 Engineering Stress-Strain Curve for Intermediate Shell Forging 05 Tensile Specimen WL3 (Tangential Orientation)

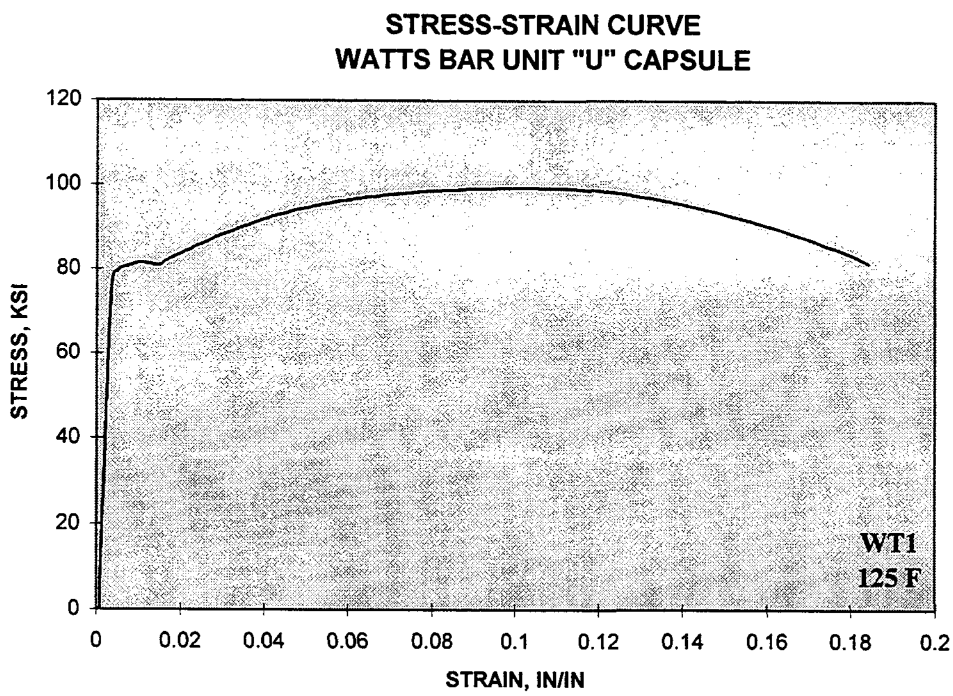

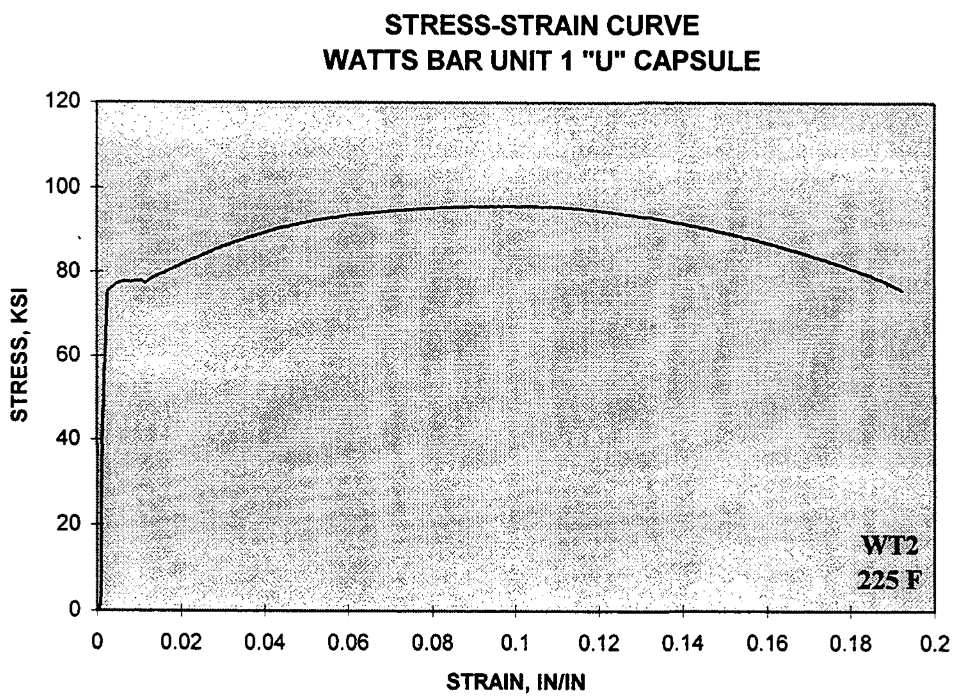

Figure 5-25 Engineering Stress-Strain Curves for Intermediate Shell Forging 05 Tensile Specimens WT1 and WT2 (Axial Orientation)

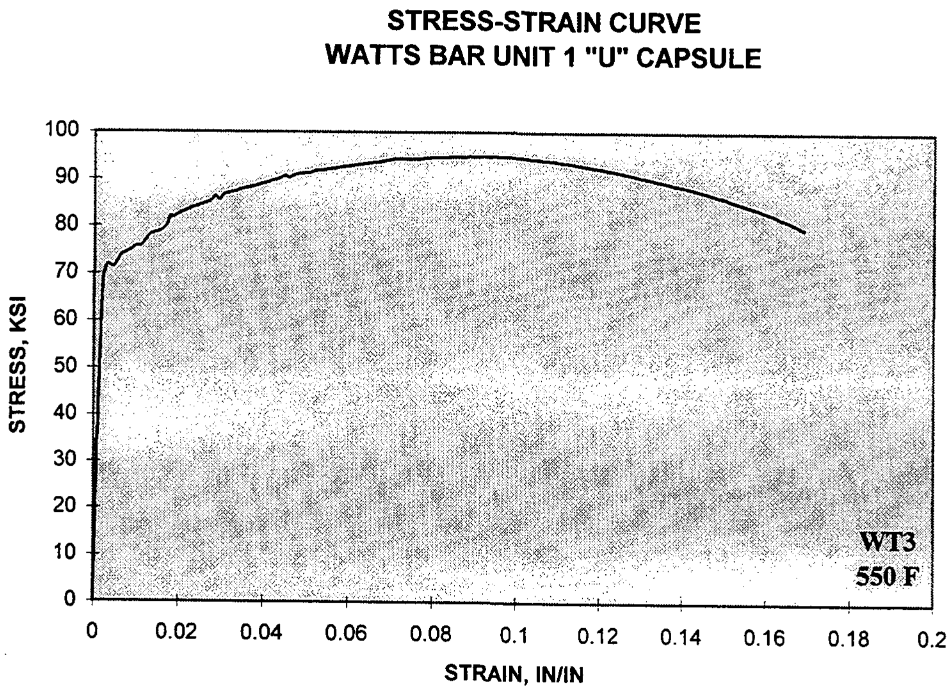

Figure 5-26 Engineering Stress-Strain Curve for Intermediate Shell Forging 05 Tensile Specimen WT3 (Axial Orientation)

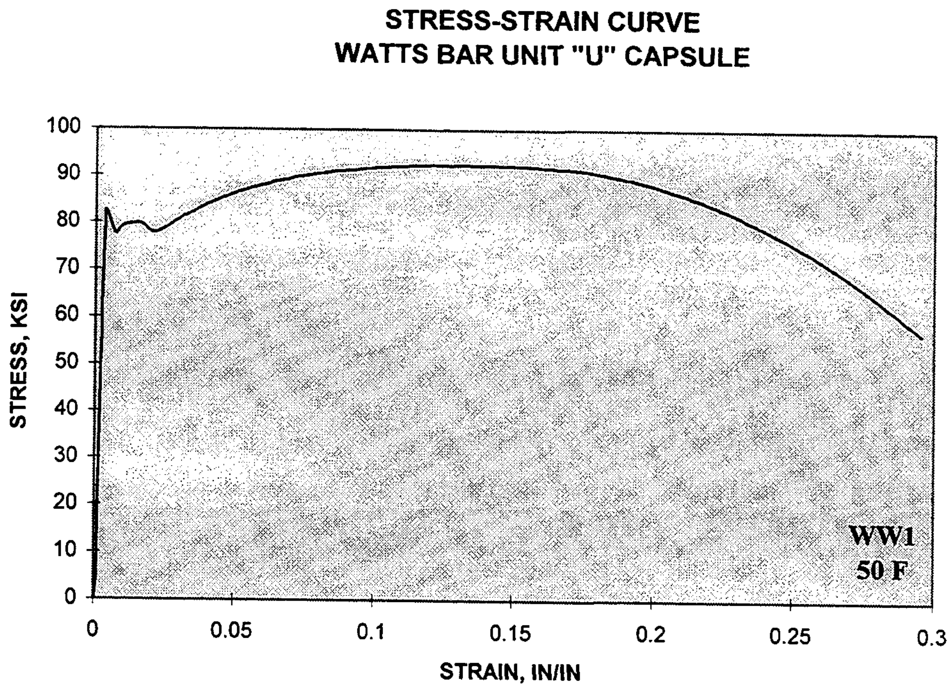

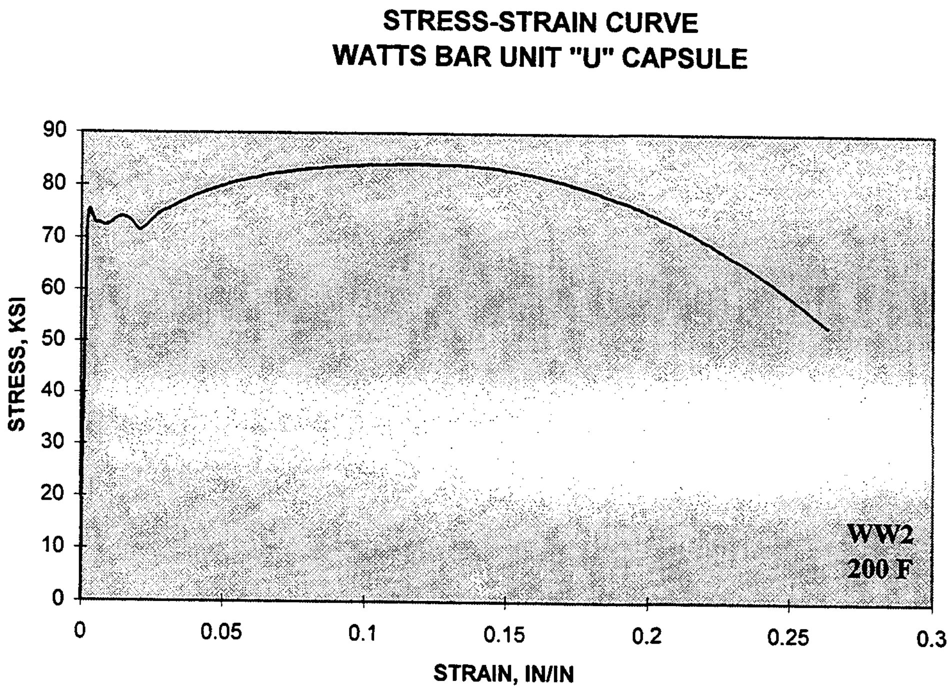

Figure 5-27 Engineering Stress-Strain Curves for Weld Metal Tensile Specimens WW1 and WW2

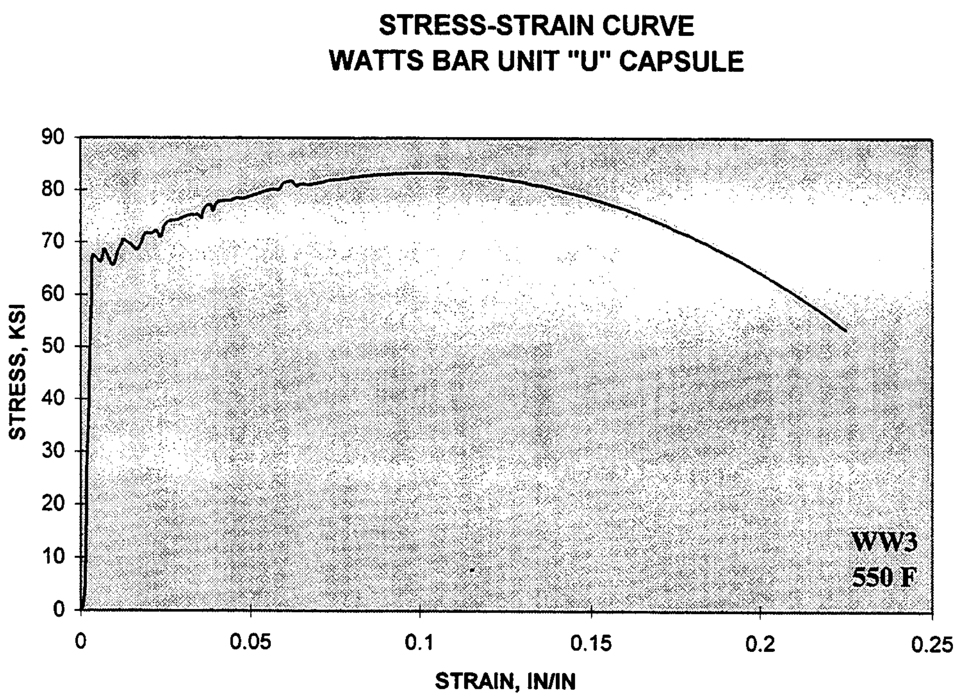

Figure 5-28 Engineering Stress-Strain Curve for Weld Metal Tensile Specimen WW3

SECTION 6.0
RADIATION ANALYSIS AND NEUTRON DOSIMETRY

6.1 Introduction

Knowledge of the neutron environment within the reactor vessel and surveillance capsule geometry is required as an integral part of LWR reactor vessel surveillance programs for two reasons. First, in order to interpret the neutron radiation induced material property changes observed in the test specimens, the neutron environment (energy spectrum, flux, fluence) to which the test specimens were exposed must be known. Second, in order to relate the changes observed in the test specimens to the present and future condition of the reactor vessel, a relationship must be established between the neutron environment at various positions within the reactor vessel and that experienced by the test specimens. The former requirement is normally met by employing a combination of rigorous analytical techniques and measurements obtained with passive neutron flux monitors contained in each of the surveillance capsules. The latter information is generally derived solely from analysis.

The use of fast neutron fluence (E > 1.0 MeV) to correlate measured material property changes to the neutron exposure of the material has traditionally been accepted for development of damage trend curves as well as for the implementation of trend curve data to assess vessel condition. In recent years, however, it has been suggested that an exposure model that accounts for differences in neutron energy spectra between surveillance capsule locations and positions within the vessel wall could lead to an improvement in the uncertainties associated with damage trend curves as well as to a more accurate evaluation of damage gradients through the reactor vessel wall.

Because of this potential shift away from a threshold fluence toward an energy dependent damage function for data correlation, ASTM Standard Practice E853, "Analysis and Interpretation of Light-Water Reactor Surveillance Results," recommends reporting displacements per iron atom (dpa) along with fluence (E > 1.0 MeV) to provide a data base for future reference. The energy dependent dpa function to be used for this evaluation is specified in ASTM Standard Practice E693, "Characterizing Neutron Exposures in Iron and Low Alloy Steels in Terms of Displacements per Atom." The application of the dpa parameter to the assessment of embrittlement gradients through the thickness of the reactor vessel wall has already been promulgated in Revision 2 to Regulatory Guide 1.99, "Radiation Embrittlement of Reactor Vessel Materials."

This section provides the results of the neutron dosimetry evaluations performed in conjunction with the analysis of test specimens contained in surveillance Capsule U, which was withdrawn at the end of the first fuel cycle. This evaluation is based on current state-of-the-art methodology and nuclear data including recently released neutron transport and dosimetry cross-section libraries derived from the ENDF/B-VI data base. This report provides a consistent up-to-date neutron exposure data base for use in evaluating the material properties of the Watts Bar Unit 1 reactor vessel.

In each capsule dosimetry evaluation, fast neutron exposure parameters in terms of neutron fluence (E > 1.0 MeV), neutron fluence (E > 0.1 MeV), and iron atom displacements (dpa) are established for the capsule irradiation history. The analytical formalism relating the measured capsule exposure to the exposure of the vessel wall is described and used to project the integrated exposure of the vessel wall. Also, uncertainties associated with the derived exposure parameters at the surveillance capsules and with the projected exposure of the reactor vessel are provided.

6.2 Discrete Ordinates Analysis

A plan view of the reactor geometry at the core midplane is shown in Figure 4-1. Six irradiation capsules attached to the neutron pads are included in the reactor design to constitute the reactor vessel surveillance program. The capsules are located at azimuthal angles of 56°, 58.5°, 124°, 236°, 238.5°, and 304° relative to the core cardinal axis as shown in Figure 4-1.

A plan view of a dual surveillance capsule holder attached to the neutron pad is shown in Figure 6-1. The stainless steel specimen containers are 1.182 by 1-inch and approximately 56 inches in height. The containers are positioned axially such that the test specimens are centered on the core midplane, thus spanning the central 5 feet of the 12-foot high reactor core.

From a neutronic standpoint, the surveillance capsules and associated support structures are significant. The presence of these materials has a marked effect on both the spatial distribution of neutron flux and the neutron energy spectrum in the water annulus between the neutron pad and the reactor vessel. In order to determine the neutron environment at the test specimen location, the capsules themselves must be included in the analytical model.

In performing the fast neutron exposure evaluations for the surveillance capsules and reactor vessel, two distinct sets of transport calculations were carried out. The first, a single computation in the conventional forward mode, was used primarily to obtain relative neutron energy distributions throughout the reactor geometry as well as to establish relative radial distributions of exposure parameters {ϕ(E > 1.0 MeV), ϕ(E > 0.1 MeV), and dpa/sec} through the vessel wall. The neutron spectral information was required for the interpretation of neutron dosimetry withdrawn from the surveillance capsule as well as for the determination of exposure parameter ratios, i.e., [dpa/sec]/[ϕ(E > 1.0 MeV)], within the reactor vessel geometry. The relative radial gradient information was required to permit the projection of measured exposure parameters to locations interior to the reactor vessel wall, i.e., the ¼T and ¾T locations.

The second set of calculations consisted of a series of adjoint analyses relating the fast neutron flux, ϕ(E > 1.0 MeV), at surveillance capsule positions and at several azimuthal locations on the reactor vessel inner radius to neutron source distributions within the reactor core. The source importance functions generated from these adjoint analyses provided the basis for all absolute exposure calculations and comparison with measurement. These importance functions, when combined with fuel cycle specific neutron source distributions, yielded absolute predictions of neutron exposure at the locations of interest for each cycle of irradiation. They also established the means to perform similar predictions and dosimetry evaluations for all subsequent fuel cycles. It is important to note that the cycle specific neutron source distributions utilized in these analyses included not only spatial variations of fission rates within the reactor core but also accounted for the effects of varying neutron yield per fission and fission spectrum introduced by the build-up of plutonium as the burnup of individual fuel assemblies increased.

The absolute cycle-specific data from the adjoint evaluations together with the relative neutron energy spectra and radial distribution information from the reference forward calculation provided the means to:

1 - Evaluate neutron dosimetry obtained from surveillance capsules,
2 - Relate dosimetry results to key locations at the inner radius and through the thickness of the reactor vessel wall,
3 - Enable a direct comparison of analytical prediction with measurement, and
4 - Establish a mechanism for projection of reactor vessel exposure as the design of each new fuel cycle evolves.

The forward transport calculation for the reactor model summarized in Figures 4-1 and 6-1 was carried out in R,θ geometry using the DORT two-dimensional discrete ordinates code Version 2.8.14 [12] and the BUGLE-93 cross-section library [13]. The BUGLE-93 library is a 47 energy group ENDF/B-VI based data set produced specifically for light water reactor applications. In these analyses, anisotropic scattering was treated with a P_3 expansion of the scattering cross-sections and the angular discretization was modeled with an S_8 order of angular quadrature.

The core power distribution utilized in the reference forward transport calculation was derived from statistical studies of long-term operation of Westinghouse 4-loop plants. Inherent in the development of this reference core power distribution is the use of an out-in fuel management strategy, i.e., fresh fuel on the core periphery. Furthermore, for the peripheral fuel assemblies, the neutron source was increased by a 2σ margin derived from the statistical evaluation of plant-to-plant and cycle-to-cycle variations in peripheral power. Since it is unlikely that any single reactor would exhibit power levels on the core periphery at the nominal + 2σ value for a large number of fuel cycles, the use of this reference distribution is expected to yield somewhat conservative results.

All adjoint calculations were also carried out using an S_8 order of angular quadrature and the P_3 cross-section approximation from the BUGLE-93 library. Adjoint source locations were chosen at several azimuthal locations along the reactor vessel inner radius as well as at the geometric center of each surveillance capsule. Again, these calculations were run in R,θ geometry to provide neutron source distribution importance functions for the exposure parameter of interest, in this case $\phi(E > 1.0\text{ MeV})$.

Having the importance functions and appropriate core source distributions, the response of interest could be calculated as:

$$R(r,\theta) = \int_r \int_\theta \int_E I(r,\theta,E)\, S(r,\theta,E)\, r\, dr\, d\theta\, dE$$

where:

$R(r,\theta)$ =	$\phi(E > 1.0\text{ MeV})$ at radius r and azimuthal angle θ.
$I(r,\theta,E)$=	Adjoint source importance function at radius r, azimuthal angle θ, and neutron source energy E.
$S(r,\theta,E)$=	Neutron source strength at core location r,θ and energy E.

Although the adjoint importance functions used in this analysis were based on a response function defined by the threshold neutron flux $\phi(E > 1.0$ MeV), prior calculations [14] have shown that, while the implementation of low leakage loading patterns significantly impacts both the magnitude and spatial distribution of the neutron field, changes in the relative neutron energy spectrum are of second order. Thus, for a given location, the ratio of [dpa/sec]/[$\phi(E > 1.0$ MeV)] is insensitive to changing core source distributions. In the application of these adjoint importance functions to the Watts Bar Unit 1 reactor, therefore, the iron atom displacement rates (dpa/sec) and the neutron flux $\phi(E > 0.1$ MeV) were computed on a cycle-specific basis by using [dpa/sec]/[$\phi(E > 1.0$ MeV)] and[$\phi(E > 0.1$ MeV)]/[$\phi(E > 1.0$ MeV)] ratios from the forward analysis in conjunction with the cycle specific $\phi(E > 1.0$ MeV) solutions from the individual adjoint evaluations.

The reactor core power distributions used in the plant specific adjoint calculations were taken from the fuel cycle design reports for the first operating cycle of Watts Bar Unit 1 [15, 16].

Selected results from the neutron transport analyses are provided in Tables 6-1 through 6-5. The data listed in these tables establish the means for absolute comparisons of analysis and measurement for the Capsule U irradiation period and provide the means to correlate dosimetry results with the corresponding exposure of the reactor vessel wall.

In Table 6-1, the calculated exposure parameters [$\phi(E > 1.0$ MeV), $\phi(E > 0.1$ MeV), and dpa/sec] are given at the geometric center of the two azimuthally symmetric surveillance capsule positions (31.5° and 34°) for both the reference and the plant specific core power distributions. The plant-specific data, based on the adjoint transport analysis, are meant to establish the absolute comparison of measurement with analysis. The reference data derived from the forward calculation are provided as a conservative exposure evaluation against which plant specific fluence calculations can be compared. Similar data are given in Table 6-2 for the reactor vessel inner radius. Again, the three pertinent exposure parameters are listed for the reference and Cycle 1 plant specific power distributions.

It is important to note that the data for the vessel inner radius were taken at the clad/base metal interface, and, thus, represent the maximum predicted exposure levels of the vessel plates and welds.

Radial gradient information applicable to $\phi(E > 1.0$ MeV), $\phi(E > 0.1$ MeV), and dpa/sec is given in Tables 6-3, 6-4, and 6-5, respectively. The data, obtained from the reference forward neutron transport calculation, are presented on a relative basis for each exposure parameter at several azimuthal locations.

Exposure distributions through the vessel wall may be obtained by normalizing the calculated or projected exposure at the vessel inner radius to the gradient data listed in Tables 6-3 through 6-5. For example, the neutron flux $\phi(E > 1.0\ MeV)$ at the ¼T depth in the reactor vessel wall along the 0° azimuth is given by:

$$\phi_{1/4T}(0°) = \phi(220.35, 0°)\ F(225.87, 0°)$$

where:

$\phi_{1/4T}(0°)$	=	Projected neutron flux at the ¼T position on the 0° azimuth.
$\phi(220.35, 0°)$	=	Projected or calculated neutron flux at the vessel inner radius on the 0° azimuth.
$F(225.87, 0°)$	=	Ratio of the neutron flux at the ¼T position to the flux at the vessel inner radius for the 0° azimuth. This data is obtained from Table 6-3.

Similar expressions apply for exposure parameters expressed in terms of $\phi(E > 0.1\ MeV)$ and dpa/sec where the attenuation function F is obtained from Tables 6-4 and 6-5, respectively.

6.3 Neutron Dosimetry

The passive neutron sensors included in the Watts Bar Unit 1 surveillance program are listed in Table 6-6. Also given in Table 6-6 are the primary nuclear reactions and associated nuclear constants that were used in the evaluation of the neutron energy spectrum within the surveillance capsules and in the subsequent determination of the various exposure parameters of interest [$\phi(E > 1.0\ MeV)$, $\phi(E > 0.1\ MeV)$, dpa/sec]. The relative locations of the neutron sensors within the capsules are shown in Figure 4-2. The iron, nickel, copper, and cobalt-aluminum monitors, in wire form, were placed in holes drilled in spacers at several axial levels within the capsules. The cadmium shielded uranium and neptunium fission monitors were accommodated within the dosimeter block located near the center of the capsule.

The use of passive monitors such as those listed in Table 6-6 does not yield a direct measure of the energy dependent neutron flux at the point of interest. Rather, the activation or fission process is a measure of the integrated effect that the time and energy dependent neutron flux has on the target material over the course of the irradiation period. An accurate assessment of the average neutron flux level incident on the various monitors may be derived from the activation measurements only if the irradiation parameters are well known. In particular, the following variables are of interest:

- The measured specific activity of each monitor,
- The physical characteristics of each monitor,
- The operating history of the reactor [17],
- The energy response of each monitor, and
- The neutron energy spectrum at the monitor location.

The specific activity of each of the neutron monitors was determined using established ASTM procedures [18 through 31]. Following sample preparation and weighing, the activity of each monitor was determined by means of a lithium-drifted germanium, Ge(Li), gamma spectrometer. The irradiation history of the Watts Bar Unit 1 reactor was obtained from Tennessee Valley Authority personnel [17] as reported in NUREG-0020, "Licensed Operating Reactors Status Summary Report," for the Cycle 1 operating period. The irradiation history applicable to the exposure of Capsule U is given in Table 6-7.

Having the measured specific activities, the physical characteristics of the sensors, and the operating history of the reactor, reaction rates referenced to full-power operation were determined from the following equation:

$$R = \frac{A}{N_0 \, F \, Y \sum \frac{P_j}{P_{ref}} \, C_j \, [1 - e^{-\lambda t_j}] \, [e^{-\lambda t_d}]}$$

where:

R	=	Reaction rate averaged over the irradiation period and referenced to operation at a core power level of P_{ref} (rps/nucleus).
A	=	Measured specific activity (dps/gm).
N_0	=	Number of target element atoms per gram of sensor.
F	=	Weight fraction of the target isotope in the sensor material.
Y	=	Number of product atoms produced per reaction.
P_j	=	Average core power level during irradiation period j (MW).
P_{ref}	=	Maximum or reference power level of the reactor (MW).
C_j	=	Calculated ratio of $\phi(E > 1.0$ MeV) during irradiation period j to the time weighted average $\phi(E > 1.0$ MeV) over the entire irradiation period.
λ	=	Decay constant of the product isotope (1/sec).
t_j	=	Length of irradiation period j (sec).
t_d	=	Decay time following irradiation period j (sec).

and the summation is carried out over the total number of monthly intervals comprising the irradiation period.

In the equation describing the reaction rate calculation, the ratio $[P_j]/[P_{ref}]$ accounts for month-by-month variation of reactor core power level within any given fuel cycle as well as over multiple fuel cycles. The ratio C_j, which can be calculated for each fuel cycle using the adjoint transport technology discussed in Section 6.2, accounts for the change in sensor reaction rates caused by variations in flux level induced by changes in core spatial power distributions from fuel cycle to fuel cycle. For a single cycle irradiation, C_j is normally taken to be 1.0. However, for multiple -cycle irradiations, particularly those employing low leakage fuel management, the additional C_j term should be employed. The impact of changing flux levels for constant power operation can be quite significant for sensor sets that have been irradiated for many cycles in a reactor that has transitioned from non-low leakage to low leakage fuel management or for sensor sets contained in surveillance capsules that have been moved from one capsule location to another.

For the irradiation history of Capsule U, the flux level term in the reaction rate calculations was set to 1.0. Measured and saturated reaction product specific activities as well as the derived full power reaction rates are listed in Table 6-8. The specific activities and reaction rates of the ^{238}U sensors provided in Table 6-8 include corrections for ^{235}U impurities, plutonium build-in, and gamma ray induced fissions. Corrections for gamma ray induced fissions were also included in the specific activities and reaction rates for the ^{237}Np sensors as well.

Values of key fast neutron exposure parameters were derived from the measured reaction rates using the FERRET least squares adjustment code [32]. The FERRET approach used the measured reaction rate data, sensor reaction cross-sections, and a calculated trial spectrum as input and proceeded to adjust the group fluxes from the trial spectrum to produce a best fit (in a least squares sense) within the constraints of the parameter uncertainties. The best estimate exposure parameters, along with the associated uncertainties, were then obtained from the best estimate spectrum.

In the FERRET evaluations, a log-normal least squares algorithm weights both the a priori values and the measured data in accordance with the assigned uncertainties and correlations. In general, the measured values, f, are linearly related to the flux, ϕ, by some response matrix, A:

$$f_i^{(s,\alpha)} = \sum_g A_{ig}^{(s)} \, \phi_g^{(\alpha)}$$

where i indexes the measured values belonging to a single data set s, g designates the energy group, and α delineates spectra that may be simultaneously adjusted. For example,

$$R_i = \sum_g \sigma_{ig} \phi_g$$

relates a set of measured reaction rates, R_i, to a single spectrum, ϕ_g, by the multi-group reaction cross-section, σ_{ig}. The log-normal approach automatically accounts for the physical constraint of positive fluxes, even with large assigned uncertainties.

In the least squares adjustment, the continuous quantities (i.e., neutron spectra and cross-sections) were approximated in a multi-group format consisting of 53 energy groups. The trial input spectrum was converted to the FERRET 53 group structure using the SAND-II code[33]. This procedure was carried out by first expanding the 47 group calculated spectrum into the SAND-II 620 group structure using a SPLINE interpolation procedure in regions where group boundaries do not coincide. The 620 point spectrum was then re-collapsed into the group structure used in FERRET.

The sensor set reaction cross-sections, obtained from the ENDF/B-VI dosimetry file [34], were also collapsed into the 53 energy group structure using the SAND-II code. In this instance, the trial spectrum, as expanded to 620 groups, was employed as a weighting function in the cross-section collapsing procedure. Reaction cross-section uncertainties in the form of a 53 × 53 covariance matrix for each sensor reaction were also constructed from the information contained on the ENDF/B-VI data files. These matrices included energy group to energy group uncertainty correlations for each of the individual reactions. However, correlation's between cross-sections for different sensor reactions were not included. The omission of this additional uncertainty information does not significantly impact the results of the adjustment.

Due to the importance of providing a trial spectrum that exhibits a relative energy distribution close to the actual spectrum at the sensor set locations, the neutron spectrum input to the FERRET evaluation was taken from the center of the surveillance capsule modeled in the reference forward transport calculation. While the 53 × 53 group covariance matrices applicable to the sensor reaction cross-sections were developed from the ENDF/B-VI data files, the covariance matrix for the input trial spectrum was constructed from the following relation:

$$M_{g'g} = R_n^2 + R_g \, R_{g'} \, P_{g'g}$$

where R_n specifies an overall fractional normalization uncertainty (i.e., complete correlation) for the set of values. The fractional uncertainties, R_g, specify additional random uncertainties for group g that are correlated with a correlation matrix given by:

$$P_{g'g} = [1-\theta] \, \delta_{g'g} + \theta \, e^{-H}$$

where:

$$H = \frac{(g-g')^2}{2\,\gamma^2}$$

The first term in the correlation matrix equation specifies purely random uncertainties, while the second term describes short range correlation's over a group range γ (θ specifies the strength of the latter term). The value of δ is 1 when $g = g'$ and 0 otherwise. For the trial spectrum used in the current evaluations, a short range correlation of $\gamma = 6$ groups was used. This choice implies that neighboring groups are strongly correlated when θ is close to 1. Strong long-range correlations (or anti-correlations) were justified based on information presented by R. E. Maerker[35]. The uncertainties associated with the measured reaction rates included both statistical (counting) and systematic components. The systematic component of the overall uncertainty accounts for counter efficiency, counter calibrations, irradiation history corrections, and corrections for competing reactions in the individual sensors.

Results of the FERRET evaluation of the Capsule U dosimetry are given in Table 6-9. The data summarized in this table include fast neutron exposure evaluations in terms of $\Phi(E > 1.0 \text{ MeV})$, $\Phi(E > 0.1 \text{ MeV})$, and dpa. In general, excellent results were achieved in the fits of the best estimate spectra to the individual measured reaction rates. The measured, calculated and best estimate reaction rates for each reaction are given in Table 6-10. An examination of Table 6-10 shows that, in all cases, reaction rates calculated with the best estimate spectra match the measured reaction rates to better than 17%. The best estimate spectra from the least squares evaluation is given in Table 6-11 in the FERRET 53 energy group structure.

In Table 6-12, absolute comparisons of the best estimate and calculated fluence at the center of Capsule U are presented. The result for the Capsule U dosimetry evaluation (BE/C ratio of 1.081 for $\Phi(E > 1.0$ MeV)) are consistent with results obtained from similar evaluations of dosimetry from other reactors using methodologies based on ENDF/B-VI cross-sections.

6.4 Projections of Reactor Vessel Exposure

The best estimate exposure of the Watts Bar Unit 1 reactor vessel was developed using a combination of absolute plant specific transport calculations and all available plant specific measurement data. In the case of Watts Bar Unit 1, the measurement data base contains one surveillance capsule discussed in this report.

Combining this measurement data base with the plant-specific calculations, the best estimate vessel exposure is obtained from the following relationship:

$$\Phi_{Best\ Est.} = K\ \Phi_{Calc.}$$

where:

$\Phi_{Best.\ Est.}$	=	The best estimate fast neutron exposure at the location of interest.
K	=	The plant specific best estimate/calculation (BE/C) bias factor derived from the surveillance capsule dosimetry data.
$\Phi_{Calc.}$	=	The absolute calculated fast neutron exposure at the location of interest.

The approach defined in the above equation is based on the premise that the measurement data represent the most accurate plant-specific information available at the locations of the dosimetry; and, further that the use of the measurement data on a plant-specific basis essentially removes biases present in the analytical approach and mitigates the uncertainties that would result from the use of analysis alone.

That is, at the measurement points the uncertainty in the best estimate exposure is dominated by the uncertainties in the measurement process. At locations within the reactor vessel wall, additional uncertainty is incurred due to the analytically determined relative ratios among the various measurement points and locations within the reactor vessel wall.

For Watts Bar Unit 1, the derived plant specific bias factors were 1.081, 1.213, and 1.155 for $\Phi(E > 1.0$ MeV), $\Phi(E > 0.1$ MeV), and dpa, respectively. Bias factors of this magnitude are fully consistent with experience using the BUGLE-93 cross-section library.

The use of the bias factors derived from the measurement data base acts to remove plant-specific biases associated with the definition of the core source, actual versus assumed reactor dimensions, and operational variations in water density within the reactor. As a result, the overall uncertainty in the best estimate exposure projections within the vessel wall depends on the individual uncertainties in the measurement process, the uncertainty in the dosimetry location, and, in the uncertainty in the calculated ratio of the neutron exposure at the point of interest to that at the measurement location.

The uncertainty in the derived neutron flux for an individual measurement is obtained directly from the results of a least squares evaluation of dosimetry data. The least squares approach combines individual uncertainty in the calculated neutron energy spectrum, the uncertainties in dosimetry cross-sections, and the uncertainties in measured foil specific activities to produce a net uncertainty in the derived neutron flux at the measurement point. The associated uncertainty in the plant specific bias factor, K, derived from the BE/C data base, in turn, depends on the total number of available measurements as well as on the uncertainty of each measurement.

In developing the overall uncertainty associated with the reactor vessel exposure, the positioning uncertainties for dosimetry are taken from parametric studies of sensor position performed as part a series of analytical sensitivity studies included in the qualification of the methodology. The uncertainties in the exposure ratios relating dosimetry results to positions within the vessel wall are again based on the analytical sensitivity studies of the vessel thickness tolerance, downcomer water density variations, and vessel inner radius tolerance. Thus, this portion of the overall uncertainty is controlled entirely by dimensional tolerances associated with the reactor design and by the operational characteristics of the reactor.

The net uncertainty in the bias factor, K, is combined with the uncertainty from the analytical sensitivity study to define the overall fluence uncertainty at the reactor vessel wall. However, since the present

Watts Bar Unit 1 measurement data base only contains one surveillance capsule, the net uncertainty in K is the same as the uncertainty that was derived from the FERRET calculations.

Based on this best estimate approach, neutron exposure projections at key locations on the reactor vessel inner radius are given in Table 6-13; furthermore, calculated neutron exposure projections are also provided for comparison purposes. Along with the current (1.20 EFPY) exposure, projections are also provided for exposure periods of 16 EFPY and 32 EFPY. Projections for future operation were based on the assumption that the design basis exposure rates would continue to be applicable throughout plant life.

In the derivation of best estimate and calculated exposure gradients within the reactor vessel wall for the Watts Bar Unit 1 reactor vessel, exposure projections to 16 and 32 EFPY were also employed. Data based on both a $\Phi(E > 1.0\ \text{MeV})$ slope and a plant-specific dpa slope through the vessel wall are provided in Table 6-14.

In order to access RT_{NDT} versus fluence curves, dpa equivalent fast neutron fluence levels for the ¼T and ¾T positions were defined by the relations:

$$\phi(\tfrac{1}{4}T) = \phi(0T)\,\frac{dpa(\tfrac{1}{4}T)}{dpa(0T)}$$

and

$$\phi(\tfrac{3}{4}T) = \phi(0T)\,\frac{dpa(\tfrac{3}{4}T)}{dpa(0T)}$$

Using this approach results in the dpa equivalent fluence values listed in Table 6-14.

In Table 6-15, updated lead factors are listed for each of the Watts Bar Unit 1 surveillance capsules.

Figure 6-1

Plan View Of A Dual Reactor Vessel Surveillance Capsule

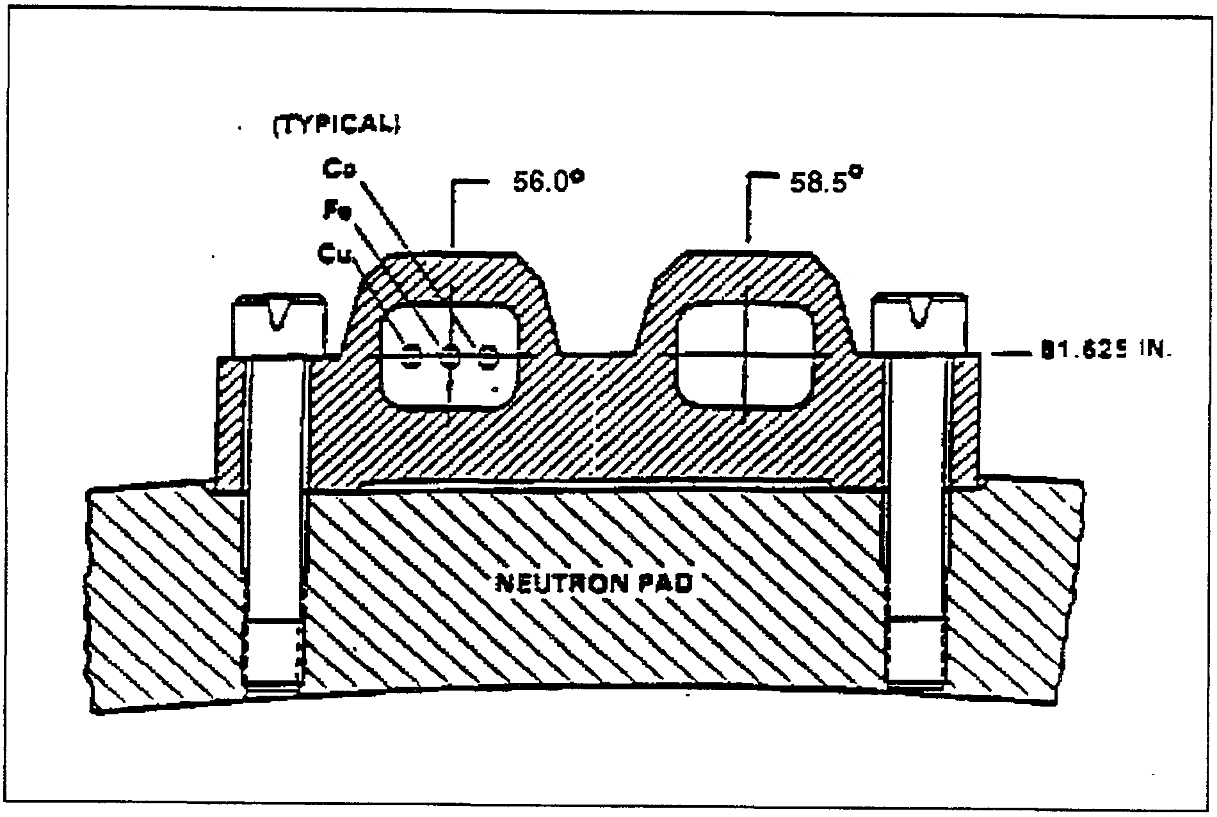

Table 6-1

Calculated Fast Neutron Exposure Rates And Iron Atom Displacement Rates At The Surveillance Capsule Center

	$\phi(E > 1.0$ MeV) (n/cm^2-sec)	
Cycle No.	31.5°	34°
Reference	1.368e+11	1.599e+11
1	1.044e+11	1.230e+11

	$\phi(E > 0.1$ MeV) (n/cm^2-sec)	
Cycle No.	31.5°	34°
Reference	5.964e+11	7.180e+11
1	4.553e+11	5.522e+11

	Displacement Rate (dpa/sec)	
Cycle No.	31.5°	34°
Reference	2.609e-10	3.095e-10
1	1.991e-10	2.381e-10

Table 6-2

Calculated Azimuthal Variation Of Fast Neutron Exposure Rates
And Iron Atom Displacement Rates At The Reactor Vessel
Clad/Base Metal Interface

$\phi(E > 1.0 \text{ MeV})$ (n/cm^2-sec)

Cycle No.	0°	15°	30°	45°
Reference	1.761e+10	2.692e+10	2.610e+10	3.120e+10
1	1.322e+10	2.012e+10	2.017e+10	2.491e+10

$\phi(E > 0.1 \text{ MeV})$ (n/cm^2-sec)

Cycle No.	0°	15°	30°	45°
Reference	3.706e+10	5.733e+10	5.982e+10	7.880e+10
1	2.784e+10	4.283e+10	4.623e+10	6.291e+10

Displacement Rate (dpa/sec)

Cycle No.	0°	15°	30°	45°
Reference	2.727e-11	4.131e-11	4.057e-11	4.938e-11
1	2.047e-11	3.086e-11	3.136e-11	3.943e-11

Table 6-3

Relative Radial Distribution Of ϕ (E > 1.0 Mev)
Within The Reactor Vessel Wall

RADIUS (cm)	AZIMUTHAL ANGLE 0°	15°	30°	45°
220.35	1.000	1.000	1.000	1.000
221.00	0.959	0.958	0.960	0.957
222.30	0.852	0.850	0.851	0.846
223.60	0.739	0.736	0.737	0.729
224.89	0.634	0.630	0.632	0.622
225.87	0.561	0.557	0.559	0.547
227.01	0.486	0.481	0.484	0.471
228.63	0.395	0.390	0.392	0.380
230.09	0.325	0.320	0.323	0.311
231.39	0.273	0.269	0.271	0.259
232.68	0.229	0.225	0.227	0.216
234.14	0.187	0.183	0.186	0.175
235.76	0.149	0.146	0.148	0.139
236.90	0.127	0.124	0.126	0.117
237.88	0.110	0.107	0.109	0.101
239.18	0.091	0.088	0.090	0.082
240.47	0.074	0.072	0.074	0.067
241.77	0.061	0.058	0.060	0.053
242.42	0.058	0.055	0.057	0.050

Note: Base Metal Inner Radius = 220.35 cm
Base Metal ¼T = 225.87 cm
Base Metal ½T = 231.39 cm
Base Metal ¾T = 236.90 cm
Base Metal Outer Radius = 242.42 cm

Table 6-4

Relative Radial Distribution Of ϕ (E > 0.1 Mev)
Within The Reactor Vessel Wall

RADIUS		AZIMUTHAL ANGLE		
(cm)	0°	15°	30°	45°
220.35	1.000	1.000	1.000	1.000
221.00	1.014	1.012	1.015	1.009
222.30	1.002	0.996	1.002	0.988
223.60	0.966	0.957	0.965	0.943
224.89	0.920	0.908	0.918	0.890
225.87	0.882	0.868	0.880	0.848
227.01	0.835	0.820	0.833	0.797
228.63	0.768	0.752	0.767	0.726
230.09	0.708	0.691	0.707	0.663
231.39	0.654	0.637	0.654	0.608
232.68	0.602	0.585	0.602	0.554
234.14	0.544	0.528	0.545	0.496
235.76	0.481	0.467	0.484	0.434
236.90	0.438	0.425	0.442	0.392
237.88	0.401	0.389	0.405	0.356
239.18	0.353	0.343	0.359	0.309
240.47	0.307	0.298	0.313	0.263
241.77	0.262	0.250	0.264	0.216
242.42	0.253	0.240	0.254	0.206

Note: Base Metal Inner Radius = 220.35 cm
Base Metal ¼T = 225.87 cm
Base Metal ½T = 231.39 cm
Base Metal ¾T = 236.90 cm
Base Metal Outer Radius = 242.42 cm

Table 6-5

Relative Radial Distribution Of dpa/sec
Within The Reactor Vessel Wall

RADIUS (cm)	AZIMUTHAL ANGLE 0°	15°	30°	45°
220.35	1.000	1.000	1.000	1.000
221.00	0.965	0.965	0.968	0.965
222.30	0.877	0.876	0.882	0.878
223.60	0.785	0.783	0.793	0.787
224.89	0.699	0.696	0.708	0.702
225.87	0.638	0.635	0.649	0.642
227.01	0.575	0.571	0.587	0.579
228.63	0.495	0.491	0.508	0.499
230.09	0.432	0.428	0.446	0.436
231.39	0.383	0.378	0.397	0.386
232.68	0.339	0.334	0.352	0.341
234.14	0.295	0.291	0.308	0.296
235.76	0.252	0.248	0.264	0.251
236.90	0.224	0.221	0.237	0.223
237.88	0.202	0.199	0.214	0.199
239.18	0.175	0.172	0.186	0.171
240.47	0.150	0.147	0.160	0.144
241.77	0.127	0.123	0.135	0.118
242.42	0.123	0.118	0.130	0.113

Note: Base Metal Inner Radius = 220.35 cm
Base Metal ¼T = 225.87 cm
Base Metal ½T = 231.39 cm
Base Metal ¾T = 236.90 cm
Base Metal Outer Radius = 242.42 cm

Table 6-6

Nuclear Parameters Used In The Evaluation Of Neutron Sensors

Monitor Material	Reaction of Interest	Target Atom Fraction	Response Range	Product Half-life	Fission Yield (%)
Copper	^{63}Cu (n,α)	0.6917	E > 4.7 MeV	5.271 y	
Iron	^{54}Fe (n,p)	0.0585	E > 1.0 MeV	312.1 d	
Nickel	^{58}Ni (n,p)	0.6808	E > 1.0 MeV	70.88 d	
Uranium-238	^{238}U (n,f)	1.0000	E > 0.4 MeV	30.07 y	6.02
Neptunium-237	^{237}Np (n,f)	1.0000	E > 0.08 MeV	30.07 y	6.17
Cobalt-Al	^{59}Co (n,γ)	0.0015	E > 0.015 MeV	5.271 y	

Note: ^{238}U and ^{237}Np monitors are cadmium shielded.

Table 6-7

Monthly Thermal Generation During The First Fuel Cycle
Of The Watts Bar Unit 1 Reactor

Cycle 1

Month	Thermal Gen. MWt-hr
Jan-96	9519
Feb-96	49773
Mar-96	475248
Apr-96	999029
May-96	1713718
Jun-96	2348718
Jul-96	2523691
Aug-96	2525629
Sep-96	2184725
Oct-96	1114619
Nov-96	2202224
Dec-96	2523130
Jan-97	1956638
Feb-97	2147746
Mar-97	1645462
Apr-97	2236507
May-97	2519097
Jun-97	2237128
Jul-97	2399891
Aug-97	1934439
Sep-97	262258

Table 6-8

Measured Sensor Activities And Reaction Rates

Surveillance Capsule U

Reaction	Location	Measured Activity (dps/gm)	Saturated Activity (dps/gm)	Reaction Rate (rps/atom)
^{63}Cu (n,α) ^{60}Co	Top	5.05E+04	3.68E+05	5.62E-17
	Middle	5.34E+04	3.90E+05	5.94E-17
	Bottom	5.25E+04	3.83E+05	5.84E-17
^{54}Fe (n,p) ^{54}Mn	Top	1.62E+06	3.86E+06	6.11E-15
	Middle	1.71E+06	4.07E+06	6.45E-15
	Bottom	1.71E+06	4.07E+06	6.45E-15
^{58}Ni (n,p) ^{58}Co	Top	1.20E+07	5.96E+07	8.53E-15
	Middle	1.25E+07	6.21E+07	8.89E-15
	Bottom	1.26E+07	6.26E+07	8.96E-15
^{59}Co (n,γ) ^{60}Co	Top	1.55E+07	1.13E+08	7.38E-12
	Top	1.28E+07	9.34E+07	6.09E-12
	Middle	1.43E+07	1.04E+08	6.80E-12
	Middle	1.19E+07	8.68E+07	5.66E-12
	Bottom	1.41E+07	1.03E+08	6.71E-12
	Bottom	1.22E+07	8.90E+07	5.81E-12
^{59}Co (n,γ) ^{60}Co (Cd)	Top	7.59E+06	5.54E+07	3.61E-12
	Middle	7.06E+06	5.15E+07	3.36E-12
	Bottom	7.10E+06	5.18E+07	3.38E-12
^{238}U (n,f) ^{137}Cs				
	Middle	2.34E+05	8.65E+06	5.68E-14
^{237}Np (n,f) ^{137}Cs				
	Middle	1.94E+06	7.17E+07	4.57E-13

Table 6-9

Summary Of Neutron Dosimetry Results
Surveillance Capsule U

Best Estimate Flux and Fluence for Capsule U

Quantity	Flux [n/cm^2-sec]	Quantity	Fluence [n/cm^2]	Uncertainty
ϕ (E > 1.0 MeV)	1.329e+11	Φ (E > 1.0 MeV)	5.050e+18	7%
ϕ (E > 0.1 MeV)	6.698e+11	Φ (E > 0.1 MeV)	2.545e+19	15%
ϕ (E < 0.414 eV)	1.277e+11	Φ (E < 0.414 eV)	4.853e+18	28%
dpa/sec	2.750e-10	dpa	1.045e-02	11%

Table 6-10

Comparison Of Measured, Calculated, And Best Estimate Reaction Rates At The Surveillance Capsule Center

Surveillance Capsule U

Reaction	Measured	Calculated	Best Estimate	Meas/Calc	BE/Meas	BE/Calc
^{63}Cu (n,α)	5.80e-17	5.71e-17	5.62e-17	1.02	0.97	0.98
^{54}Fe (n,p)	6.34e-15	6.83e-15	6.50e-15	0.93	1.03	0.95
^{58}Ni (n,p)	8.79e-15	9.65e-15	9.34e-15	0.91	1.06	0.97
^{238}U (n,f) (Cd)	4.75e-14	3.83e-14	3.95e-14	1.24	0.83	1.03
^{237}Np (n,f)	4.53e-13	3.83e-13	4.45e-13	1.18	0.98	1.16
^{59}Co (n,γ)	6.41e-12	5.46e-12	6.38e-12	1.17	1.00	1.17
^{59}Co (n,γ) (Cd)	3.45e-12	3.84e-12	3.47e-12	0.90	1.01	0.90

Table 6-11

Best Estimate Neutron Energy Spectrum At The Center Of Surveillance Capsule

Capsule U

Group #	Energy (MeV)	Flux (n/cm^2-sec)	Group #	Energy (MeV)	Flux (n/cm^2-sec)
1	1.73e+01	7.69E+06	28	9.12E-03	2.89E+10
2	1.49e+01	1.63E+07	29	5.53E-03	3.67E+10
3	1.35e+01	5.97E+07	30	3.36E-03	1.14E+10
4	1.16e+01	1.63E+08	31	2.84E-03	1.08E+10
5	1.00e+01	3.66E+08	32	2.40E-03	1.04E+10
6	8.61e+00	6.37E+08	33	2.04E-03	3.03E+10
7	7.41e+00	1.53E+09	34	1.23E-03	2.89E+10
8	6.07e+00	2.35E+09	35	7.49E-04	2.60E+10
9	4.97e+00	5.03E+09	36	4.54E-04	2.29E+10
10	3.68e+00	6.28E+09	37	2.75E-04	2.49E+10
11	2.87e+00	1.31E+10	38	1.67E-04	2.39E+10
12	2.23e+00	1.96E+10	39	1.01E-04	2.59E+10
13	1.74e+00	2.87E+10	40	6.14E-05	2.59E+10
14	1.35e+00	3.40E+10	41	3.73E-05	2.58E+10
15	1.11e+00	6.18E+10	42	2.26E-05	2.54E+10
16	8.21e-01	7.47E+10	43	1.37E-05	2.47E+10
17	6.39e-01	8.34E+10	44	8.32E-06	2.38E+10
18	4.98e-01	5.74E+10	45	5.04E-06	2.29E+10
19	3.88e-01	8.69E+10	46	3.06E-06	2.26E+10
20	3.02e-01	9.08E+10	47	1.86E-06	2.24E+10
21	1.83e-01	8.94E+10	48	1.13E-06	1.57E+10
22	1.11e-01	6.49E+10	49	6.83E-07	1.77E+10
23	6.74e-02	4.99E+10	50	4.14E-07	2.47E+10
24	4.09e-02	2.66E+10	51	2.51E-07	2.36E+10
25	2.55e-02	3.08E+10	52	1.52E-07	2.20E+10
26	1.99e-02	1.46E+10	53	9.24E-08	5.75E+10
27	1.50e-02	2.52E+10			

Note: Tabulated energy levels represent the upper energy in each group.

Table 6-12

Comparison Of Calculated And Best Estimate Integrated Neutron Exposure Of Watts Bar Unit 1 Surveillance Capsule U

CAPSULE U

	Calculated	Best Estimate	BE/C
$\Phi(E > 1.0\ MeV)$ [n/cm²]	4.673e+18	5.050e+18	1.081
$\Phi(E > 0.1\ MeV)$ [n/cm²]	2.098e+19	2.545e+19	1.213
dpa	9.047e-03	1.045e-02	1.155

AVERAGE BE/C RATIOS

	BE/C
Φ (E > 1.0 MeV) [n/cm²]	1.081
Φ (E > 0.1 MeV) [n/cm²]	1.213
dpa	1.155

Table 6-13

Azimuthal Variations Of The Neutron Exposure Projections
On The Reactor Vessel Clad/Base Metal Interface At Core Midplane

Best Estimate Exposure (1.20 EFPY) at the Reactor Vessel Inner Radius

	0°	15°	30° (15° N Pad)	30° (20° N Pad)	45°
Φ (E > 1.0 MeV)	5.43e+17	8.26e+17	8.28e+17	5.69e+17	1.02e+18
Φ (E > 0.1 MeV)	1.28e+18	1.97e+18	2.13e+18	1.90e+18	2.90e+18
dpa	8.99e-04	1.35e-03	1.38e-03	1.04e-03	1.73e-03

Best Estimate Exposure (16 EFPY) at the Reactor Vessel Inner Radius

	0°	15°	30° (15° N Pad)	30° (20° N Pad)	45°
Φ (E > 1.0 MeV)	9.43e+18	1.45e+19	1.39e+19	9.55e+18	1.68e+19
Φ (E > 0.1 MeV)	2.23e+19	3.48e+19	3.59e+19	3.20e+19	4.76e+19
dpa	1.56e-02	2.38e-02	2.31e-02	1.74e-02	2.84e-02

Best Estimate Exposure (32 EFPY) at the Reactor Vessel Inner Radius

	0°	15°	30° (15° N Pad)	30° (20° N Pad)	45°
Φ (E > 1.0 MeV)	1.90e+19	2.94e+19	2.80e+19	1.93e+19	3.38e+19
Φ (E > 0.1 MeV)	4.50e+19	7.02e+19	7.24e+19	6.45e+19	9.58e+19
dpa	3.15e-02	4.82e-02	4.66e-02	3.51e-02	5.72e-02

Table 6-13 Cont'd

Azimuthal Variations Of The Neutron Exposure Projections
On The Reactor Vessel Clad/Base Metal Interface At Core Midplane

Calculated Exposure (1.20 EFPY) at the Reactor Vessel Inner Radius

	0°	15°	30° (15° N Pad)	30° (20° N Pad)	45°
Φ (E > 1.0 MeV)	5.03e+17	7.64e+17	7.66e+17	5.27e+17	9.46e+17
Φ (E > 0.1 MeV)	1.06e+18	1.63e+18	1.76e+18	1.56e+18	2.39e+18
dpa	7.78e-04	1.17e-03	1.19e-03	8.97e-04	1.50e-03

Calculated Exposure (16 EFPY) at the Reactor Vessel Inner Radius

	0°	15°	30° (15° N Pad)	30° (20° N Pad)	45°
Φ (E > 1.0 MeV)	8.73e+18	1.35e+19	1.29e+19	8.84e+18	1.55e+19
Φ (E > 0.1 MeV)	1.84e+19	2.87e+19	2.96e+19	2.64e+19	3.92e+19
dpa	1.35e-02	2.06e-02	2.00e-02	1.51e-02	2.46e-02

Calculated Exposure (32 EFPY) at the Reactor Vessel Inner Radius

	0°	15°	30° (15° N Pad)	30° (20° N Pad)	45°
Φ (E > 1.0 MeV)	1.76e+19	2.72e+19	2.59e+19	1.78e+19	3.13e+19
Φ (E > 0.1 MeV)	3.71e+19	5.79e+19	5.97e+19	5.32e+19	7.90e+19
dpa	2.73e-02	4.17e-02	4.04e-02	3.04e-02	4.95e-02

Table 6-14

Neutron Exposure Values Within The
Watts Bar Unit 1 Reactor Vessel

BEST ESTIMATE FLUENCE BASED ON E > 1.0 MeV SLOPE

16 EFPY Φ (E > 1.0 MeV) [n/cm^2]

	0°	15°	30° (15° N Pad)	30° (20° N Pad)	45°
Surface	9.43e+18	1.45e+19	1.39e+19	9.55e+18	1.68e+19
¼ T	5.29e+18	8.09e+18	7.76e+18	5.34e+18	9.17e+18
¾ T	1.20e+18	1.80e+18	1.75e+18	1.20e+18	1.96e+18

32 EFPY Φ (E > 1.0 MeV) [n/cm^2]

	0°	15°	30° (15° N Pad)	30° (20° N Pad)	45°
Surface	1.90e+19	2.94e+19	2.80e+19	1.93e+19	3.38e+19
¼ T	1.07e+19	1.63e+19	1.57e+19	1.08e+19	1.85e+19
¾ T	2.41e+18	3.63e+18	3.52e+18	2.42e+18	3.96e+18

CALCULATED FLUENCE BASED ON E > 1.0 MeV SLOPE

16 EFPY Φ (E > 1.0 MeV) [n/cm^2]

	0°	15°	30° (15° N Pad)	30° (20° N Pad)	45°
Surface	8.73e+18	1.35e+19	1.29e+19	8.94e+18	1.55e+19
¼ T	4.89e+18	7.49e+18	7.18e+18	4.94e+18	8.49e+18
¾ T	1.11e+18	1.67e+18	1.62e+18	1.11e+18	1.82e+18

32 EFPY Φ (E > 1.0 MeV) [n/cm^2]

	0°	15°	30° (15° N Pad)	30° (20° N Pad)	45°
Surface	1.76e+19	2.72e+19	2.59e+19	1.78e+19	3.13e+19
¼ T	9.88e+18	1.51e+19	1.45e+19	9.96e+18	1.71e+19
¾ T	2.23e+18	3.36e+18	3.26e+18	2.24e+18	3.66e+18

Table 6-14 Cont'd

Neutron Exposure Values Within The
Watts Bar Unit 1 Reactor Vessel

BEST ESTIMATE FLUENCE BASED ON dpa SLOPE

16 EFPY Φ (E > 1.0 MeV) [n/cm²]

	0°	15°	30° (15° N Pad)	30° (20° N Pad)	45°
Surface	9.43e+18	1.45e+19	1.39e+19	9.55e+18	1.68e+19
¼ T	6.02e+18	9.23e+18	9.02e+18	6.20e+18	1.08e+19
¾ T	2.11e+18	3.21e+18	3.29e+18	2.26e+18	3.74e+18

32 EFPY Φ (E > 1.0 MeV) [n/cm²]

	0°	15°	30° (15° N Pad)	30° (20° N Pad)	45°
Surface	1.90e+19	2.94e+19	2.80e+19	1.93e+19	3.38e+19
¼ T	1.21e+19	1.86e+19	1.82e+19	1.25e+19	2.17e+19
¾ T	4.27e+18	6.49e+18	6.63e+18	4.56e+18	7.53e+18

CALCULATED FLUENCE BASED ON dpa SLOPE

16 EFPY Φ (E > 1.0 MeV) [n/cm²]

	0°	15°	30° (15° N Pad)	30° (20° N Pad)	45°
Surface	8.73e+18	1.35e+19	1.29e+19	8.84e+18	1.55e+19
¼ T	5.57e+18	8.54e+18	8.35e+18	5.74e+18	9.96e+18
¾ T	1.96e+18	2.97e+18	3.04e+18	2.09e+18	3.46e+18

32 EFPY Φ (E > 1.0 MeV) [n/cm²]

	0°	15°	30° (15° N Pad)	30° (20° N Pad)	45°
Surface	1.76e+19	2.72e+19	2.59e+19	1.78e+19	3.13e+19
¼ T	1.12e+19	1.72e+19	1.68e+19	1.16e+19	2.01e+19
¾ T	3.95e+18	6.00e+18	6.13e+18	4.22e+18	6.97e+18

Table 6-15

Updated Lead Factors For Watts Bar Unit 1
Surveillance Capsules

Capsule	Lead Factor
U[a]	4.94
V[b]	4.19
W[b]	4.94
X[b]	4.94
Y[b]	4.19
Z(b]	4.94

[a] - Withdrawn at the end of Cycle 1.
[b] - Not withdrawn; on standby.

SECTION 7.0
SURVEILLANCE CAPSULE REMOVAL SCHEDULE

The following surveillance capsule removal schedule meets the requirements of ASTM E185-82 and is recommended for future capsules to be removed from the Watts Bar Unit 1 reactor vessel. This recommended removal schedule is applicable to 32 EFPY of operation.

TABLE 7-1

Watts Bar Unit 1 Reactor Vessel Surveillance Capsule Withdrawal Schedule

Capsule	Location	Lead Factor[a]	Removal Time (EFPY)[b]	Fluence (n/cm^2, E > 1.0 MeV)[a]
U	56°	4.94	1.20	5.05×10^{18} (c)
W	124°	4.94	3.9	2.03×10^{19} (d)
X	236°	4.94	6.5	3.38×10^{19} (e)
Z	304°	4.94	9.7	5.07×10^{19} (f)
V(g)	58.5°	4.19	Standby	---
Y(g)	238.5°	4.19	Standby	---

Notes:

(a) Updated in Capsule U dosimetry analysis, See Section 6 of this Report.

(b) Effective Full Power Years (EFPY) from plant startup.

(c) Plant specific evaluation.

(d) This fluence is the approximate fluence at 1/4T at end-of-life (32 EFPY).

(e) This fluence is equal to the calculated peak reactor vessel surface fluence at EOL (32 EFPY).

(f) This fluence is not less than once or greater than twice the peak EOL fluence, and is approximately equal to the peak vessel fluence at 48 EFPY.

(g) These capsules will reach a fluence of 5.07×10^{19} (48 EFPY Peak Fluence) at approximately 11.5 EFPY.

SECTION 8.0
REFERENCES

1. Regulatory Guide 1.99, Revision 2, *Radiation Embrittlement of Reactor Vessel Materials*, U.S. Nuclear Regulatory Commission, May, 1988.

2. Code of Federal Regulations, 10CFR50, Appendix G, *Fracture Toughness Requirements*, and Appendix H, *Reactor Vessel Material Surveillance Program Requirements*, U.S. Nuclear Regulatory Commission, Washington, D.C.

3. WCAP-9298, "Tennessee Valley Authority Watts Bar Unit 1 Reactor Vessel Radiation Surveillance Program", P. A. Peter, August, 1995.

4. Section XI of the ASME Boiler and Pressure Vessel Code, Appendix G, *Fracture Toughness Criteria for Protection Against Failure*.

5. ASTM E208, *Standard Test Method for Conducting Drop-Weight Test to Determine Nil-Ductility Transition Temperature of Ferritic Steels*, in ASTM Standards, Section 3, American Society for Testing and Materials, Philadelphia, PA.

6. ASTM E185-82, *Standard Practice for Conducting Surveillance Tests for Light-Water Cooled Nuclear Power Reactor Vessels, E706 (IF)*, in ASTM Standards, Section 3, American Society for Testing and Materials, Philadelphia, PA, 1993.

7. ASTM E23-93a, *Standard Test Methods for Notched Bar Impact Testing of Metallic Materials*, in ASTM Standards, Section 3, American Society for Testing and Materials, Philadelphia, PA, 1993.

8. ASTM A370-92, *Standard Test Methods and Definitions for Mechanical Testing of Steel Products*, in ASTM Standards, Section 3, American Society for Testing and Materials, Philadelphia, PA, 1993.

9. ASTM E8-93, *Standard Test Methods for Tension Testing of Metallic Materials*, in ASTM Standards, Section 3, American Society for Testing and Materials, Philadelphia, PA, 1993.

10. ASTM E21-92, *Standard Test Methods for Elevated Temperature Tension Tests of Metallic Materials,* in ASTM Standards, Section 3, American Society for Testing and Materials, Philadelphia, PA, 1993.

11. ASTM E83-93, *Standard Practice for Verification and Classification of Extensometers*, in ASTM Standards, Section 3, American Society for Testing and Materials, Philadelphia, PA, 1993.

12. RSIC Computer Code Collection CCC-543, "TORT-DORT Two- and Three-Dimensional Discrete Ordinates Transport, Version 2.8.14", January 1994.

13. RSIC Data Library Collection DLC-175, "BUGLE-93, Production and Testing of the VITAMIN-B6 Fine Group and the BUGLE-93 Broad Group Neutron/Photon Cross-Section Libraries Derived from ENDF/B-VI Nuclear Data", April 1994.

14. R. E. Maerker, et al., *Accounting for Changing Source Distributions in Light Water Reactor Surveillance Dosimetry Analysis*, Nuclear Science and Engineering, Volume 94, Pages 291-308, 1986.

15. N. A. Pogorzelski, et al., "Nuclear Parameters and Operations Package for Watts Bar Unit 1, Cycle 1", WCAP-13444, Revision 1, March 1993. [Westinghouse Proprietary Class 2]

16. A. J. Hartshorn, et al., "Nuclear Parameters and Operations Package for Watts Bar Unit 1, Cycle 2", WCAP-14960, Revision 0, October 1997. [Westinghouse Proprietary Class 2]

17. C. S. Faulkner (Tennessee Valley Authority) electronic mail to G. K. Roberts (Westinghouse) transmitting selected Watts Bar Unit 1 operating plant history data, January 22, 1998.

18. ASTM Designation E482-89 (Re-approved 1996), *Standard Guide for Application of Neutron Transport Methods for Reactor Vessel Surveillance*, in ASTM Standards, Section 12, American Society for Testing and Materials, Philadelphia, PA, 1997.

19. ASTM Designation E560-84 (Re-approved 1996), *Standard Recommended Practice for Extrapolating Reactor Vessel Surveillance Dosimetry Results*, in ASTM Standards, Section 12, American Society for Testing and Materials, Philadelphia, PA, 1997.

20. ASTM Designation E693-94, *Standard Practice for Characterizing Neutron Exposures in Iron and Low Alloy Steels in Terms of Displacements per Atom (dpa)*, in ASTM Standards, Section 12, American Society for Testing and Materials, Philadelphia, PA, 1997.

21. ASTM Designation E706-87 (Re-approved 1994), *Standard Master Matrix for Light-Water Reactor Pressure Vessel Surveillance Standard*, in ASTM Standards, Section 12, American Society for Testing and Materials, Philadelphia, PA, 1997.

22. ASTM Designation E853-87 (Re-approved 1995), *Standard Practice for Analysis and Interpretation of Light-Water Reactor Surveillance Results*, in ASTM Standards, Section 12, American Society for Testing and Materials, Philadelphia, PA, 1997.

23. ASTM Designation E261-96, *Standard Practice for Determining Neutron Fluence Rate, Fluence, and Spectra by Radioactivation Techniques*, in ASTM Standards, Section 12, American Society for Testing and Materials, Philadelphia, PA, 1997.

24. ASTM Designation E262-86 (Re-approved 1991), *Standard Method for Determining Thermal Neutron Reaction and Fluence Rates by Radioactivation Techniques*, in ASTM Standards, Section 12, American Society for Testing and Materials, Philadelphia, PA, 1997.

25. ASTM Designation E263-93, *Standard Method for Measuring Fast-Neutron Reaction Rates by Radioactivation of Iron*, in ASTM Standards, Section 12, American Society for Testing and Materials, Philadelphia, PA, 1997.

26. ASTM Designation E264-92 (Re-approved 1996), *Standard Method for Measuring Fast-Neutron Reaction Rates by Radioactivation of Nickel*, in ASTM Standards, Section 12, American Society for Testing and Materials, Philadelphia, PA, 1997.

27. ASTM Designation E481-86 (Re-approved 1991), *Standard Method for Measuring Neutron-Fluence Rate by Radioactivation of Cobalt and Silver*, in ASTM Standards, Section 12, American Society for Testing and Materials, Philadelphia, PA, 1997.

28. ASTM Designation E523-92 (Re-approved 1996), *Standard Test Method for Measuring Fast-Neutron Reaction Rates by Radioactivation of Copper*, in ASTM Standards, Section 12, American Society for Testing and Materials, Philadelphia, PA, 1997.

29. ASTM Designation E704-96, *Standard Test Method for Measuring Reaction Rates by 7adioactivation of Uranium-238*, in ASTM Standards, Section 12, American Society for Testing and Materials, Philadelphia, PA, 1997.

30. ASTM Designation E705-96, *Standard Test Method for Measuring Reaction Rates by Radioactivation of Neptunium-237*, in ASTM Standards, Section 12, American Society for Testing and Materials, Philadelphia, PA, 1997.

31. ASTM Designation E1005-84 (Re-approved 1991), *Standard Test Method for Application and Analysis of Radiometric Monitors for Reactor Vessel Surveillance*, in ASTM Standards, Section 12, American Society for Testing and Materials, Philadelphia, PA, 1997.

32. F. A. Schmittroth, *FERRET Data Analysis Core*, HEDL-TME 79-40, Hanford Engineering Development Laboratory, Richland, WA, September 1979.

33. W. N. McElroy, S. Berg and T. Crocket, *A Computer-Automated Iterative Method of Neutron Flux Spectra Determined by Foil Activation*, AFWL-TR-7-41, Vol. I-IV, Air Force Weapons Laboratory, Kirkland AFB, NM, July 1967.

34. RSIC Data Library Collection DLC-178, "SNLRML Recommended Dosimetry Cross-Section Compendium", July 1994.

35. EPRI-NP-2188, *Development and Demonstration of an Advanced Methodology for LWR Dosimetry Applications*, R. E. Maerker, et al., 1981.

36. WCAP-13587, Rev. 1, "Reactor Vessel Upper Shelf Energy Bounding Evaluation For Westinghouse Pressurized Water Reactors", M.J. Malone, et. al., September 1993.

APPENDIX A

Load-Time Records for Charpy Specimen Tests

Curve 784472-AF13

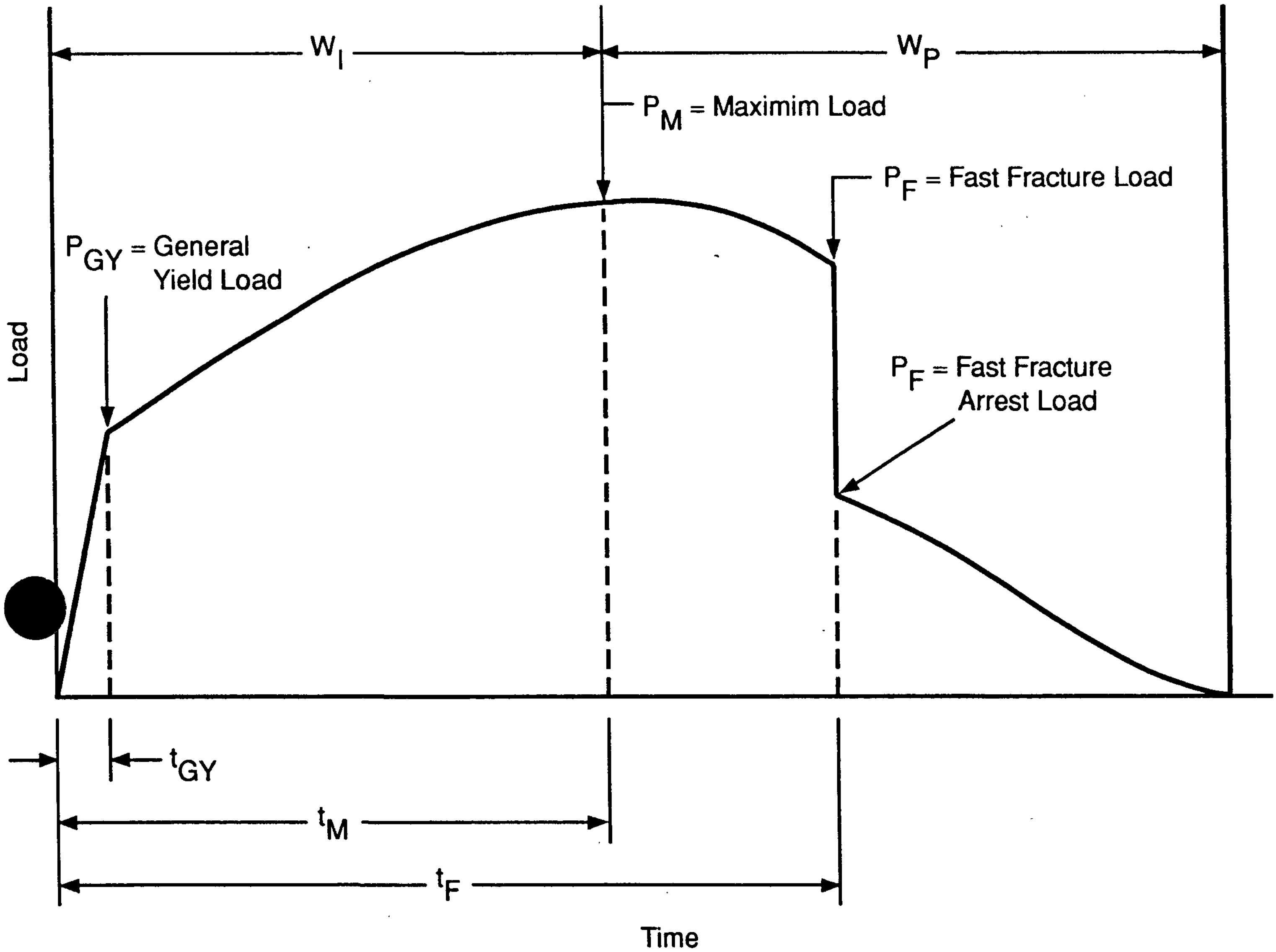

W_I = Fracture Initiation Region
W_P = Fracture Propagation Region

t_{GY} = Time to General Yielding
t_M = Time to Maximum Load
t_F = Time to Fast (Brittle) Fracture Start

Fig. A-1-Idealized load-time record

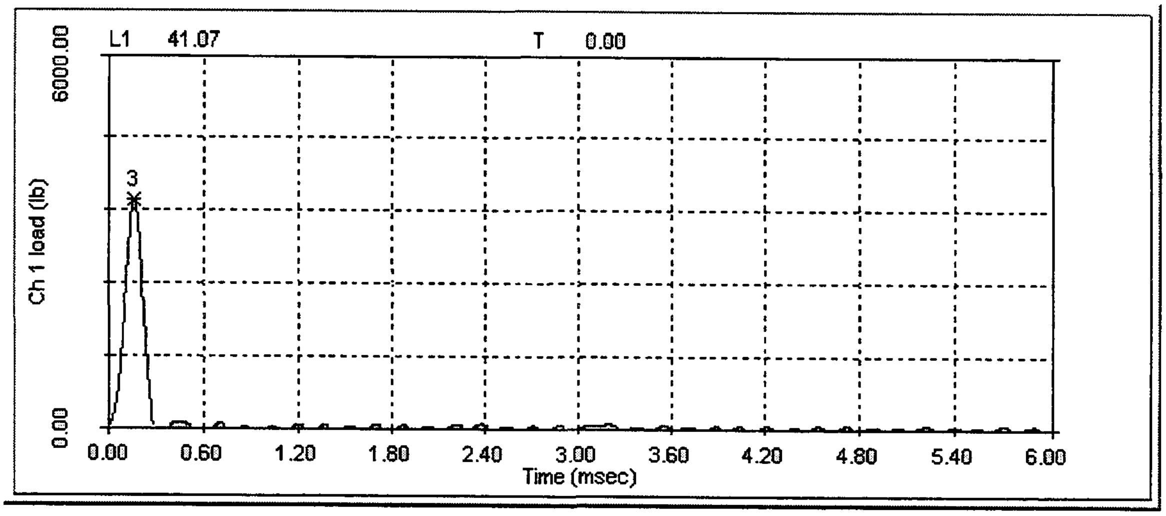

Figure A-2 Load-Time record for tangential specimen WL7 tested at -105°F.

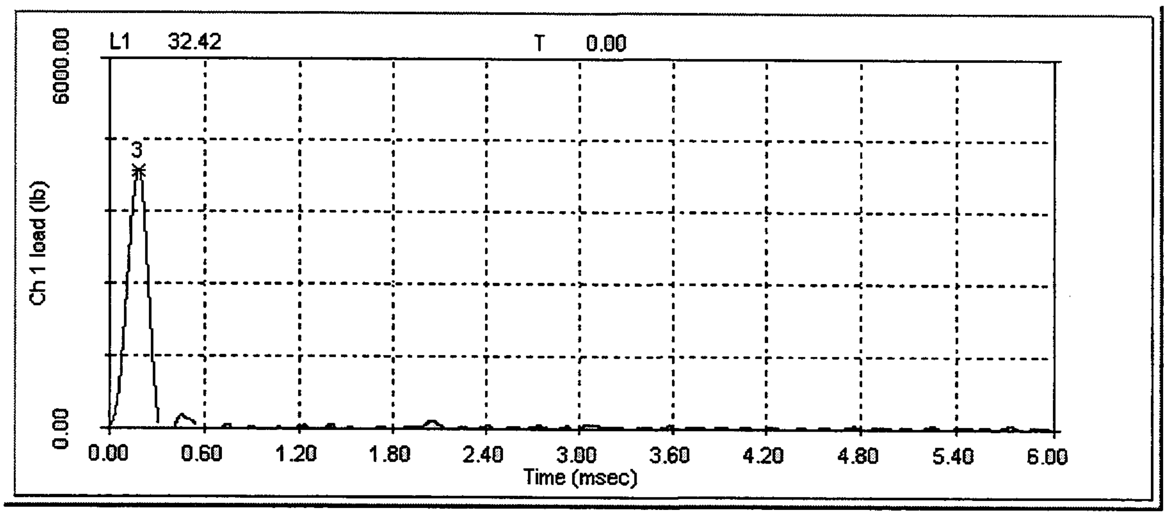

Figure A-3 Load-Time record for tangential specimen WL1 tested at -25°F.

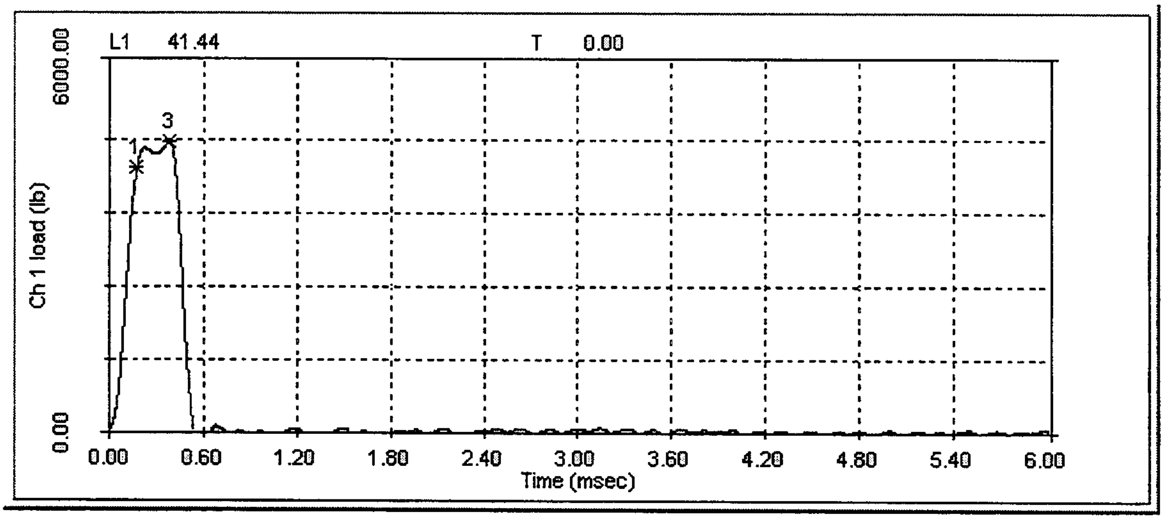

Figure A-4 Load-Time record for tangential specimen WL9 test at 0°F.

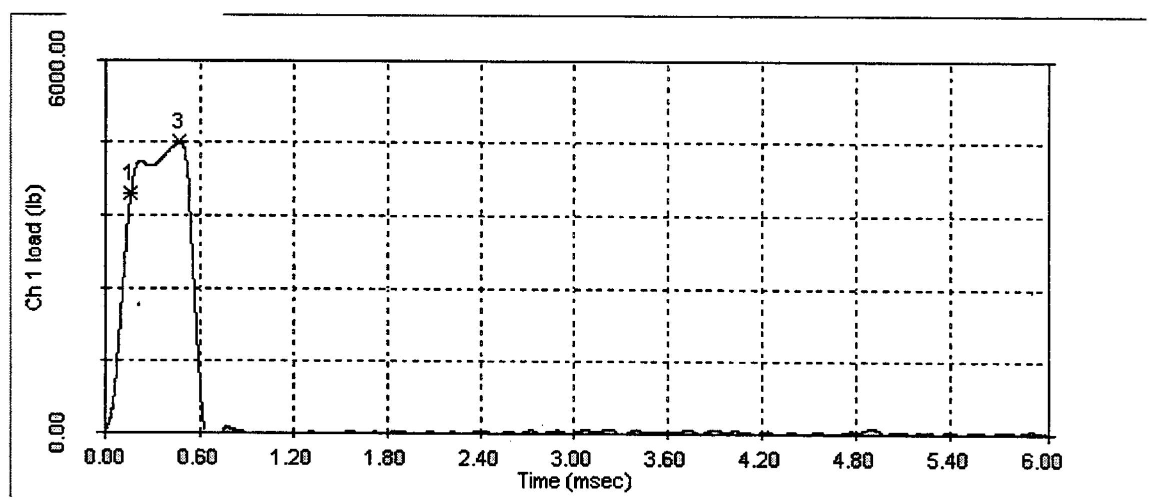

Figure A-5 Load-Time record for tangential specimen WL12 tested at 10°F.

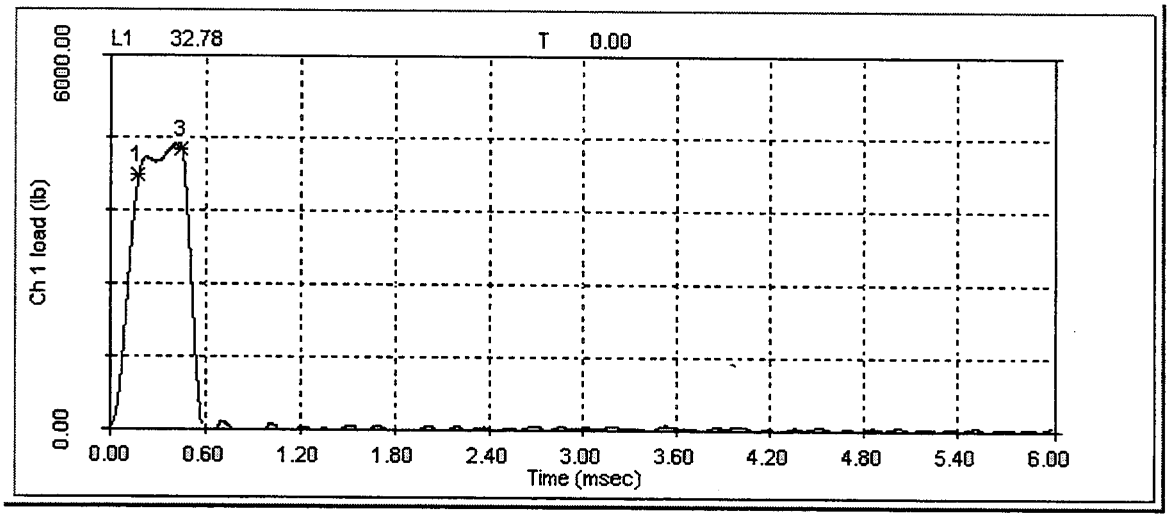

Figure A-6 Load-Time record for tangential specimen WL2 tested at 25°F.

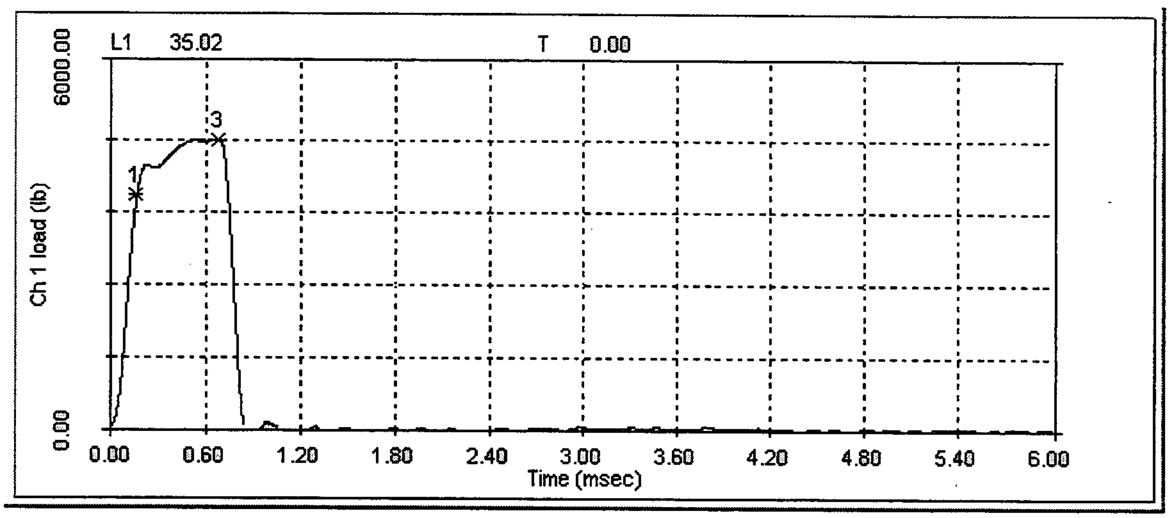

Figure A-7 Load-Time record for tangential specimen WL4 tested at 50°F.

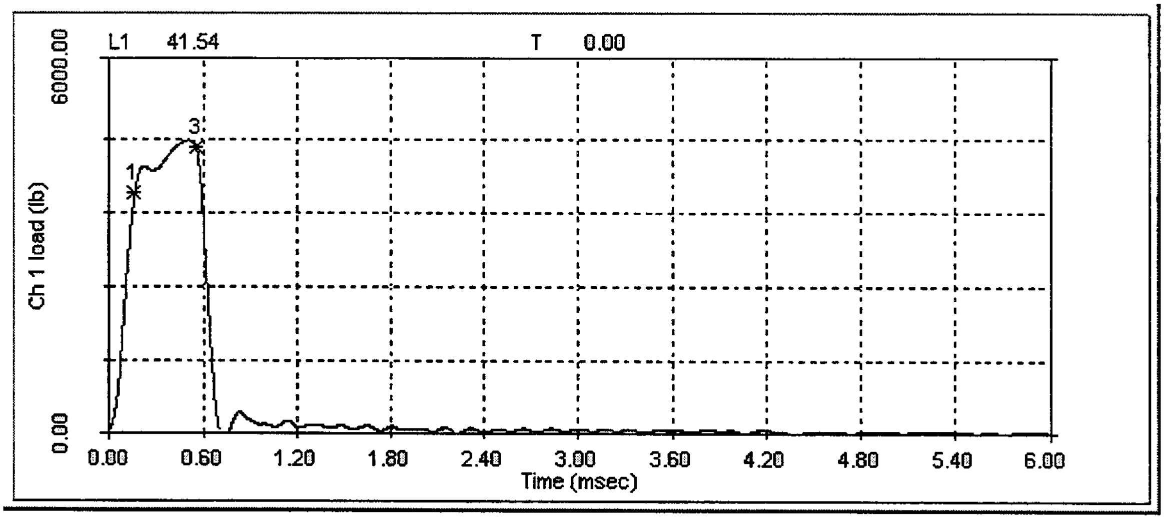

Figure A-8 Load-Time record for tangential specimen WL3 tested at 70°F.

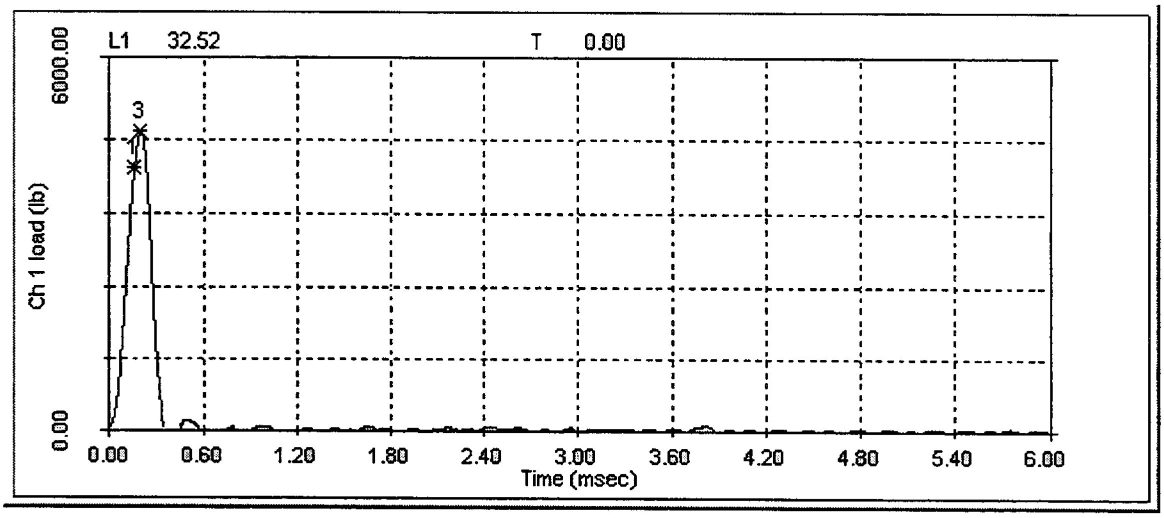

Figure A-9 Load-Time record for tangential specimen WL11 tested at 75°F.

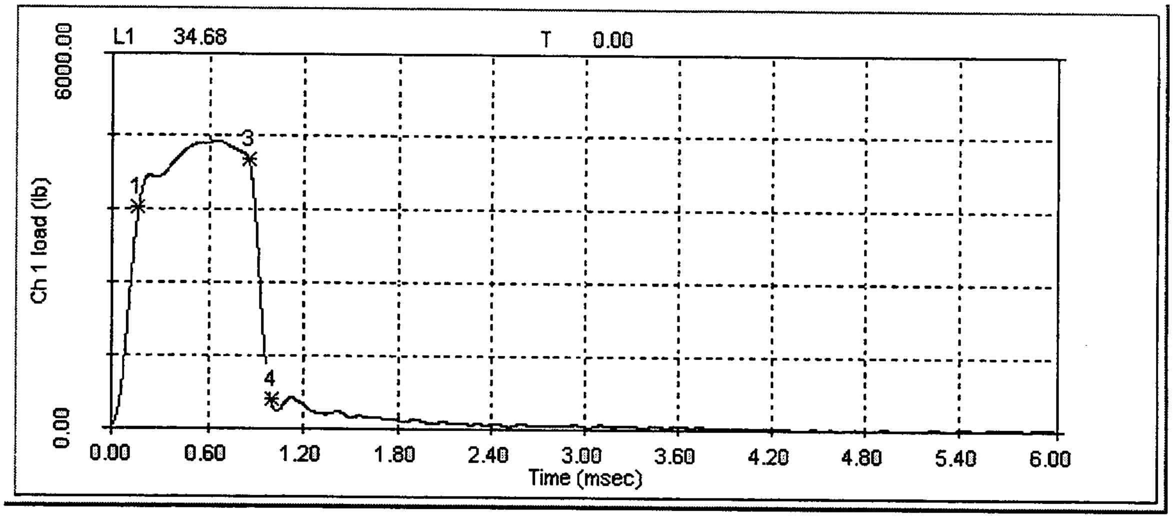

Figure A-10 Load-Time record for tangential specimen WL5 tested at 100°F.

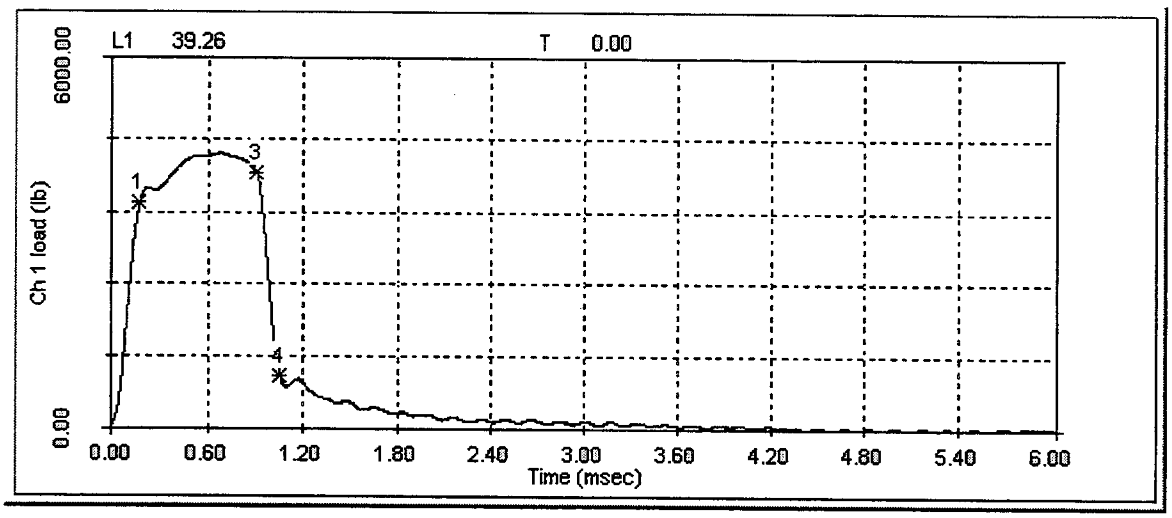

Figure A-11 Load-Time record for tangential specimen WL13 tested at 125°F.

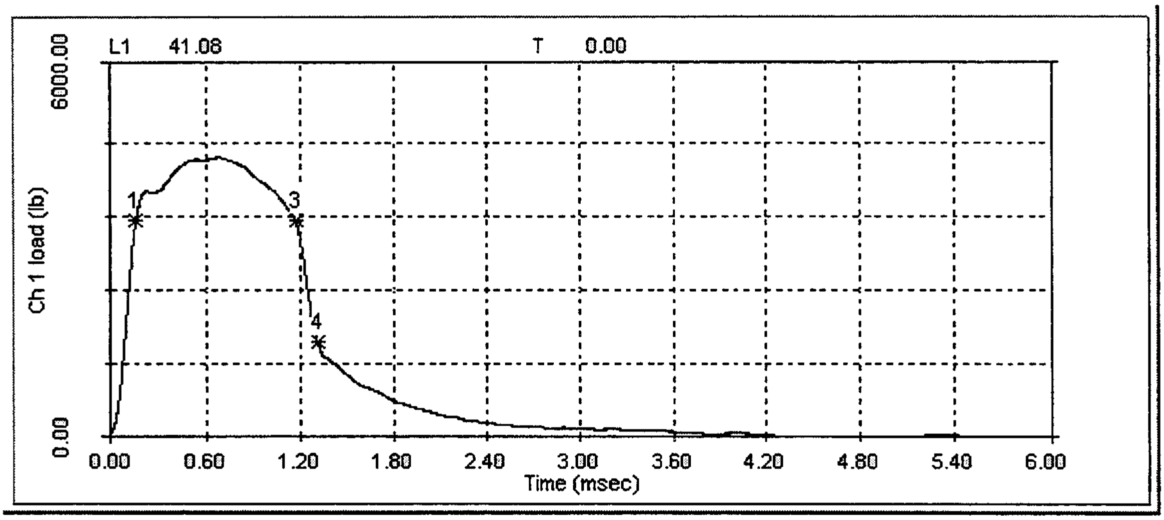

Figure A-12 Load-Time record for tangential specimen WL10 tested at 150°F.

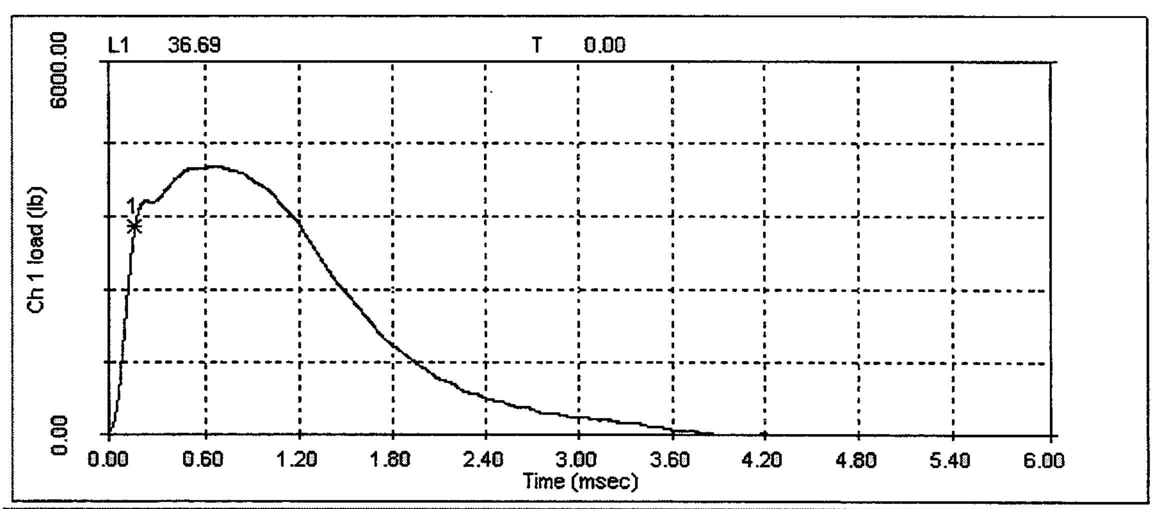

Figure A-13 Load-Time record for tangential specimen WL6 tested at 200°F.

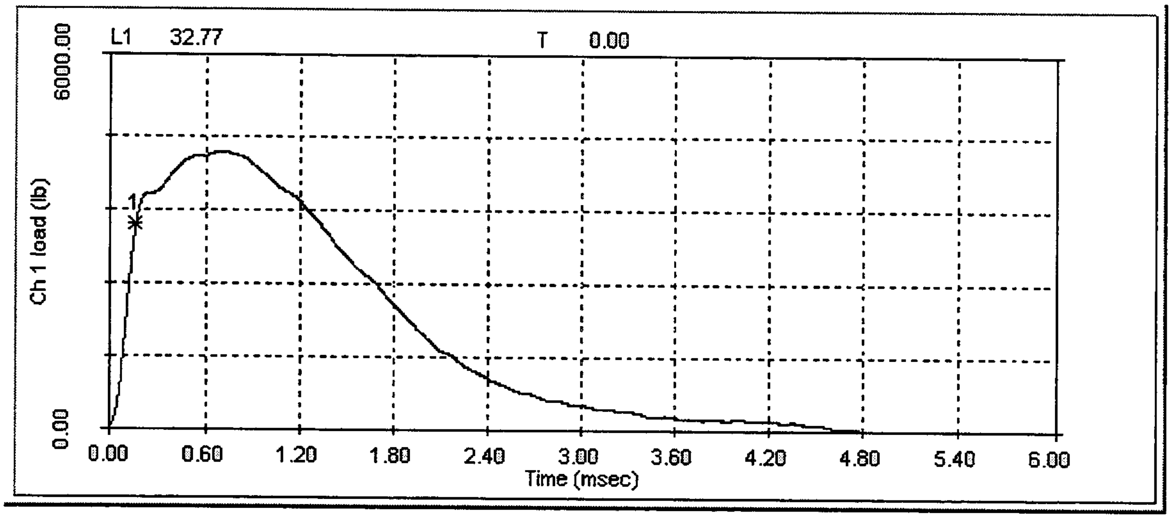

Figure A-14 Load-Time record for tangential specimen WL14 tested at 250°F.

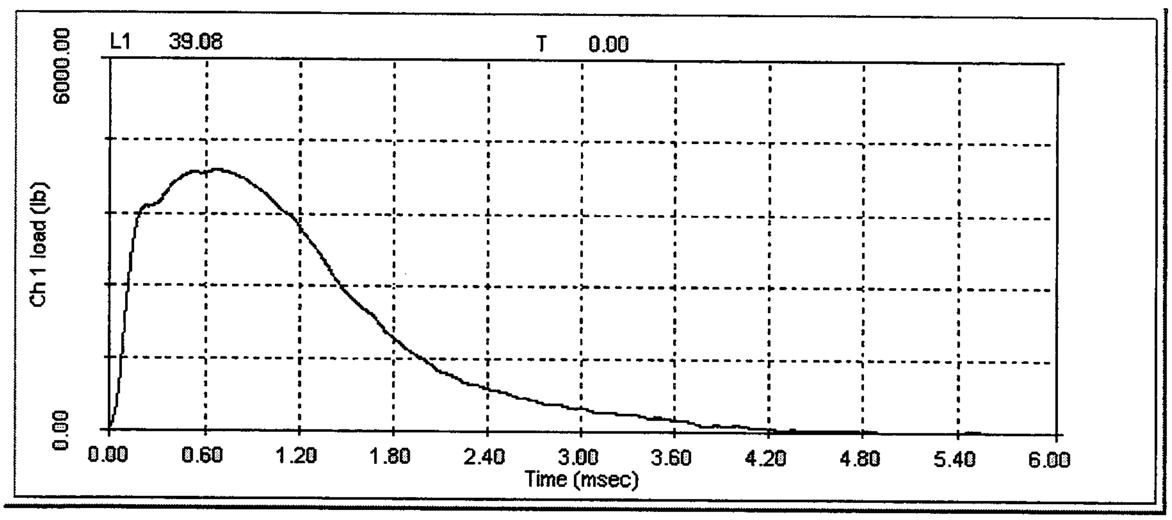

Figure A-15 Load-Time record for tangential specimen WL8 tested at 300°F.

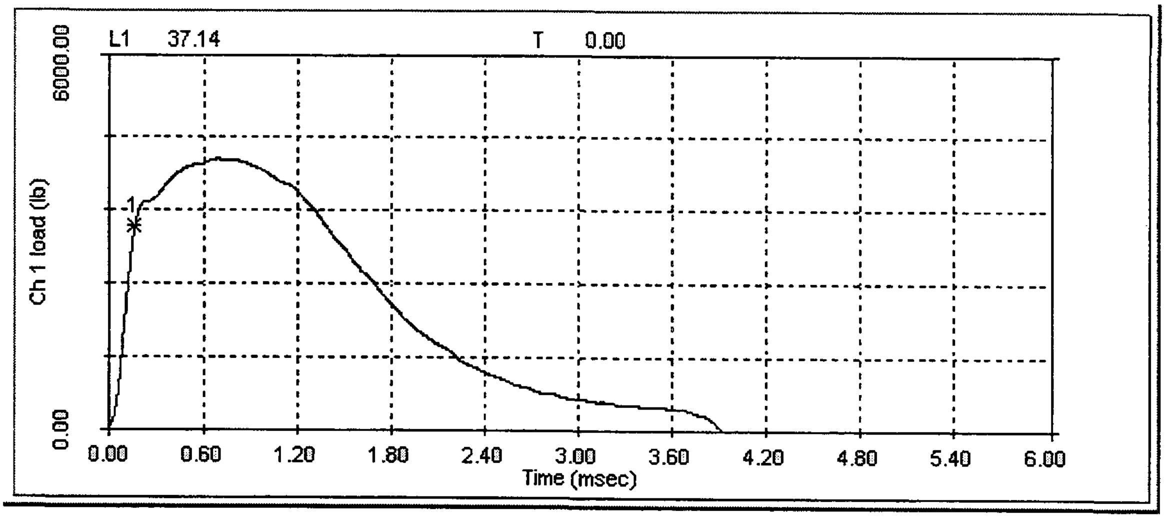

Figure A-16 Load-Time record for tangential specimen WL15 tested at 350°F.

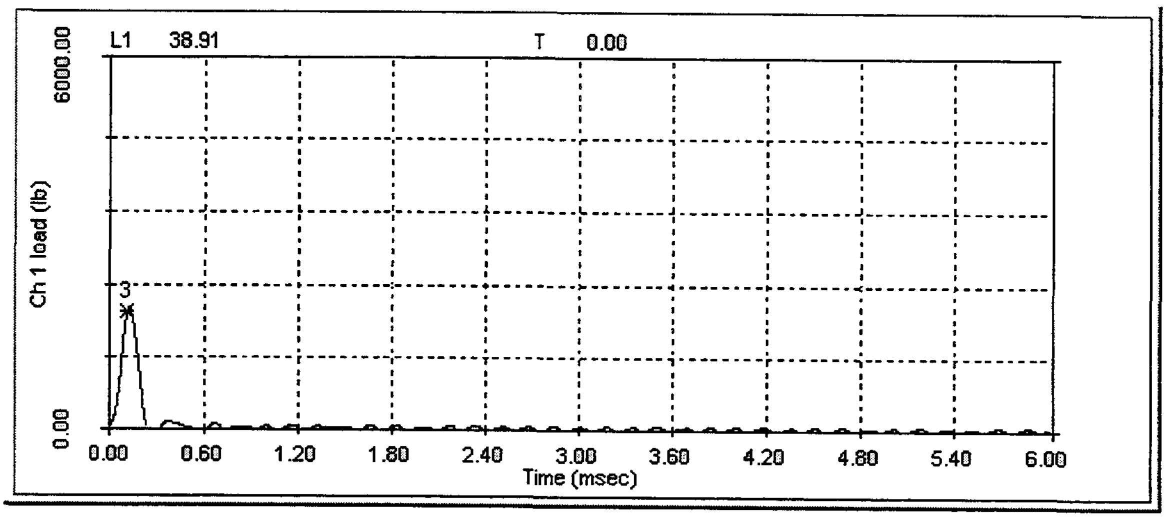

Figure A-17 Load-Time record for axial specimen WT5 tested at -100°F.

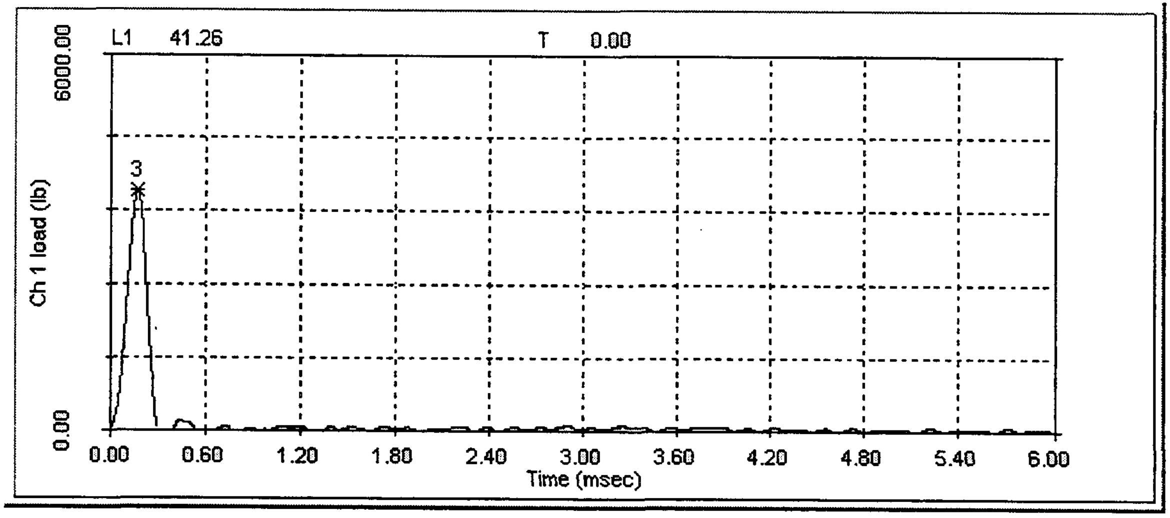

Figure A-18 Load-Time record for axial specimen WT12 tested at -20°F.

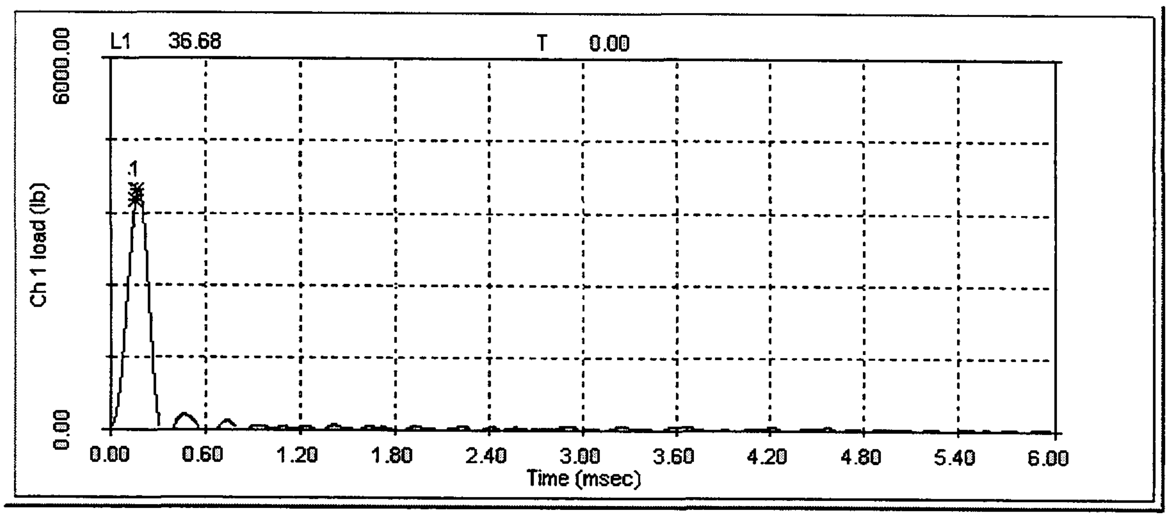

Figure A-19 Load-Time record for axial specimen WT2 tested at 10°F.

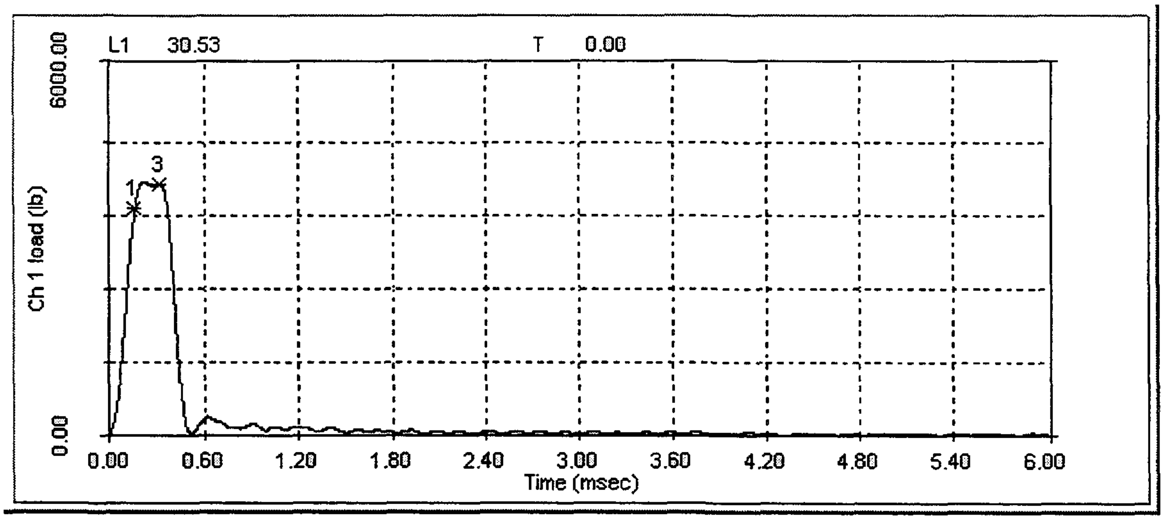

Figure A-20 Load-Time record for axial specimen WT14 tested at 50°F.

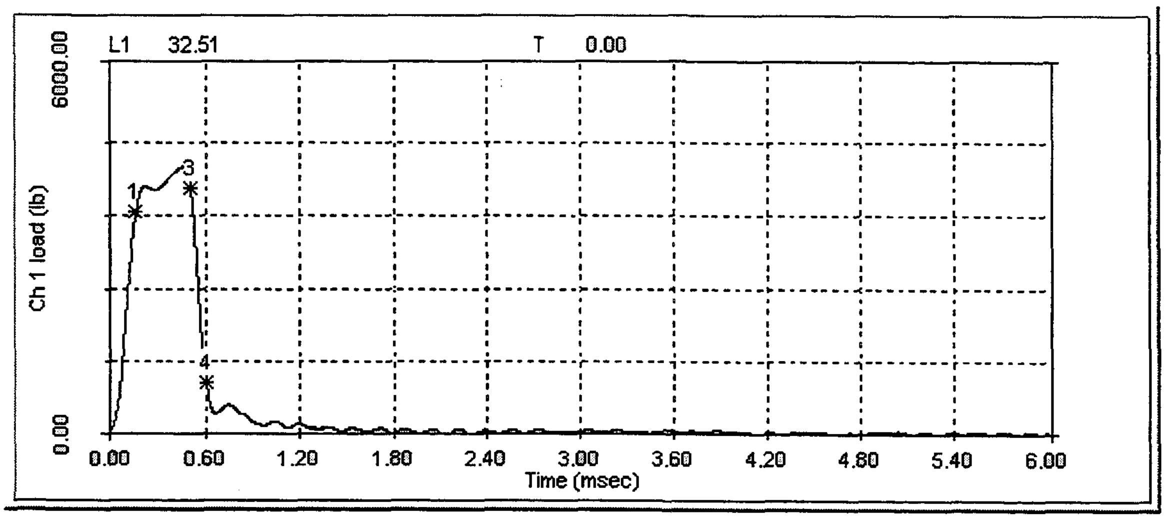

Figure A-21 Load-Time record for axial specimen WT6 tested at 75°F.

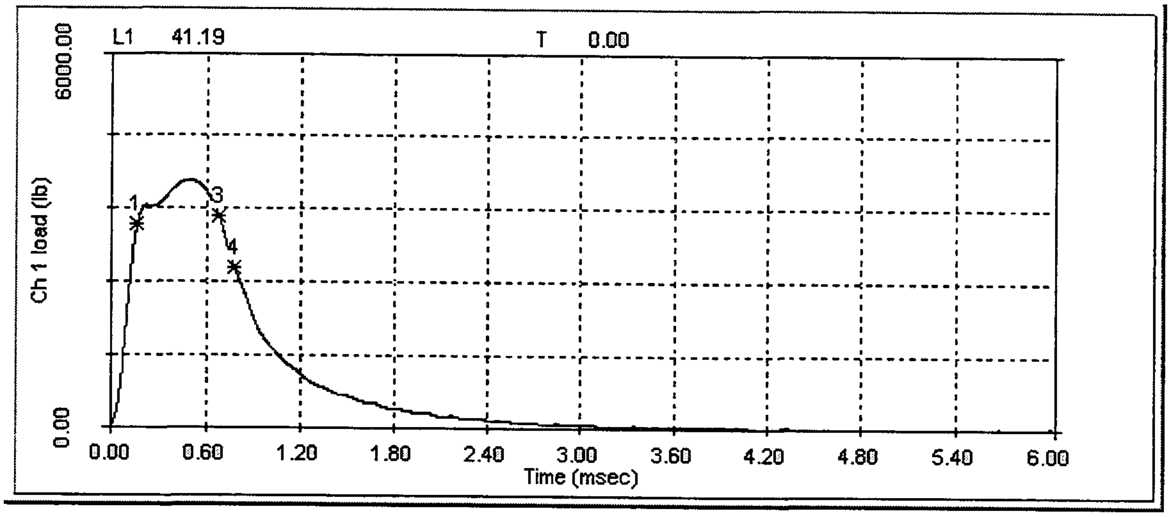

Figure A-22 Load-Time record for axial specimen WT7 tested at 75°F.

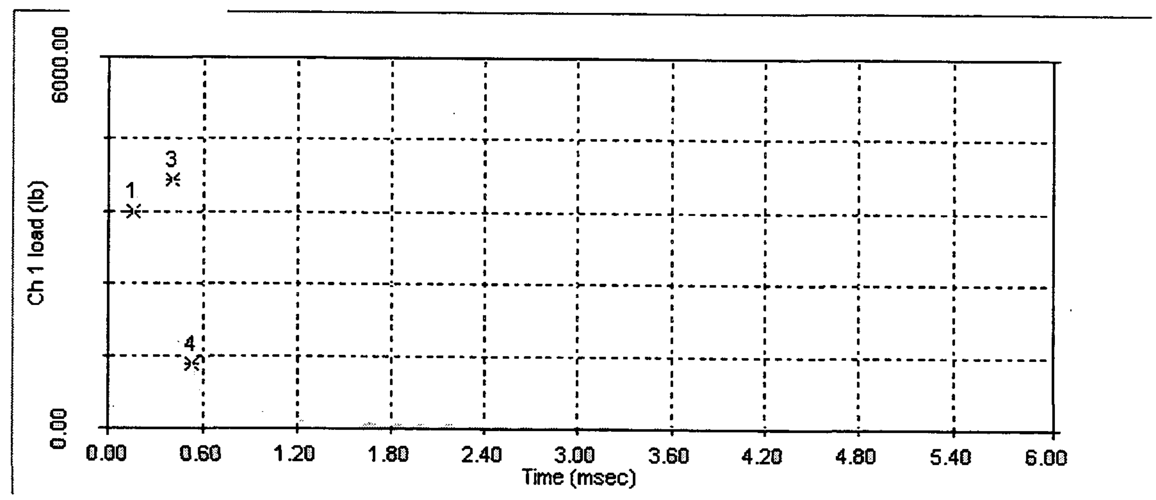

Figure A-23 Load-Time record for axial specimen WT11 tested at 100°F.

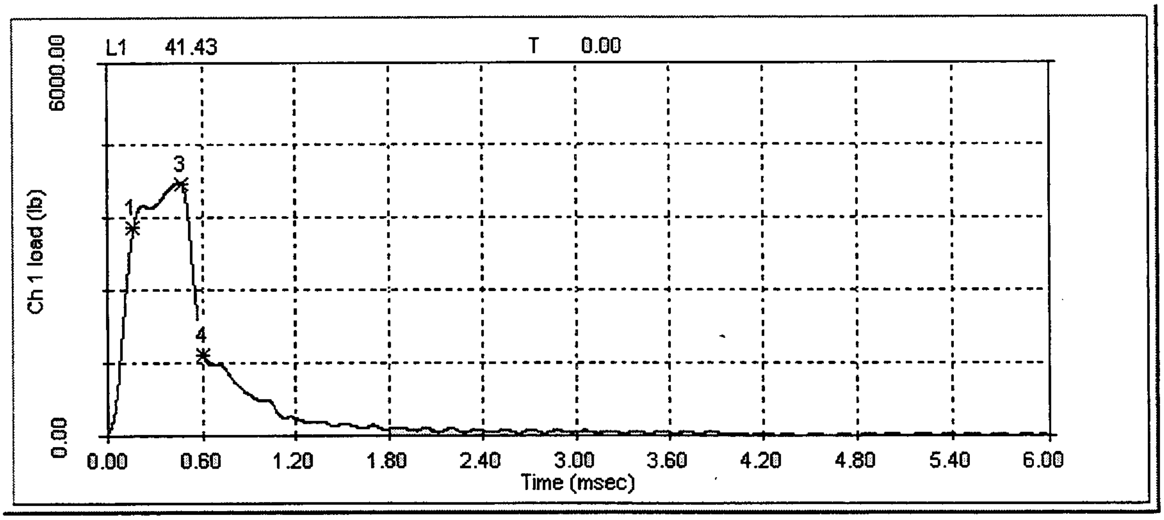

Figure A-24 Load-Time record for axial specimen WT3 tested at 125°F.

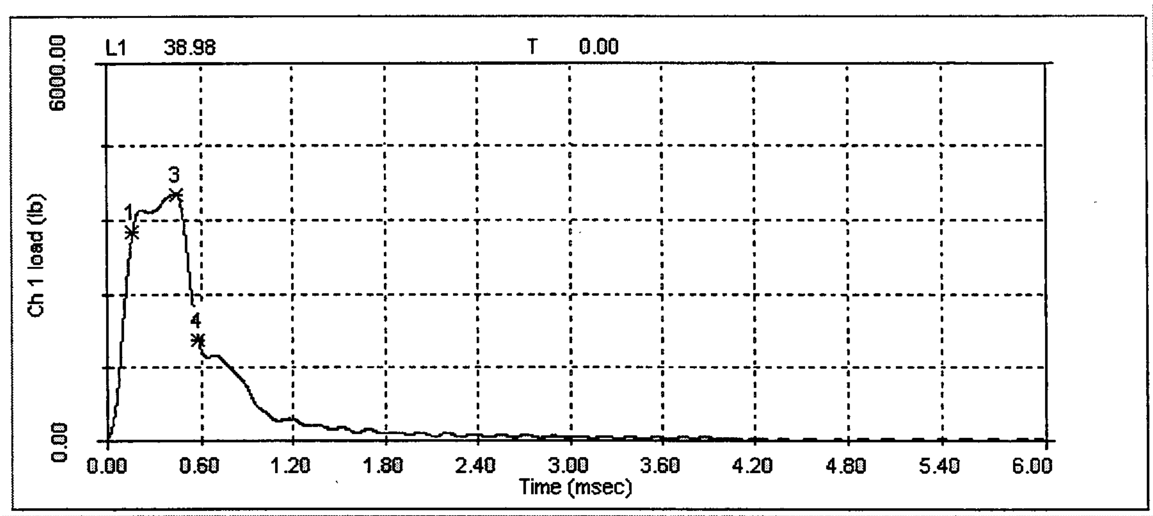

Figure A-25 Load-Time record for axial specimen WT9 tested at 150°F.

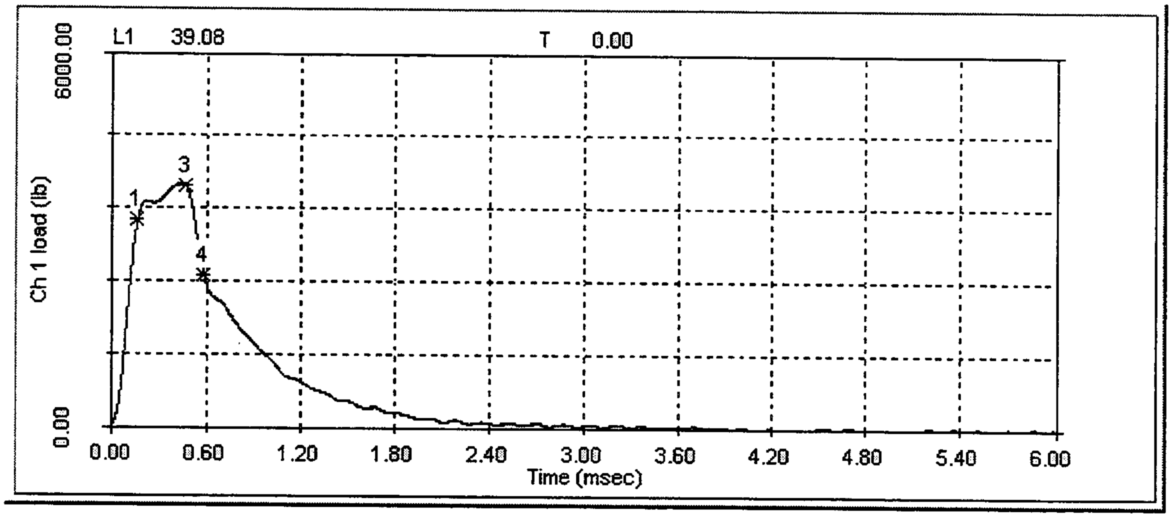

Figure A-26 Load-Time record for axial specimen WT4 tested at 175°F.

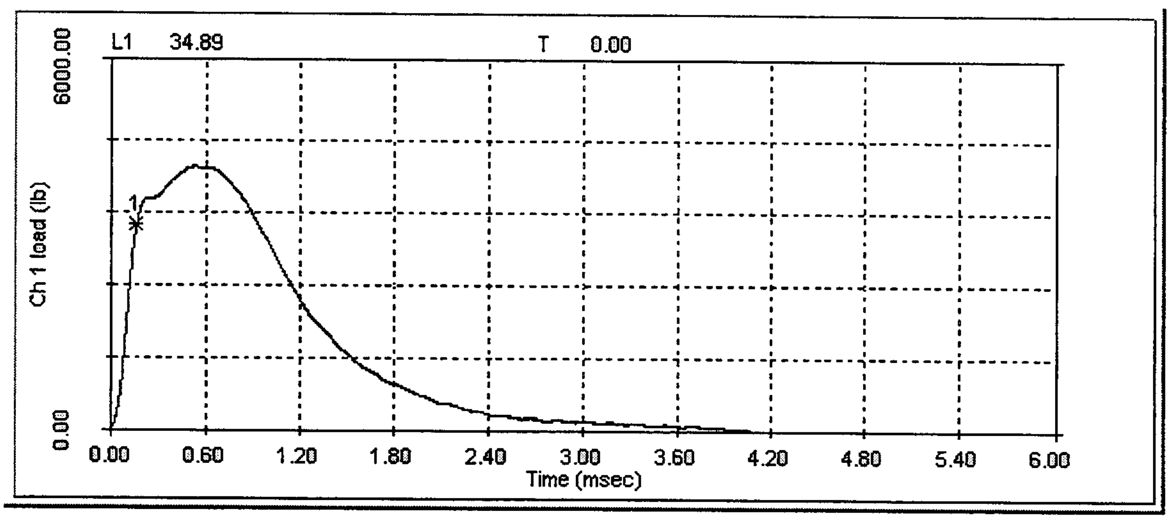

Figure A-27 Load-Time record for axial specimen WT1 tested at 225°F.

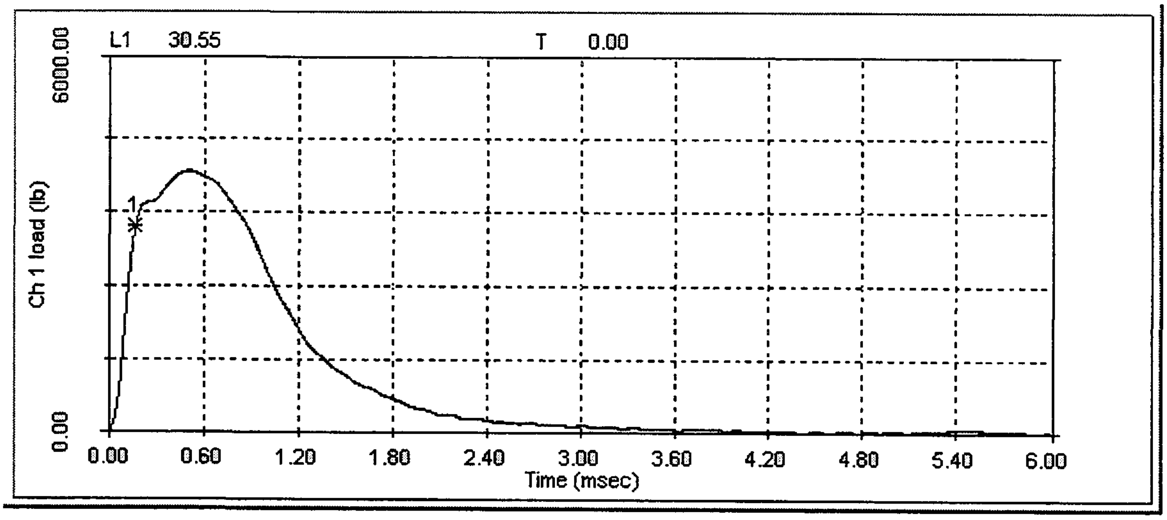

Figure A-28 Load-Time record for axial specimen WT13 tested at 250°F.

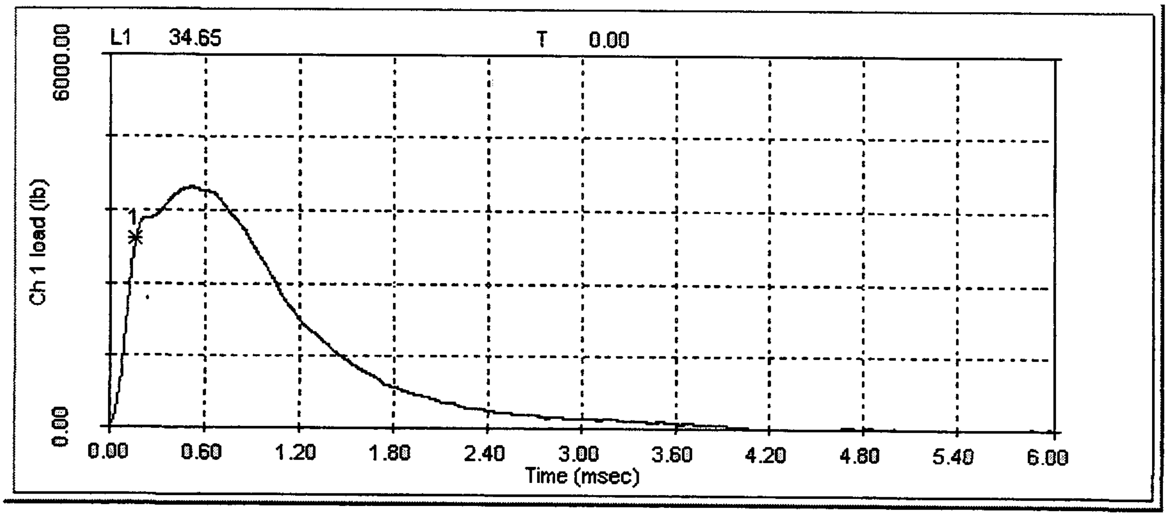

Figure A-29 Load-Time record for axial specimen WT10 tested at 300°F.

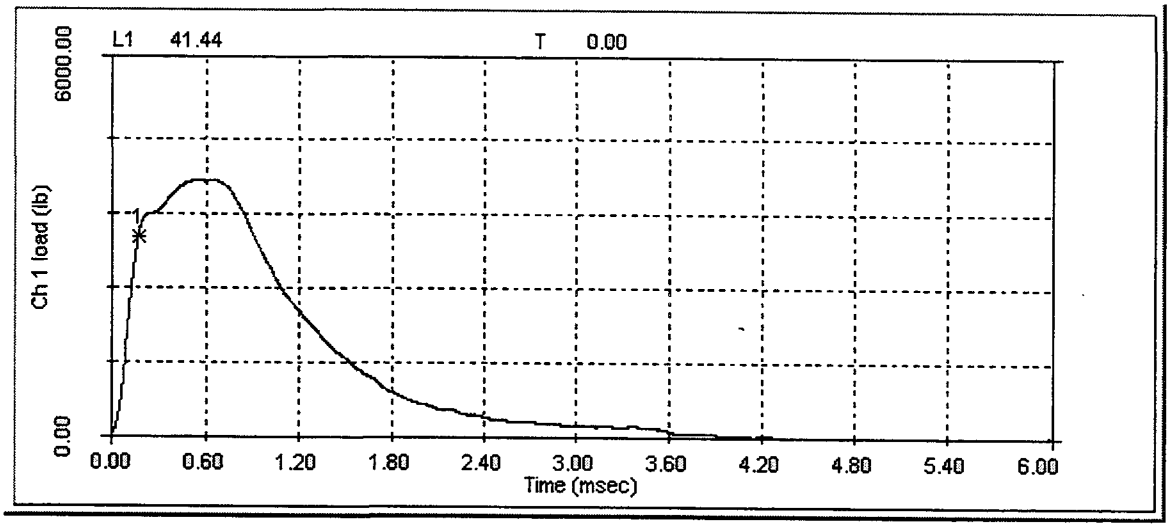

Figure A-30 Load-Time record for axial specimen WT8 tested at 350°F.

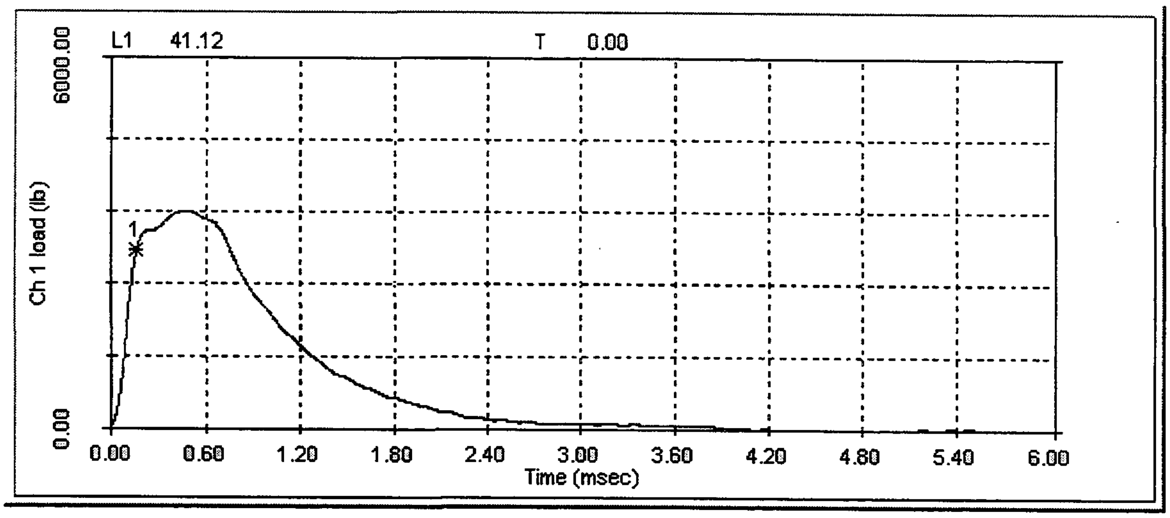

Figure A-31 Load-Time record for axial specimen WT15 tested at 400°F.

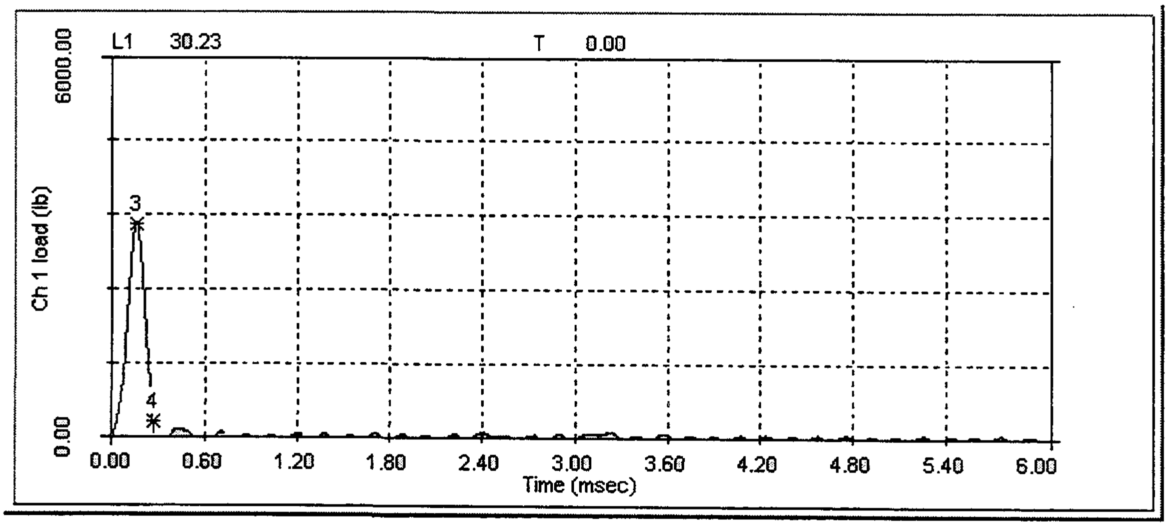

Figure A-32 Load-Time record for weld specimen WW6 tested at -100°F.

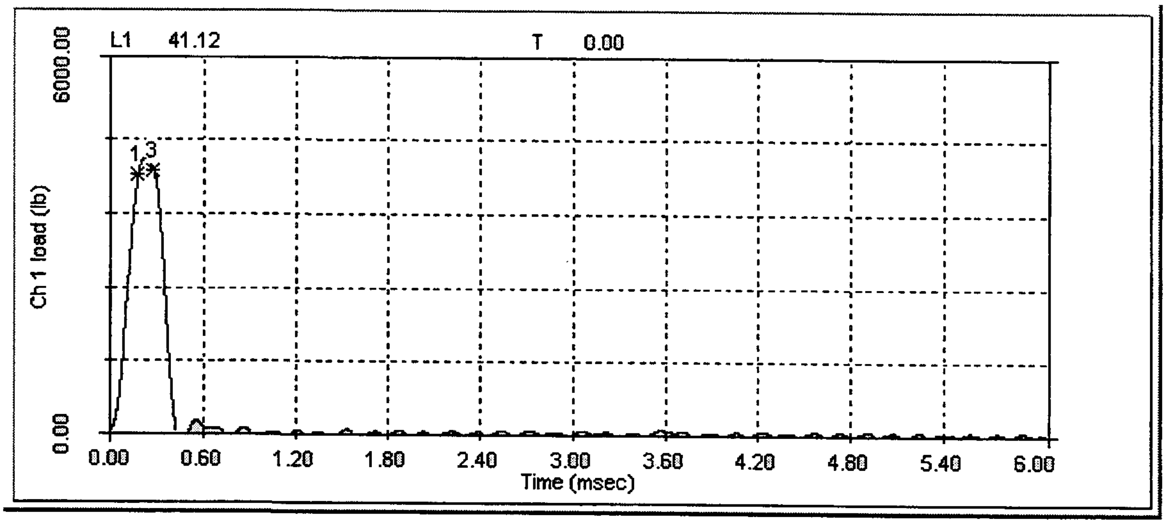

Figure A-33 Load-Time record for weld specimen WW4 tested at -50°F.

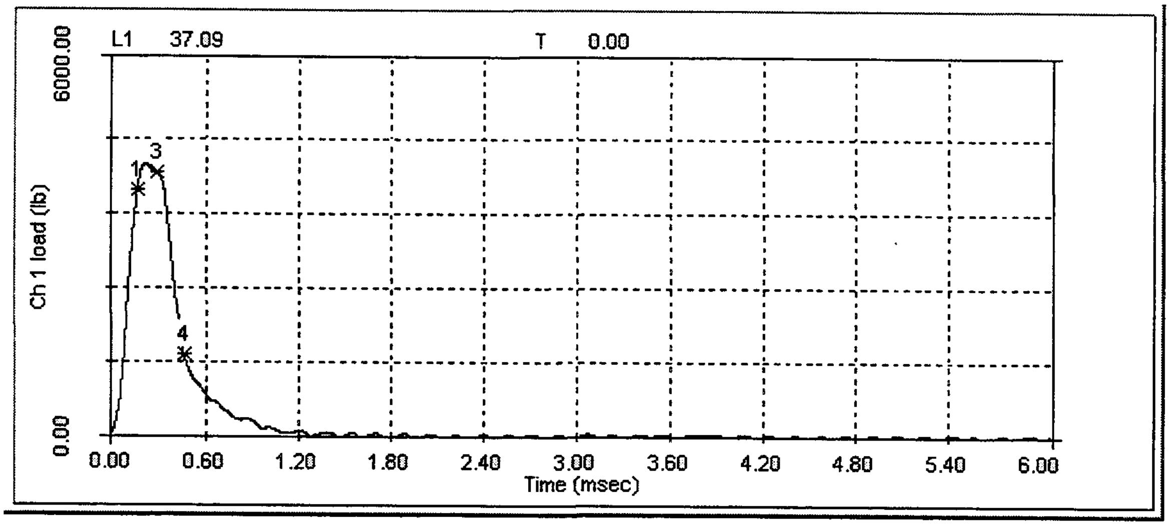

Figure A-34 Load-Time record for weld specimen WW1 tested at -25°F.

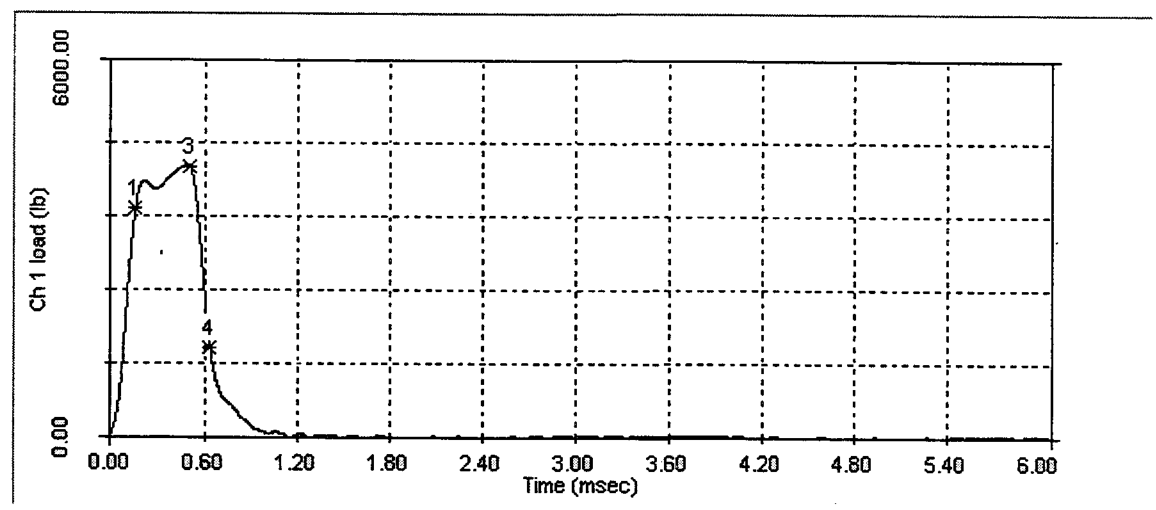

Figure A-35 Load-Time record for axial specimen WW7 tested at 0°F.

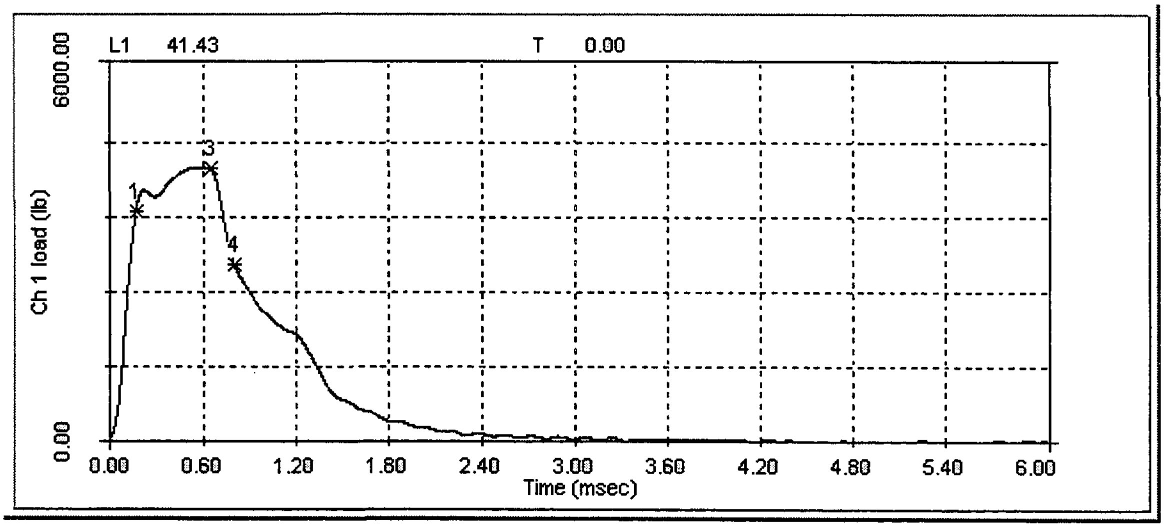

Figure A-36 Load-Time record for weld specimen WW11 tested at 20°F.

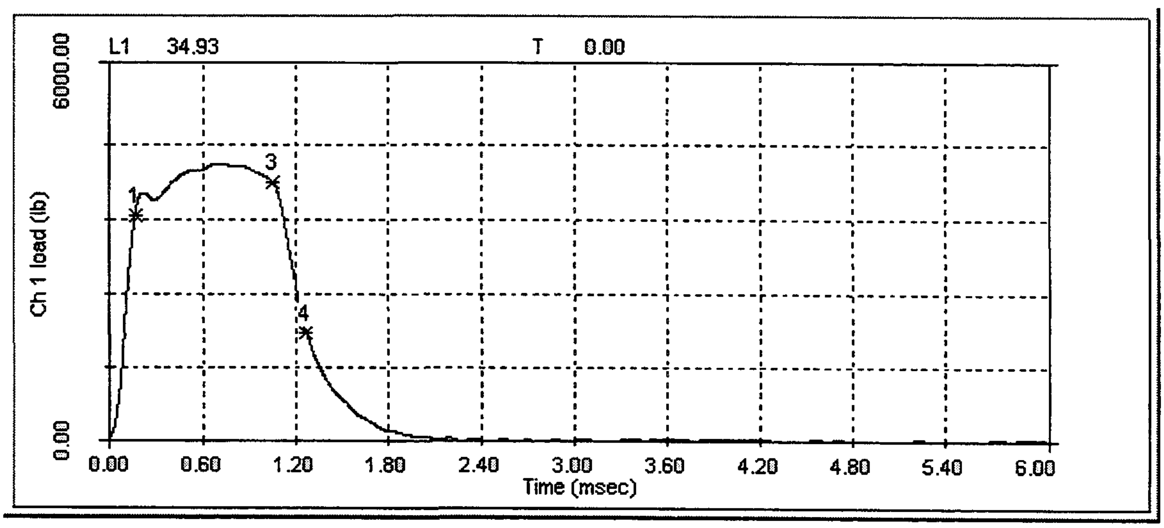

Figure A-37 Load-Time record for weld specimen WW10 tested at 35°F.

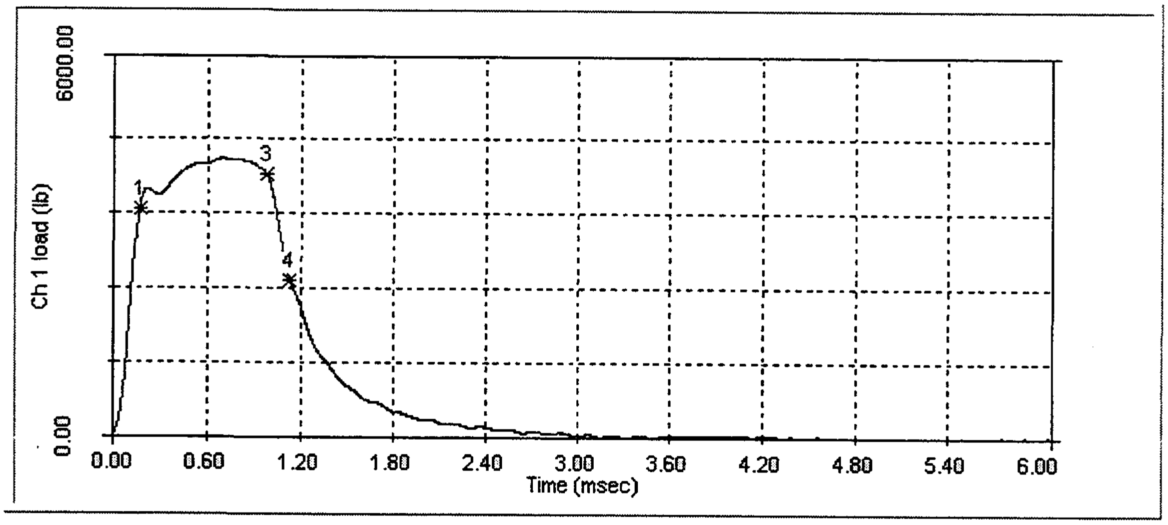

Figure A-38 Load-Time record for weld specimen WW12 tested at 50°F.

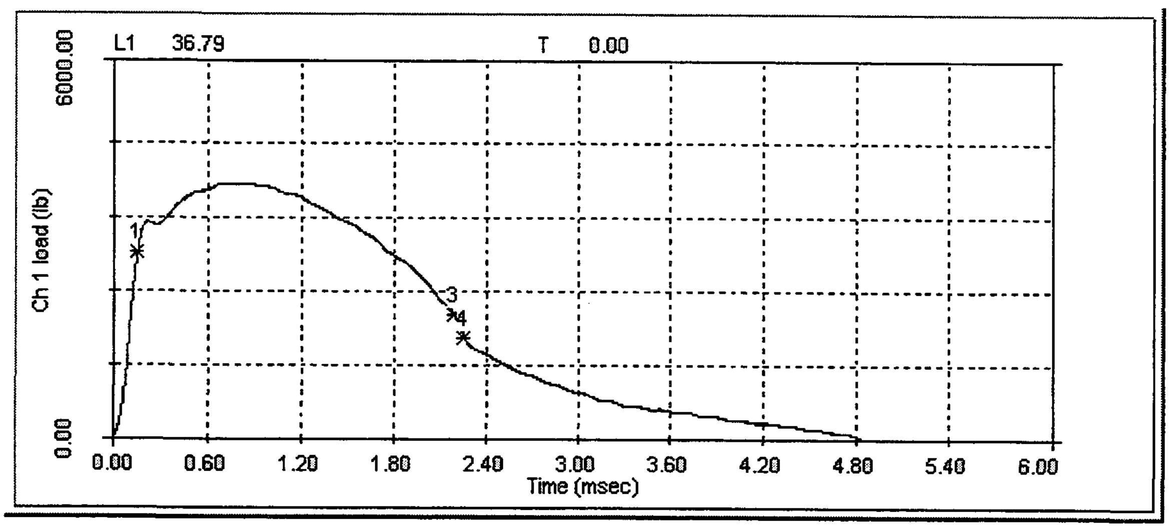

Figure A-39 Load-Time record for weld specimen WW13 tested at 75°F.

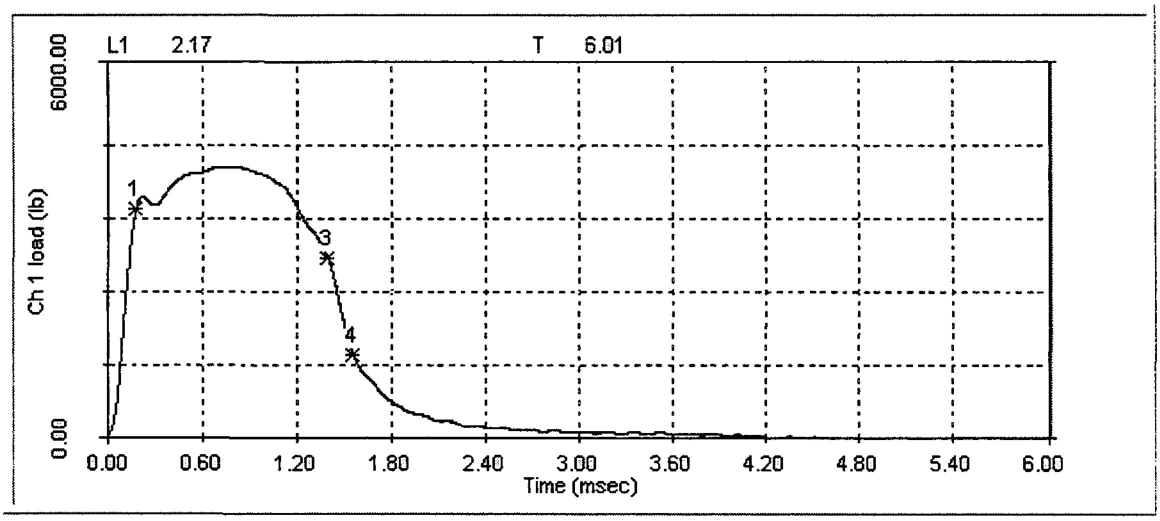

Figure A-40 Load-Time record for weld specimen WW8 tested at 75°F.

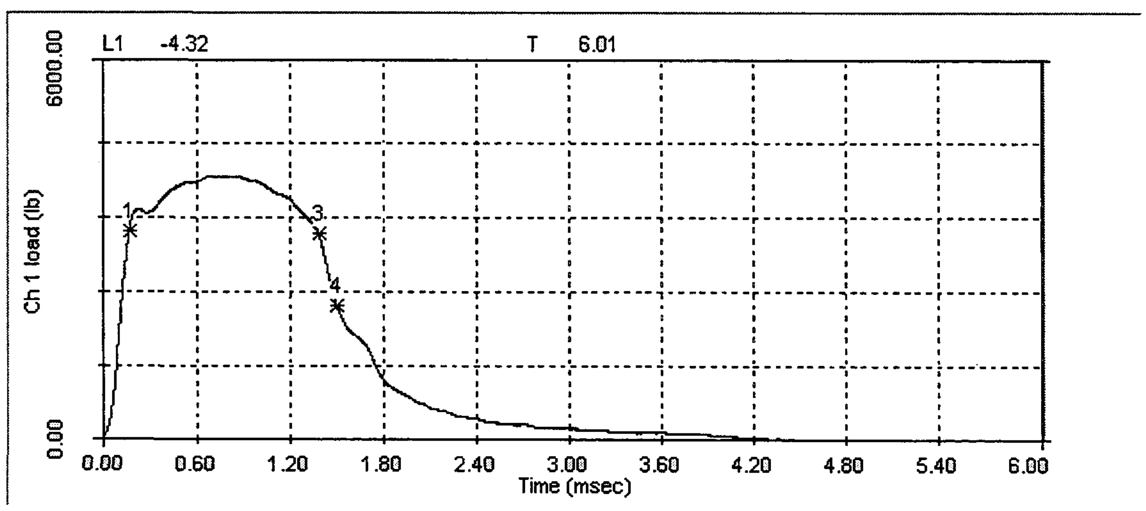

Figure A-41 Load-Time record for weld specimen WW9 tested at 100°F.

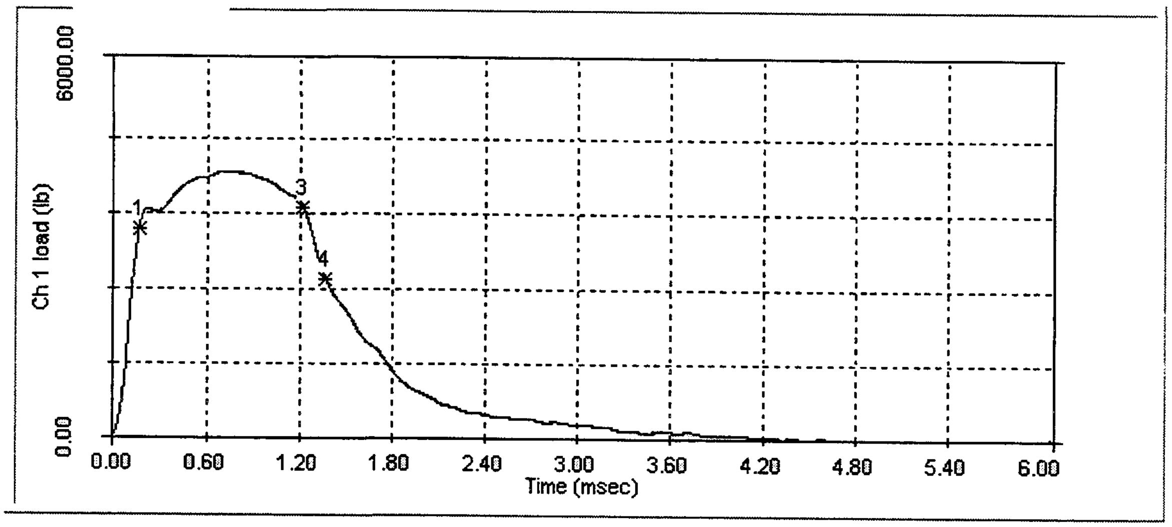

Figure A-42 Load-Time record for weld specimen WW2 tested at 125°F.

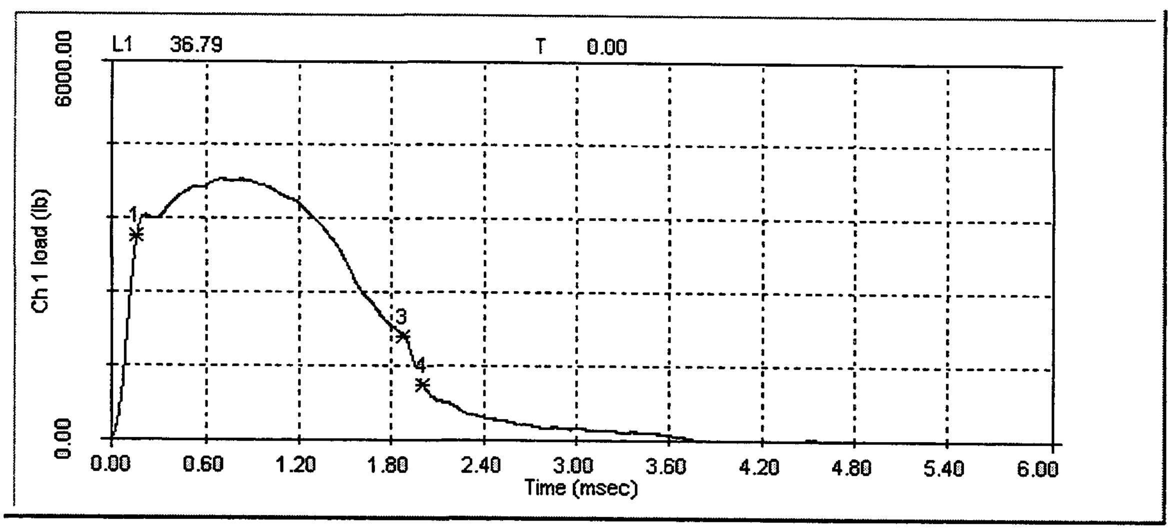

Figure A-43 Load-Time record for weld specimen WW5 tested at 150°F.

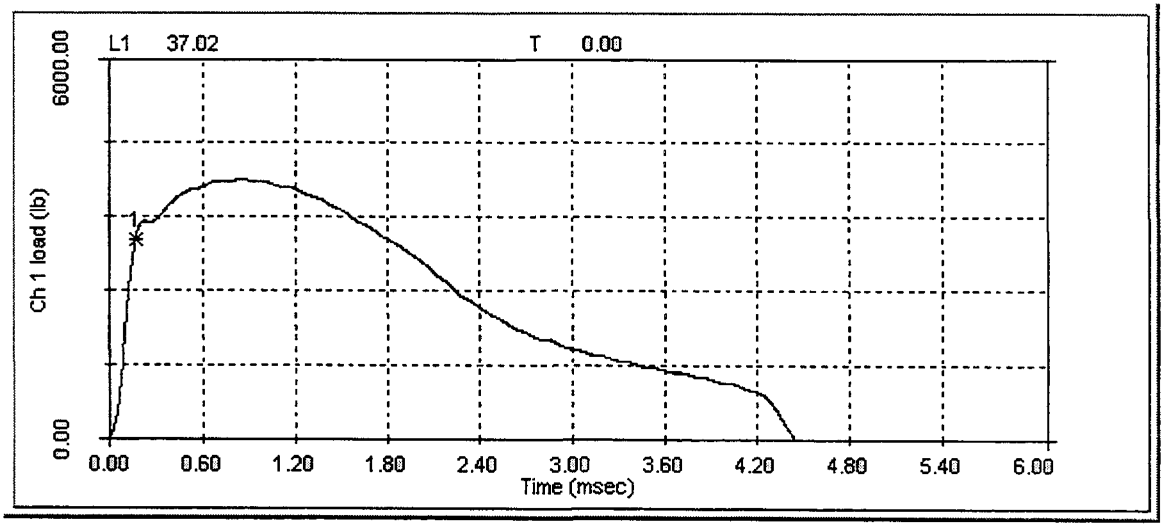

Figure A-44 Load-Time record for weld specimen WW15 tested at 250°F.

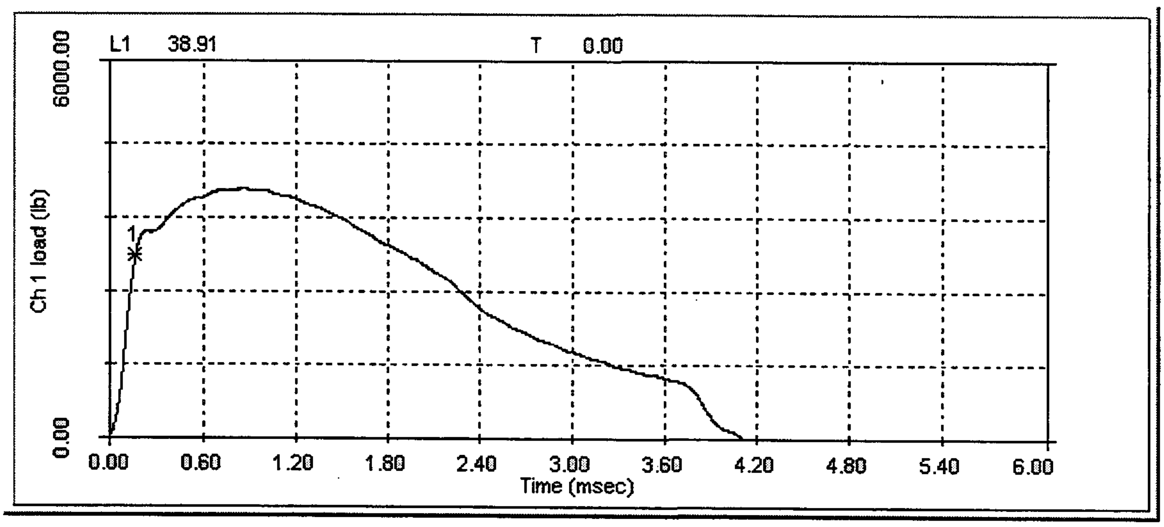

Figure A-45 Load-Time record for weld specimen WW3 tested at 300°F.

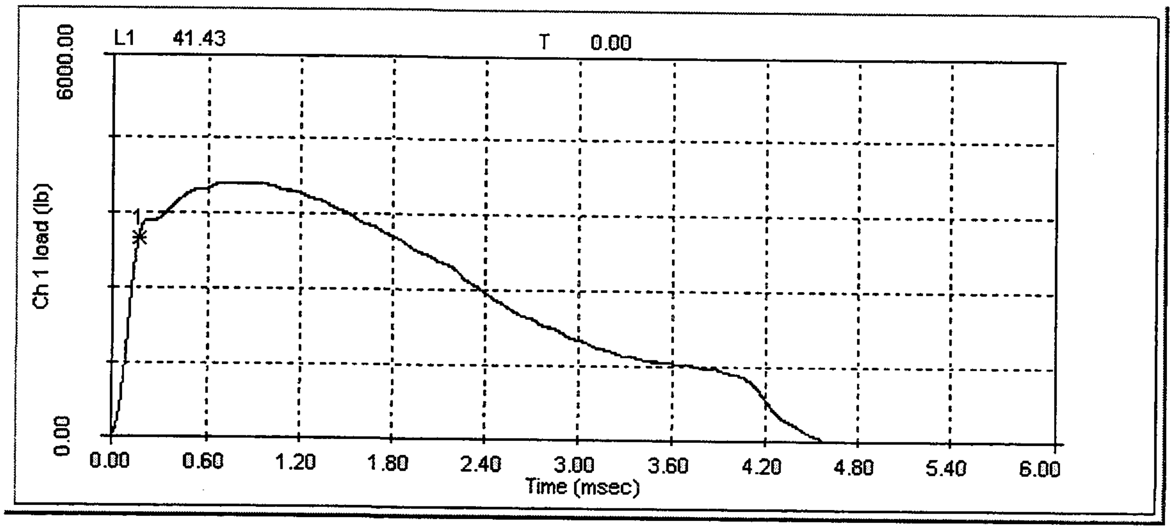

Figure A-46 Load-Time record for weld specimen WW14 tested at 350°F.

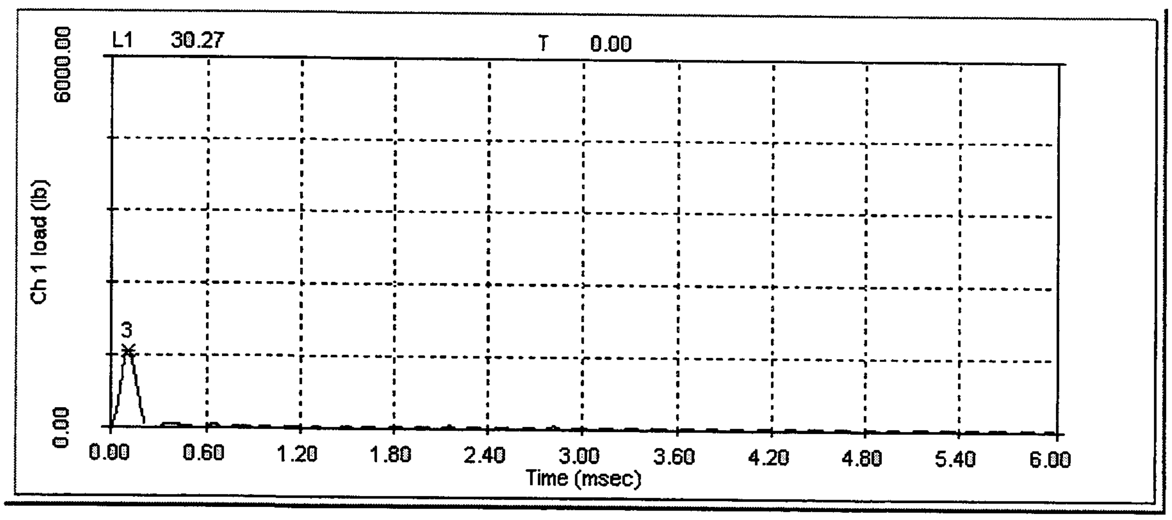

Figure A-47 Load-Time record for HAZ specimen WH11 tested at -175°F.

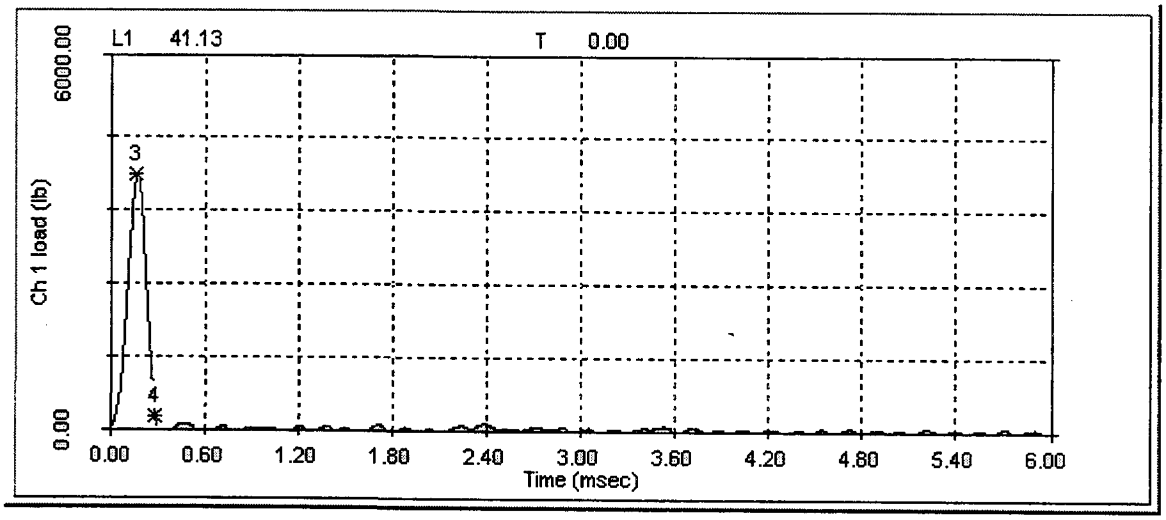

Figure A-48 Load-Time record for HAZ specimen WH9 tested at -100°F.

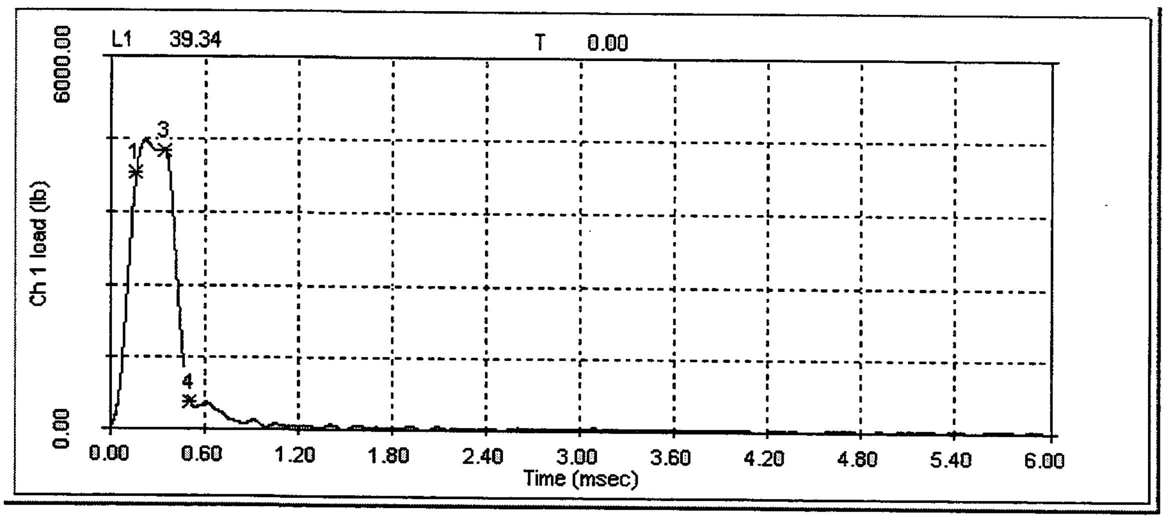

Figure A-49 Load-Time record for HAZ specimen WH2 tested at -25°F.

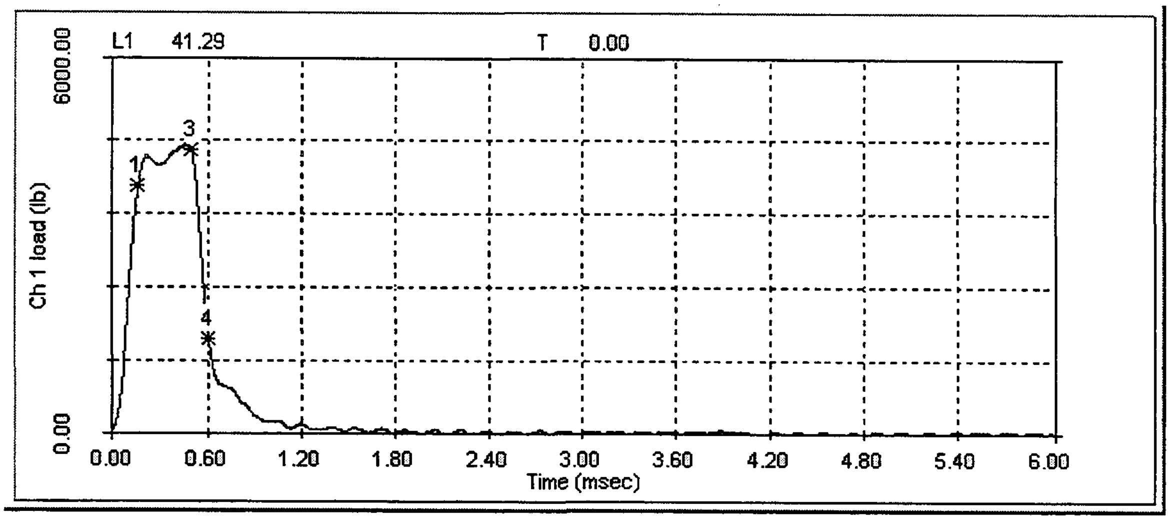

Figure A-50 Load-Time record for HAZ specimen WH14 tested at 0°F.

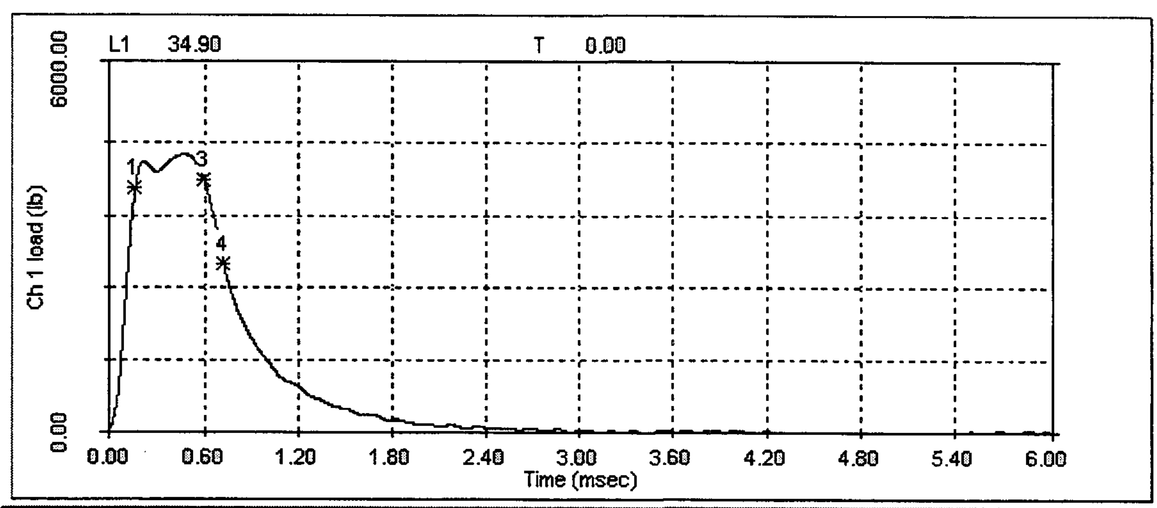

Figure A-51 Load-Time record for HAZ specimen WH5 tested at 25°F.

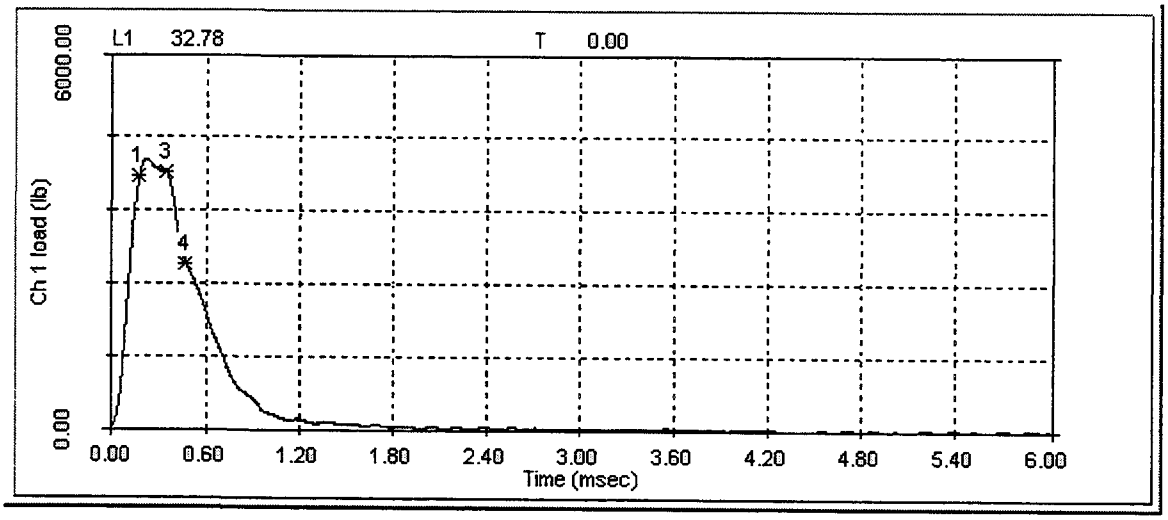

Figure A-52 Load-Time record for HAZ specimen WH15 tested at 40°F.

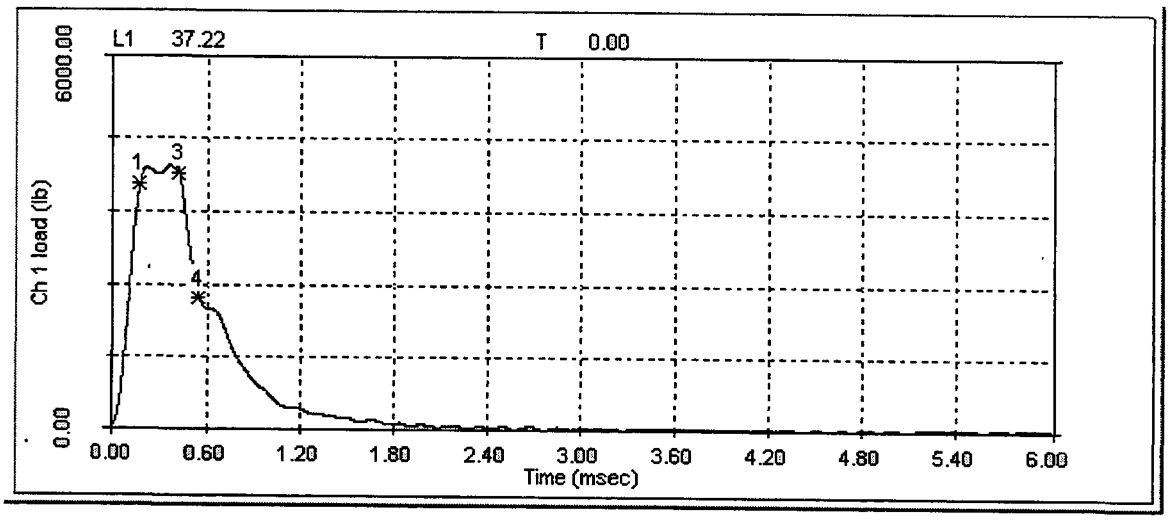

Figure A-53 Load-Time record for HAZ specimen WW7 tested at 50°F.

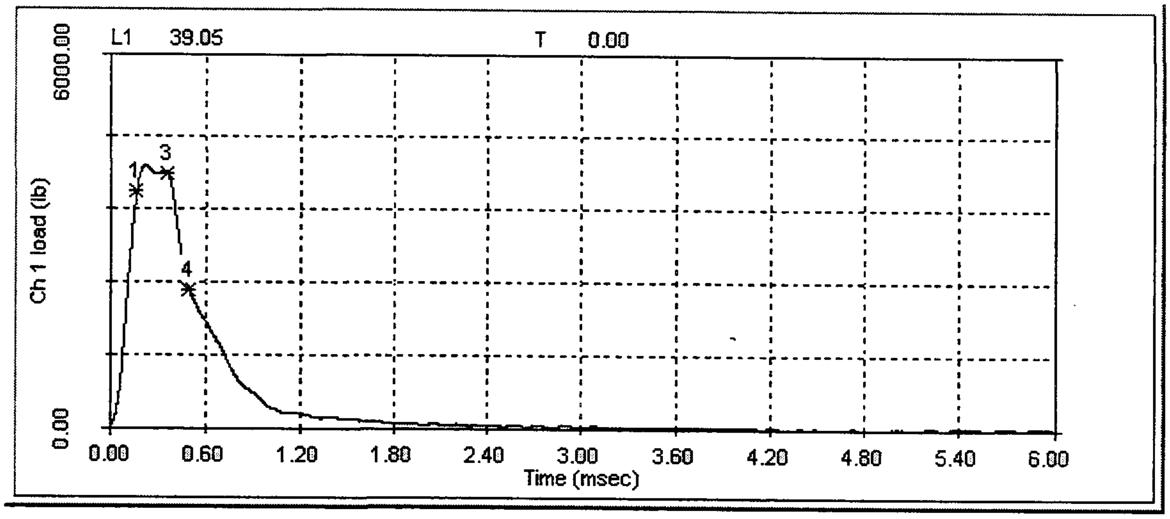

Figure A-54 Load-Time record for HAZ specimen WH13 tested at 60°F.

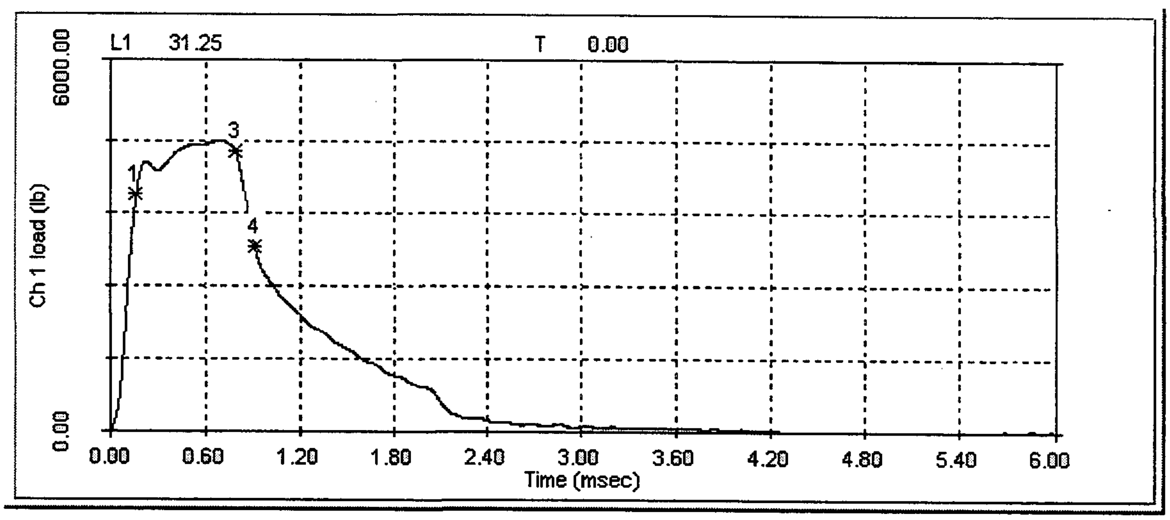

Figure A-55 Load-Time record for HAZ specimen WH8 tested at 70°F.

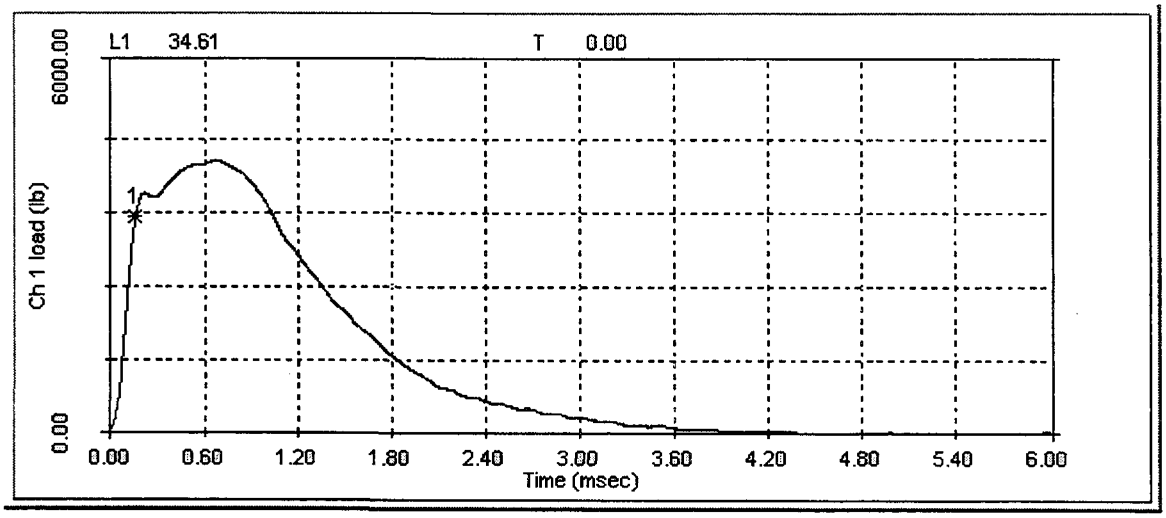

Figure A-56 Load-Time record for HAZ specimen WH12 tested at 75°F.

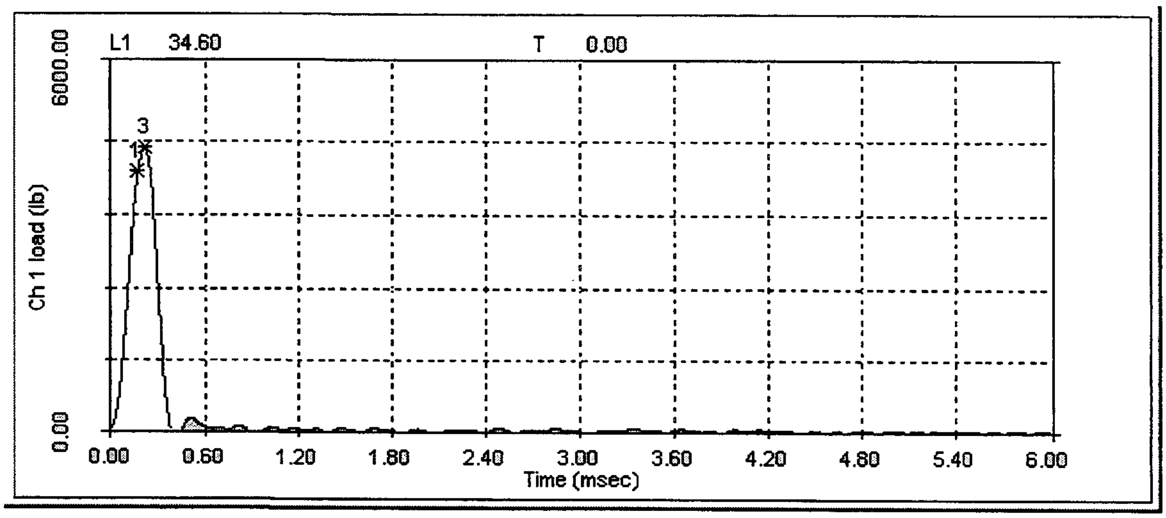

Figure A-57 Load-Time record for HAZ specimen WH3 tested at 75°F.

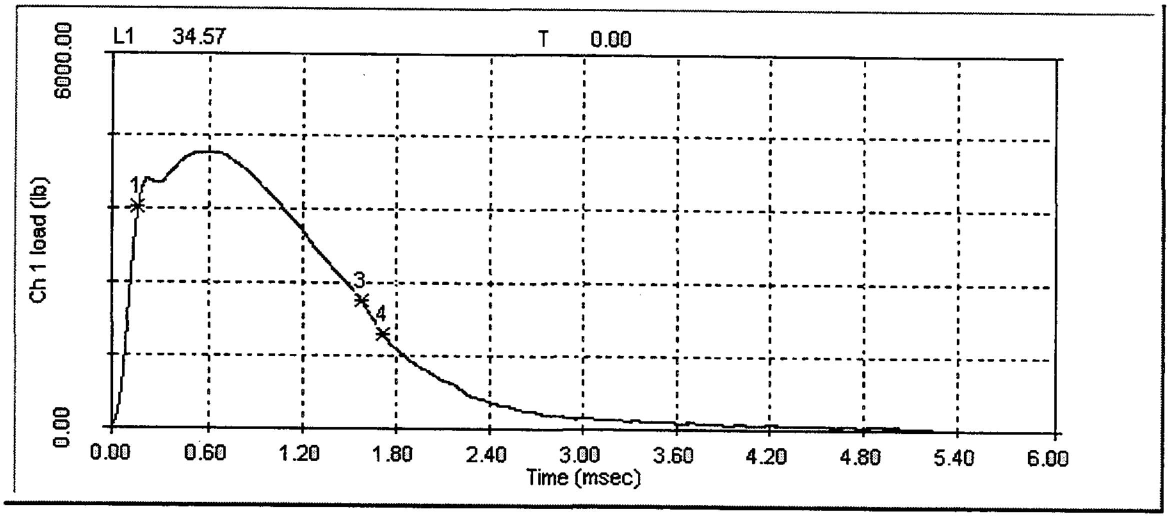

Figure A-58 Load-Time record for HAZ specimen WH10 tested at 100°F.

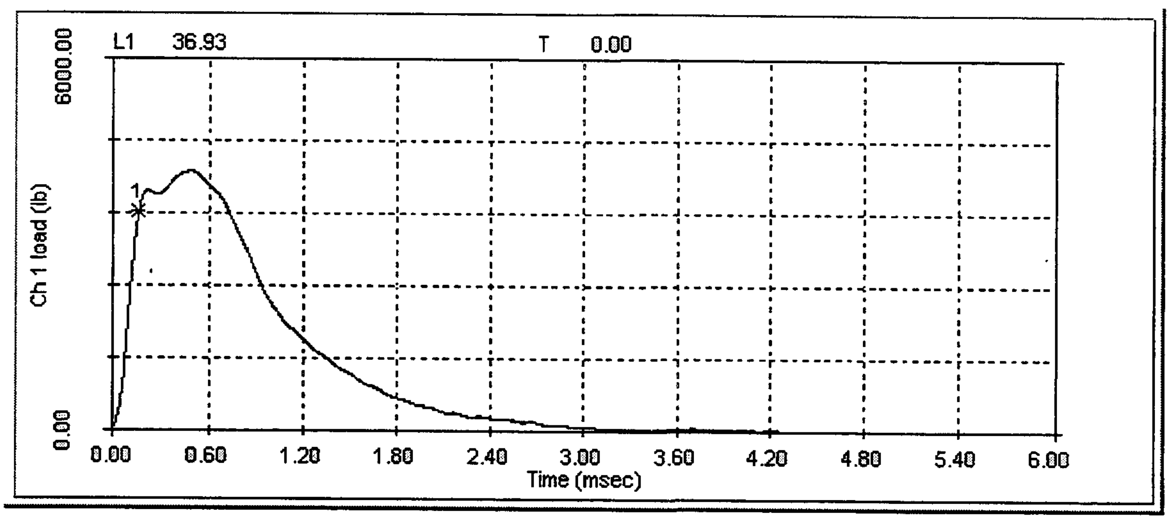

Figure A-59 Load-Time record for HAZ specimen WH1 tested at 150°F.

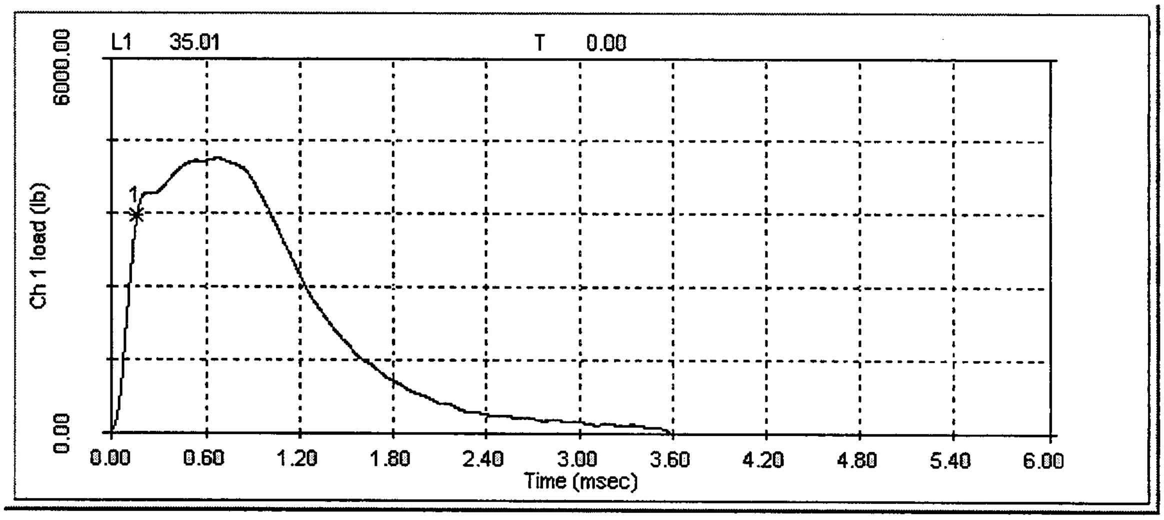

Figure A-60 Load-Time record for HAZ specimen WH4 tested at 250°F.

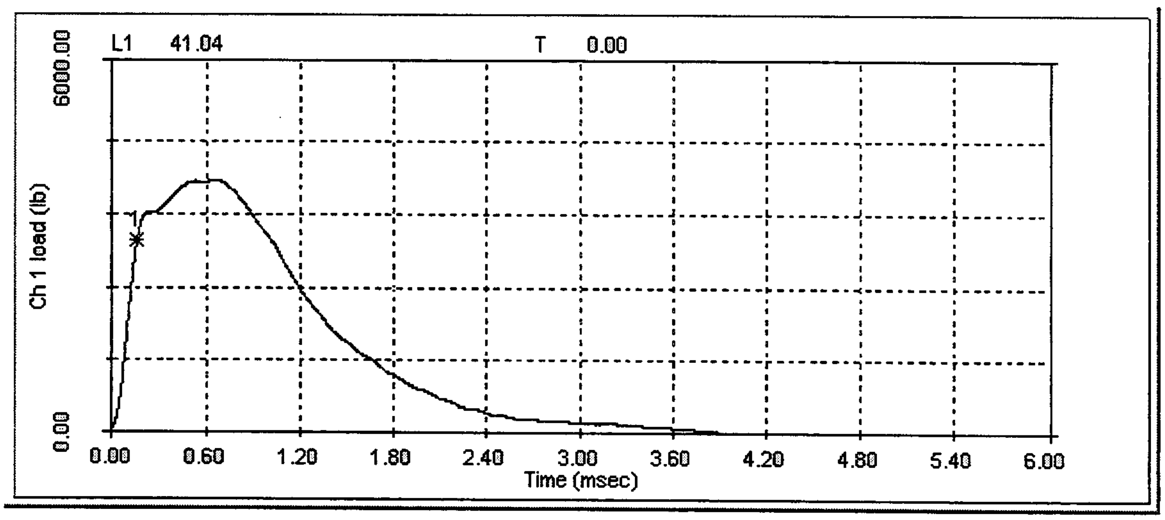

Figure A-61 Load-Time record for HAZ specimen WH6 tested at 300°F.

APPENDIX B

Charpy V-Notch Plots for Each Capsule Using Hyperbolic Tangent Curve-Fitting Method

Contained in Table B-1 are the upper shelf energy values used as input for the generation of the Charpy V-notch plots using CVGRAPH, Version 4.1. Lower shelf energy values were fixed at 2.2 ft-lb. The unirradiated and irradiated upper shelf energy values were calculated per the ASTM E185-82 definition of upper shelf energy.

TABLE B-1

Upper Shelf Energy Values Fixed in CVGRAPH

Material	Unirradiated	Capsule U
Intermediate Shell Forging 05 (Tangential Orientation)	132 ft-lb	107 ft-lb
Intermediate Shell Forging 05 (Axial Orientation)	62 ft-lb	72 ft-lb
Weld Metal (Heat # 895075)	131 ft-lb	143 ft-lb
HAZ Material	89 ft-lb	79 ft-lb

CAPSULE–U TANGENTIAL

CVGRAPH 4.1 Hyperbolic Tangent Curve Printed at 12:43:30 on 02-24-1998

Page 1

Coefficients of Curve 1

A = 54.34	B = 52.15	C = 107.5	T0 = 95.13

Equation is: CVN = A + B * [tanh((T - T0)/C)]

Upper Shelf Energy: 106.5 Fixed   Temp. at 30 ft-lbs: 40.7   Temp. at 50 ft-lbs: 86.1   Lower Shelf Energy: 2.19 Fixed

Material: FORGING SA508CL2   Heat Number: 527536 (RING 05)   Orientation: LT

Capsule: U   Total Fluence:

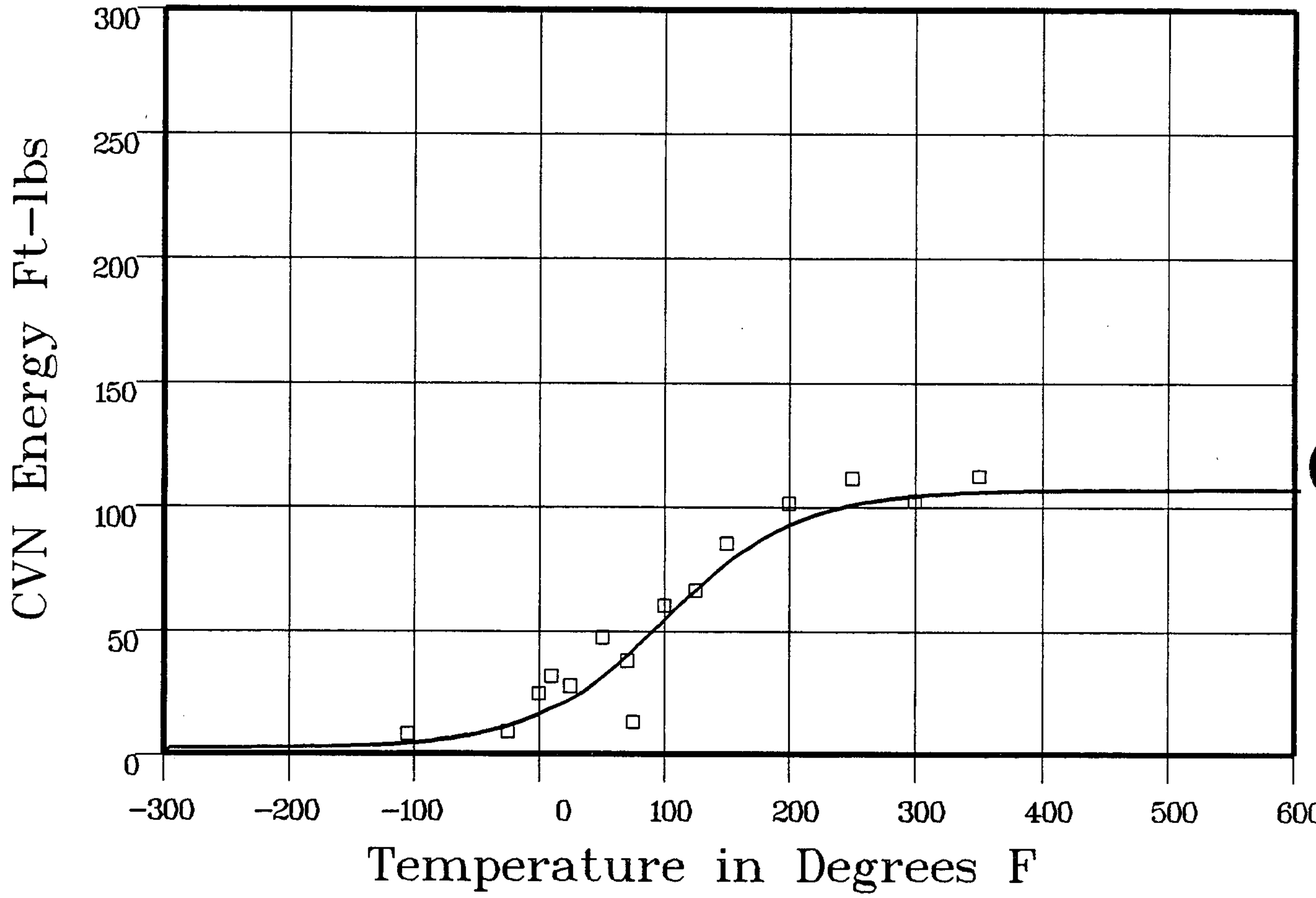

Data Set(s) Plotted

Plant: WB1   Cap.: U   Material: FORGING SA508CL2   Ori.: LT   Heat #: 527536 (RING 05)

Charpy V-Notch Data

Temperature	Input CVN Energy	Computed CVN Energy	Differential
-105	8	4.66	3.33
-25	9	12.28	-3.28
0	25	17.38	7.61
10	32	19.95	12.04
25	28	24.45	3.54
50	47	33.65	13.34
70	38	42.37	-4.37
75	13	44.69	-31.69
100	60	56.7	3.29

**** Data continued on next page ****

CAPSULE–U TANGENTIAL

Page 2

Material: FORGING SA508CL2 Heat Number: 527536 (RING 05) Orientation: LT

Capsule: U Total Fluence:

Charpy V–Notch Data (Continued)

Temperature	Input CVN Energy	Computed CVN Energy	Differential
125	66	68.47	-2.47
150	85	78.87	6.12
200	101	93.51	7.48
250	111	100.96	10.03
300	102	104.24	-2.24
350	112	105.59	6.4

SUM of RESIDUALS = 29.15

CAPSULE–U TANGENTIAL

CVGRAPH 4.1 Hyperbolic Tangent Curve Printed at 13:20:25 on 02-24-1998

Page 1

Coefficients of Curve 1

A = 38.73	B = 37.73	C = 99.5	T0 = 101.36

Equation is: L.E. = A + B * [tanh((T - T0)/C)]

Upper Shelf L.E.: 76.47 Temperature at L.E. 35: 91.4 Lower Shelf L.E.: 1 Fixed

Material: FORGING SA508CL2 Heat Number: 527536 (RING 05) Orientation: LT

Capsule: U Total Fluence:

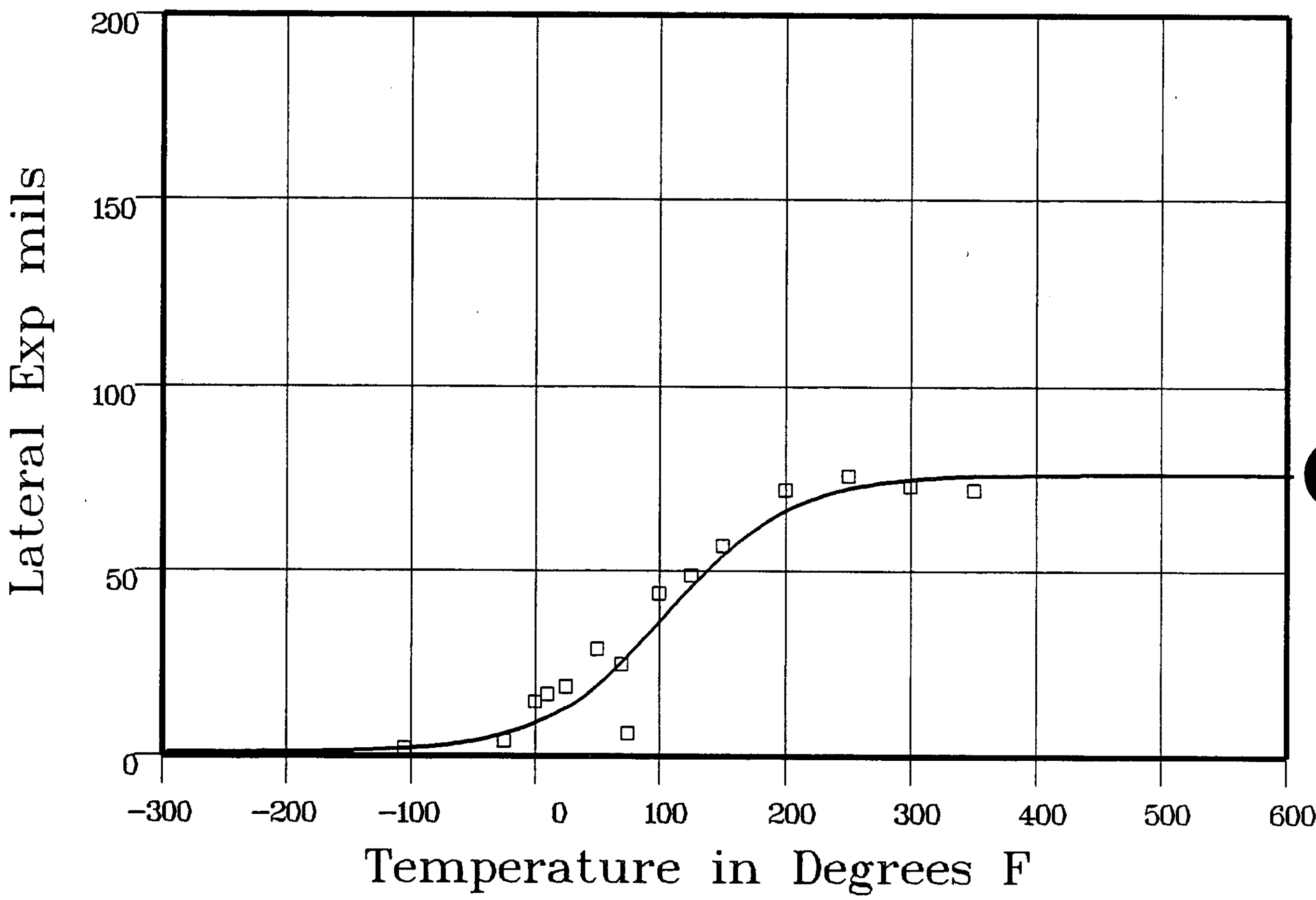

Data Set(s) Plotted

Plant: WB1 Cap.: U Material: FORGING SA508CL2 Ori.: LT Heat #: 527536 (RING 05)

Charpy V-Notch Data

Temperature	Input Lateral Expansion	Computed L.E.	Differential
-105	2	2.17	-.17
-25	4	6.51	-2.51
0	15	9.7	5.29
10	17	11.37	5.62
25	19	14.38	4.61
50	29	20.82	8.17
70	25	27.22	-2.22
75	6	28.96	-22.96
100	44	38.22	5.77

**** Data continued on next page ****

CAPSULE–U TANGENTIAL

Page 2

Material: FORGING SA508CL2 Heat Number: 527536 (RING 05) Orientation: LT

Capsule: U Total Fluence:

Charpy V–Notch Data (Continued)

Temperature	Input Lateral Expansion	Computed L.E.	Differential
125	49	47.53	1.46
150	57	55.84	1.15
200	72	67.34	4.65
250	76	72.85	3.14
300	73	75.11	-2.11
350	72	75.97	-3.97

SUM of RESIDUALS = 5.94

CAPSULE–U TANGENTIAL

CVGRAPH 4.1 Hyperbolic Tangent Curve Printed at 13:38:58 on 02-24-1998

Page 1

Coefficients of Curve 1

A = 50	B = 50	C = 63.58	T0 = 126.56

Equation is: Shear% = A + B * [tanh((T – T0)/C)]

Temperature at 50% Shear: 126.5

Material: FORGING SA508CL2 Heat Number: 527536 (RING 05) Orientation: LT

Capsule: U Total Fluence:

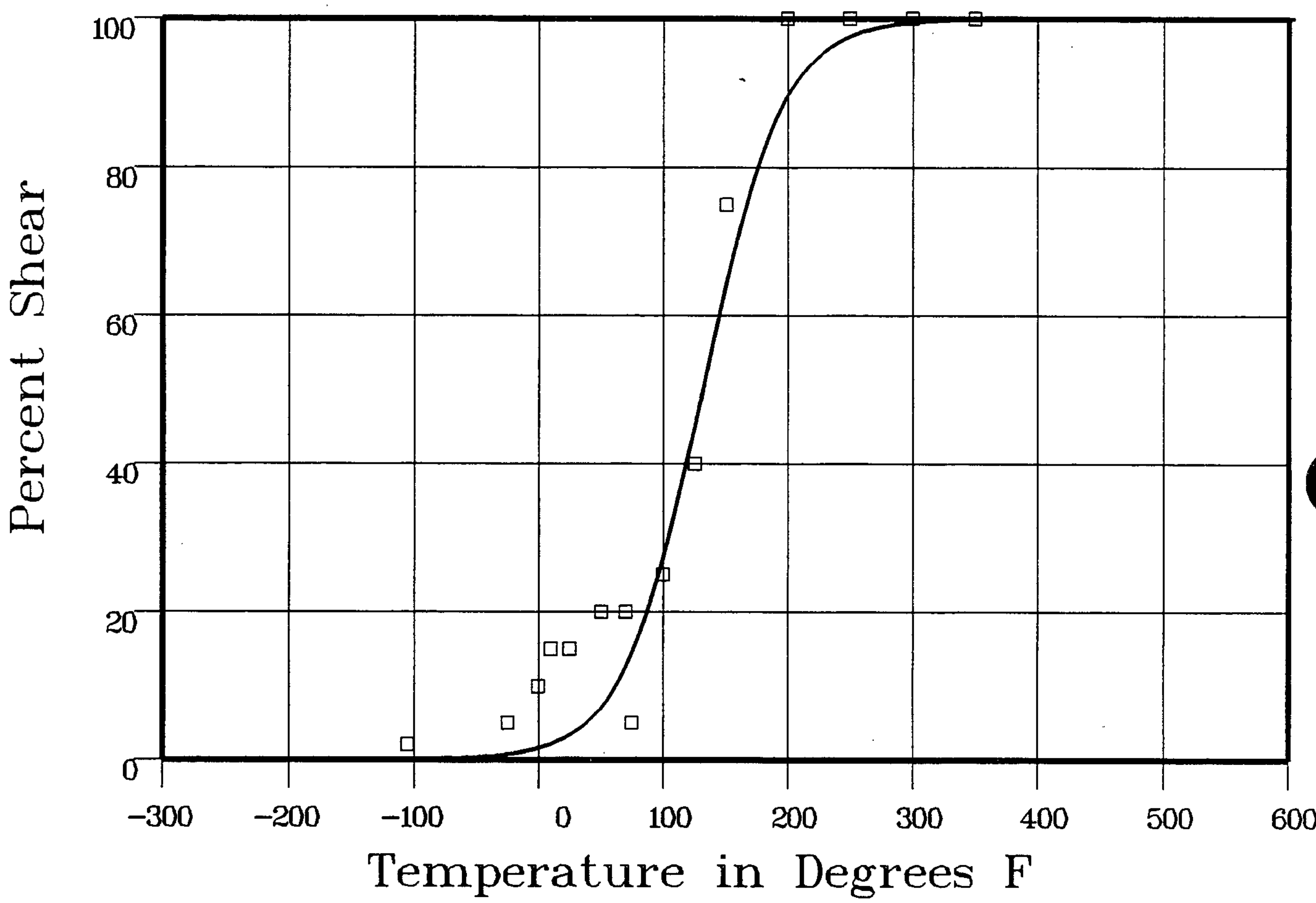

Data Set(s) Plotted

Plant: WB1 Cap.: U Material: FORGING SA508CL2 Ori.: LT Heat #: 527536 (RING 05)

Charpy V–Notch Data

Temperature	Input Percent Shear	Computed Percent Shear	Differential
-105	2	.06	1.93
-25	5	.84	4.15
0	10	1.83	8.16
10	15	2.49	12.5
25	15	3.93	11.06
50	20	8.25	11.74
70	20	14.43	5.56
75	5	16.49	-11.49
100	25	30.24	-5.24

**** Data continued on next page ****

CAPSULE–U TANGENTIAL

Page 2

Material: FORGING SA508CL2 Heat Number: 527536 (RING 05) Orientation: LT

Capsule: U Total Fluence:

Charpy V–Notch Data (Continued)

Temperature	Input Percent Shear	Computed Percent Shear	Differential
125	40	48.77	-8.77
150	75	67.63	7.36
200	100	90.97	9.02
250	100	97.98	2.01
300	100	99.57	.42
350	100	99.91	.08

SUM of RESIDUALS = 48.54

CAPSULE–U AXIAL

CVGRAPH 4.1 Hyperbolic Tangent Curve Printed at 13:46:40 on 02-24-1998

Page 1

Coefficients of Curve 1

A = 37.19	B = 35	C = 126.34	T0 = 100.19

Equation is: CVN = A + B * [tanh((T - T0)/C)]

Upper Shelf Energy: 72.19 Fixed Temp. at 30 ft-lbs: 73.8 Temp. at 50 ft-lbs: 148.6 Lower Shelf Energy: 2.19 Fixed

Material: FORGING SA508CL2 Heat Number: 527536 (RING 05) Orientation: TL

Capsule: U Total Fluence:

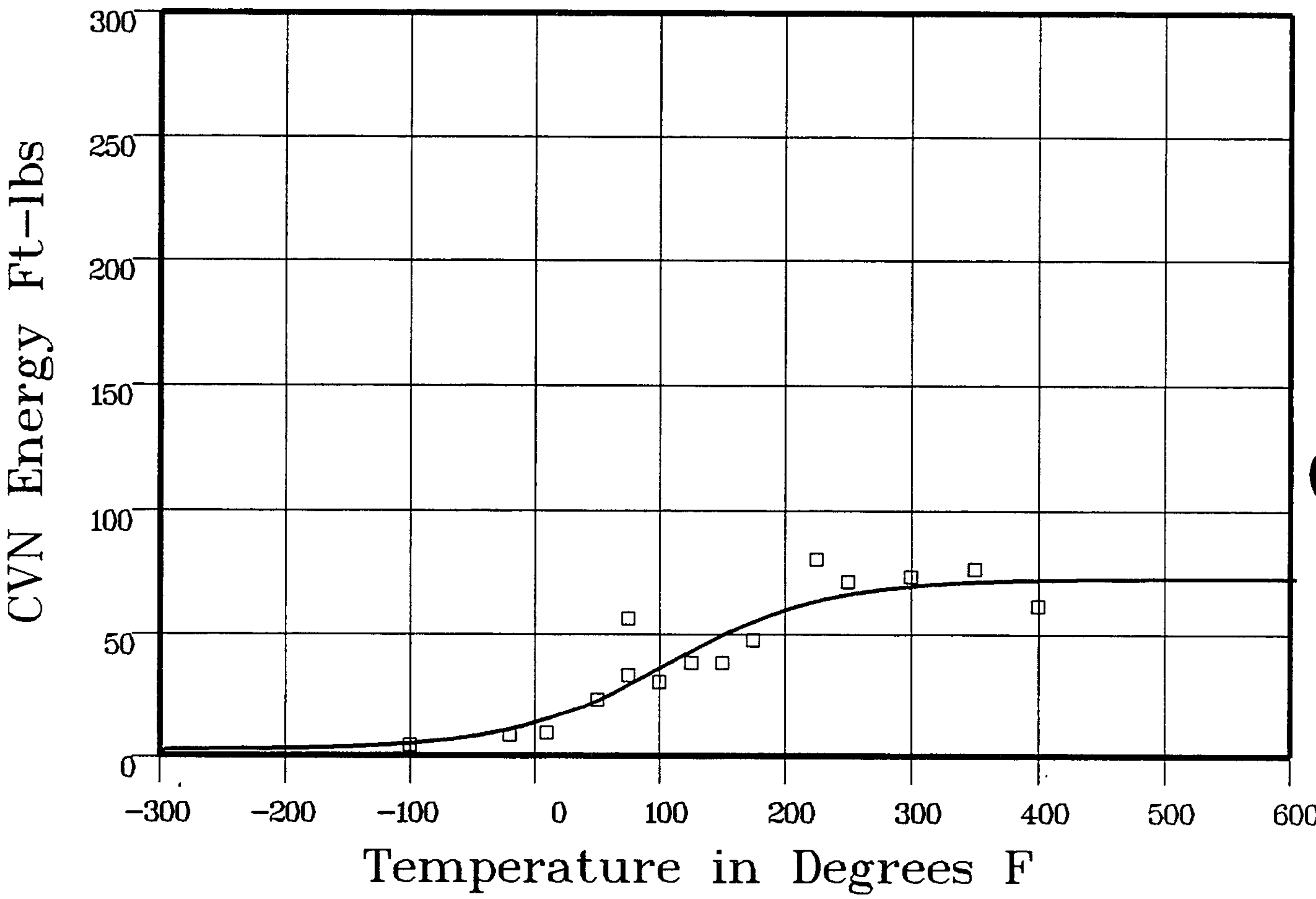

Data Set(s) Plotted

Plant: WB1 Cap.: U Material: FORGING SA508CL2 Ori.: TL Heat #: 527536 (RING 05)

Charpy V-Notch Data

Temperature	Input CVN Energy	Computed CVN Energy	Differential
-100	4	5.02	-1.02
-20	8	11.28	-3.28
10	9	15.74	-6.74
50	23	23.98	-.98
75	56	30.31	25.68
75	33	30.31	2.68
100	30	37.14	-7.14
125	38	43.98	-5.98
150	38	50.32	-12.32

**** Data continued on next page ****

CAPSULE–U AXIAL

Page 2

Material: FORGING SA508CL2 Heat Number: 527536 (RING 05) Orientation: TL

Capsule: U Total Fluence:

Charpy V–Notch Data (Continued)

Temperature	Input CVN Energy	Computed CVN Energy	Differential
175	47	55.79	−8.79
225	80	63.67	16.32
250	71	66.22	4.77
300	73	69.35	3.64
350	76	70.88	5.11
400	61	71.59	−10.59

SUM of RESIDUALS = 1.35

CAPSULE–U AXIAL

CVGRAPH 4.1 Hyperbolic Tangent Curve Printed at 13:50:52 on 02-24-1998

Page 1

Coefficients of Curve 1

A = 29.19	B = 28.19	C = 110.16	T0 = 90.58

Equation is: L.E. = A + B * [tanh((T - T0)/C)]

Upper Shelf L.E.: 57.39 Temperature at L.E. 35: 113.5 Lower Shelf L.E.: 1 Fixed

Material: FORGING SA508CL2 Heat Number: 527536 (RING 05) Orientation: TL

Capsule: U Total Fluence:

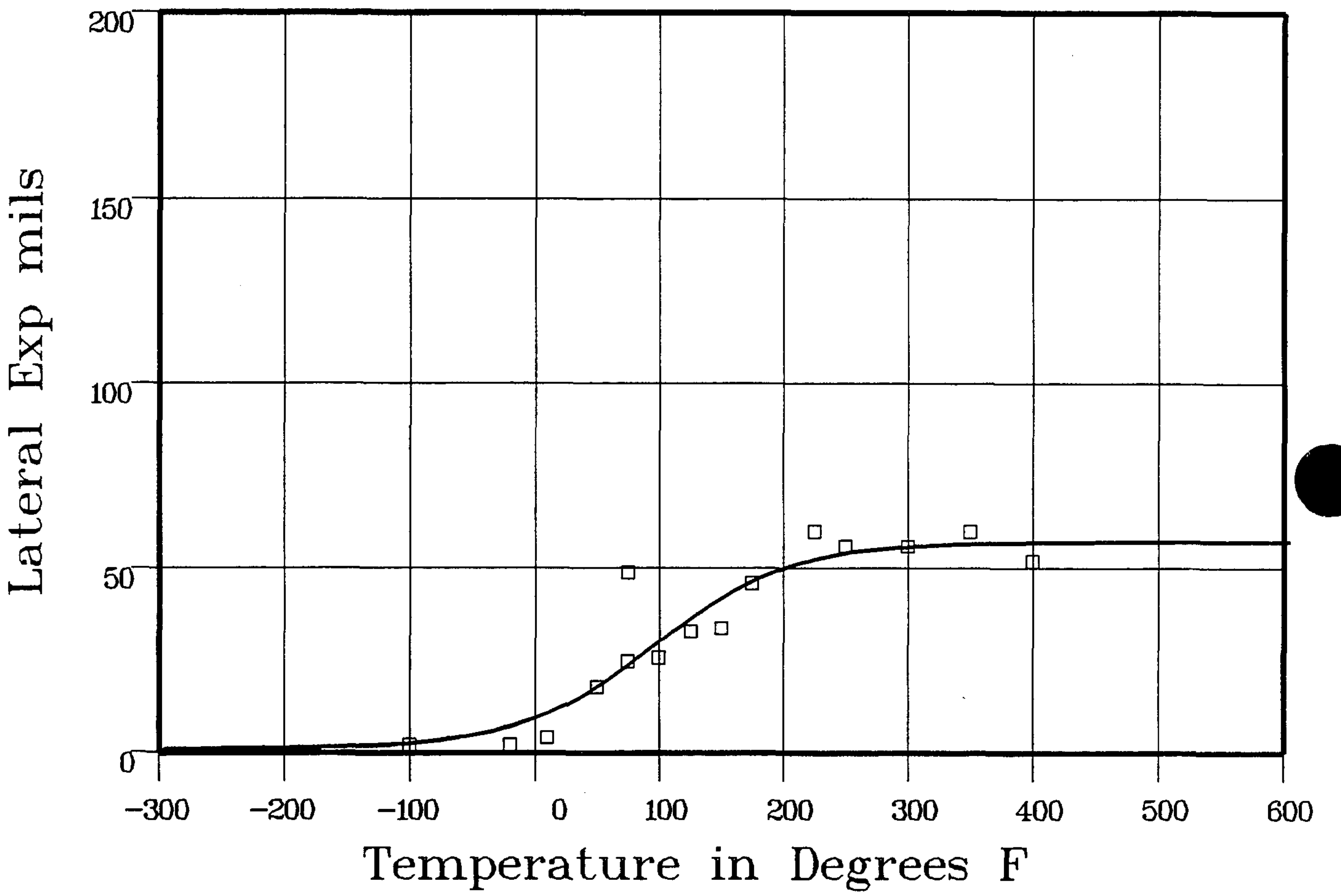

Data Set(s) Plotted

Plant: WB1 Cap.: U Material: FORGING SA508CL2 Ori.: TL Heat #: 527536 (RING 05)

Charpy V-Notch Data

Temperature	Input Lateral Expansion	Computed L.E.	Differential
-100	2	2.71	-.71
-20	2	7.67	-5.67
10	4	11.6	-7.6
50	18	19.25	-1.25
75	49	25.23	23.76
75	25	25.23	-.23
100	26	31.6	-5.6
125	33	37.72	-4.72
150	34	43.08	-9.08

**** Data continued on next page ****

CAPSULE–U AXIAL

Page 2

Material: FORGING SA508CL2 Heat Number: 527536 (RING 05) Orientation: TL

Capsule: U Total Fluence:

Charpy V–Notch Data (Continued)

Temperature	Input Lateral Expansion	Computed L.E.	Differential
175	46	47.37	−1.37
225	60	52.87	7.12
250	56	54.43	1.56
300	56	56.15	−.15
350	60	56.88	3.11
400	52	57.18	−5.18

SUM of RESIDUALS = −6.04

CAPSULE–U AXIAL

CVGRAPH 4.1 Hyperbolic Tangent Curve Printed at 14:07:12 on 02-24-1998

Page 1

Coefficients of Curve 1

A = 50	B = 50	C = 108.75	T0 = 144.42

Equation is: Shear% = A + B * [tanh((T - T0)/C)]

Temperature at 50% Shear: 144.4

Material: FORGING SA508CL2   Heat Number: 527536 (RING 05)   Orientation: TL

Capsule: U   Total Fluence:

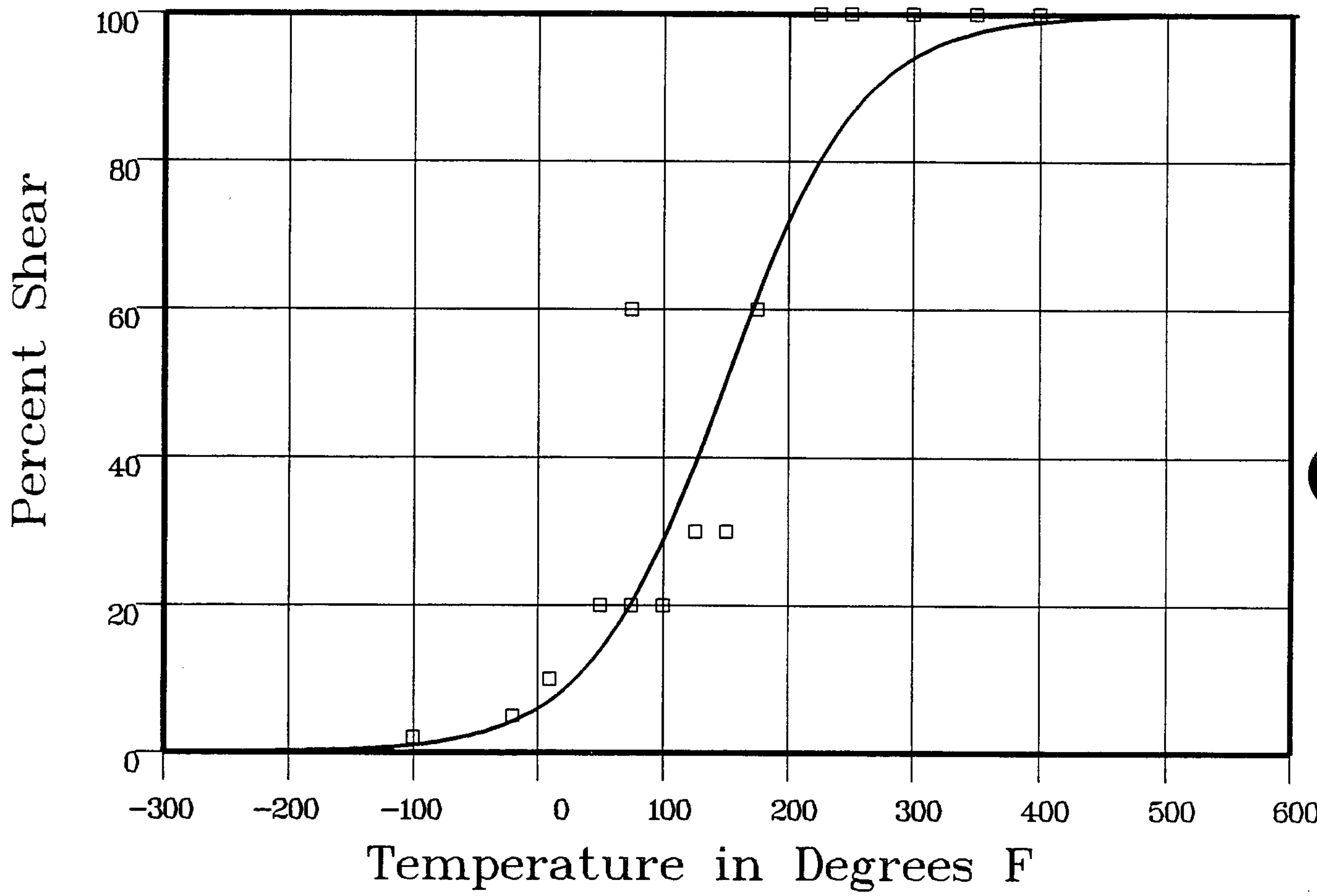

Data Set(s) Plotted

Plant: WB1   Cap.: U   Material: FORGING SA508CL2   Ori.: TL   Heat #: 527536 (RING 05)

Charpy V-Notch Data

Temperature	Input Percent Shear	Computed Percent Shear	Differential
-100	2	1.1	.89
-20	5	4.63	.36
10	10	7.78	2.21
50	20	14.97	5.02
75	60	21.81	38.18
75	20	21.81	-1.81
100	20	30.64	-10.64
125	30	41.16	-11.16
150	30	52.56	-22.56

**** Data continued on next page ****

CAPSULE–U AXIAL

Page 2

Material: FORGING SA508CL2 Heat Number: 527536 (RING 05) Orientation: TL

Capsule: U Total Fluence:

Charpy V–Notch Data (Continued)

Temperature	Input Percent Shear	Computed Percent Shear	Differential
175	60	63.69	-3.69
225	100	81.48	18.51
250	100	87.45	12.54
300	100	94.58	5.41
350	100	97.76	2.23
400	100	99.09	.9

SUM of RESIDUALS = 36.41

CAPSULE–U WELD

CVGRAPH 4.1 Hyperbolic Tangent Curve Printed at 10:03:55 on 02–26–1998

Page 1

Coefficients of Curve 1

A = 72.75	B = 70.55	C = 120.39	T0 = 46.4

Equation is: CVN = A + B * [tanh((T - T0)/C)]

Upper Shelf Energy: 143.3 Fixed   Temp. at 30 ft-lbs: -38.1   Temp. at 50 ft-lbs: 6.1   Lower Shelf Energy: 2.19 Fixed

Material: WELD   Heat Number: WIRE HEAT:895075   Orientation:

Capsule: U   Total Fluence:

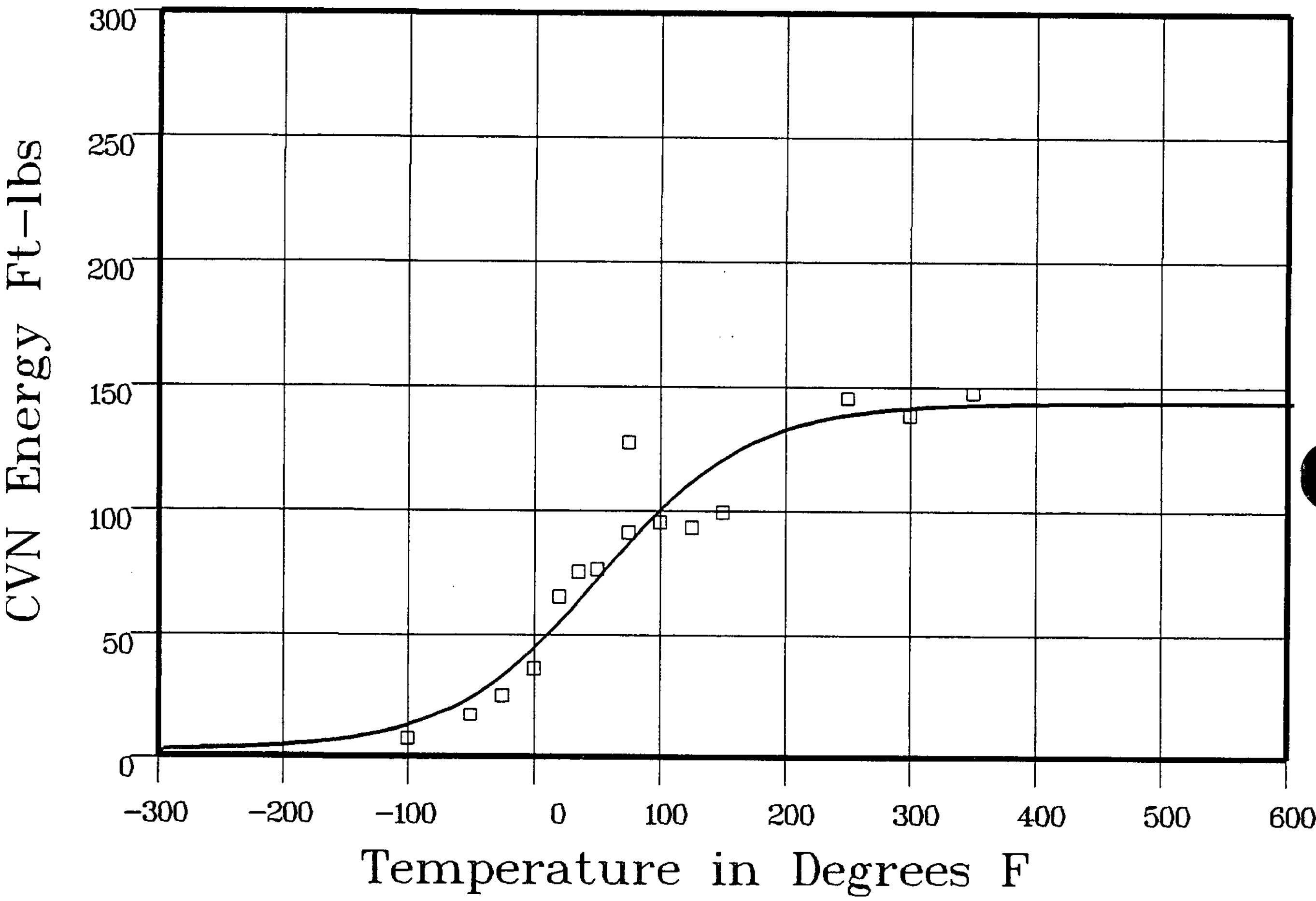

Data Set(s) Plotted

Plant: WB1   Cap.: U   Material: WELD   Ori.:   Heat #: WIRE HEAT:895075

Charpy V–Notch Data

Temperature	Input CVN Energy	Computed CVN Energy	Differential
-100	7	13.59	-6.59
-50	17	25.87	-8.87
-25	25	35.2	-10.2
0	36	46.82	-10.82
20	65	57.51	7.48
35	75	66.08	8.91
50	76	74.85	1.14
75	91	89.19	1.8
75	127	89.19	37.8

**** Data continued on next page ****

CAPSULE–U WELD

Page 2

Material: WELD　　Heat Number: WIRE HEAT:895075　　Orientation:

Capsule: U　　Total Fluence:

Charpy V–Notch Data (Continued)

Temperature	Input CVN Energy	Computed CVN Energy	Differential
100	95	102.23	-7.23
125	93	113.21	-20.21
150	99	121.88	-22.88
250	145	138.66	6.33
300	138	141.24	-3.24
350	147	142.39	4.6

SUM of RESIDUALS = -21.99

CAPSULE-U WELD

CVGRAPH 4.1 Hyperbolic Tangent Curve Printed at 10:25:15 on 02-26-1998
Page 1
Coefficients of Curve 1

A = 38.73	B = 37.73	C = 63.56	T0 = 14.06

Equation is: L.E. = A + B * [tanh((T - T0)/C)]

Upper Shelf L.E.: 76.46 Temperature at L.E. 35: 7.7 Lower Shelf L.E.: 1 Fixed

Material: WELD Heat Number: WIRE HEAT:895075 Orientation:

Capsule: U Total Fluence:

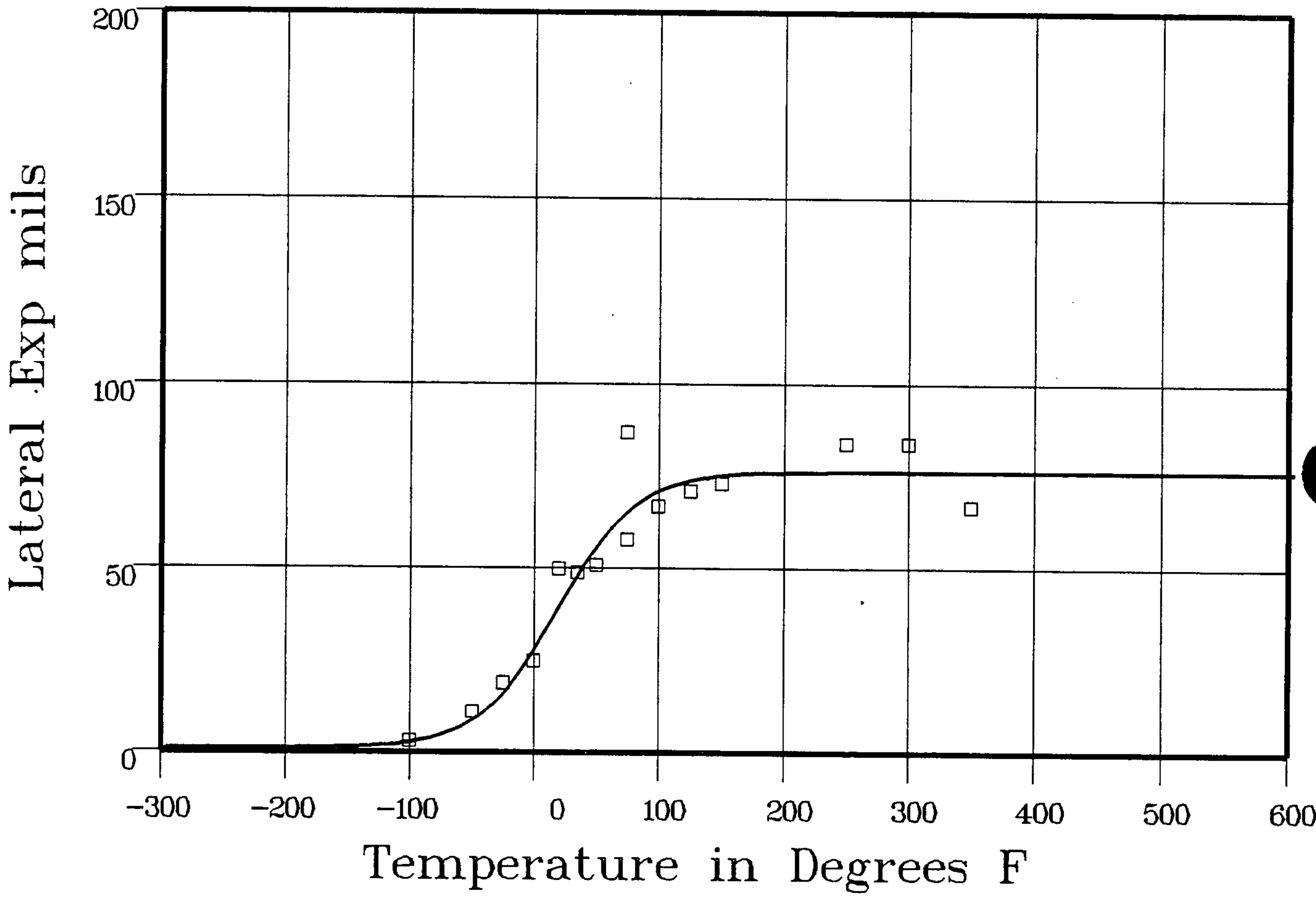

Data Set(s) Plotted
Plant: WB1 Cap.: U Material: WELD Ori.: Heat #: WIRE HEAT:895075

Charpy V-Notch Data

Temperature	Input Lateral Expansion	Computed L.E.	Differential
-100	3	3.02	-.02
-50	11	9.87	1.12
-25	19	18.08	.91
0	25	30.51	-5.51
20	50	42.24	7.75
35	49	50.73	-1.73
50	51	58.05	-7.05
75	58	66.79	-8.79
75	87	66.79	20.2

**** Data continued on next page ****

CAPSULE–U WELD

Page 2

Material: WELD   Heat Number: WIRE HEAT:895075   Orientation:

Capsule: U   Total Fluence:

Charpy V–Notch Data (Continued)

Temperature	Input Lateral Expansion	Computed L.E.	Differential
100	67	71.73	−4.73
125	71	74.23	−3.23
150	73	75.43	−2.43
250	84	76.42	7.57
300	84	76.45	7.54
350	67	76.46	−9.46

SUM of RESIDUALS = 2.12

CAPSULE–U WELD

CVGRAPH 4.1 Hyperbolic Tangent Curve Printed at 10:28:15 on 02-26-1998
Page 1
Coefficients of Curve 1

A = 50	B = 50	C = 52.48	T0 = 9.66

Equation is: Shear% = A + B * [tanh((T - T0)/C)]

Temperature at 50% Shear: 9.6

Material: WELD   Heat Number: WIRE HEAT:895075   Orientation:

Capsule: U   Total Fluence:

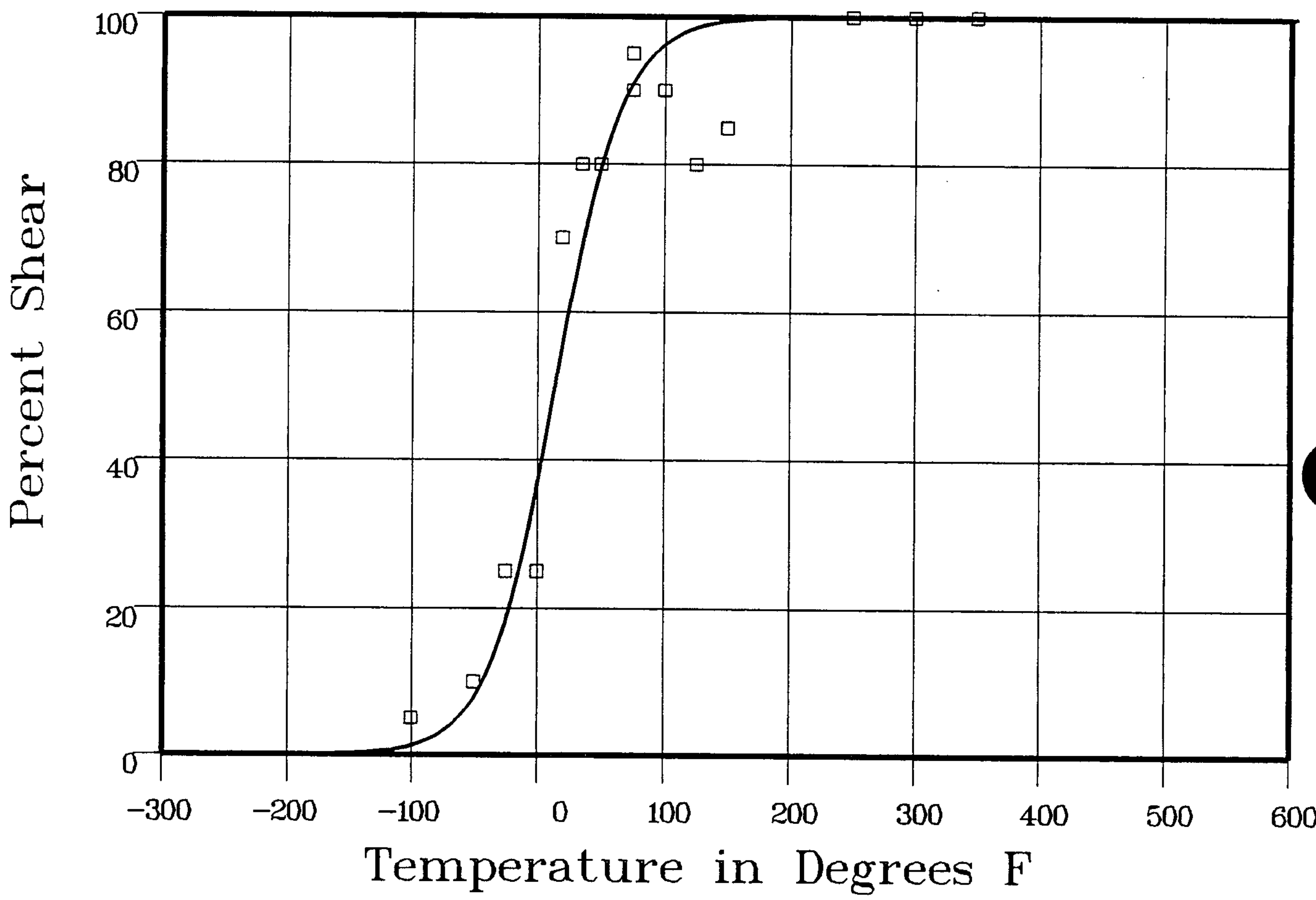

Data Set(s) Plotted
Plant: WB1   Cap.: U   Material: WELD   Ori.:   Heat #: WIRE HEAT:895075

Charpy V-Notch Data

Temperature	Input Percent Shear	Computed Percent Shear	Differential
-100	5	1.5	3.49
-50	10	9.33	.66
-25	25	21.06	3.93
0	25	40.89	-15.89
20	70	59.71	10.28
35	80	72.41	7.58
50	80	82.3	-2.3
75	90	92.34	-2.34
75	95	92.34	2.65

**** Data continued on next page ****

CAPSULE–U WELD

Page 2

Material: WELD Heat Number: WIRE HEAT:895075 Orientation:

Capsule: U Total Fluence:

Charpy V–Notch Data (Continued)

Temperature	Input Percent Shear	Computed Percent Shear	Differential
100	90	96.89	-6.89
125	80	98.78	-18.78
150	85	99.52	-14.52
250	100	99.98	.01
300	100	99.99	0
350	100	99.99	0

SUM of RESIDUALS = -32.11

CAPSULE–U HEAT–AFFECTED–ZONE

CVGRAPH 4.1 Hyperbolic Tangent Curve Printed at 15:01:03 on 02-26-1998

Page 1

Coefficients of Curve 1

A = 40.59	B = 38.4	C = 92.11	T0 = 20.62

Equation is: CVN = A + B * [tanh((T - T0)/C)]

Upper Shelf Energy: 79 Fixed   Temp. at 30 ft-lbs: -5.4   Temp. at 50 ft-lbs: 43.6   Lower Shelf Energy: 2.19 Fixed

Material: HEAT AFF'D ZONE   Heat Number: WIRE HEAT:895075   Orientation:

Capsule: U   Total Fluence:

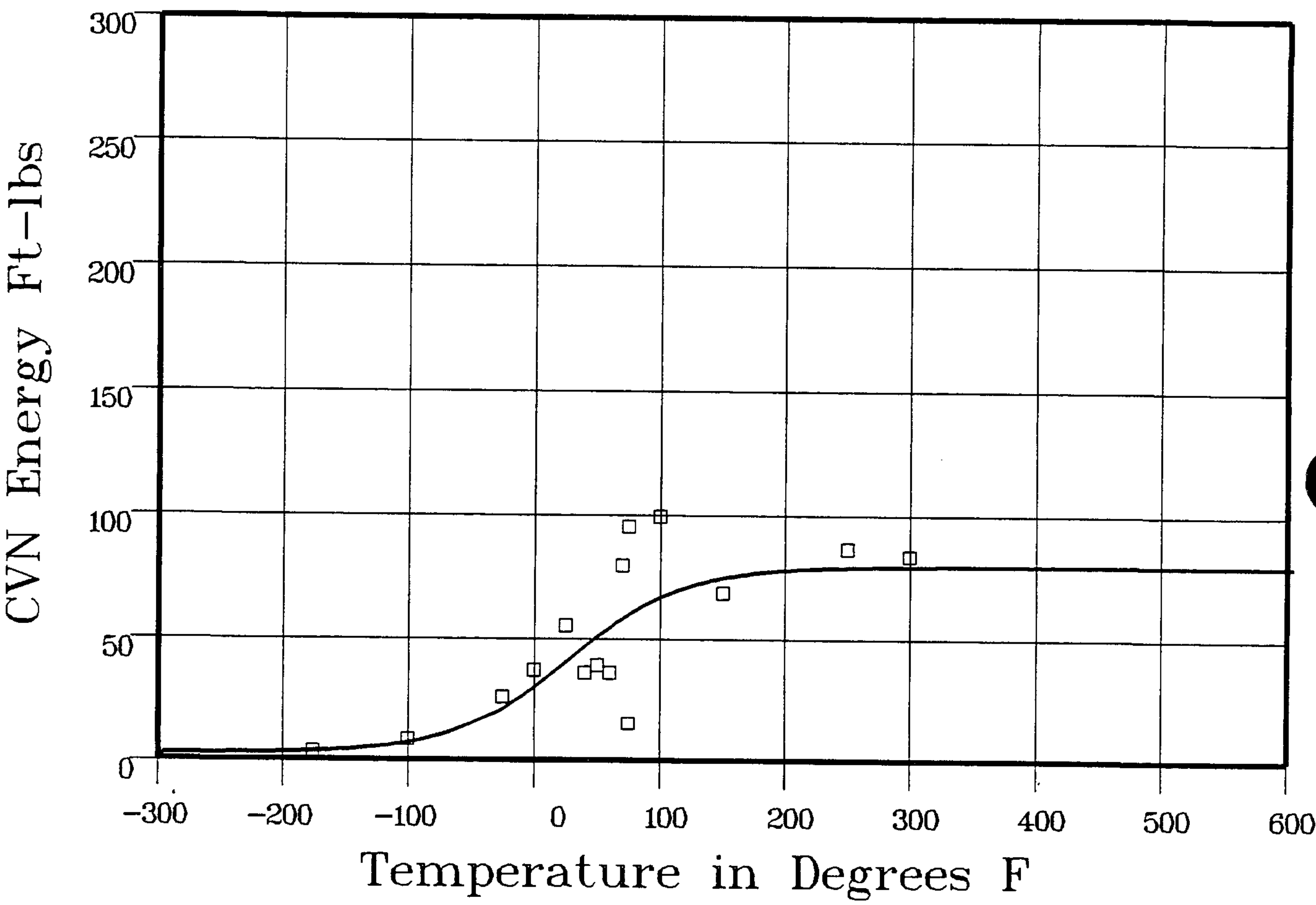

Data Set(s) Plotted

Plant: WB1   Cap.: U   Material: HEAT AFF'D ZONE   Ori.:   Heat #: WIRE HEAT:895075

Charpy V-Notch Data

Temperature	Input CVN Energy	Computed CVN Energy	Differential
-175	3	3.28	-.28
-100	8	7.41	.58
-25	26	22.99	3
0	37	32.14	4.85
25	55	42.42	12.57
40	36	48.55	-12.55
50	39	52.44	-13.44
60	36	56.08	-20.08
70	79	59.41	19.58

**** Data continued on next page ****

CAPSULE–U HEAT–AFFECTED–ZONE

Material: HEAT AFF'D ZONE   Heat Number: WIRE HEAT:895075   Orientation:

Capsule: U   Total Fluence:

Charpy V–Notch Data (Continued)

Temperature	Input CVN Energy	Computed CVN Energy	Differential
75	15	60.95	–45.95
75	95	60.95	34.04
100	99	67.36	31.63
150	68	74.63	–6.63
250	86	78.47	7.52
300	83	78.82	4.17

SUM of RESIDUALS = 19.02

CAPSULE–U HEAT–AFFECTED–ZONE

CVGRAPH 4.1 Hyperbolic Tangent Curve Printed at 15:28:53 on 02-26-1998

Page 1

Coefficients of Curve 1

A = 27.73	B = 26.73	C = 78.82	T0 = 29.72

Equation is: L.E. = A + B * [tanh((T - T0)/C)]

Upper Shelf L.E.: 54.47 Temperature at L.E. 35: 51.6 Lower Shelf L.E.: 1 Fixed

Material: HEAT AFF'D ZONE Heat Number: WIRE HEAT:895075 Orientation:

Capsule: U Total Fluence:

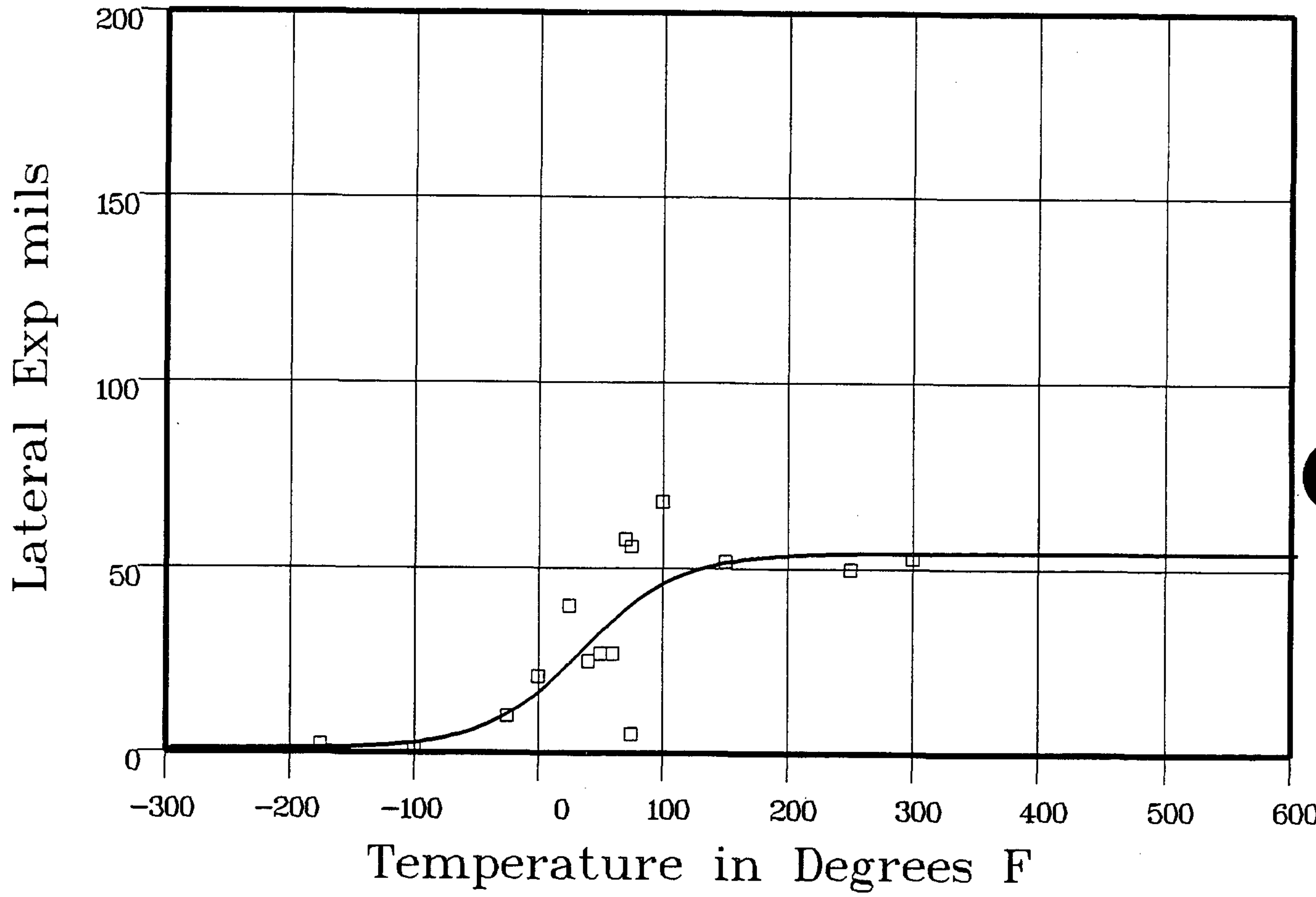

Data Set(s) Plotted

Plant: WB1 Cap.: U Material: HEAT AFF'D ZONE Ori.: Heat #: WIRE HEAT:895075

Charpy V-Notch Data

Temperature	Input Lateral Expansion	Computed L.E.	Differential
-175	2	1.29	.7
-100	1	2.91	-1.91
-25	10	11.67	-1.67
0	21	18.1	2.89
25	40	26.13	13.86
40	25	31.2	-6.2
50	27	34.46	-7.46
60	27	37.53	-10.53
70	58	40.32	17.67

**** Data continued on next page ****

CAPSULE–U HEAT–AFFECTED–ZONE

Page 2

Material: HEAT AFF'D ZONE   Heat Number: WIRE HEAT:895075   Orientation:

Capsule: U   Total Fluence:

Charpy V–Notch Data (Continued)

Temperature	Input Lateral Expansion	Computed L.E.	Differential
75	5	41.6	–36.6
75	56	41.6	14.39
100	68	46.78	21.21
150	52	52.06	–.06
250	50	54.27	–4.27
300	53	54.42	–1.42

SUM of RESIDUALS = .58

CAPSULE–U HEAT–AFFECTED–ZONE

CVGRAPH 4.1 Hyperbolic Tangent Curve Printed at 10:00:52 on 03-13-1998
Page 1
Coefficients of Curve 1

A = 50	B = 50	C = 37.41	T0 = 88.18

Equation is: Shear% = A + B * [tanh((T − T0)/C)]

Temperature at 50% Shear: 88.1

Material: HEAT AFF'D ZONE Heat Number: WIRE HEAT:895075 Orientation:

Capsule: U Total Fluence:

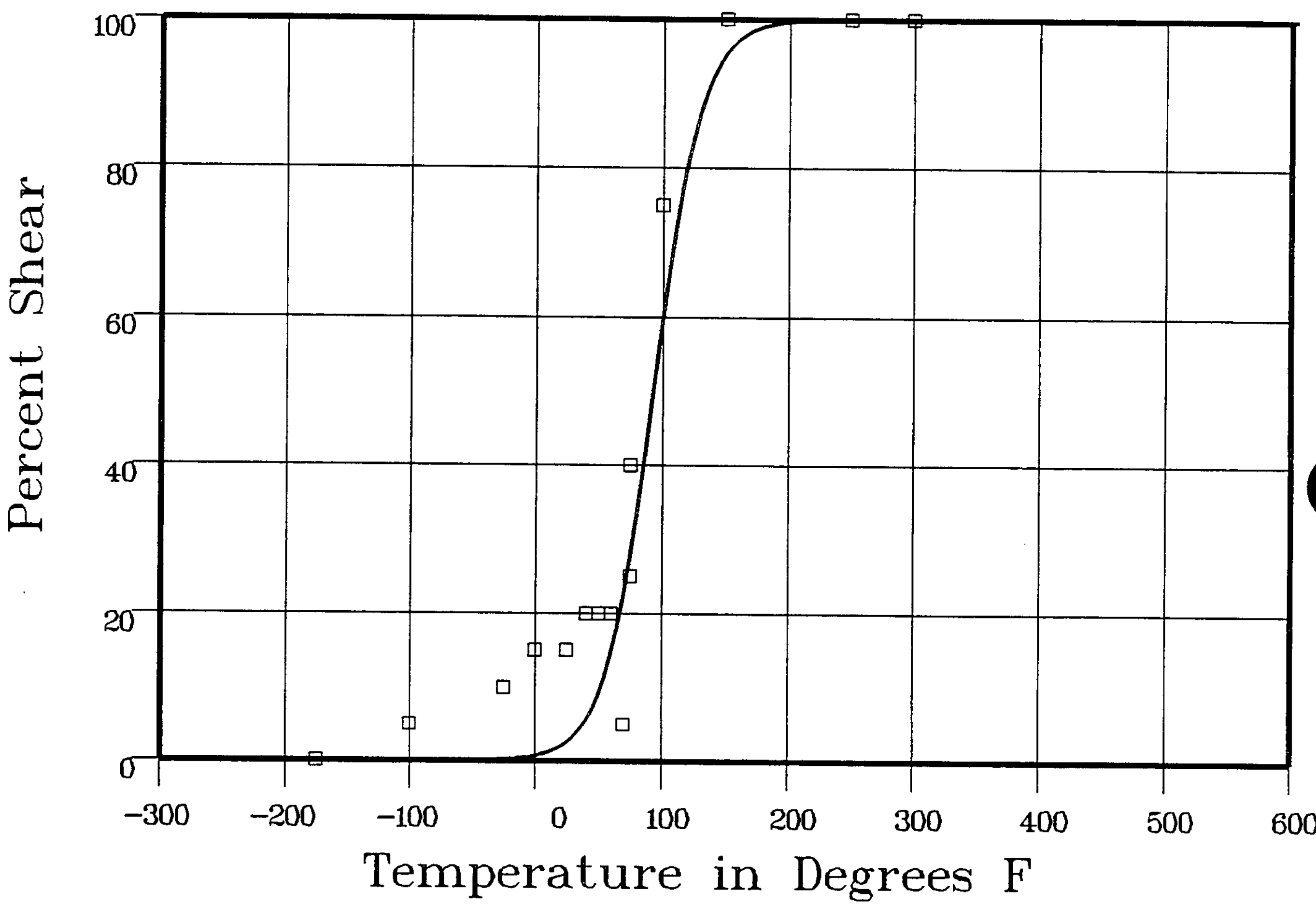

Data Set(s) Plotted

Plant: WB1 Cap.: U Material: HEAT AFF'D ZONE Ori.: Heat #: WIRE HEAT:895075

Charpy V–Notch Data

Temperature	Input Percent Shear	Computed Percent Shear	Differential
-175	0	0	0
-100	5	0	4.99
-25	10	.23	9.76
0	15	.88	14.11
25	15	3.3	11.69
40	20	7.07	12.92
50	20	11.49	8.5
60	20	18.14	1.85
70	5	27.44	-22.44

**** Data continued on next page ****

CAPSULE–U HEAT–AFFECTED–ZONE

Page 2

Material: HEAT AFFD ZONE Heat Number: WIRE HEAT:895075 Orientation:

Capsule: U Total Fluence:

Charpy V–Notch Data (Continued)

Temperature	Input Percent Shear	Computed Percent Shear	Differential
75	40	33.07	6.92
75	25	33.07	-8.07
100	75	65.28	9.71
150	100	96.45	3.54
250	100	99.98	.01
300	100	99.99	0

SUM of RESIDUALS = 53.52

SHELL FORGING 05 TANGENTIAL

CVGRAPH 4.1 Hyperbolic Tangent Curve Printed at 10:04:36 on 02-23-1998

Page 1

Coefficients of Curve 1

A = 66.84	B = 64.65	C = 109.35	T0 = 13.59

Equation is: CVN = A + B * [tanh((T - T0)/C)]

Upper Shelf Energy: 131.5 Fixed Temp. at 30 ft-lbs: -57.2 Temp. at 50 ft-lbs: -15.5 Lower Shelf Energy: 2.19 Fixed

Material: FORGING SA508CL2 Heat Number: 527536 (RING 05) Orientation: LT

Capsule: UNIRR Total Fluence:

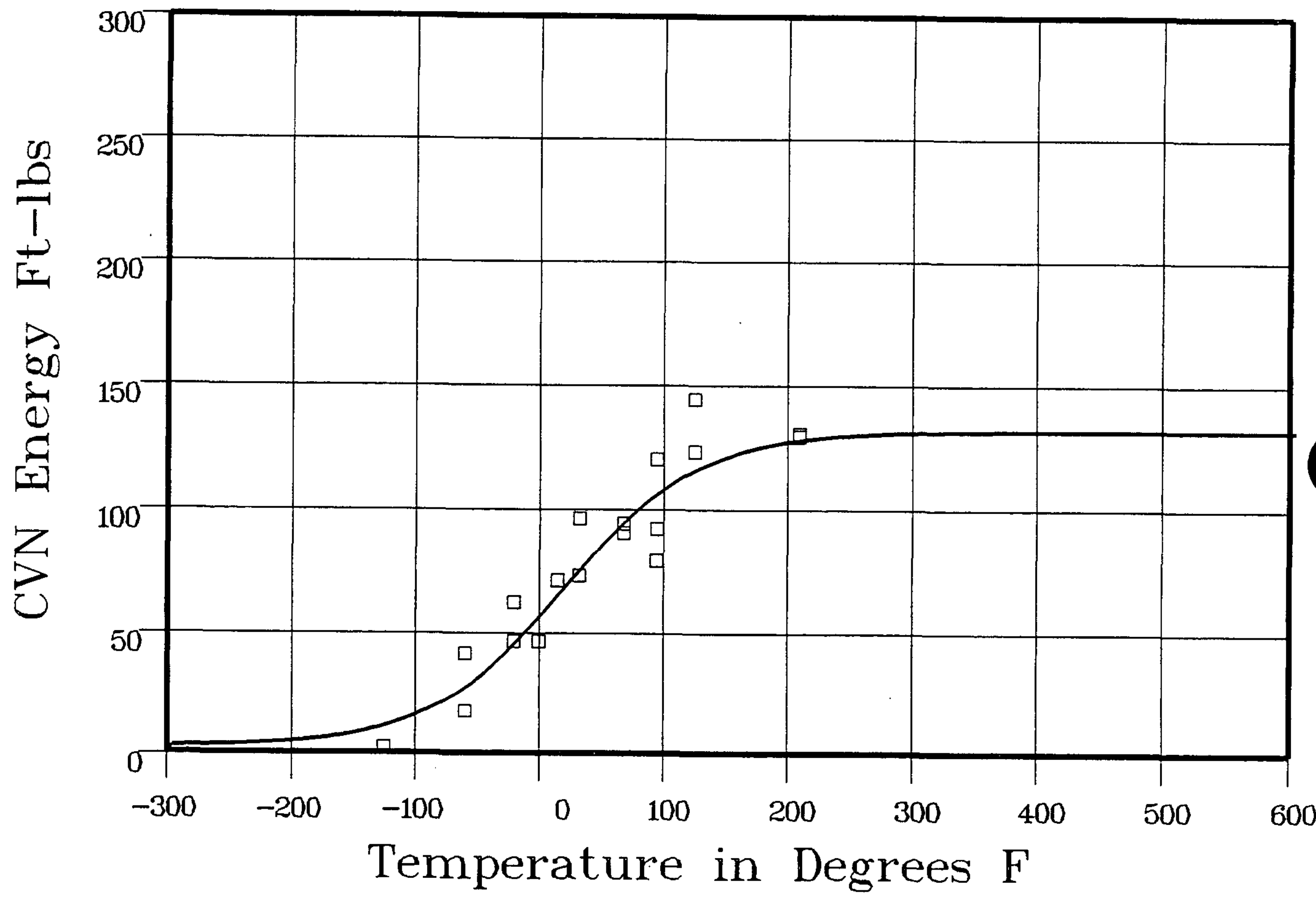

Data Set(s) Plotted

Plant: WB1 Cap.: UNIRR Material: FORGING SA508CL2 Ori.: LT Heat #: 527536 (RING 05)

Charpy V-Notch Data

Temperature	Input CVN Energy	Computed CVN Energy	Differential
-125	2	11.69	-9.69
-60	17	28.9	-11.9
-60	41	28.9	12.09
-20	62	47.59	14.4
-20	46	47.59	-1.59
0	46	58.85	-12.85
15	71	67.68	3.31
32	96	77.62	18.37
32	73	77.62	-4.62

**** Data continued on next page ****

SHELL FORGING 05 TANGENTIAL

Page 2

Material: FORGING SA508CL2 Heat Number: 527536 (RING 05) Orientation: LT

Capsule: UNIRR Total Fluence:

Charpy V-Notch Data (Continued)

Temperature	Input CVN Energy	Computed CVN Energy	Differential
68	90	96.59	-6.59
68	94	96.59	-2.59
95	92	107.69	-15.69
95	120	107.69	12.3
95	79	107.69	-28.69
125	144	116.58	27.41
125	123	116.58	6.41
210	129	128.03	.96
210	130	128.03	1.96

SUM of RESIDUALS = 2.98

SHELL FORGING 05 TANGENTIAL

CVGRAPH 4.1 Hyperbolic Tangent Curve Printed at 10:10:39 on 02-23-1998

Page 1

Coefficients of Curve 1

A = 40.64	B = 39.64	C = 85.15	T0 = 3.28

Equation is: L.E. = A + B * [tanh((T - T0)/C)]

Upper Shelf L.E.: 80.28 Temperature at L.E. 35: -8.9 Lower Shelf L.E.: 1 Fixed

Material: FORGING SA508CL2 Heat Number: 527536 (RING 05) Orientation: LT

Capsule: UNIRR Total Fluence:

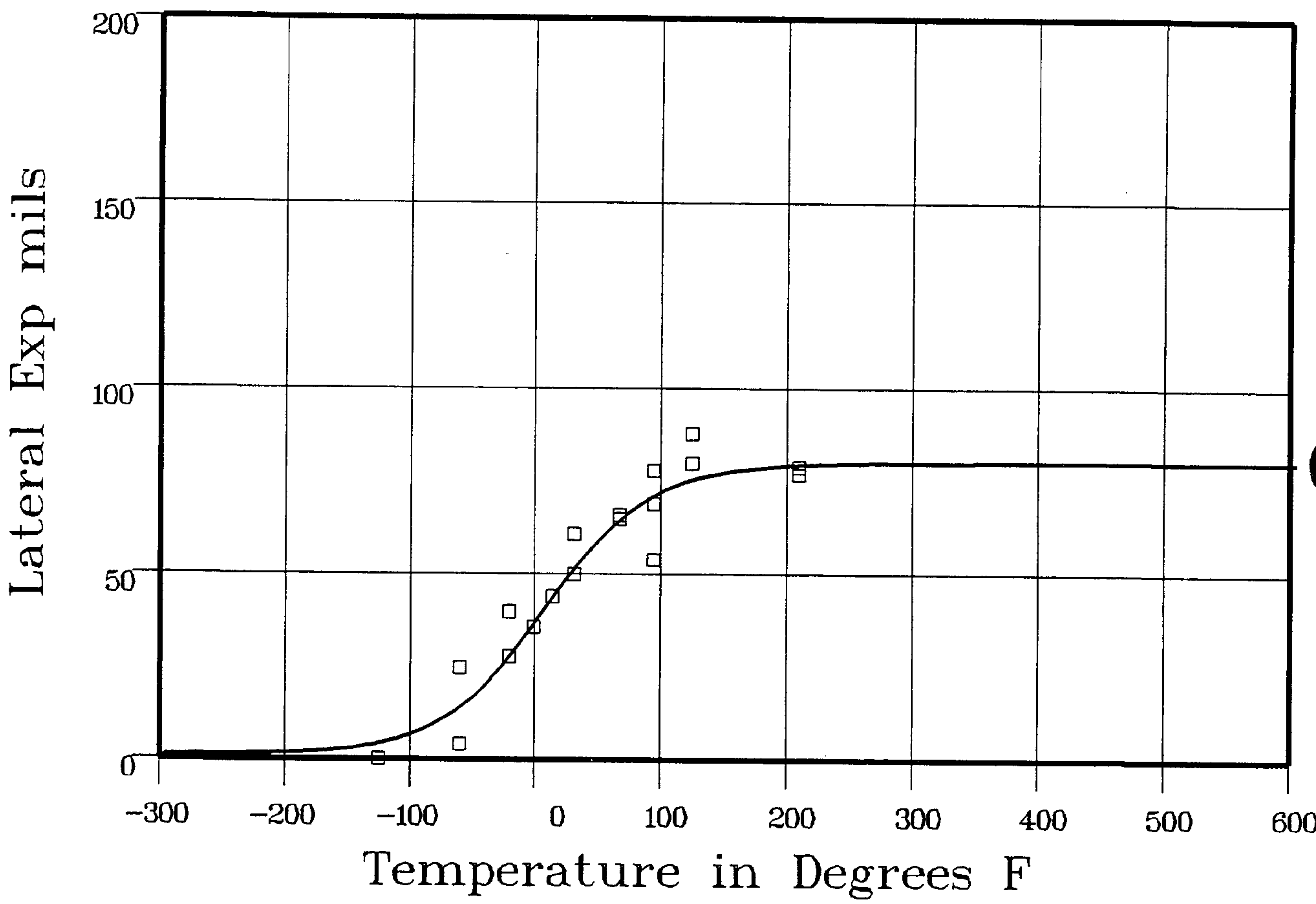

Data Set(s) Plotted

Plant: WB1 Cap.: UNIRR Material: FORGING SA508CL2 Ori.: LT Heat #: 527536 (RING 05)

Charpy V-Notch Data

Temperature	Input Lateral Expansion	Computed L.E.	Differential
-125	0	4.71	-4.71
-60	4	15.62	-11.62
-60	25	15.62	9.37
-20	40	30.06	9.93
-20	28	30.06	-2.06
0	36	39.11	-3.11
15	44	46.06	-2.06
32	61	53.52	7.47
32	50	53.52	-3.52

**** Data continued on next page ****

SHELL FORGING 05 TANGENTIAL

Page 2

Material: FORGING SA508CL2 Heat Number: 527536 (RING 05) Orientation: LT

Capsule: UNIRR Total Fluence:

Charpy V-Notch Data (Continued)

Temperature	Input Lateral Expansion	Computed L.E.	Differential
68	66	66.05	-.05
68	65	66.05	-1.05
95	69	72.04	-3.04
95	78	72.04	5.95
95	54	72.04	-18.04
125	88	75.98	12.01
125	80	75.98	4.01
210	79	79.66	-.66
210	77	79.66	-2.66

SUM of RESIDUALS = -3.84

SHELL FORGING 05 TANGENTIAL

CVGRAPH 4.1 Hyperbolic Tangent Curve Printed at 10:18:37 on 02-23-1998

Page 1

Coefficients of Curve 1

A = 50	B = 50	C = 94.49	T0 = 34.88

Equation is: Shear% = A + B * [tanh((T - T0)/C)]

Temperature at 50% Shear: 34.8

Material: FORGING SA508CL2 Heat Number: 527536 (RING 05) Orientation: LT

Capsule: UNIRR Total Fluence:

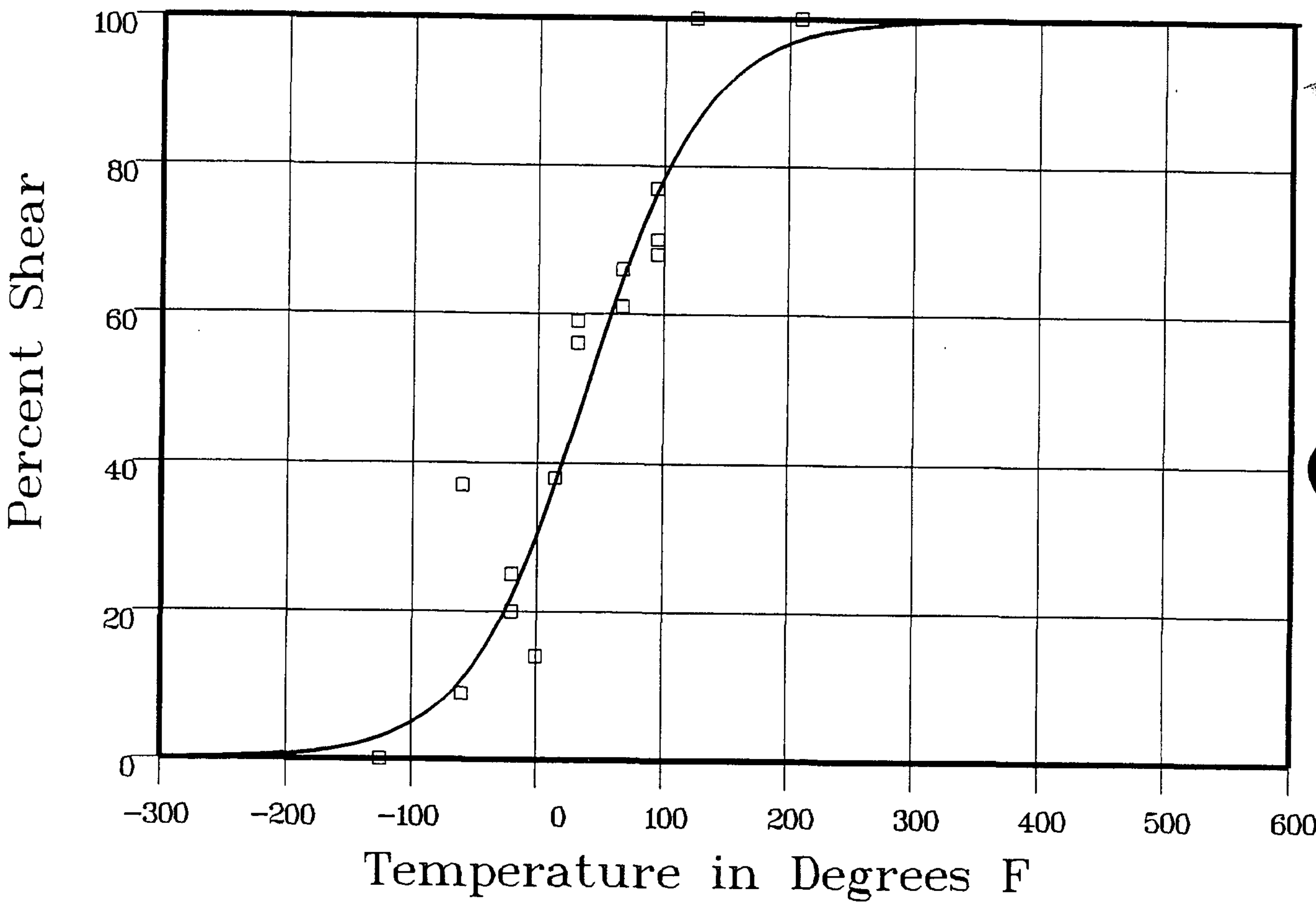

Data Set(s) Plotted

Plant: WB1 Cap.: UNIRR Material: FORGING SA508CL2 Ori.: LT Heat #: 527536 (RING 05)

Charpy V-Notch Data

Temperature	Input Percent Shear	Computed Percent Shear	Differential
-125	0	3.28	-3.28
-60	9	11.83	-2.83
-60	37	11.83	25.16
-20	25	23.83	1.16
-20	20	23.83	-3.83
0	14	32.33	-18.33
15	38	39.63	-1.63
32	59	48.47	10.52
32	56	48.47	7.52

**** Data continued on next page ****

SHELL FORGING 05 TANGENTIAL

Page 2

Material: FORGING SA508CL2 Heat Number: 527536 (RING 05) Orientation: LT

Capsule: UNIRR Total Fluence:

Charpy V-Notch Data (Continued)

Temperature	Input Percent Shear	Computed Percent Shear	Differential
68	66	66.83	-.83
68	61	66.83	-5.83
95	68	78.11	-10.11
95	77	78.11	-1.11
95	70	78.11	-8.11
125	100	87.07	12.92
125	100	87.07	12.92
210	100	97.6	2.39
210	100	97.6	2.39

SUM of RESIDUALS = 19.07

SHELL FORGING 05 AXIAL

CVGRAPH 4.1 Hyperbolic Tangent Curve Printed at 10:43:23 on 02-23-1998

Page 1

Coefficients of Curve 1

A = 31.89	B = 29.69	C = 90.03	T0 = 50.62

Equation is: CVN = A + B * [tanh((T - T0)/C)]

Upper Shelf Energy: 61.59 Fixed Temp. at 30 ft-lbs: 44.8 Temp. at 50 ft-lbs: 114.3 Lower Shelf Energy: 2.2 Fixed

Material: FORGING SA508CL2 Heat Number: 527536 (RING 05) Orientation: TL

Capsule: UNIRR Total Fluence:

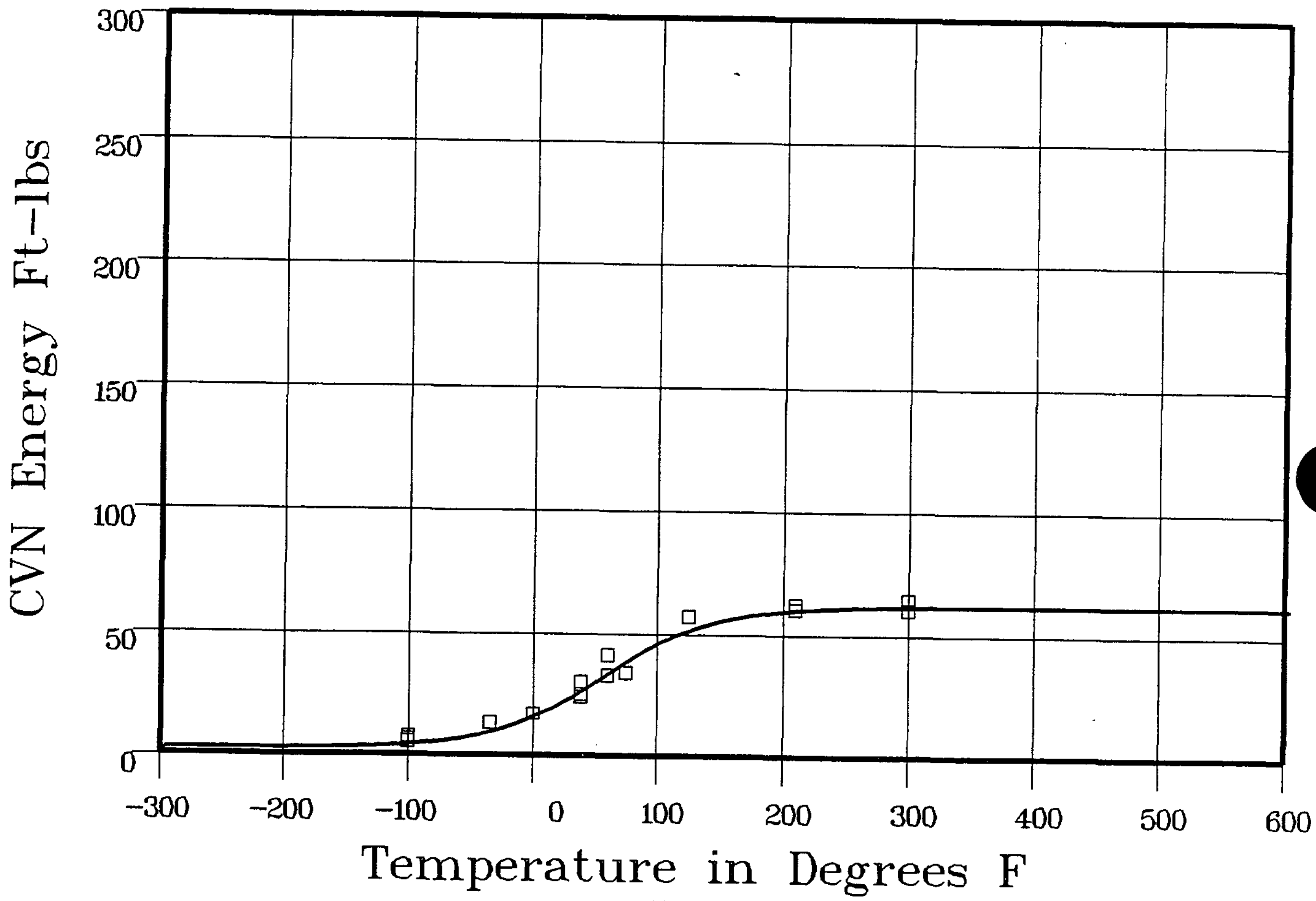

Data Set(s) Plotted

Plant: WB1 Cap.: UNIRR Material: FORGING SA508CL2 Ori.: TL Heat #: 527536 (RING 05)

Charpy V-Notch Data

Temperature	Input CVN Energy	Computed CVN Energy	Differential
-100	7	4.22	2.77
-100	6	4.22	1.77
-100	5	4.22	.77
-35	13	9.91	3.08
0	17	16.76	.23
0	17	16.76	.23
38	24	27.76	-3.76
38	25	27.76	-2.76
38	30	27.76	2.23

**** Data continued on next page ****

SHELL FORGING 05 AXIAL

Material: FORGING SA508CL2 Heat Number: 527536 (RING 05) Orientation: TL

Capsule: UNIRR Total Fluence:

Charpy V-Notch Data (Continued)

Temperature	Input CVN Energy	Computed CVN Energy	Differential
60	33	34.98	-1.98
60	41	34.98	6.01
75	34	39.74	-5.74
125	57	52.04	4.95
210	60	59.92	.07
210	62	59.92	2.07
210	62	59.92	2.07
300	64	61.36	2.63
300	60	61.36	-1.36

SUM of RESIDUALS = 13.33

SHELL FORGING 05 AXIAL

CVGRAPH 4.1 Hyperbolic Tangent Curve Printed at 10:48:01 on 02-23-1998

Page 1

Coefficients of Curve 1

A = 29.58	B = 28.58	C = 96.31	T0 = 65.62

Equation is: L.E. = A + B * [tanh((T - T0)/C)]

Upper Shelf L.E.: 58.17 Temperature at L.E. 35: 84 Lower Shelf L.E.: 1 Fixed

Material: FORGING SA508CL2 Heat Number: 527536 (RING 05) Orientation: TL

Capsule: UNIRR Total Fluence:

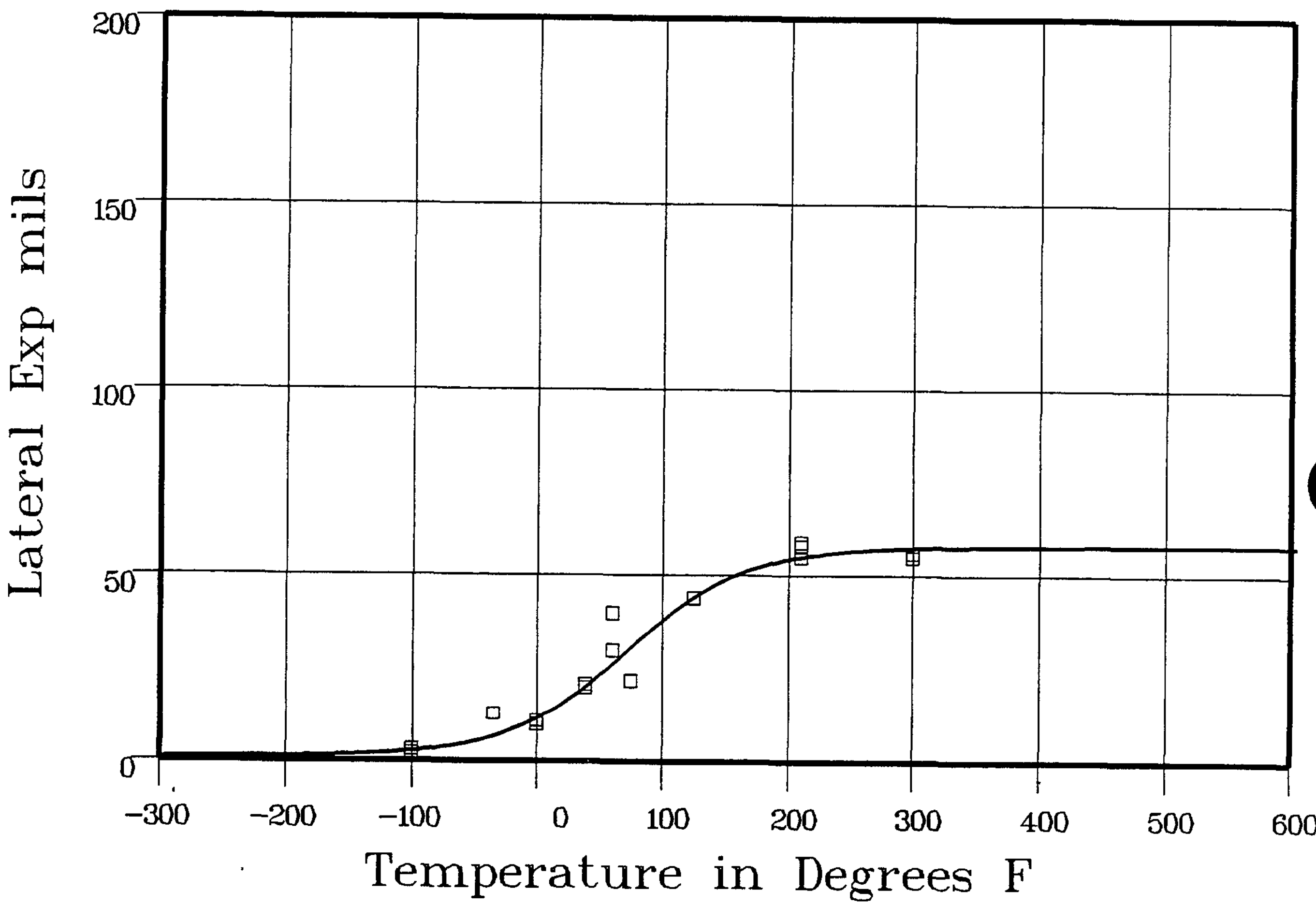

Data Set(s) Plotted

Plant: WB1 Cap.: UNIRR Material: FORGING SA508CL2 Ori.: TL Heat #: 527536 (RING 05)

Charpy V-Notch Data

Temperature	Input Lateral Expansion	Computed L.E.	Differential
-100	3	2.77	.22
-100	2	2.77	-.77
-100	1	2.77	-1.77
-35	13	7.29	5.7
0	10	12.65	-2.65
0	11	12.65	-1.65
38	20	21.6	-1.6
38	21	21.6	-.6
38	21	21.6	-.6

**** Data continued on next page ****

SHELL FORGING 05 AXIAL

Material: FORGING SA508CL2 Heat Number: 527536 (RING 05) Orientation: TL

Capsule: UNIRR Total Fluence:

Charpy V-Notch Data (Continued)

Temperature	Input Lateral Expansion	Computed L.E.	Differential
60	30	27.91	2.08
60	40	27.91	12.08
75	22	32.36	-10.36
125	44	45.27	-1.27
210	55	55.45	-.45
210	58	55.45	2.54
210	59	55.45	3.54
300	56	57.73	-1.73
300	55	57.73	-2.73

SUM of RESIDUALS = -.05

SHELL FORGING 05 AXIAL

CVGRAPH 4.1 Hyperbolic Tangent Curve Printed at 10:52:45 on 02-23-1998

Page 1

Coefficients of Curve 1

A = 50	B = 50	C = 95.06	T0 = 54.84

Equation is: Shear% = A + B * [tanh((T - T0)/C)]

Temperature at 50% Shear: 54.8

Material: FORGING SA508CL2 Heat Number: 527536 (RING 05) Orientation: TL

Capsule: UNIRR Total Fluence:

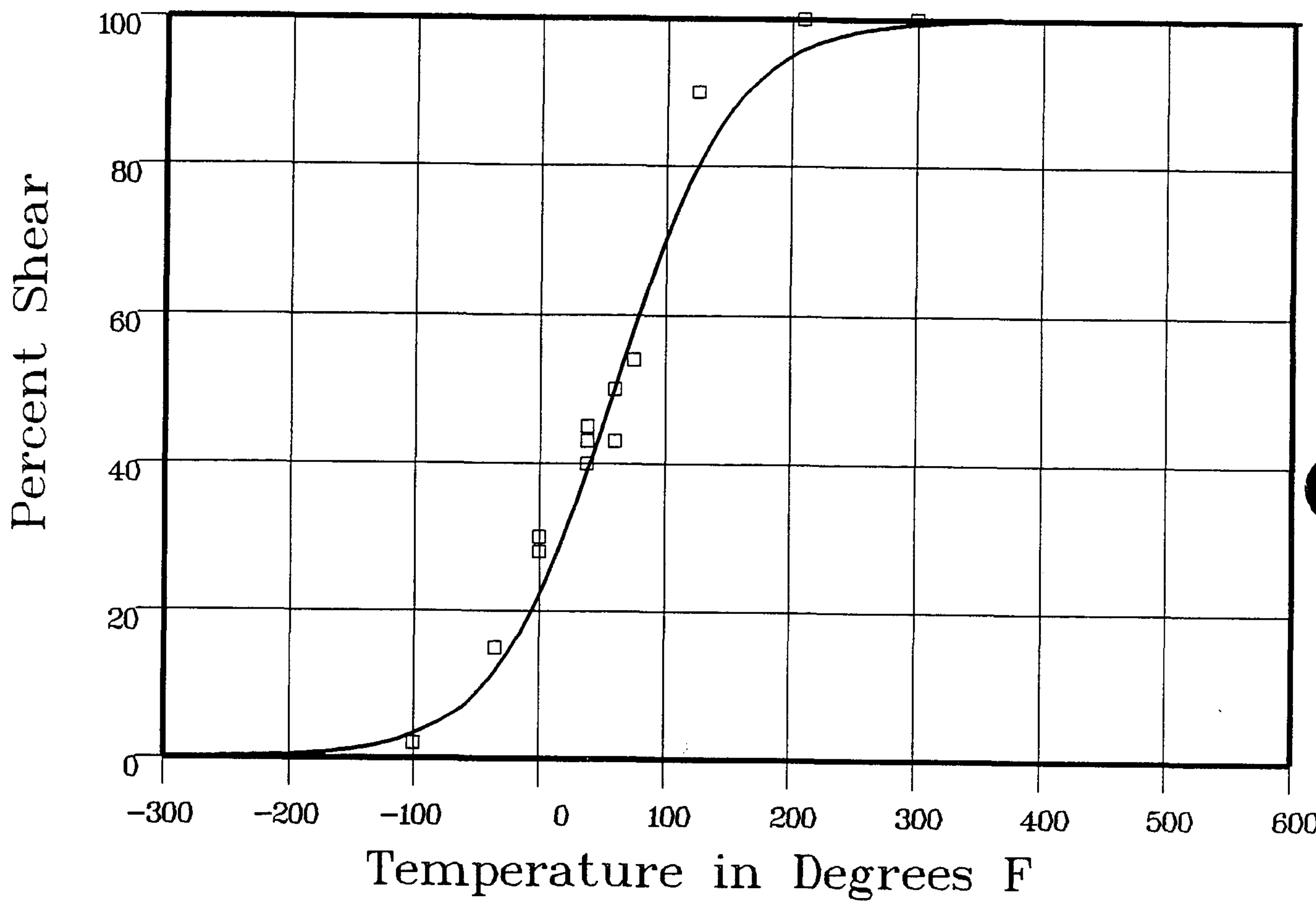

Data Set(s) Plotted

Plant: WB1 Cap.: UNIRR Material: FORGING SA508CL2 Ori.: TL Heat #: 527536 (RING 05)

Charpy V-Notch Data

Temperature	Input Percent Shear	Computed Percent Shear	Differential
-100	2	3.7	-1.7
-100	2	3.7	-1.7
-100	2	3.7	-1.7
-35	15	13.12	1.87
0	28	23.98	4.01
0	30	23.98	6.01
38	40	41.23	-1.23
38	45	41.23	3.76
38	43	41.23	1.76

**** Data continued on next page ****

SHELL FORGING 05 AXIAL

Page 2

Material: FORGING SA508CL2 Heat Number: 527536 (RING 05) Orientation: TL

Capsule: UNIRR Total Fluence:

Charpy V-Notch Data (Continued)

Temperature	Input Percent Shear	Computed Percent Shear	Differential
60	43	52.7	-9.7
60	50	52.7	-2.7
75	54	60.44	-6.44
125	90	81.39	8.6
210	100	96.31	3.68
210	100	96.31	3.68
210	100	96.31	3.68
300	100	99.42	.57
300	100	99.42	.57

SUM of RESIDUALS = 13.03

UNIRRADIATED WELD

CVGRAPH 4.1 Hyperbolic Tangent Curve Printed at 08:20:17 on 02-24-1998

Page 1

Coefficients of Curve 1

A = 66.5	B = 64.3	C = 66.58	T0 = 11.25

Equation is: CVN = A + B * [tanh((T - T0)/C)]

Upper Shelf Energy: 130.8 Fixed Temp. at 30 ft-lbs: -31.6 Temp. at 50 ft-lbs: -6.2 Lower Shelf Energy: 2.19 Fixed

Material: WELD Heat Number: WIRE HEAT:895075 Orientation:

Capsule: UNIRR Total Fluence:

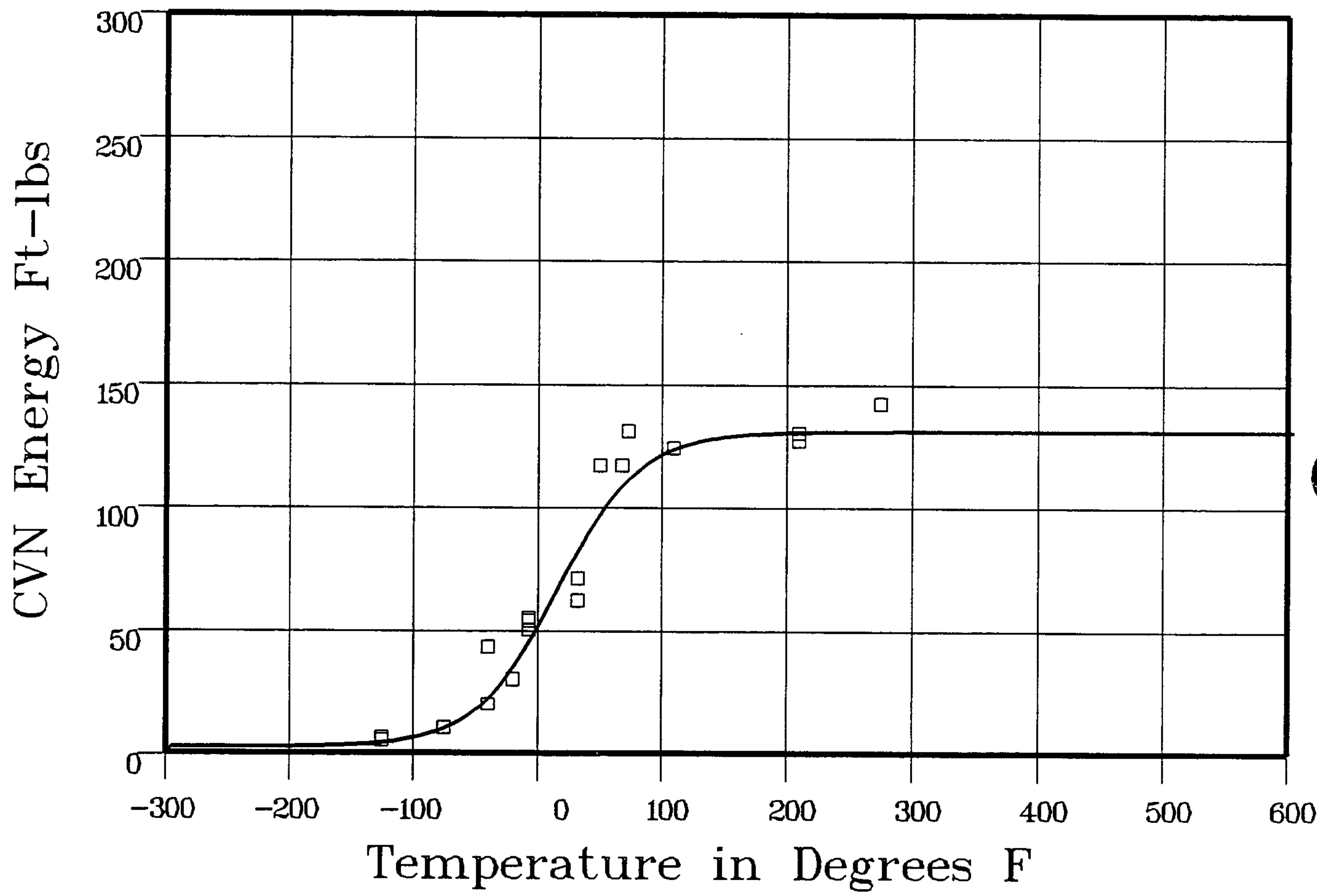

Data Set(s) Plotted

Plant: WB1 Cap.: UNIRR Material: WELD Ori.: Heat #: WIRE HEAT:895075

Charpy V-Notch Data

Temperature	Input CVN Energy	Computed CVN Energy	Differential
-125	5	4.31	.68
-125	6	4.31	1.68
-75	10	11.16	-1.16
-40	43	24.91	18.08
-40	20	24.91	-4.91
-20	30	38.35	-8.35
-7	55	49.3	5.69
-7	50	49.3	.69
-7	54	49.3	4.69

**** Data continued on next page ****

UNIRRADIATED WELD

Material: WELD   Heat Number: WIRE HEAT:895075   Orientation:

Capsule: UNIRR   Total Fluence:

Charpy V-Notch Data (Continued)

Temperature	Input CVN Energy	Computed CVN Energy	Differential
32	62	85.91	-23.91
32	71	85.91	-14.91
50	117	100.19	16.8
68	117	111.01	5.98
73	131	113.39	17.6
110	124	124.5	-.5
210	127	130.47	-3.47
210	130	130.47	-.47
275	142	130.75	11.24

SUM of RESIDUALS = 25.46

UNIRRADIATED WELD

CVGRAPH 4.1 Hyperbolic Tangent Curve Printed at 08:36:31 on 02-24-1998
Page 1
Coefficients of Curve 1

A = 44.42	B = 43.42	C = 64.07	T0 = 4.68

Equation is: L.E. = A + B * [tanh((T - T0)/C)]

Upper Shelf L.E.: 87.85 Temperature at L.E. 35: -9.4 Lower Shelf L.E.: 1 Fixed

Material: WELD Heat Number: WIRE HEAT:895075 Orientation:

Capsule: UNIRR Total Fluence:

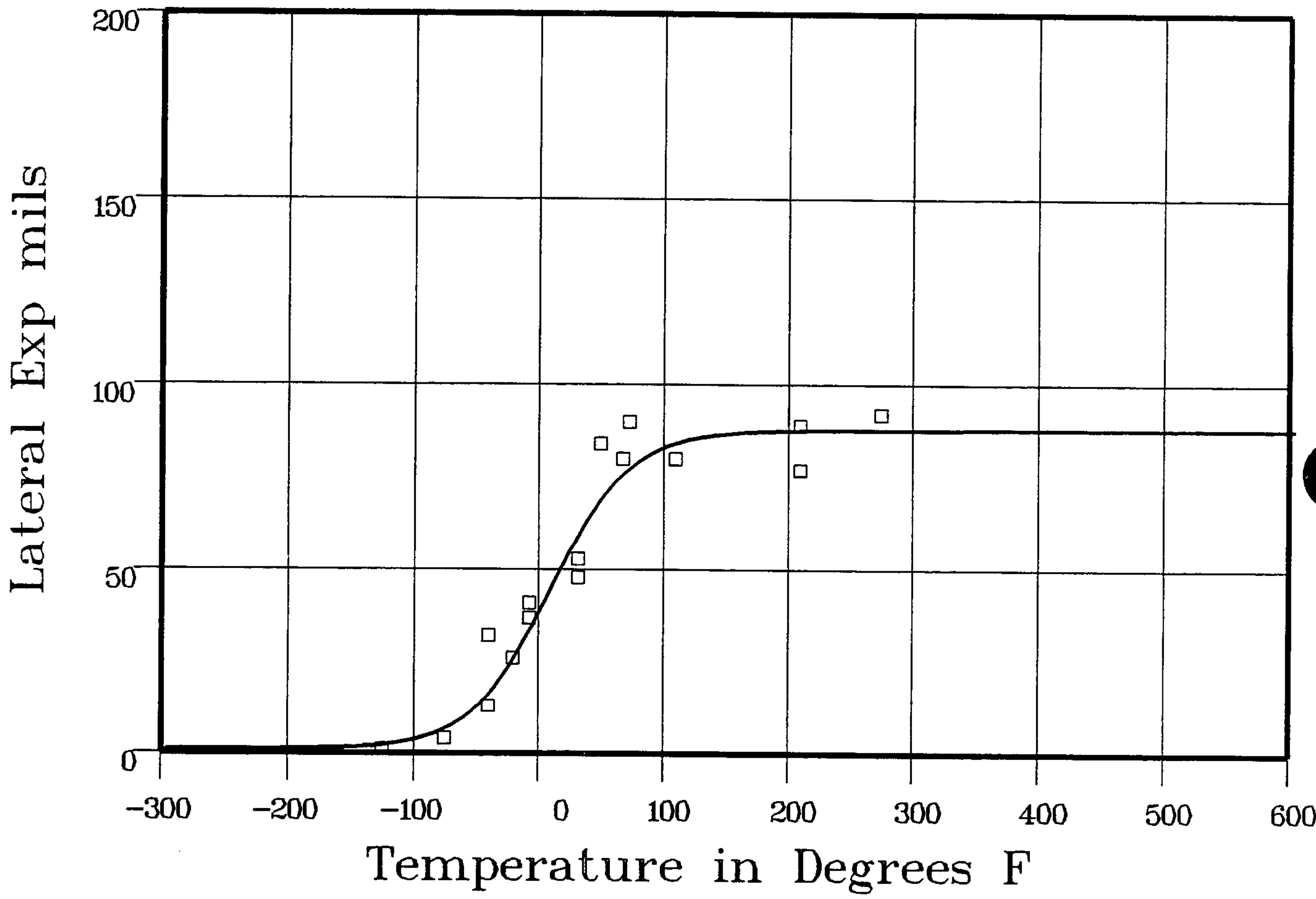

Data Set(s) Plotted
Plant: WB1 Cap.: UNIRR Material: WELD Ori.: Heat #: WIRE HEAT:895075

Charpy V-Notch Data

Temperature	Input Lateral Expansion	Computed L.E.	Differential
-125	1	2.49	-1.49
-125	1	2.49	-1.49
-75	4	7.66	-3.66
-40	32	18.25	13.74
-40	13	18.25	-5.25
-20	26	28.47	-2.47
-7	41	36.59	4.4
-7	37	36.59	.4
-7	37	36.59	.4

**** Data continued on next page ****

UNIRRADIATED WELD

Page 2

Material: WELD   Heat Number: WIRE HEAT:895075   Orientation:

Capsule: UNIRR   Total Fluence:

Charpy V-Notch Data (Continued)

Temperature	Input Lateral Expansion	Computed L.E.	Differential
32	48	61.88	-13.88
32	53	61.88	-8.88
50	84	70.86	13.13
68	80	77.27	2.72
73	90	78.64	11.35
110	80	84.72	-4.72
210	77	87.7	-10.7
210	89	87.7	1.29
275	92	87.83	4.16

SUM of RESIDUALS = -.93

UNIRRADIATED WELD

CVGRAPH 4.1 Hyperbolic Tangent Curve Printed at 08:42:01 on 02-24-1998

Page 1

Coefficients of Curve 1

A = 50	B = 50	C = 91.74	T0 = -1.4

Equation is: Shear% = A + B * [tanh((T - T0)/C)]

Temperature at 50% Shear: -1.4

Material: WELD Heat Number: WIRE HEAT:895075 Orientation:

Capsule: UNIRR Total Fluence:

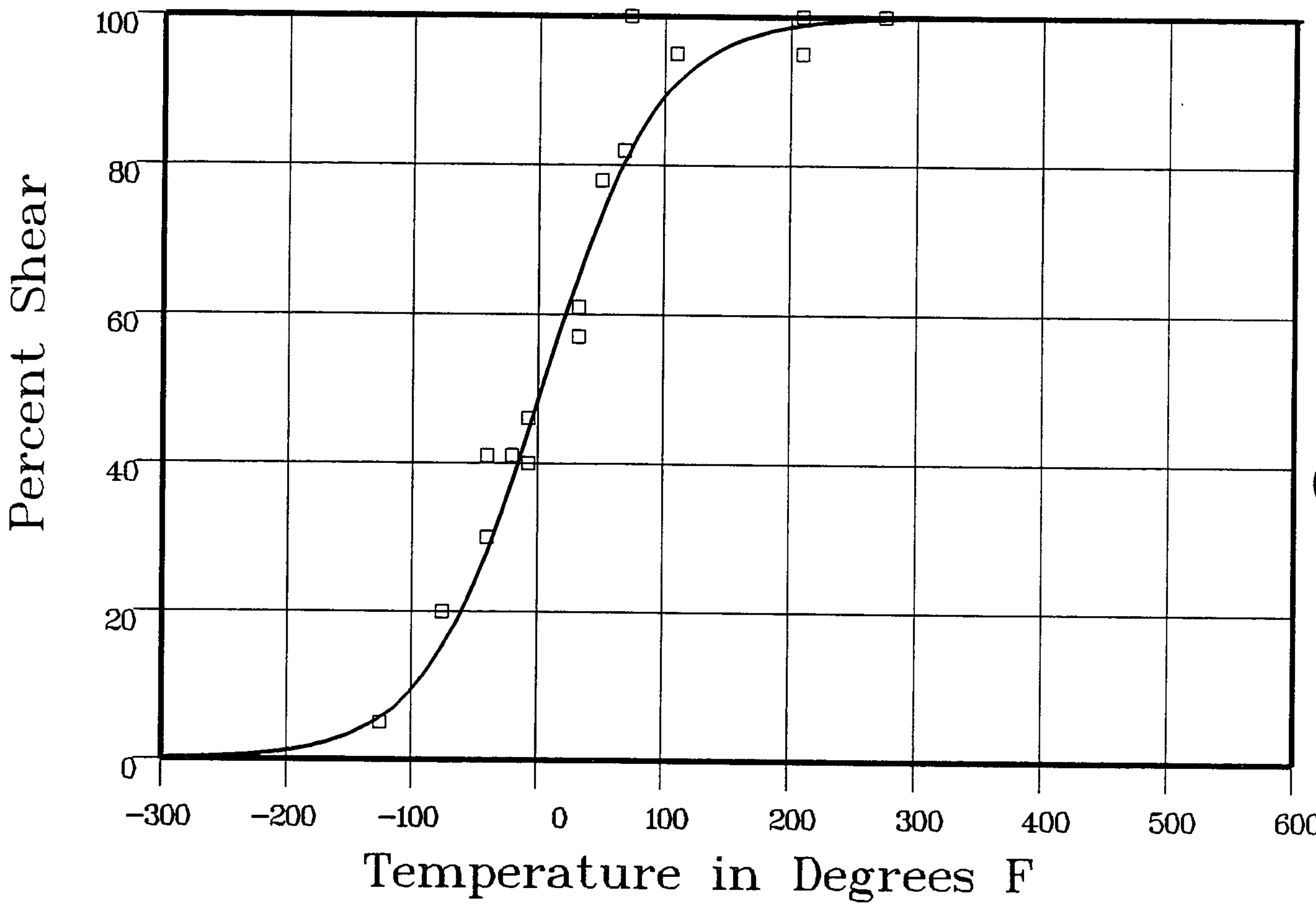

Data Set(s) Plotted

Plant: WB1 Cap.: UNIRR Material: WELD Ori.: Heat #: WIRE HEAT:895075

Charpy V-Notch Data

Temperature	Input Percent Shear	Computed Percent Shear	Differential
-125	5	6.33	-1.33
-125	5	6.33	-1.33
-75	20	16.73	3.26
-40	41	30.12	10.87
-40	30	30.12	-.12
-20	41	40	.99
-7	46	46.95	-.95
-7	46	46.95	-.95
-7	40	46.95	-6.95

**** Data continued on next page ****

UNIRRADIATED WELD

Material: WELD Heat Number: WIRE HEAT:895075 Orientation:

Capsule: UNIRR Total Fluence:

Charpy V-Notch Data (Continued)

Temperature	Input Percent Shear	Computed Percent Shear	Differential
32	57	67.44	-10.44
32	61	67.44	-6.44
50	78	75.41	2.58
68	82	81.95	.04
73	100	83.5	16.49
110	95	91.89	3.1
210	95	99.01	-4.01
210	100	99.01	.98
275	100	99.75	.24

SUM of RESIDUALS = 6.04

UNIRRADIATED HEAT-AFFECTED-ZONE

CVGRAPH 4.1 Hyperbolic Tangent Curve Printed at 08:49:06 on 02-24-1998

Page 1

Coefficients of Curve 1

A = 45.59	B = 43.4	C = 99.48	T0 = -19.21

Equation is: CVN = A + B * [tanh((T - T0)/C)]

Upper Shelf Energy: 89 Fixed Temp. at 30 ft-lbs: -56.6 Temp. at 50 ft-lbs: -9 Lower Shelf Energy: 2.19 Fixed

Material: HEAT AFF'D ZONE Heat Number: WIRE HEAT:895075 Orientation:

Capsule: UNIRR Total Fluence:

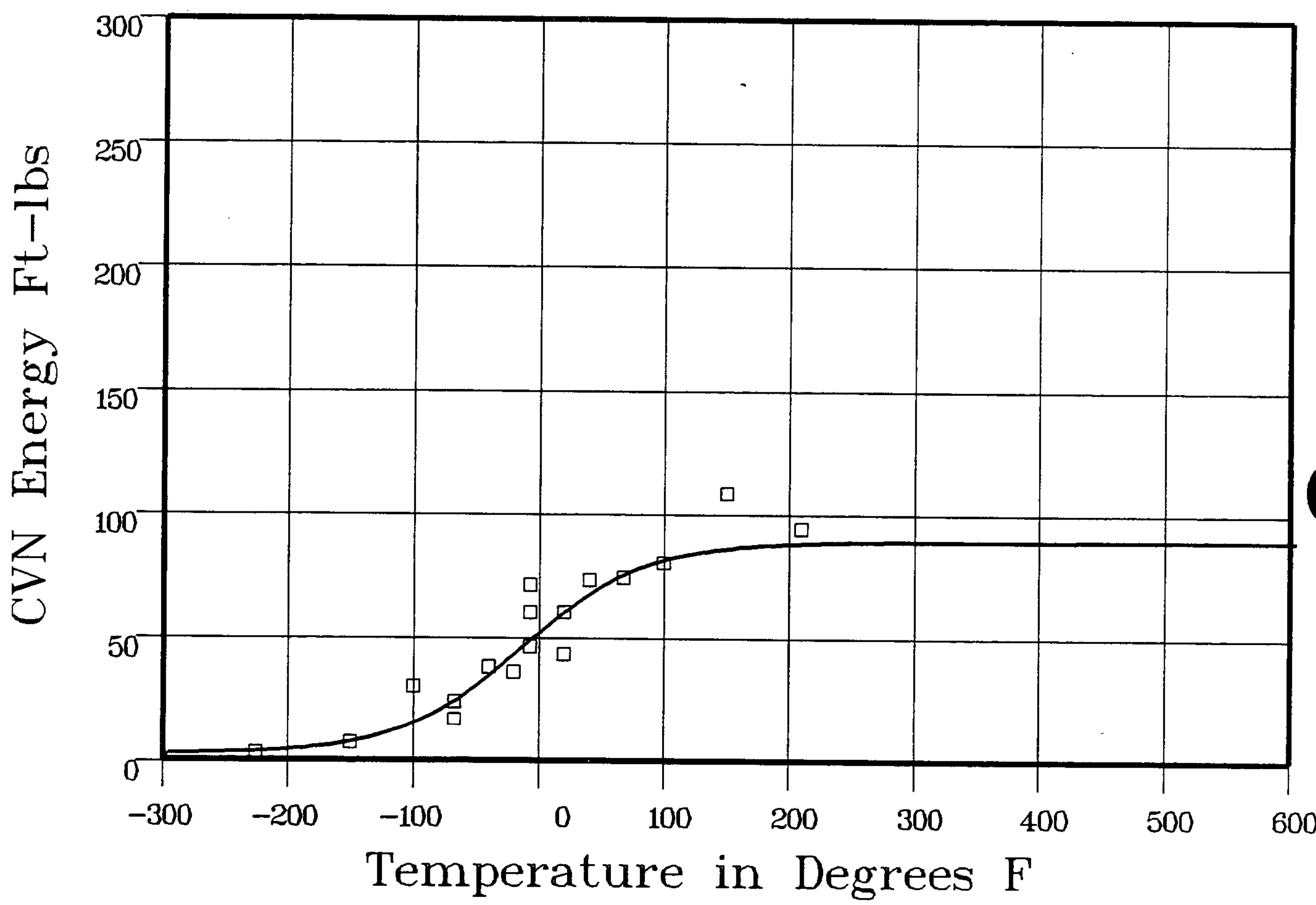

Data Set(s) Plotted

Plant: WB1 Cap.: UNIRR Material: HEAT AFF'D ZONE Ori.: Heat #: WIRE HEAT:895075

Charpy V-Notch Data

Temperature	Input CVN Energy	Computed CVN Energy	Differential
-225	3	3.56	-.56
-225	3	3.56	-.56
-150	7	8.03	-1.03
-100	30	16.49	13.5
-67	24	26.22	-2.22
-67	17	26.22	-9.22
-40	38	36.66	1.33
-20	36	45.25	-9.25
-7	60	50.9	9.09

**** Data continued on next page ****

UNIRRADIATED HEAT-AFFECTED-ZONE

Page 2

Material: HEAT AFF'D ZONE Heat Number: WIRE HEAT:895075 Orientation:

Capsule: UNIRR Total Fluence:

Charpy V-Notch Data (Continued)

Temperature	Input CVN Energy	Computed CVN Energy	Differential
-7	71	50.9	20.09
-7	46	50.9	-4.9
20	60	61.87	-1.87
20	43	61.87	-18.87
40	73	68.76	4.23
68	74	76.18	-2.18
100	80	81.75	-1.75
150	108	86.2	21.79
210	94	88.14	5.85

SUM of RESIDUALS = 23.47

UNIRRADIATED HEAT-AFFECTED-ZONE

CVGRAPH 4.1 Hyperbolic Tangent Curve Printed at 08:55:39 on 02-24-1998

Page 1

Coefficients of Curve 1

A = 33.35	B = 32.35	C = 110.6	T0 = -6.09

Equation is: L.E. = A + B * [tanh((T - T0)/C)]

Upper Shelf L.E.: 65.71 Temperature at L.E. 35: -.4 Lower Shelf L.E.: 1 Fixed

Material: HEAT AFFD ZONE Heat Number: WIRE HEAT:895075 Orientation:

Capsule: UNIRR Total Fluence:

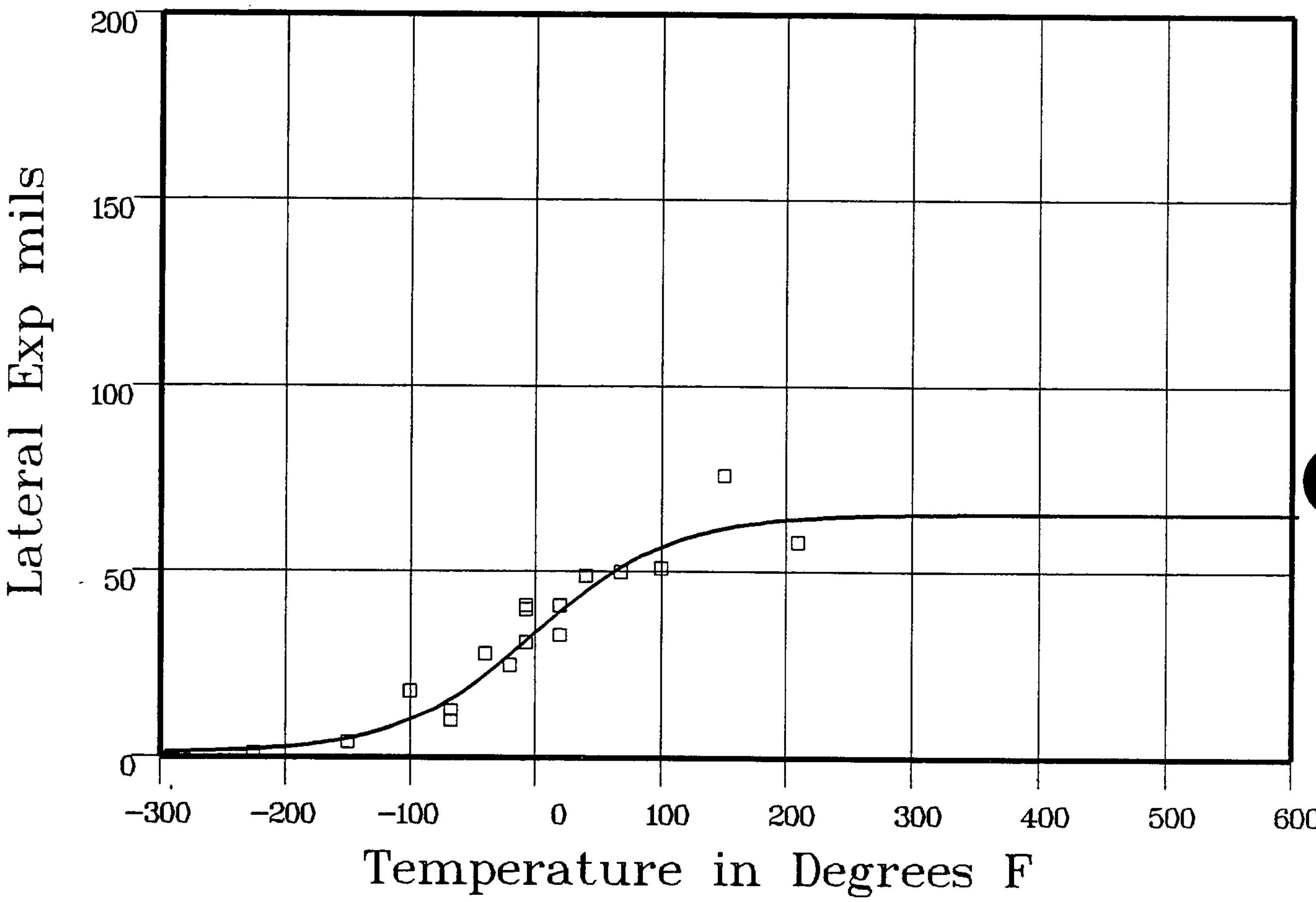

Data Set(s) Plotted

Plant: WB1 Cap.: UNIRR Material: HEAT AFFD ZONE Ori.: Heat #: WIRE HEAT:895075

Charpy V-Notch Data

Temperature	Input Lateral Expansion	Computed L.E.	Differential
-225	1	2.21	-1.21
-225	1	2.21	-1.21
-150	4	5.46	-1.46
-100	18	11.01	6.98
-67	13	17.14	-4.14
-67	10	17.14	-7.14
-40	28	23.73	4.26
-20	25	29.31	-4.31
-7	40	33.09	6.9

**** Data continued on next page ****

UNIRRADIATED HEAT-AFFECTED-ZONE

Page 2

Material: HEAT AFF'D ZONE   Heat Number: WIRE HEAT:895075   Orientation:

Capsule: UNIRR   Total Fluence:

Charpy V-Notch Data (Continued)

Temperature	Input Lateral Expansion	Computed L.E.	Differential
-7	41	33.09	7.9
-7	31	33.09	-2.09
20	41	40.85	.14
20	33	40.85	-7.85
40	49	46.11	2.88
68	50	52.28	-2.28
100	51	57.43	-6.43
150	76	62.08	13.91
210	58	64.44	-6.44

SUM of RESIDUALS = -1.59

UNIRRADIATED HEAT-AFFECTED-ZONE

CVGRAPH 4.1 Hyperbolic Tangent Curve Printed at 08:59:55 on 02-24-1998

Page 1

Coefficients of Curve 1

A = 50	B = 50	C = 94.61	T0 = -22.37

Equation is: Shear% = A + B * [tanh((T - T0)/C)]

Temperature at 50% Shear: -22.3

Material: HEAT AFF'D ZONE Heat Number: WIRE HEAT:895075 Orientation:

Capsule: UNIRR Total Fluence:

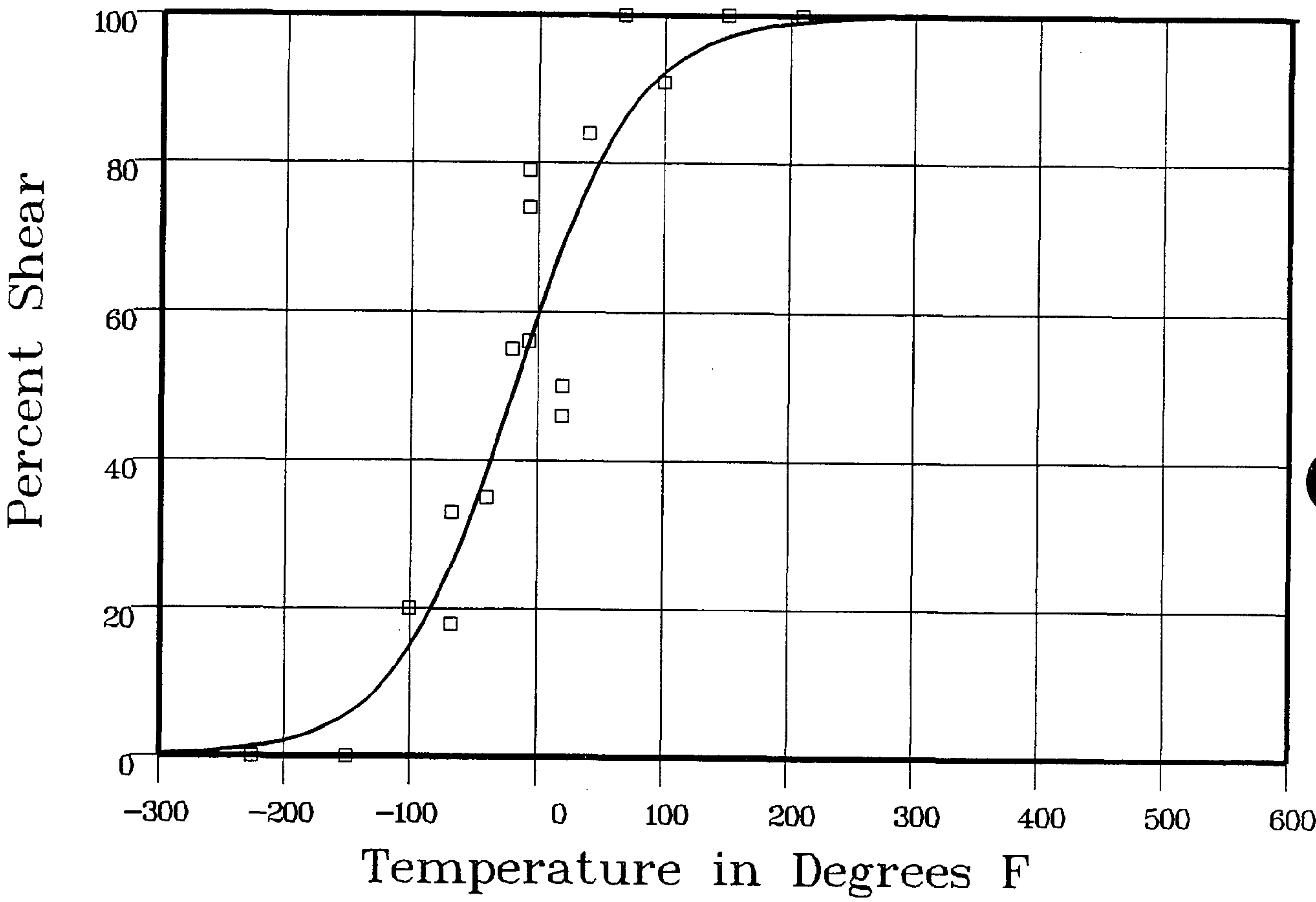

Data Set(s) Plotted

Plant: WB1 Cap.: UNIRR Material: HEAT AFF'D ZONE Ori.: Heat #: WIRE HEAT:895075

Charpy V-Notch Data

Temperature	Input Percent Shear	Computed Percent Shear	Differential
-225	0	1.36	-1.36
-225	0	1.36	-1.36
-150	0	6.31	-6.31
-100	20	16.23	3.76
-67	33	28.02	4.97
-67	18	28.02	-10.02
-40	35	40.79	-5.79
-20	55	51.25	3.74
-7	74	58.05	15.94

**** Data continued on next page ****

UNIRRADIATED HEAT-AFFECTED-ZONE

Material: HEAT AFF'D ZONE   Heat Number: WIRE HEAT:895075   Orientation:

Capsule: UNIRR   Total Fluence:

Charpy V-Notch Data (Continued)

Temperature	Input Percent Shear	Computed Percent Shear	Differential
-7	79	58.05	20.94
-7	56	58.05	-2.05
20	46	71	-25
20	50	71	-21
40	84	78.89	5.1
68	100	87.1	12.89
100	91	93	-2
150	100	97.45	2.54
210	100	99.26	.73

SUM of RESIDUALS = -4.26